

Post-Tensioning Anchorage Zones in Bridge Decks

APPROVED:

John E. Breen

John L. Tassoulas

For all those who have suffered

For all those who will suffer

For all those who never give up and never give in

For something that should win

Post-Tensioning Anchorage Zones in Bridge Decks

by

Brian Albert Falconer, B.S.

THESIS

Presented to the Faculty of the Graduate School of
The University of Texas at Austin
in Partial Fulfillment
of the Requirements
for the degree of

MASTER OF SCIENCE IN ENGINEERING

THE UNIVERSITY OF TEXAS AT AUSTIN

MAY 1990

ACKNOWLEDGEMENTS

The author wishes to thank everyone involved with this investigation and thesis for their contributions. In particular, Dr. John Breen, Dr. John Tassoulas, Gregor Wollman, Olivier Burdet, David Sanders, Carin Roberts have my appreciation for their guidance, and Charles Crisman, David Dorr, and Martin Gonzalez have all earned my appreciation for their assistance.

The support of the National Cooperative Highway Research Program (NCHRP), Phil M. Ferguson Structural Engineering Laboratory (FSEL), the Center for High Performance Computing of the University of Texas System (CHPC), and the Graduate School of the University of Texas at Austin were all essential to the successful completion of this investigation and this thesis.

Brian Albert Falconer

Table of Contents

Chapter 1 Introduction.....	1
1.1 Background.....	1
1.2 Objective and Scope of Investigation.....	2
1.3 Review of Literature Pertaining To Bridge Deck Anchorage Zones.....	5
Chapter 2 Analytical Program.....	8
2.1 General.....	8
2.2 Finite Element Analysis.....	8
2.2.1 General.....	8
2.2.2 Horizontal Plane Analysis.....	8
2.2.3 Vertical Plane Analysis.....	18
2.2.4 Predicted Failure.....	20
2.3 Strut and Tie Modeling.....	21
2.3.1 General.....	21
2.3.2 Horizontal Plane Analysis.....	23
2.3.3 Vertical Plane Analysis.....	30
2.3.4 Predicted Failure.....	33
Chapter 3 Experimental Program.....	38
3.1 General.....	38
3.2 Slab Fabrication.....	38
3.2.1 General.....	38
3.2.2 Anchors and Spacings.....	41
3.2.3 Pre-Formed Vertical Cracks.....	42
3.2.4 Anchorage Reinforcement Details.....	43
3.3 Instrumentation and Loading System.....	45
3.3.1 General.....	45

Table of Contents (cont.)

3.3.2	Embedded Strain Gages.....	45
3.3.3	Reinforcement Strain Gages.....	47
3.3.4	Loading Hardware and Process.....	48
3.4	Materials Tests.....	51
3.4.1	General.....	51
3.4.2	Concrete.....	51
3.4.3	Reinforcing Steel.....	52
Chapter 4 Test Results		55
4.1	General.....	55
4.2	Half-Scale Four Strand Anchors Horizontal Orientation....	58
4.2.1	General.....	58
4.2.2	Unreinforced Anchorage Zones.....	60
4.2.2.1	General.....	60
4.2.2.2	Effects of Stressing Sequence.....	64
4.2.2.3	Loading to Failure.....	71
4.2.3	Anchorage Zones with Horizontal Reinforcement....	72
4.2.3.1	General.....	72
4.2.3.2	Effects of Stressing Sequence.....	76
4.2.3.3	Loading to Failure.....	76
4.2.4	Detail B - Back-up Bars.....	81
4.2.5	Detail P - Hairpins and Back-up Bars.....	86
4.2.6	Detail C - Cross Ties and Back-up Bars.....	86
4.2.7	Detail S - Spiral and Back-up Bars.....	90
4.2.8	Detail H - Hoops and Back-up Bars.....	90
4.2.9	Detail HP - Hairpin Hoops and Back-up Bars.....	93
4.2.10	Control Detail.....	93
4.3	Half-Scale Four Strand Anchors Vertical Orientation....	93
4.3.1	General.....	93

Table of Contents (cont.)

4.3.2 Detail B – Back-up Bars.....	97
4.3.3 Detail P – Hairpins and Back-up Bars.....	97
4.3.4 Detail C – Cross Ties and Back-up Bars.....	97
4.3.5 Detail S – Spiral and Back-up Bars.....	102
4.3.6 Control Detail.....	102
4.4 Half-Scale Four Strand Anchors with Diagonal Tendons...	103
4.4.1 General.....	103
4.4.2 Horizontal Anchorage Zone Reinforcement Only...	103
4.4.3 Detail P – Hairpins.....	103
4.4.4 Detail C – Cross Ties.....	109
4.4.5 Detail S – Spiral.....	109
4.4.6 Control Detail.....	109
4.5 Full-Scale Monostrand Anchors.....	112
4.5.1 General.....	112
4.5.2 Detail B – Back-up Bars.....	113
4.5.3 Detail P – Hairpins and Back-up Bars.....	116
4.5.4 Detail C – Cross Ties and Back-up Bars.....	118
4.5.5 Detail S – Spiral and Back-up Bars.....	118
4.5.6 Control Detail.....	118
Chapter 5 Comparison and Discussion of Test Results.....	121
5.1 General.....	121
5.2 Evaluation of Anchorages.....	122
5.2.1 General.....	122
5.2.2 Exterior Anchors and Edge Distance.....	125
5.2.3 Anchor Spacing and Stressing Sequence.....	131
5.2.4 Effects of Anchor Orientation, Anchor Type and Tendon Inclination.....	137

Table of Contents (cont.)

5.2.5	Evaluation of Anchorage Zone Reinforcing Details.....	143
5.3	Evaluation of Finite Element Analysis Predictions.....	147
5.4	Evaluation of Strut and Tie Model Predictions.....	150
5.4.1	General.....	150
5.4.2	Strut Failure Predictions.....	154
5.4.3	Node Failure Predictions.....	155
5.4.4	Tie Failure Predictions.....	160
5.4.5	Strut-and-tie Model Predicted Failure Load Levels.....	161
5.5	Analysis Recommendations.....	161
5.6	Design Recommendations.....	161
5.6.1	General.....	161
5.6.2	Anchorage Reinforcing Details.....	162
5.6.3	Edge Distance.....	162
5.6.4	Anchor Spacing and Stressing Sequence.....	162
5.6.5	Anchor Orientation.....	163
5.6.6	Anchor Types.....	163
5.7	Recommendations for AASHTO Bridge Design Specifications and Commentary.....	164
Chapter 6 Summary and Conclusions.....		166
6.1	Summary of the Investigation.....	166
6.2	Conclusions.....	166
6.3	Recommendations.....	167
Appendix.....		169
Bibliography.....		190
Vita.....		192

List of Tables

3.1 Physical Properties of the Experimental Program.....	40
3.2 Concrete Strength of Slabs.....	51
4.1 Failure of Four-strand Horizontal Oriented Anchors at Half-scale.....	61
4.2 Failure of Four-strand Vertical Oriented Anchors at Half-scale in Slab #4.....	96
4.3 Failure of Four-strand Anchors with Inclined Tendons at Half-scale in Slab #5.....	106
4.4 Failure of Monostrand Anchors at Full Scale in Slab #6.....	115
5.1 Exterior Anchor Failures.....	129
5.2 Anchor Failures for Interior Anchors with and without Adjacent Anchor Loads.....	136
5.3 Finite Element Predicted Anchor Failure Loads and Actual Failure Loads.....	148
5.4 Average Strut-and-tie predicted Anchor Failure Loads for Various Anchors.....	152
5.5 Strut-and-tie Predicted Anchor Failure Loads for Horizontal Oriented Four-strand Anchors.....	155
5.6 Strut-and-tie Predicted Anchor Failure Loads for Vertical Oriented Four-strand Anchors.....	156
5.7 Strut-and-tie Predicted Anchor Failure Loads for Anchors with Inclined Tendons.....	157
5.8 Strut-and-tie Predicted Anchor Failure Loads for Monostrand Anchors.....	159

List of Figures

1.1	Post-tensioned Segmental Box Girder Bridge in Construction.....	1
1.2	Four-strand Post-Tensioning Anchorage.....	3
1.3	Monostrand Post-Tensioning Anchorage.....	4
1.4	Detail of Post-Tensioned Anchorage Zone in Slab which is Separated from the Wall.....	7
1.5	Detail of Post-Tensioned Anchorage Zone in Slab which is Cast Monolithically with the Wall.....	7
2.1	Dimensions of Finite Element Slab Models.....	9
2.2	Horizontal Plane Principle Stresses Under Varied Load Configurations.....	11
2.3	Horizontal Plane Principle Stresses During Stressing Sequence.....	12
2.4	Interior Anchor Horizontal Bursting Stresses.....	14
2.5	Exterior Anchor Horizontal Bursting Stresses.....	16
2.6	Leading Loaded Anchor Horizontal Bursting Stresses.....	17
2.7	Vertical Plane Bursting Stresses.....	19
2.8	Strut-and-tie Model Ahead of Uniformly Loaded Anchor.....	22
2.9	Horizontal Plane Strut-and-Tie Model #1 for Load on an Interior Anchor.....	24
2.10	Horizontal Plane Strut-and-Tie Model #2 for Load on an Interior Anchor.....	25
2.11	Horizontal Plane Strut-and-Tie Model #3 for Load on an Interior Anchor.....	26
2.12	Horizontal Plane Strut-and-Tie Model #4 for Load on an Interior Anchor.....	28
2.13	Horizontal Plane Strut-and-Tie Model for Load on an End Anchor.....	29

List of Figures (cont.)

2.14 Horizontal Plane Strut-and-Tie Model for Loads on Alternate Anchors.....	31
2.15 Horizontal Plane Strut-and-Tie Model for Loads on All Anchors.....	32
2.16 Transverse Slab Plane Strut-and-Tie Model.....	33
2.17 Bursting Stress in a Concrete Section.....	35
2.18 Strut Modeling in the Anchorage Zone.....	36
3.1 Slab 3 During Testing.....	38
3.2 Representative Half-Scale Slab.....	39
3.3 Anchor Orientation, Edge Distance, and Spacing.....	41
3.4 Preformed Cracks in Slab 2	42
3.5 Horizontal Reinforcement in Slab 6.....	43
3.6 Anchorage Zone Reinforcing Details.....	44
3.7 Control Detail.....	46
3.8 Embedded Strain Gage.....	47
3.9 Hydraulic Ram Loading Anchor with Threaded Bar.....	48
3.10 Hydraulic Ram Loading Anchor with Strands.....	49
3.11 Hydraulic Pump Monitored by Strain Indicator.....	50
3.12 Swedish #2 Reinforcing Bar Stress-Strain Curve.....	53
3.13 #3 Reinforcing Bar Stress-Strain Curve.....	53
3.14 Welded Wire Fabric Stress-Strain Curve.....	54
4.1 Single Edge Anchorage Failures.....	56
4.2 Shear Cone Ahead of Anchor in Slab #3.....	57
4.3 Slab 3 at Failed Anchor A.....	57
4.4 Average Failure Loads of Four-strand Horizontal Oriented Anchors.....	59

List of Figures (cont.)

4.5	Average Ratio of Bearing Stress at Failure to Concrete Compressive Strength for Four-strand Horizontal Oriented Anchors.....	60
4.6	Plan of Slab 1.....	62
4.7	Plan of Slab 3.....	63
4.8	First Cracking at Anchor E of Slab 1.....	64
4.9	Maximum Calculated Horizontal Bursting Stresses in Slab 1....	66
4.10	Maximum Calculated Horizontal Bursting Stresses in Slab 3....	67
4.11	Adjacent Anchor Loading Effects on Calculated Stresses in Slab 1.....	68
4.12	Adjacent Anchor Loading Effects on Calculated Stresses in Slab 3.....	69
4.13	Exterior Anchor Effects on Calculated Stresses in Slab 1....	70
4.14	Failed Anchor A in Slab 1.....	71
4.15	Slab 1 Failure at Anchor A.....	72
4.16	Slab 1 Failure at Anchor H.....	73
4.17	Slab 3 Failure at Anchor A.....	74
4.18	Slab 3 Failure at Anchor C.....	75
4.19	Plan of Slab 2.....	77
4.20	Maximum Calculated Force in #2 Reinforcing Bars of Slab 2....	78
4.21	Adjacent Anchor Loading Effects on Calculated Forces in Slab 2.....	79
4.22	Cross Tie Reinforcing in Slab 2.....	80
4.23	Cracking Along the Preformed Crack in Slab 2.....	82
4.24	Slab 2 Failure at Anchor A.....	83
4.25	Slab 2 Failure at Anchor D.....	84
4.26	Slab 2 Failure at Anchor H.....	85
4.27	Slab 3 Back-up Bars Detail.....	86

List of Figures (cont.)

4.28 Slab 3 Hairpin Detail.....	87
4.29 Slab 3 Cross Ties Detail.....	88
4.30 Failure in Slab 3 at Anchor H.....	89
4.31 Slab 3 Spiral Detail.....	90
4.32 Slab 4 Hoops Detail.....	91
4.33 Plan of Slab 4 (Vertical Anchors).....	92
4.34 Slab 4 Hairpin Hoops Detail.....	94
4.35 Failed Anchor J in Slab 4.....	95
4.36 Average Failure Loads for Four-strand Vertical Oriented Anchors.....	95
4.37 Average Ratio of Bearing Stress at Failure to Concrete Compressive Strength for Four-strand Vertical Oriented Anchors.....	96
4.38 Slab 4 Back-up Bars Detail.....	98
4.39 Failed Exterior Anchor L in Slab 4.....	99
4.40 Slab 4 Hairpin Detail.....	100
4.41 Slab 4 Cross Ties Detail.....	101
4.42 Slab 4 Spiral Detail.....	102
4.43 Plan of Slab 5 (Inclined Tendons).....	104
4.44 Average Failure Loads for Horizontal Anchors with Inclined Tendons.....	105
4.45 Average Ratio of Bearing Stress at Failure to Concrete Compressive Strength for Horizontal Anchors with Inclined Tendons.....	105
4.46 Failed Anchor A in Slab 5.....	106
4.47 Slab 5 Horizontal Reinforcing Detail.....	107
4.48 Slab 5 Hairpin Detail.....	108
4.49 Slab 5 Cross Ties Detail.....	110
4.50 Slab 5 Spiral Detail.....	111

List of Figures (cont.)

4.51 Plan of Slab 6.....	113
4.52 Failed Anchor B in Slab 6.....	114
4.53 Average Failure Loads for Monostrand Anchors.....	114
4.54 Average Ratio of Bearing Stress at Failure to Concrete Compressive Strength for Monostrand Anchors.....	115
4.55 Slab 6 Back-up Bars Detail.....	116
4.56 Slab 6 Hairpin Detail.....	117
4.57 Slab 6 Cross Ties Detail.....	119
4.58 Slab 6 Spiral Detail.....	120
5.1 Four Anchor Arrangements Tested.....	123
5.2 Anchorage Zone Reinforcing Details.....	124
5.3 Failure of Horizontal Oriented Four-strand Interior Anchor...	126
5.4 Failures of Vertical Oriented Four-strand Anchors.....	127
5.5 Ratio of Exterior Anchor Failure Loads to Similar Reinforced Interior Anchor Failure Loads.....	128
5.6 Horizontal Plane Principal Stresses During Stressing Sequence.....	132
5.7 Bursting Stress Distribution in Slab 1.....	133
5.8 Effects of Adjacent Anchor Loading on Calculated Stresses in Slab 1.....	135
5.9 Ratio of Failure Loads of Anchors without Adjacent Anchor Loads to Failure Loads of Anchors with Adjacent Anchor Loads.....	137
5.10 Comparison of Vertical Oriented Anchor Bearing Stress to Horizontal Oriented Anchor Bearing Stress.....	138
5.11 Geometrically Similar and Concentric Area.....	139
5.12 Comparison of Vertical Oriented Anchor Bearing Stress to Modified Horizontal Oriented Anchor Bearing Stress...	140

List of Figures (cont.)

5.13 Ratio of Monostrand Anchor Bearing Stress to Four-strand Anchor Bearing Stress.....	141
5.14 Vertical Splitting at Failed Anchor B in Slab 6.....	142
5.15 Ratio of Inclined Tendon Anchor Bearing Stress to Perpendicular Tendon Anchor Bearing Stress.....	143
5.16 Comparison of Bearing Stress for All Anchor Configuration and Reinforcing Detail.....	145
5.17 Ratio of Actual Average Anchor Failure Loads to Predicted Failure Loads from Finite Element Analysis.....	150
5.18 Finite Element Generated Bearing Stresses Ahead of an Edge Anchor.....	151
5.19 Average Predicted Strut-and-Tie Component Failure Loads for Various Anchor Types, Orientations, and Tendon Inclination.....	153
5.20 Predicted Strut-and-Tie Component Failure Loads for Horizontal Oriented Four-Strand Anchors.....	155
5.21 Predicted Strut-and-Tie Component Failure Loads for Vertical Oriented Four-Strand Anchors.....	156
5.22 Predicted Strut-and-Tie Component Failure Loads for Horizontal Oriented Four-Strand Anchors with Inclined Tendons.....	157
5.23 Predicted Strut-and-Tie Component Failure Loads for Horizontal Oriented Monostrand Anchors.....	158

Chapter 1 Introduction

1.1 Background

Post-tensioned concrete has become a familiar structural system, and with the increase in its use, structural engineers public have become aware of the appropriate analytical and design procedures which produce consistently high quality structures. A post-tensioned segmental box girder bridge is shown during its construction in Figure 1.1. One element of post-tensioned concrete



Figure 1.1 - Post-Tensioned Segmental Box Girder Bridge in Construction
(From Dywidag Catalog)

construction, however, still lacks a consistent and quantitative design procedure. This element is the post-tensioned anchorage zone.

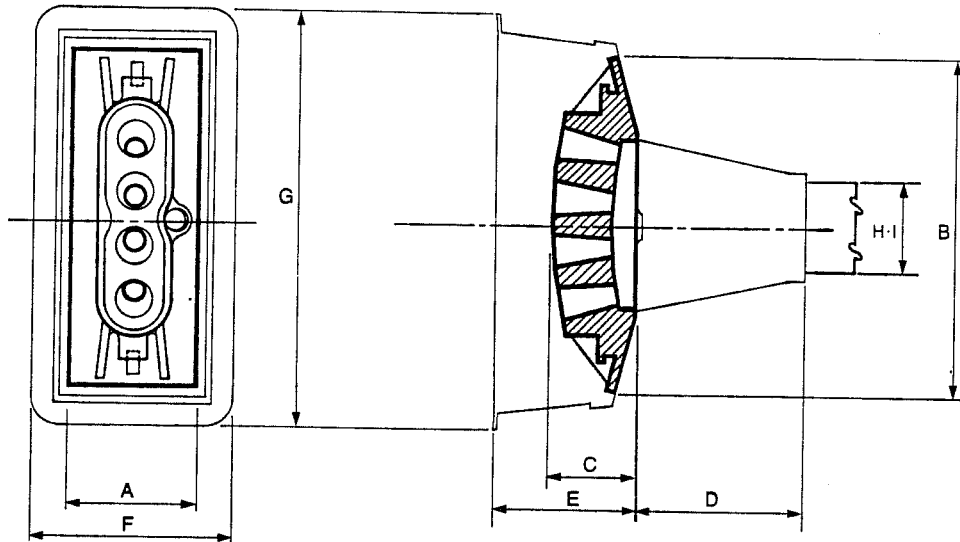
The post-tensioned anchorage zone is that region of a post-tensioned member where post-tensioning anchorage forces, which are created from the tendon stressing and are applied at a concentrated location, spread to a linear distribution of load within the member. The current American Association of Highway and Transportation Officials (AASHTO) criteria for post-tensioned anchorage zones limits the permissible bearing stress of anchors at transfer or at service loads¹. AASHTO has no specific provisions or recommended design procedures for the reinforcing of anchorage zones. For this reason, The National Cooperative Highway Research Program is sponsoring the research project Anchorage Zone Reinforcement for Post-tensioned Concrete Girders at the University of Texas at Austin. The task of the project is to develop standards for applying the strut-and-tie model to the design of reinforcement in post-tensioned anchorage zones.

Part of this project focused on the specific qualities and concerns of bridge deck edge anchorage zones. Typical bridge deck edge anchors are shown in Figures 1.2 and 1.3.

The physical experiments discussed in this thesis were performed at the Phil M. Ferguson Structural Engineering Laboratory at the University of Texas at Austin's Balcones Research Center as part of the Anchorage Zone Reinforcement for Post-Tensioned Concrete Girders project.

1.2 Objectives and Scope of Investigation

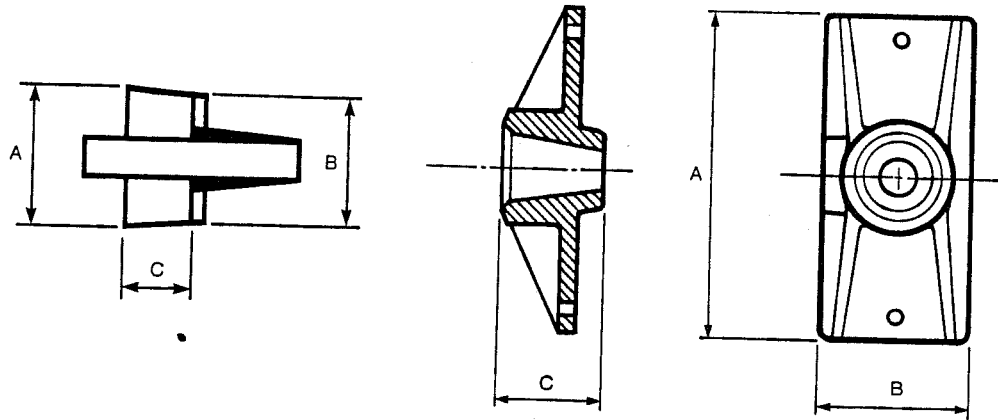
The objectives of the investigation were to explore the effects of loading multiple edge anchors on a bridge deck, to evaluate possible design criteria for bridge deck edge anchorage zones, and to recommend procedures for the analysis and design of



Anchorage Type	VSL SO5-4	SO6-4
A	3.50	3.50
B	11.00	11.00
C	2.87	2.87
D	6.25	6.25
E	5.00	5.00
F	5.62	5.62
G	13.00	13.00
H	3.00	3.00
I	1.00	1.00
J	24.00	24.00
K	4.00	4.00
L	2.50	2.50

Dimensions in inches.

Figure 1.2 - Four-Strand Post-Tensioning Anchorage (from VSL catalog)



Grommet-G

Anchorage Casting

Component	Length or Diameter	Width or Diameter	Depth or Thickness	Bearing Area (in ²)	Conc. Strength at Stressing* (lb/in ²)
	A	B	C		
S5N	5.00	2.25	1.50	11.25	2050
S5NW1	5.25	2.88	1.50	15.09	1500
S5NW2	4.00	3.50	1.50	14.00	1700
S6N	4.63	3.50	1.63	16.19	2100
S6NW	6.00	3.50	1.63	21.00	1600
G5	2.25	2.00	1.25/2.25	—	—
G6	2.50	2.13	1.25/2.25	—	—

Dimensions in inches.

*Values are based on ACI formula $f_b = 0.8 f'_c \sqrt{A_p/A_c}$, $-0.2 \leq 1.25 f'_c$ with edge distance of 1" for hardrock concrete.

Figure 1.3 - Monostrand Post-Tensioning Anchorage (from VSL catalog)

bridge deck edge anchorage zones. The scope of the investigation encompassed both an analytical program and an experimental program.

The analytical program included two-dimensional linear-elastic finite element modeling and strut-and-tie modeling of the bridge deck and its anchorage zones. The finite element analysis explored the effects of stressing sequence, adjacent anchor loading, interior anchor loading, and exterior anchor loading on bridge deck edge anchors, and was used as an indication of what the largest effects of multiple anchorage loading might be. Based on the finite element analysis, strut-and-tie models were created to reproduce the most extreme effects of multiple edge anchor loading.

The experimental program examined the effects of multiple edge anchor loading on anchorage zone strains, and the effects of adjacent anchor loading and exterior anchor edge distance on failure. Anchor types, anchor spacings, reinforcement layouts, and tendon inclination were also varied to examine their effects on anchor failure.

1.3 Review of Literature On Edge Anchors

For a thorough review of literature pertaining to post-tensioned concrete anchorage zones, refer to Burdet⁵, Roberts¹¹, and Sanders¹². For additional information on the strut-and-tie model, refer to Bergmeister, Breen, Jirsa, and Kreger³ and Schlaich, Schafer, and Jennewein¹⁴.

Burgess⁷ performed an experimental study on the behavior of closely spaced edge anchors (monostrand and four-strand) in heavily reinforced bridge decks. He concluded that interaction between closely-spaced anchors was favorable and spiral anchorage reinforcement was only moderately beneficial in heavily reinforced bridge decks. Furthermore, they emphasized that exterior anchors with small edge distances could be weaker because the width of the anchorage zone effects its strength.

Experiments on closely-spaced monostrand edge anchors performed by Sanders, Breen, and Duncan¹³, varied the anchorage zone reinforcement and rotated the anchors from horizontal orientation to vertical. They concluded that the addition of back-up bars and hairpin reinforcement increased the strength of the anchorage zone, that closely-spaced anchors cracked and failed at lower levels per anchor than single anchors, and that horizontal multiple anchors were able to withstand higher loads than vertical multiple anchors because the horizontal anchors utilized the surrounding concrete more efficiently.

Research has concentrated on the failure from jacking forces on the anchorage zone, but in 1985 a post-tensioned roof slab failed after the anchor load had been sustained for five years⁹. A crack had crept through the anchorage zones at a corner of the slab. There was no vertical reinforcement in the anchorage zones along the slab's edge, and when the crack extended far enough ahead of the anchor, the slab split apart. Anchorage zone reinforcement could have been used to provide general structural integrity rather than just for strength for initial jacking forces.

The Post Tensioning Institute suggests the use of one of two details for the edges of post-tensioned slabs (Figures 1.4 and 1.5)¹⁰. Both details incorporate vertical anchorage zone reinforcement, but the reinforcement is spread uniformly along the edge instead of being concentrated in individual anchorage zones.

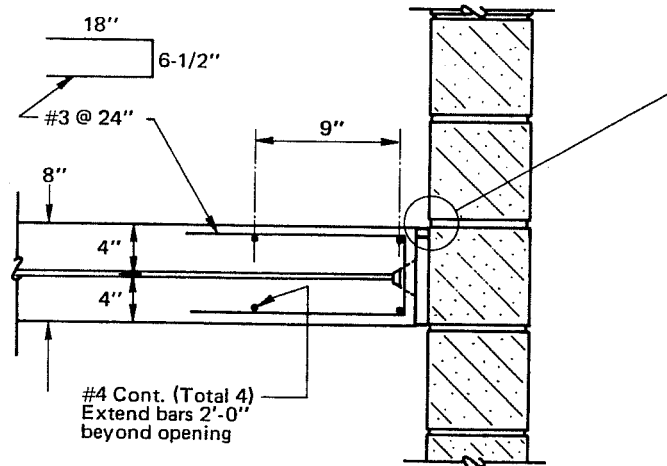


Figure 1.4 - Detail of Post-Tensioned Anchorage Zone in Slab which is Separated from the Wall

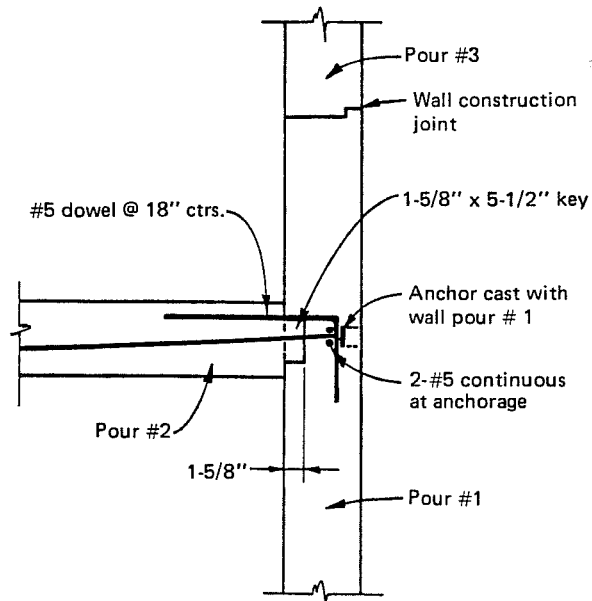


Figure 1.5 - Detail of Post-Tensioned Anchorage Zone in Slab which is cast Monolithically with Wall

Chapter 2 Analytical Program

2.1 General

The analytical program utilized two methods: linear-elastic finite element analysis and strut-and-tie modeling. The finite element analysis was conducted to estimate principal stress trajectories in a bridge deck with various in plane loads applied to its edge. It also provided estimates of stress distributions across specified cross-sections, resultant boundary forces, and first cracking loads. Strut-and-tie models (Section 1.2) were developed utilizing the load paths indicated by the finite element linear-elastic analysis. The strut-and-tie models were used to predict failure of the anchorage zones beyond first cracking.

2.2 Finite Element Analysis

2.2.1 General

Computer analysis was used to model the effects of post-tensioning loads on bridge deck edge anchors. The Abaqus finite element code⁸ was used to calculate the linear-elastic response of the bridge deck. Horizontal and vertical plane stresses were calculated independently with the two models shown in Figure 2.1. All stresses calculated assumed that 35 kip loads were placed on the anchors. This force represents the half-scale four-strand anchor maximum tendon jacking force ($0.8f_{pu}$). The horizontal plane model was used to examine the effects of sequenced loading of anchors and exterior anchor loading. The vertical plane model only examined the effect of a single loaded anchor on vertical plane stresses directly ahead of that anchor. The dimensions of both models are shown in Figure 2.1.

2.2.2 Horizontal Plane Analysis

The horizontal plane analysis concentrated mainly on the effects of anchor stressing sequences on anchorage zone stresses.

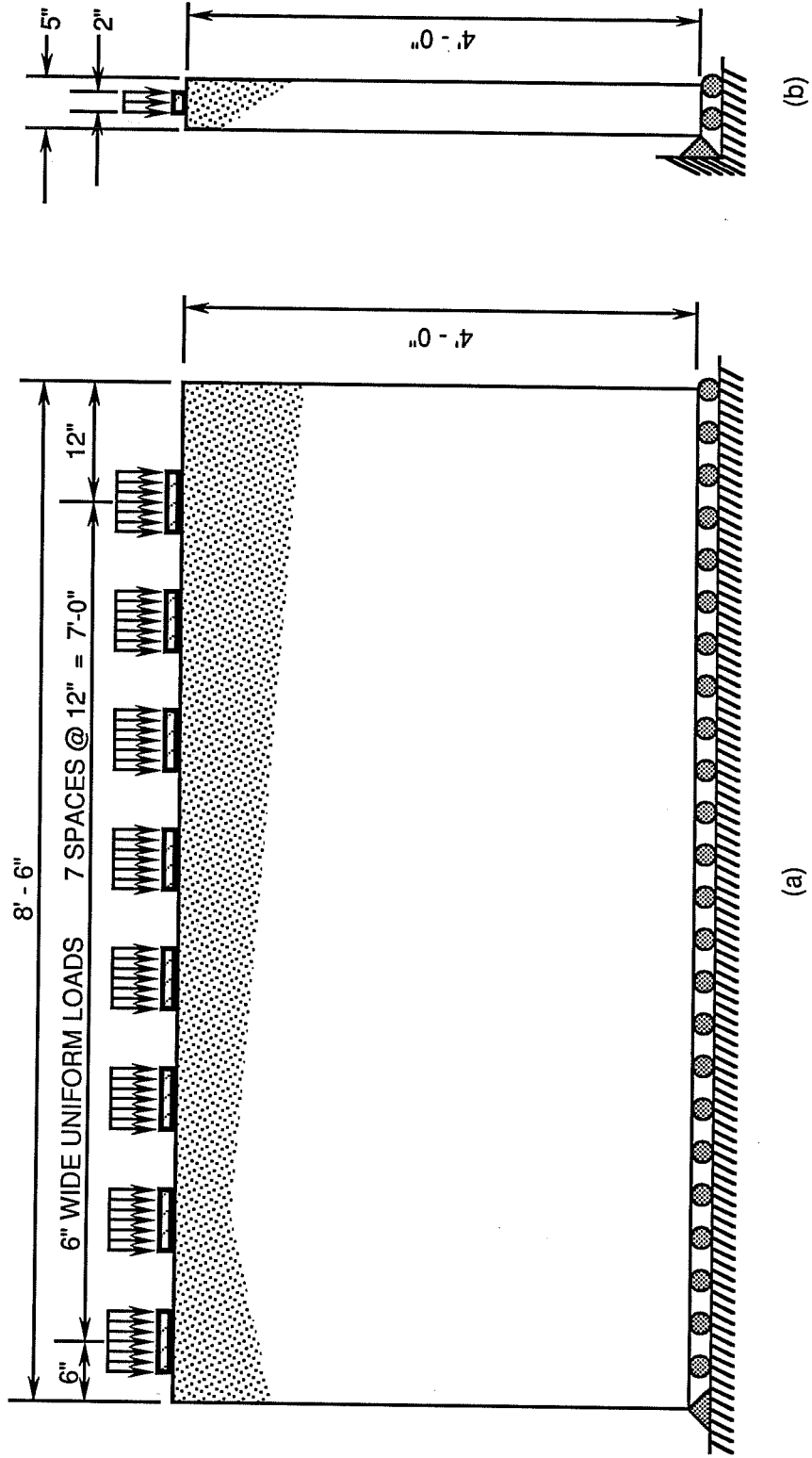


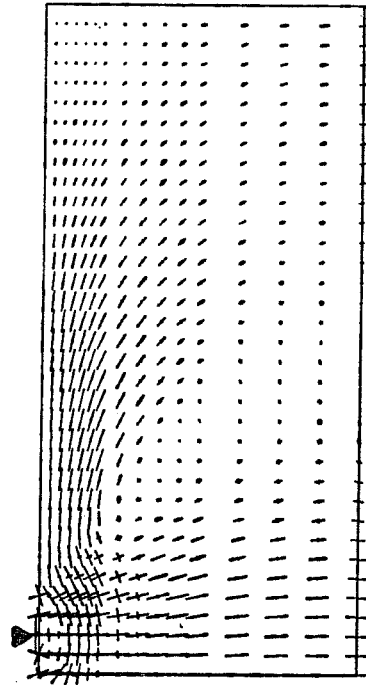
Figure 2.1 - Dimensions of Finite Element Slab Models - (a) Horizontal Plane Model; (b) Vertical Plane Model

Effects of the stressing sequence were examined by loading interior anchors, exterior anchors, adjacent anchors, and alternate anchors in the computer model. The slab model (Figure 2.1a) had eight possible anchorage plate load positions.

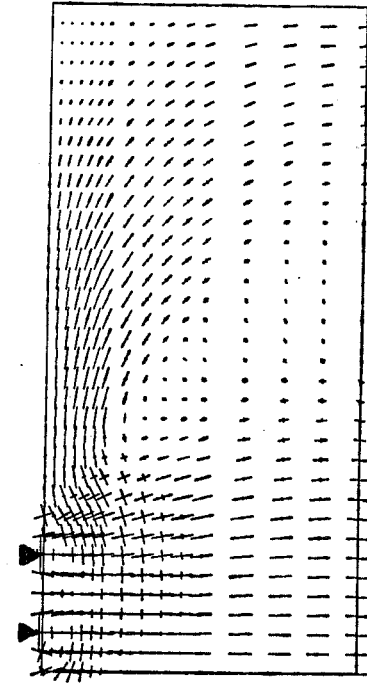
The linear-elastic response of the slab was reviewed with Prin6⁶ which graphically reproduces planar principal stress distributions and stresses across cross-sections of that plane. Slab principal stress distributions for an anchorage zone ahead of a single loaded plate are shown in Figures 2.2(a) and (b). The figures show orientation and magnitude of principal compression and tension as scaled lines at grid points in the slab's plane. Longer lines indicate higher stresses and load paths. The stresses can be classified as compressive, bursting, and spalling. The last two are both tensile stresses. Compressive stresses extend directly from the anchor and flow down to the base of the slab. The tensile stresses wrap around the anchors before extending away from them. Bursting stresses are ahead of loaded anchors and spalling stresses are along the slabs top edge beside or between loaded anchors and sometimes extend down the slab's side.

From Figures 2.2a and 2.2b, it is obvious that the anchorage zone bursting stresses are confined to a smaller region for the exterior anchor than for the interior anchor. The spalling stresses are much larger and extend over a much greater area for the exterior anchor. Figures 2.2(c) and (d) demonstrate that two loaded anchors which are close to one another (2 plate widths apart center-to-center) have one larger combined anchorage zone, but otherwise follow the general patterns of the single anchors.

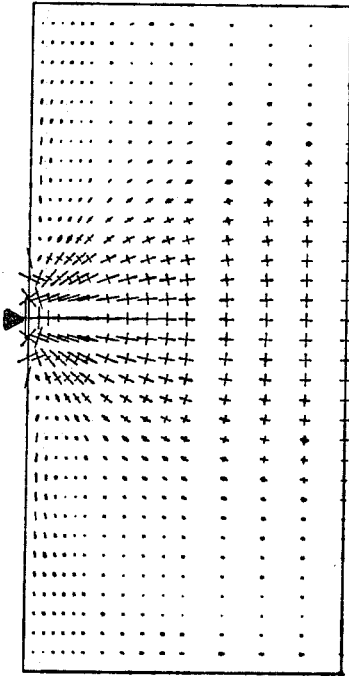
In Figure 2.3(a), two distant anchors are loaded (8 plate widths apart center-to-center). In this case the anchors are able to develop individual anchorage zones; although, substantial tension stresses develop between anchors. However, when an anchor midway between them is loaded, the spacing becomes 4 plate widths and the



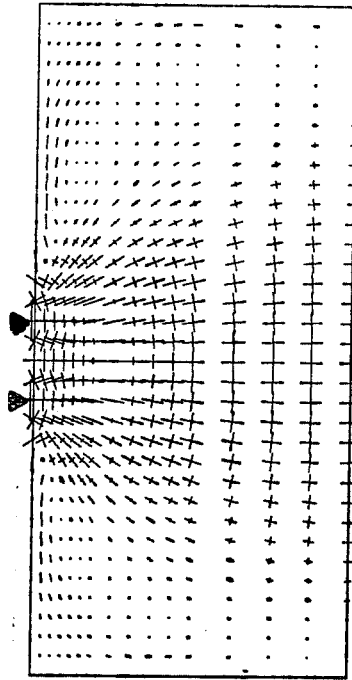
(b) Load on an End Anchor



(d) Load on a Pair of Anchors at End

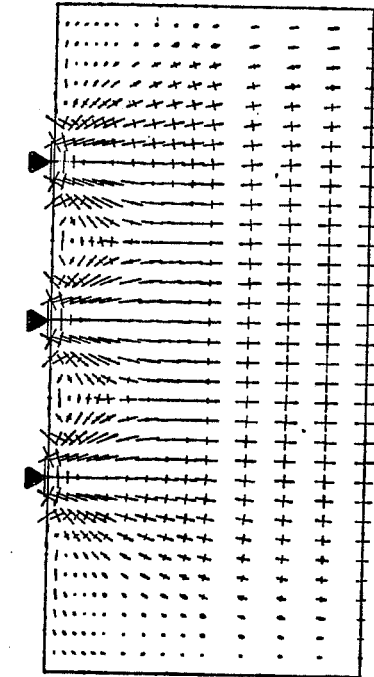


(a) Load on an Intermediate Anchor

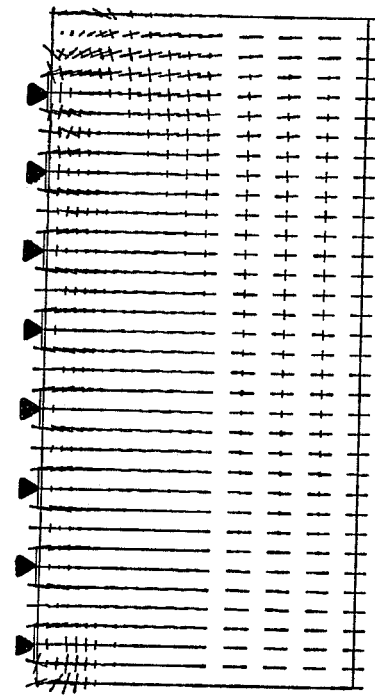


(c) Load on a Pair of Intermediate Anchors

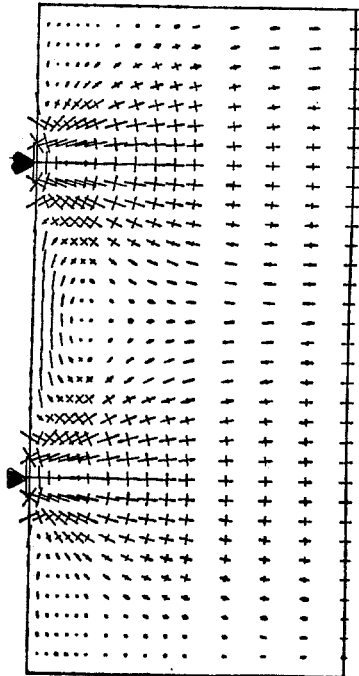
Figure 2.2 - Horizontal Plane Principal Stresses Under Varied Loading Configurations



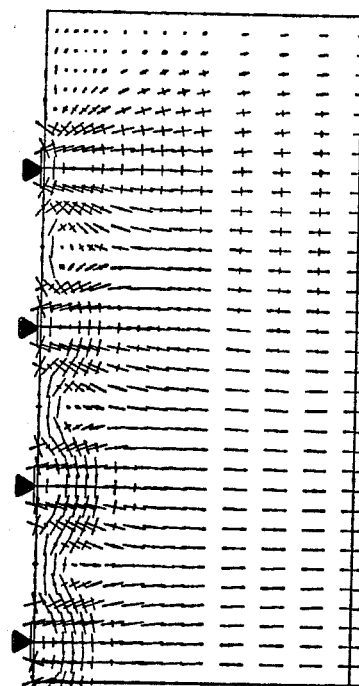
(b) Load on Three Anchors



(d) Load on All Anchors



(a) Load on Two Distant Anchors



(c) Load on Alternate Anchors

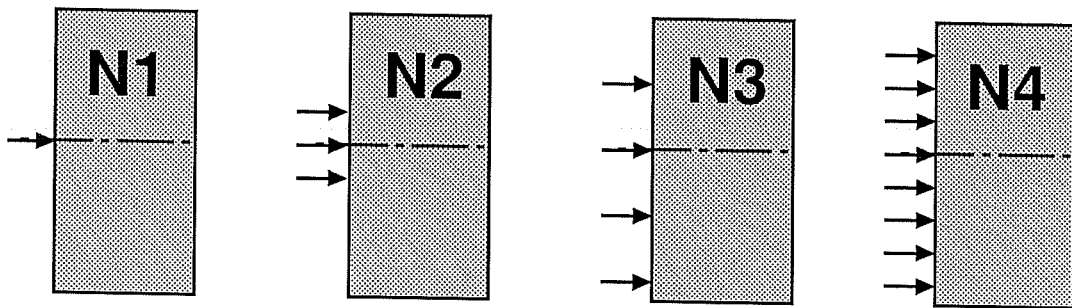
Figure 2.3 - Horizontal Plane Principal Stresses During Stressing Sequence

three anchorage zones show substantial interaction behaving more like one large anchorage zone [Figure 2.3(b)]. Bursting stresses become larger and move further ahead of the bearing plate and spalling stresses are concentrated closer to the edge. Figure 2.3(c) shows that subsequent stressing of a fourth, exterior anchor causes all of the previous three anchors to develop more distinct individual anchorage zones. The anchor spacing remains at 4 plate widths where the exterior anchor is loaded, but the smallest of the exterior anchor edge distances becomes 1 plate width. Figure 2.3(d) shows the pattern when all eight anchors are loaded on the slab edge. The two plate width spacing resembles a uniformly loaded edge in between the two exterior anchors. Substantial horizontal bursting stresses are present only ahead of the exterior anchors.

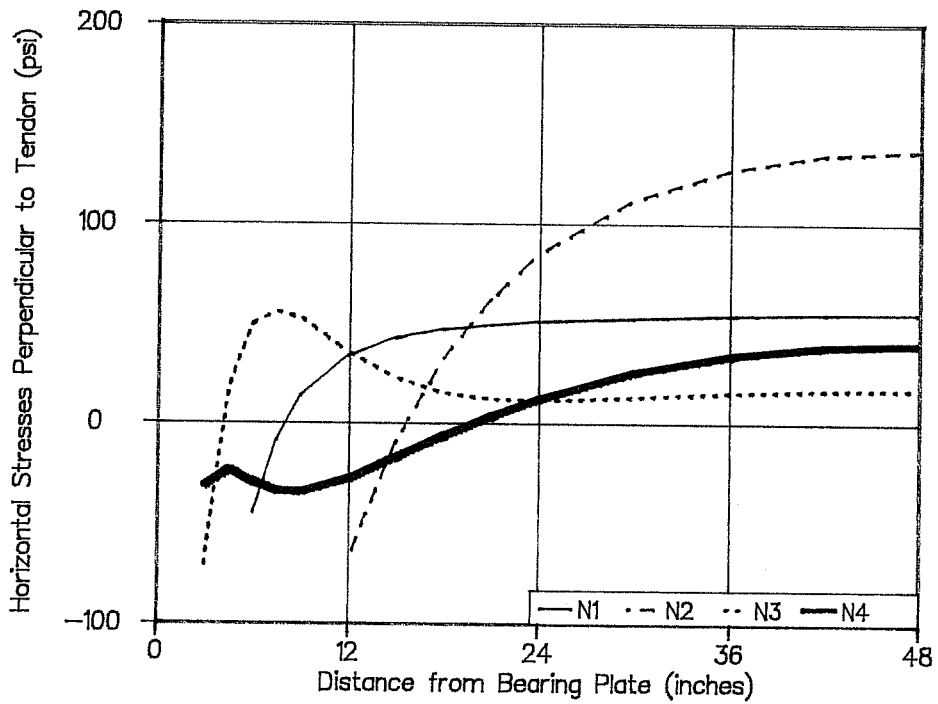
The smaller of the exterior anchor edge distance or the anchor spacing determines if the anchors will behave as one large anchor or as separate anchors. If twice the smallest edge distance is greater than the center-to-center spacing, the anchors act as one edge load. If twice the smallest edge distance is equal to or less than the center-to-center spacing, the anchors act as individual anchors on the slab edge.

Figures 2.4 through 2.6 present the finite element analysis estimates of stresses across tendon paths in a test bridge deck due to maximum tendon jacking forces ($0.8f_{pu}$) on anchors. The three figures demonstrate the stresses due to loading interior anchors, exterior anchors, and various series of anchors.

Figure 2.4 shows the bursting stresses ahead of an interior anchor as the adjacent anchor loading is changed. Loading of a single interior anchor and loading of three consecutive interior anchors (Loading Configurations N1 and N2) produced a similar horizontal bursting stress distribution but the magnitude of the maximum stress for the three loaded anchors (136 psi) was about three times larger than the single interior anchor's maximum stress



(a) Load Configurations - (Dashed Lines Indicate where Bursting Stresses are Plotted in Figure 2.4b)



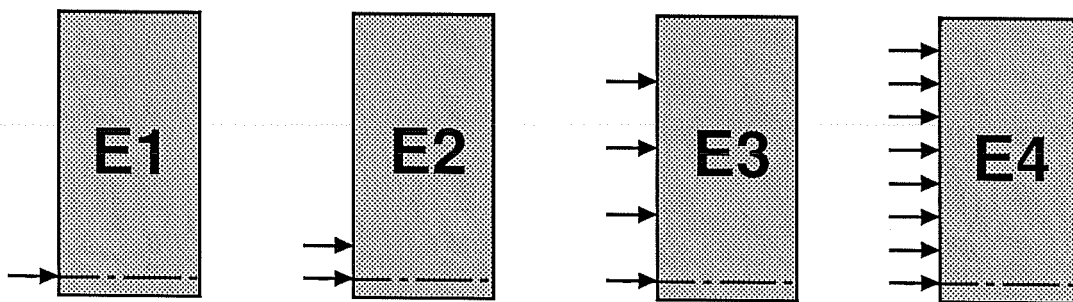
(b) Bursting Stress Ahead of the Anchor

Figure 2.4 - Interior Anchor Horizontal Bursting Stresses

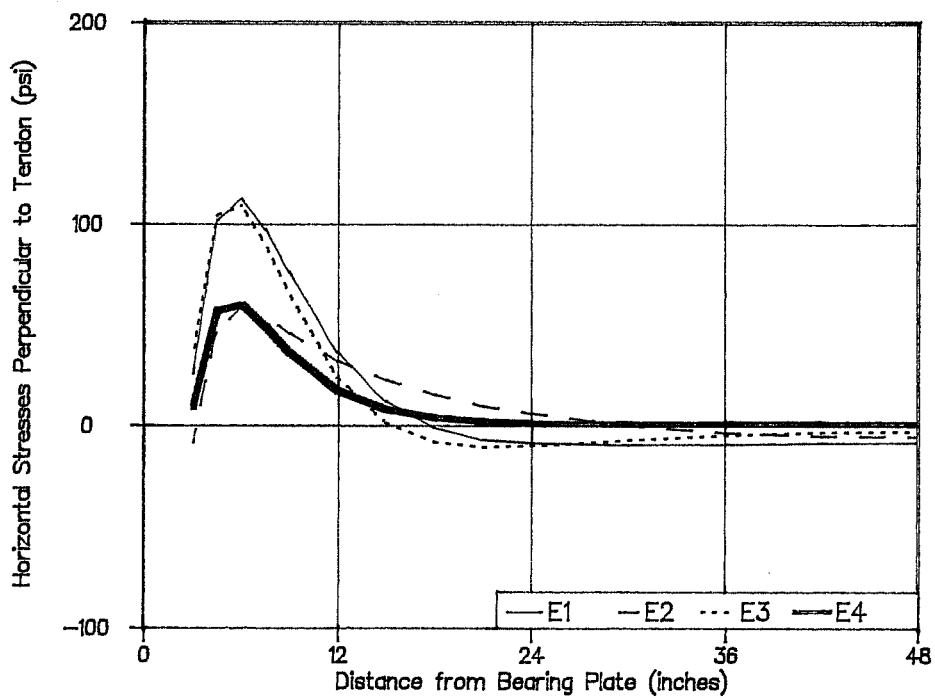
(55 psi). This supports the principal stress distribution (Figure 2.2c) that shows loads on closely spaced interior anchors behaving like load on one large anchor. When load was applied to alternate anchors (Loading Configuration N3), the bursting stress ahead of the interior anchor was concentrated closer to the anchor as shown in Figure 2.3c. Finally, loading of all the edge anchors (Loading Configuration N4) produced the lowest bursting stresses ahead of the interior anchor because that is similar to uniformly loading the slab's edge. Uniform loading produces no bursting stresses.

Horizontal bursting stresses ahead of the exterior anchor are shown in Figure 2.5. The most dramatic change in the horizontal bursting stresses ahead of the loaded exterior anchor are caused by loading of the first adjacent anchor (Loading Configuration E2). In fact, the maximum horizontal bursting stress is cut almost in half from 112 psi to 58 psi. Loading alternate anchors (Loading Configuration E3) was similar to loading just the exterior anchor, and loading of all the anchors (Loading Configuration E4) produces little change in the bursting stresses ahead of the loaded exterior anchor after the first adjacent anchor is loaded; therefore, the only way to reduce the horizontal bursting stresses ahead of an exterior anchor is to load the first adjacent anchor.

Figure 2.6 shows the horizontal bursting stresses ahead of the exterior anchor of a series of loaded anchors. This also demonstrates the horizontal bursting stresses ahead of an exterior anchor with different edge distances. Loading configurations A and B produce horizontal bursting stress distributions like an exterior anchor which are concentrated close to the edge. Loading configurations C and D produce horizontal bursting stress distributions which are concentrated at the slab's mid-section like an interior anchor. The horizontal bursting stress is greater ahead of the exterior anchor of the three loaded adjacent interior anchors

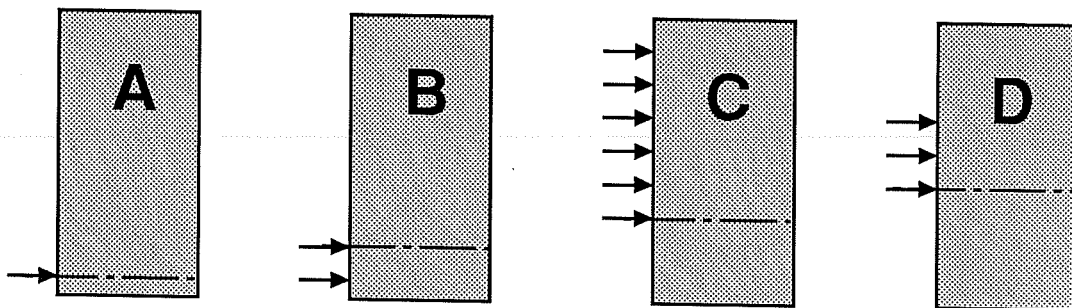


(a) Load Configurations - (Dashed Lines Indicate where Bursting Stresses are Plotted in Figure 2.5b)

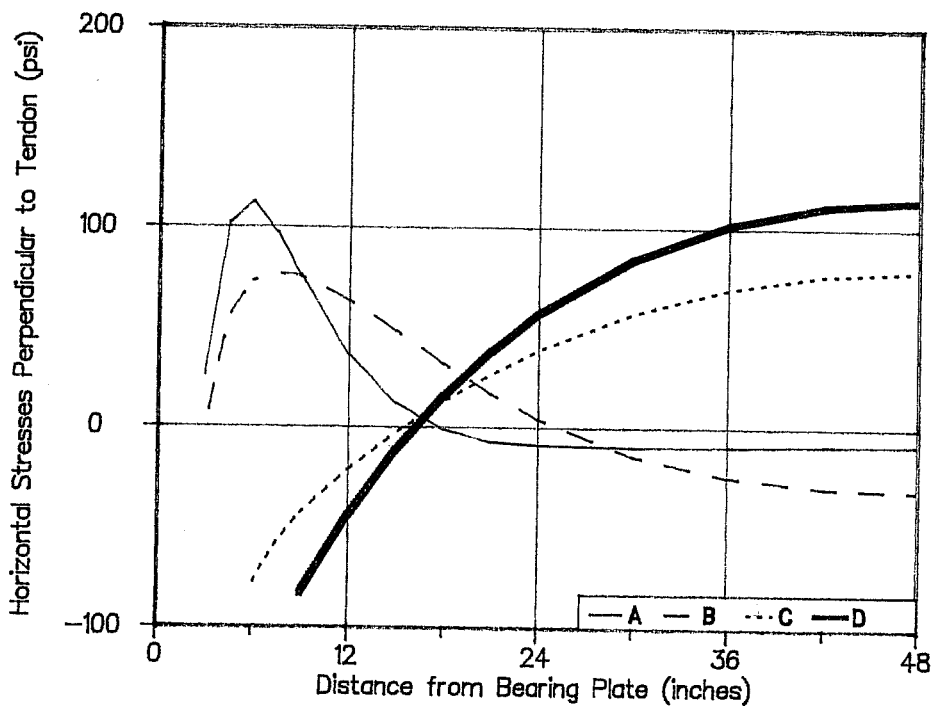


(b) Bursting Stress Ahead of the Anchor

Figure 2.5 - Exterior Anchor Horizontal Bursting Stresses



(a) Load Configurations - (Dashed Line Indicates where Bursting Stresses are Plotted in Figure 2.6b)



(b) Bursting Stress Ahead of Anchor

Figure 2.6 - Leading Loaded Anchor Horizontal Bursting Stresses

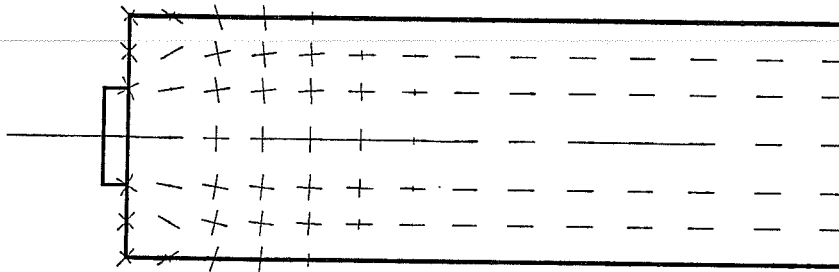
(114 psi) than ahead of the exterior anchor of the six loaded adjacent anchors (80 psi).

When stressing a post-tensioned slab, only one tendon set is usually being stressed at a given time. Anchors are loaded one at a time on the bridge deck edge, and only one anchor can be critically overloaded. The linear analysis prediction of the increase in stress due to overloading of a single anchor is identical to the stress predicted due to loading of only that anchor; therefore, stresses due to the loading of a single anchor should be used to predict stresses due to overloading. Stresses developed due to loading of multiple anchors should be added to the additional stresses due to overload of an individual anchor to predict failure during a stressing sequence. The highest horizontal plane bursting stress occurring during loading of a single anchor was predicted to be 113 psi ahead of the loaded exterior anchor which is shown in Figure 2.5 -Load Configuration E1.

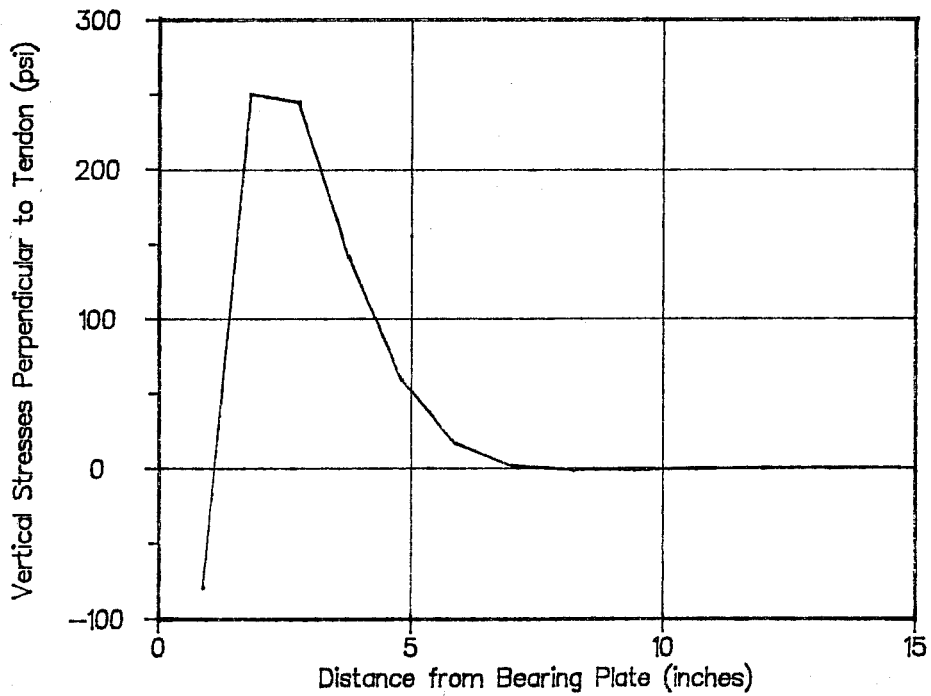
The interaction of interior anchors shown in Figure 2.3(b) is also evident in the bursting stress distribution below the center anchor. Figure 2.4 shows the increase in stress below the center anchor when service loads are applied to the adjacent anchorages. The maximum stress at the centerline raises from 55 psi to 136 psi when the two loads are added; therefore, the stress was approximately tripled with the tripled load.

2.2.3 Vertical Plane Analysis

Vertical plane stresses (Figure 2.7) were considered to be a localized effect. The computer model only represented the section of the slab directly ahead of the anchor; therefore, effects of sequenced stressing or adjacent anchor loading are not considered in the vertical plane analysis. All of the vertical plane stresses were assumed to be dispersed directly ahead of the anchor across



(a) Vertical Plane Principal Stress Trajectories Ahead of a Loaded Anchor - (Bursting Stresses are Taken across the Center-line and Plotted in Figure 2.7b)



(b) Bursting Stresses Ahead of Anchor

Figure 2.7 - Vertical Plane Bursting Stresses

it's 6" width. The calculated stresses are across the tendon path and due to maximum tendon jacking force ($0.8f_{pu}$) on the anchor.

Figure 2.7 shows both the principal stress trajectories in the cross section and the bursting stress distribution across the center of the cross section. The vertical plane bursting stresses were concentrated close to the anchor. The maximum vertical plane bursting stress under service loads was predicted to be 249 psi. This is the highest bursting stress in either plane created from loading any or all of the anchors.

2.2.4 Predicted First Cracking and Ultimate Failure

The following equation predicts the tensile strength of concrete².

$$f_t = [w(f_c)]^{\frac{1}{2}}$$

f_t = tensile strength of concrete (psi)

w = weight of concrete (pcf)

f_c = compressive strength of concrete (psi)

Concrete with a compressive strength of 4000 psi and a weight of 150 has a predicted tensile strength of 258 psi. The largest horizontal plane bursting stress predicted ahead of an anchor by the finite element analysis was 136 psi for the loading of three adjacent anchors to service load levels (Figure 2.4 - Load Configuration N2); therefore, overloading would be necessary to cause failure of anchorage zones due to horizontal plane stresses.

The maximum vertical plane bursting stress was estimated as greater than any horizontal plane bursting stress, and it is directly related to overloading because it applies to the loading of only one anchor regardless of adjacent loads. A maximum 249 psi

vertical bursting stress is estimated for a 35 kip anchor load. The linear analysis predicts a first cracking load of 36 kips for a half-scale four-strand anchor in a 5 inch thick anchorage zone made with 4000 psi compressive strength concrete. Predicted first cracking loads are provided for specific tested anchorage zones in Section 5.3.

It is suggested by Burdet⁵ that the ultimate load of a post-tensioning anchorage can be estimated by checking the compressive stress at the interface between the local and general zones. When the maximum compressive stress at that interface reaches 75% of the anchorage zones concrete compressive strength ($0.75f'_c$), failure is predicted. The compressive stresses from the vertical plane analysis are highest in this study and should be used to predict failure.

Burdet also assumes, based on typical anchorage zone reinforcement, that the depth of the local zone can be estimated as equal to the maximum lateral dimension of the anchor. For a 2 inch by 6 inch horizontal anchor plate in a 5 inch thick slab (as was used in the experimental program), the maximum compressive stress 6 inches ahead of the anchor with a 35 kip tendon load is 1404 psi. If the anchorage zone concrete compressive strength is 4000 psi, the maximum compressive stress at failure is estimated as 3000 psi and the ultimate failure load is predicted to be 74.8 kips. Predicted ultimate failure loads for the specific tested anchorage zones are provided in Section 5.3.

2.3 Strut-and-Tie Modeling

2.3.1 General

Strut-and-tie models are used to predict the lower bound failure loads of reinforced concrete structures. Strut-and-tie models predict failure loads from either tension cracking of the concrete followed by yielding of the ties, compression failure of

a concrete strut, or destruction of a node. Using a strut-and-tie model, the designer tries to predict the failure mode of a structural element. Linear-elastic finite element analysis can be used to develop strut-and-tie models according to analytical stress distributions. Strut-and-tie models represent failure modes and can vary from the undeformed linear-elastic analysis stress distributions. Many reasonable models can be used for the same applications. They all would represent lower bounds or conservative estimates of load carrying capacity; therefore, any could be used safely.

The strut-and-tie models developed in this section are based on the resultant boundary forces and principal stress trajectories predicted by the finite element analysis. Use of such models usually results in improved crack control at service load levels¹⁴. Some general rules were also applied to the development of the strut-and-tie models in order to better model the elastic stress patterns. The depth of the bursting tie was assumed as two-thirds of the lesser of twice the anchor's edge distance or its center-to-center anchor spacing. The strut-and-tie model detail directly ahead of anchors was always assumed to be the same (Figure 2.8).

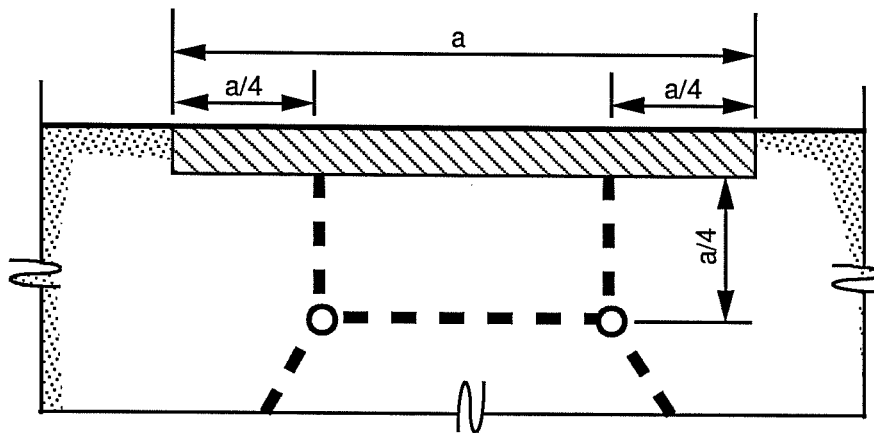


Figure 2.8 - Strut and Tie Model Ahead of Uniformly Loaded Anchor

In order to control local, compatibility induced effects next to anchor edges, spalling stress ties were placed beside all loaded anchors one and one-half inches from the slab's edge and were proportioned to carry at least 1% of the anchor load.

2.3.2 Horizontal Plane Analysis

An overview of the principal stress distribution in Figures 2.2 and 2.3 illustrates that there are four main horizontal stress distributions produced by the various loading patterns - only the exterior anchor loaded, only the interior anchor loaded, alternate anchors loaded, and all anchors loaded. Strut-and-tie models were developed to emulate these four load configurations.

The simplest models are for the single loaded interior anchor as presented in Figures 2.9 through 2.12. For the interior anchors, three models were developed to demonstrate the applicability of different models for the same element, namely the anchorage zone of a bridge deck post-tensioning edge anchor.

Figure 2.9 shows a strut-and-tie model based on linear elastic finite element analysis which matches external boundary conditions and internal principal stress distributions from elastic stress analysis. The two struts crossing the slab's mid-section were placed at the centroids of the computed compressive forces across the mid-section on each side of the loaded anchor. The ties between the two struts were placed at the centroid of the bursting stress for each half of the slab, and the tie force matches the computed linear-elastic finite element analysis horizontal bursting force. Those constraints provide the diagonal struts directly ahead of the anchor with approximately a 2:1 slope. Note that although the horizontal bursting ties carry a large force, they are far ahead of the anchor and there is plenty of space for reinforcement. The development of this model is based on the finite element solution,

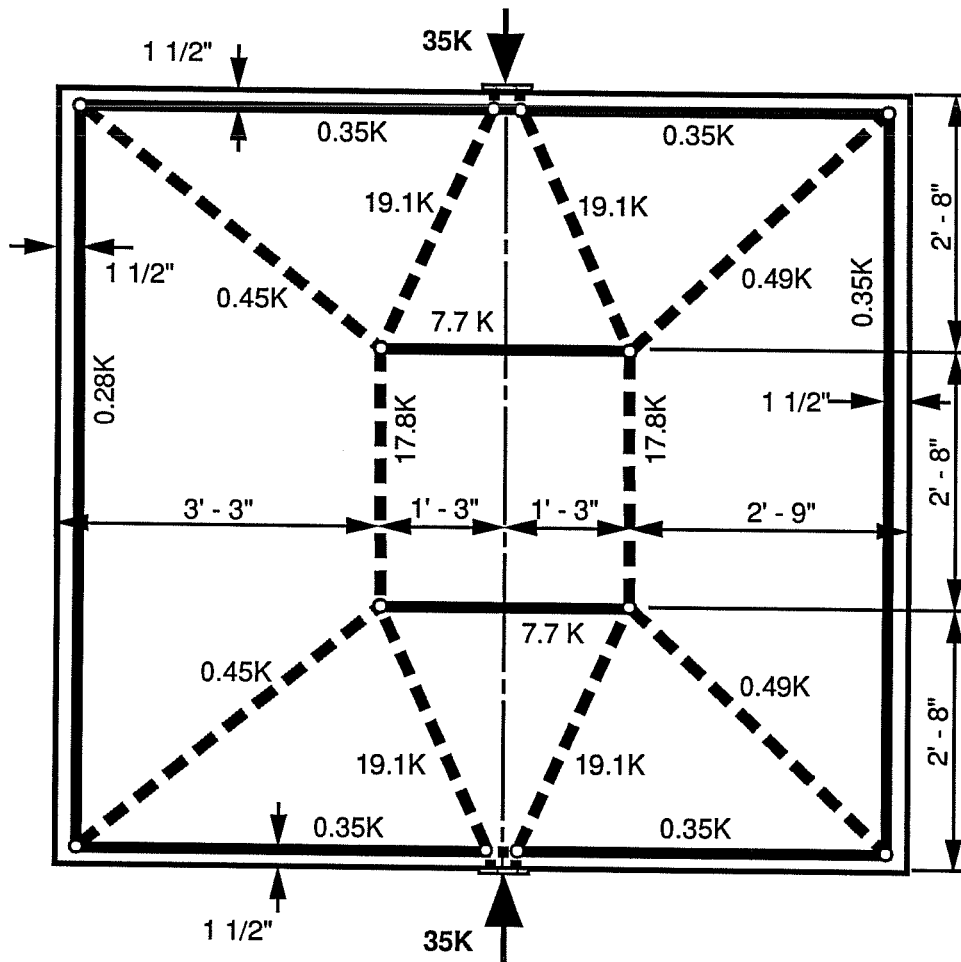


**Figure 2.9 - Horizontal Plane Strut-and-Tie Model #1 for Load on an Interior Anchor
(Based on Principle Stress Distribution at Cross-Sections)**

but the purpose of the strut-and-tie model is to design the anchorage zone without complicated analysis. Therefore, the remaining interior models were developed using the first as a comparison rather than a guide.

In Figure 2.10, a much simpler strut-and-tie model was designed making two major assumptions. Spalling forces are assumed to be either non-existent or negligible. The post-tensioning load is assumed to become evenly distributed across the slab's mid-

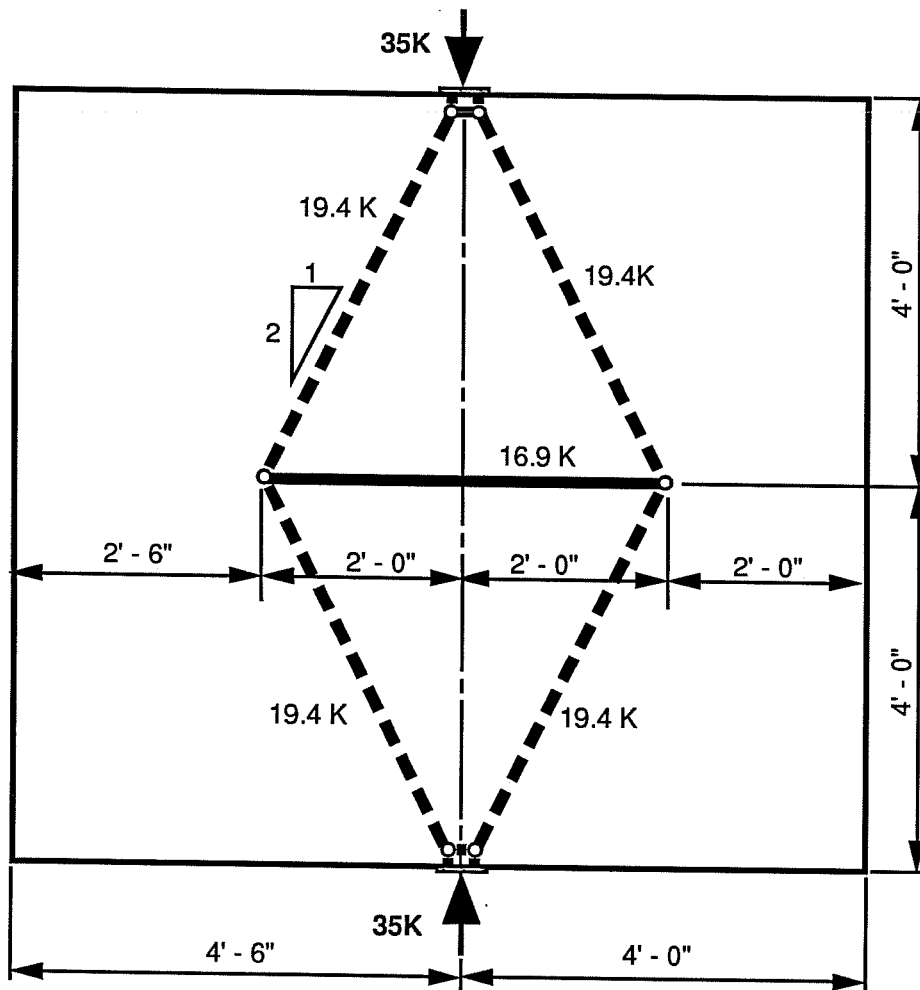


**Figure 2.10 - Horizontal Plane Strut-and-Tie Model #2 for Loaded Interior Anchor
(Based on Even Load Distribution at Mid-Section)**

section. Those two assumptions allow the mid-section nodes to be placed close to the quarter points and the ties for spalling to be left out. Note that the single bursting tie carries 16.9 kips of force as opposed to the total of 15.4 kips carried by the two layers of bursting ties of the previous model. However, this simple model does not closely match the elastic distribution of the horizontal bursting stress region (Figure 2.4 - Load Configuration N1) which

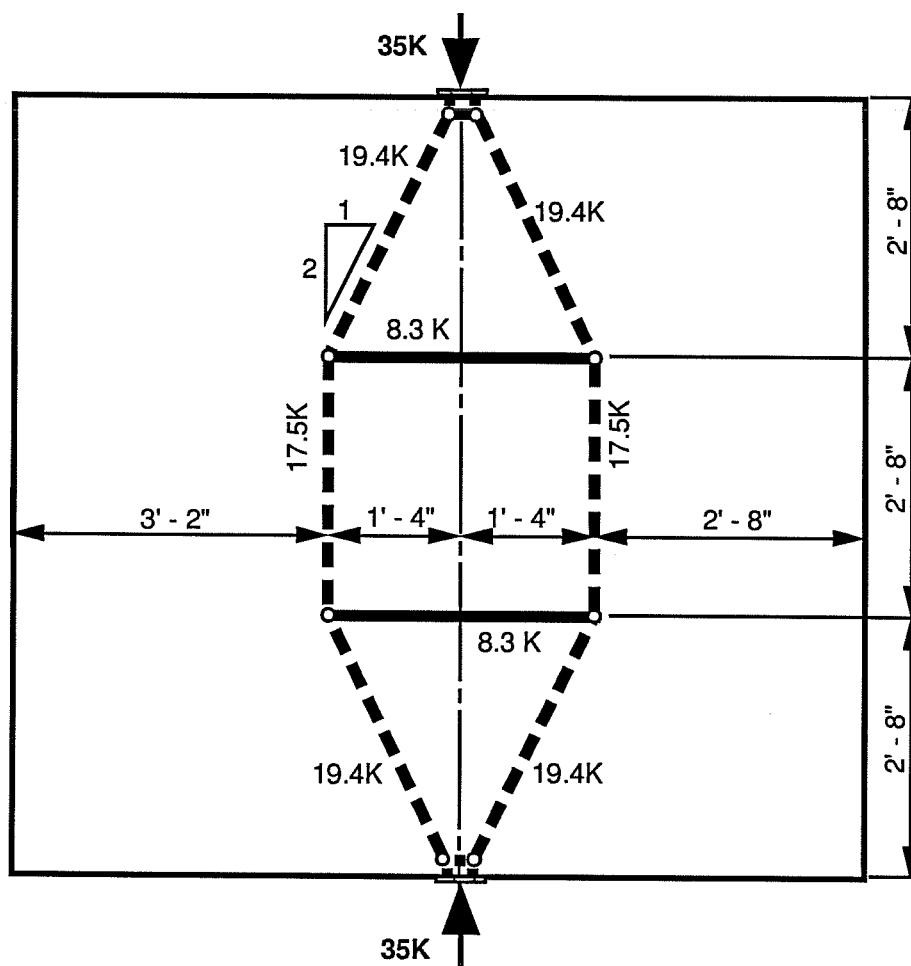


**Figure 2.11 - Horizontal Plane Strut-and-Tie Model #3 for Load on an Interior Anchor
(Struts Maintain 2:1 Slope With 2 Bursting Ties at One-Third Points)**

is centered at the mid-section but spread across most of the tendon's length.

Figure 2.11 shows an interior anchor strut-and-tie model which maintains the 2:1 slope of the diagonal struts in the previous model, but instead of having a single tie at the mid-section it has ties at the one-third points between the anchors. This model ignores spalling forces along the slab's edges, and assumes a concentration of post-tensioning compressive loads more towards the

center of the mid-section instead of an even distribution along the mid-section. The bursting ties in this model are located more like the pair of ties in the strut-and-tie model of Figure 2.9 which was based on the linear-elastic analysis. Their required capacity is higher at 8.3 kips (108%) instead of 7.7 kips. The most desirable quality of the model in Figure 2.11 over the one in Figure 2.10 is the dispersion of the bursting ties which indicate that bursting reinforcement should be spread across a broad range rather than concentrated at the middle.

In Figure 2.12 another interior anchor strut-and-tie model is created based on some assumptions about the most effective region of anchor load dispersion in the slab. The slab is symmetric about its mid-section. The transverse deviation of compressive stress should stop well before the mid-section. The distribution region (D-Region) which is bounded by the mid-section, is approximately square and is shaded in Figure 2.12. Struts are placed at the quarter points of the D-Regions base because an evenly distributed load is assumed there, and the horizontal bursting tie is located at two-thirds the depth of the D-Region ahead of the anchor to halt the transverse deviation of the struts from the anchor. Last, spalling ties and the corresponding struts should be inserted. This model is very close to the model shown in Figure 2.9 which was based on the linear-elastic finite element stress distribution results, but was far easier to construct. The ties of this model carry 6.4 kips each, which is 83% of the force carried by the ties of the model of Figure 2.9.

The strut-and-tie model for a loaded exterior anchor is shown in Figure 2.13. This strut-and-tie model was constructed by matching the resultant boundary conditions and trying to emulate the general force paths shown in the finite element study (Figure 2.2b) including the high spalling forces. Spalling stresses are caused by continuity strains and are not usually critical because they are

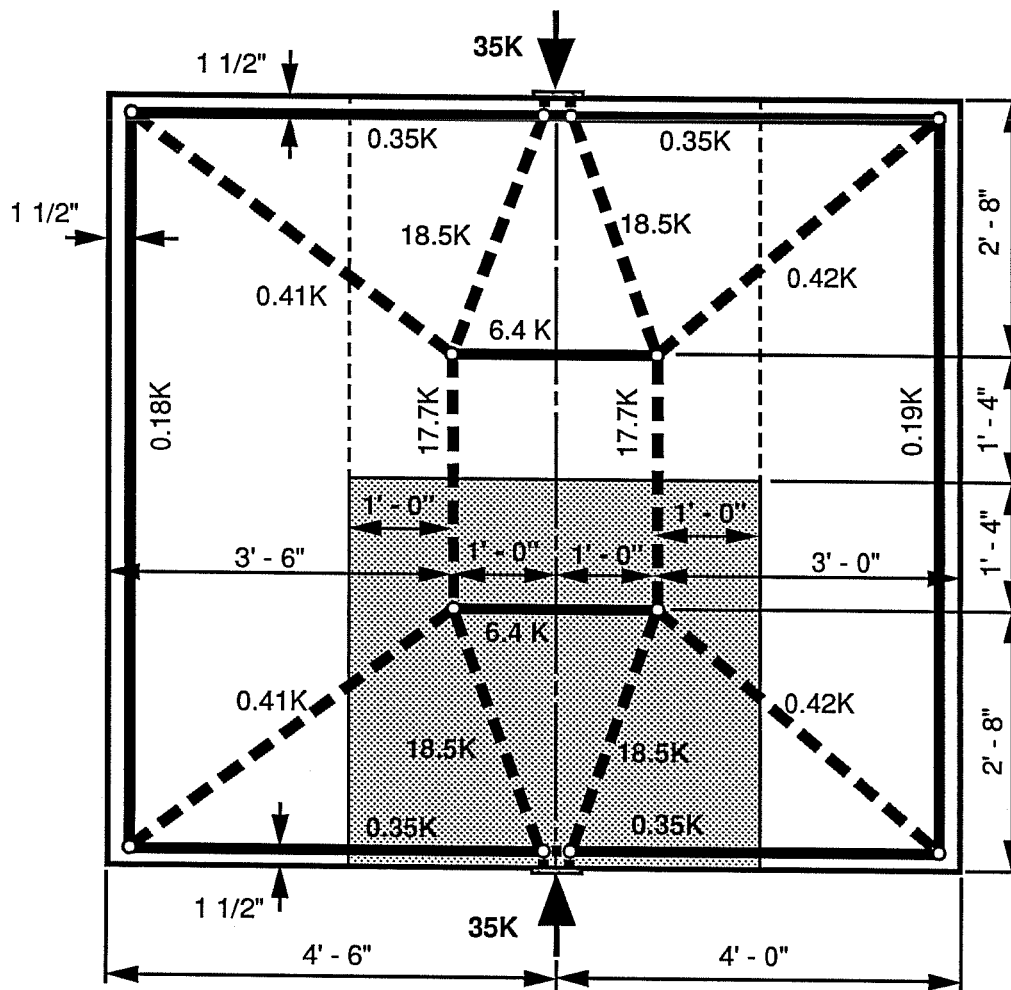


Figure 2.12 - Horizontal Plane Strut-and-Tie Model #4 for Load on an Interior Anchor
(Based on Distribution Limited to the D-Region which is shaded)

often dispersed through micro-cracking. However, with a highly eccentric anchor, tensile stresses can be set up on the far face and some reinforcement is required if concrete tensile strength is not to be depended upon. The bursting stress ahead of the exterior anchor is critical because the region is small, and in an actual slab reinforcing will need to be concentrated in the region of this tensile tie.

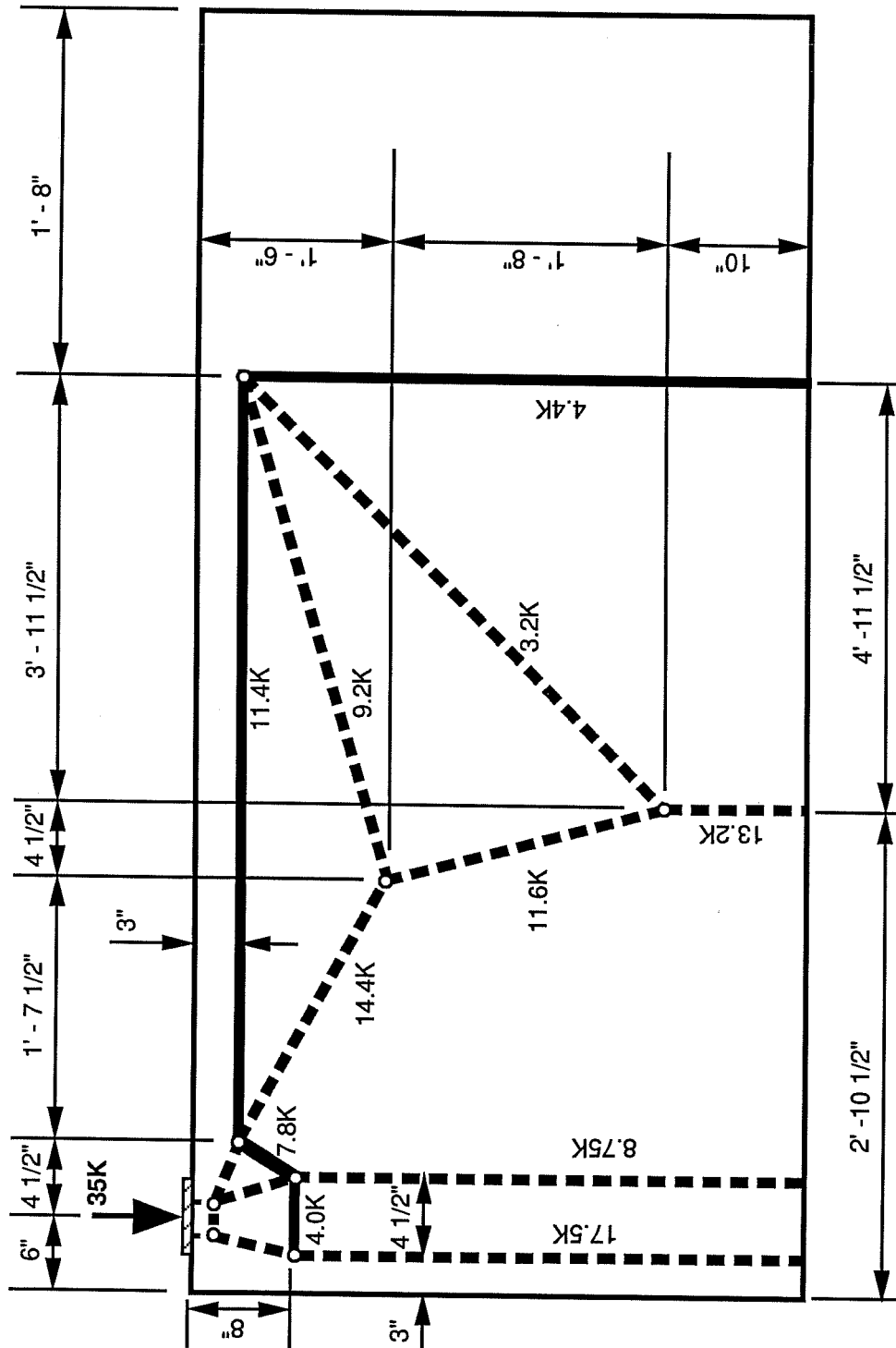


Figure 2.13 - Horizontal Plane Strut-and-Tie Model for Load on an End Anchor

In Figure 2.14, the strut-and-tie model for loaded alternate anchors has four separate bursting regions which are similar to the four separate bursting regions indicated by the finite element stress distribution. As in the exterior anchor model, a bursting tie is placed close to the exterior anchor. The other loaded anchors are assumed to have D-Regions based on their anchor spacing. Struts are placed at the quarter points of the D-Regions and run straight to the mid-section as a uniform load. Bursting ties are placed at two-thirds the depth of the D-Region. The diagonal compression struts have approximately a 2:1 slope.

Figure 2.15 shows a strut-and-tie model with all the anchors loaded (2 plate widths center-to-center). Review of the finite element analysis shows that loading close adjacent anchors reduces or negates bursting stresses immediately ahead of anchors (Figures 2.3 and 2.4). Notice that loading all the anchors is assumed to produce struts between anchors rather than ties below them as the finite element analysis indicates. The exterior anchors, however, develop their own bursting stress ties, and half the load of the exterior anchor is applied to that separate exterior anchor strut-and-tie model. The interior adjacent anchors are assumed to have D-Regions based on their spacing and develop distributed loads to the mid-section. The anchor to anchor struts were placed at two-thirds the depth of the D-Region. The exterior model places the outside vertical strut half-way to the slab's edge and the inside strut mirrors the outside strut.

2.3.3 Vertical Plane Analysis

In Figure 2.16 the vertical bursting forces are illustrated with the transverse strut-and-tie model. The magnitude of this force (5.3 kips / 35 kip anchor load) is not unusually large compared to the forces estimated by the horizontal models, but it

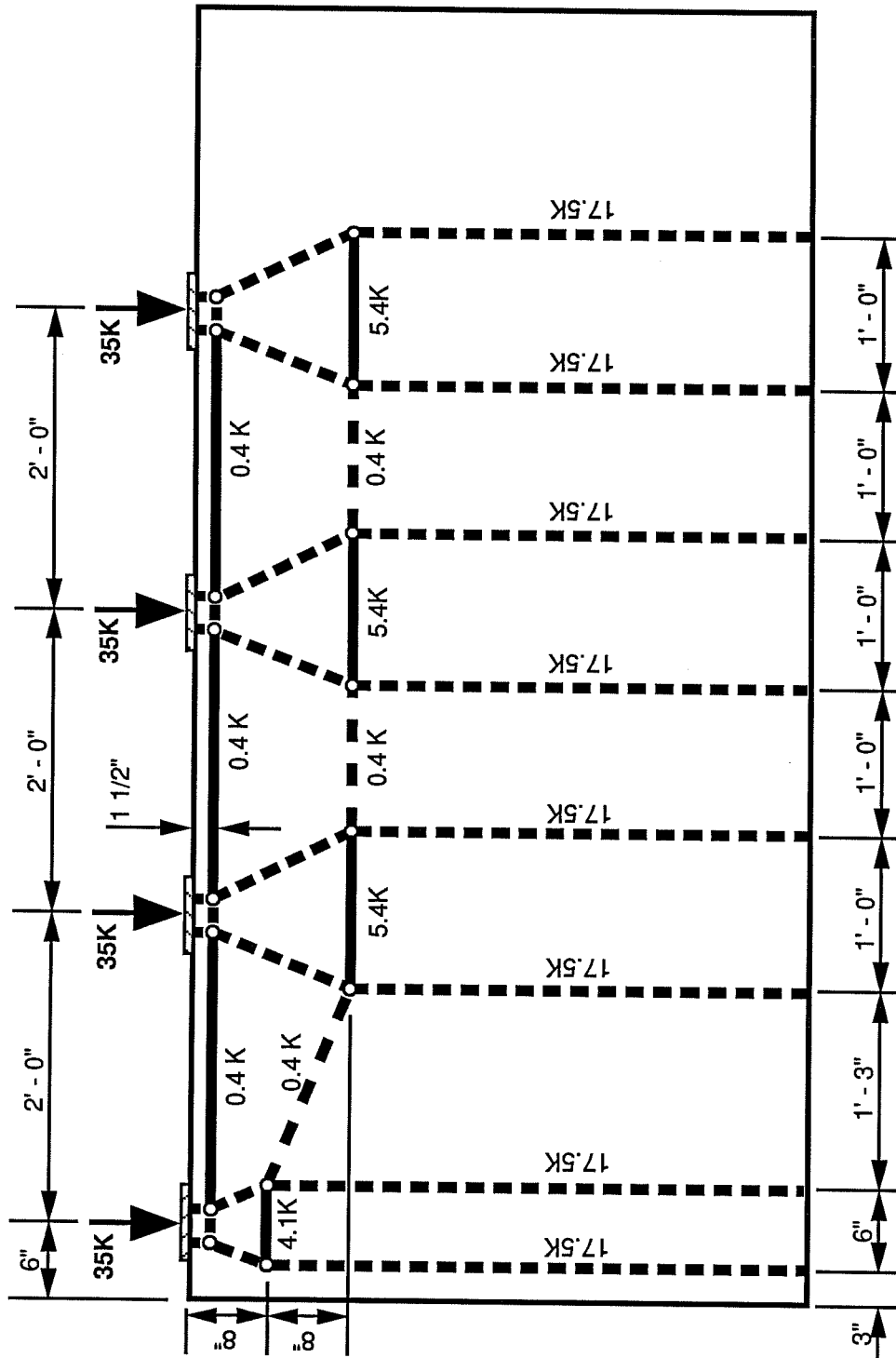


Figure 2.14 - Horizontal Plane Strut-and-Tie Model for Load on an Alternate Anchors

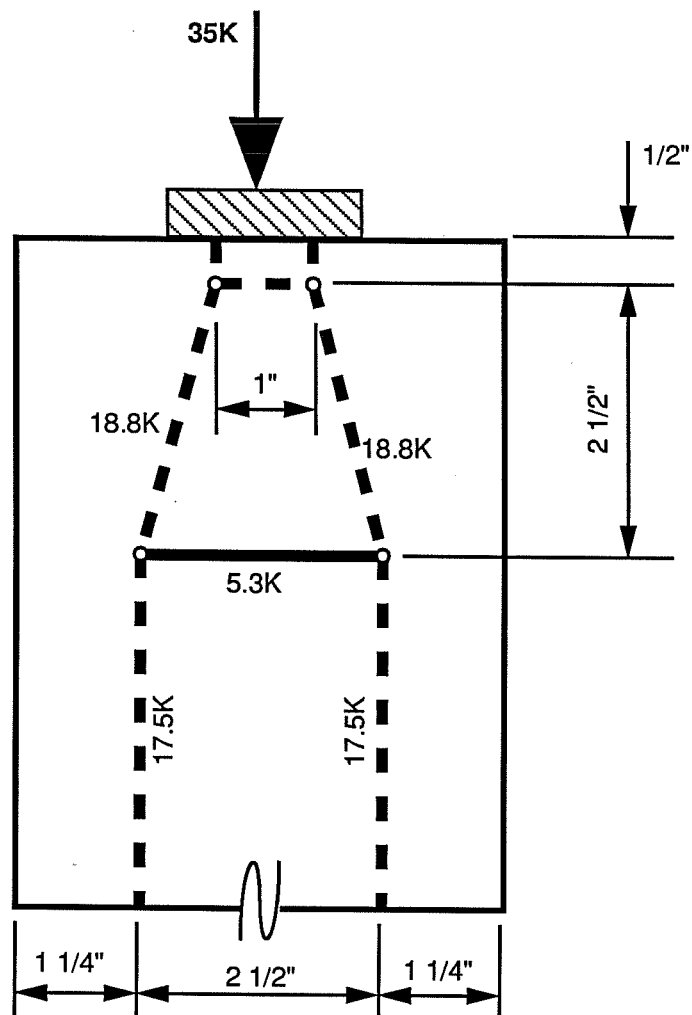


Figure 2.16 - Transverse Slab Plane Strut & Tie Model

is centered at only 3" from the slabs edge. In this confined region it will be difficult to place sufficient reinforcement to develop a tie.

2.3.4 Predicted Failure

Predicted failure from the strut-and-tie model is dependent on the strength of its components compared to the loads applied to each component under loading. The strength of the components were

calculated based on material strengths, anchorage zone geometry and assumed strut-and-tie models. Those strengths were applied to the vertical plane strut-and-tie model (Figure 2.16) which concentrates the highest loads in the smallest area.

Tie strength is easily evaluated because it depends only on the reinforcement yield strength. If two #2 Grade 60 reinforcing bars were placed vertically 3 inches ahead of the anchor with sufficient anchorage or development length, the tie failure would occur at a tendon stressing load of 39 kips (the sum of the two bars' yield strengths is 5.89 kips). From Section 2.2.4, first cracking of the concrete was estimated to be 60 kips which exceeds the strut-and-tie failure load; therefore, if first cracking transfers all the tie force to the reinforcement, this strut-and-tie model would fail at the concrete's first cracking. Transfer of vertical stress from the concrete to the reinforcing would yield the two bars. More vertical reinforcing would be required to increase the failure load beyond the first cracking load.

Contrary to the assumption that first cracking negates the effects of the concrete's tensile strength, concrete can continue to carry tension in uncracked regions and provide strength for the anchorage zone. Figure 2.17 shows that first cracking in the anchorage zone can possibly produce advantageous effects. Cracking which is in a limited region directly ahead of the anchor can redistribute concrete tensile stress to a position further ahead of the anchor. Further ahead of the anchor, smaller tension forces can support the anchor load or even a larger anchor load. The prediction of concrete tie failure is considered inaccurate, and depending on concrete tensile strength to transfer long term tie forces is unsafe.

Node failure at the anchorage was evaluated with the following equation¹¹.

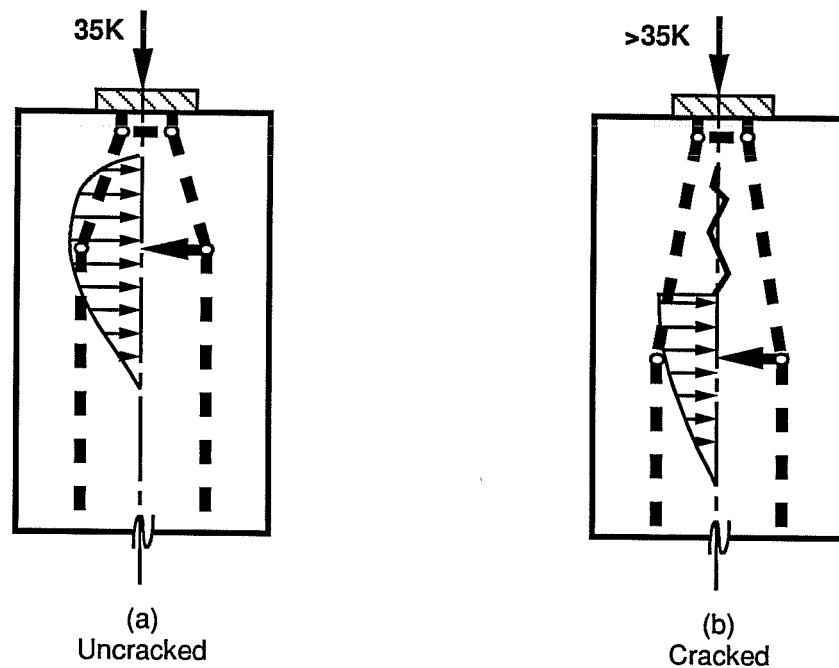


Figure 2.17 - Bursting Stresses Across the Section Ahead of the Anchor and the Corresponding Strut & Tie Model including the Concrete Tensile Strength's Contribution to the Tie

$$P_u = 0.7 f_{ci} \sqrt{\frac{A}{A_g}} (A_g) + 4.1 \left(\frac{2A_s f_y}{Ds} \right) \left(1 - \frac{s}{D} \right)^2 A_{co}$$

- P_u = predicted anchor-node failure load
 f_{ci} = concrete compressive strength
 A = maximum area of the portion of the concrete anchorage that is geometrically similar to and concentric with the area of the anchor plate
 A_g = gross area of the bearing plate.
 N = 2 if spiral confining reinforcement is used or 1 if orthogonal
 A_s = cross-sectional area of the bar used for confining reinforcement
 f_y = yield strength of the confinement reinforcement
 D = diameter or lateral dimension of the confining reinforcement
 s = spacing of confining reinforcement
 A_{co} = area of confined concrete

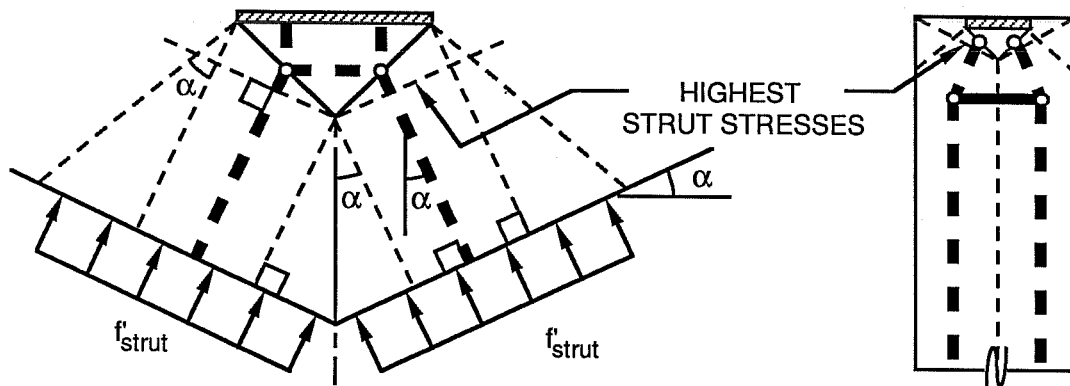


Figure 2.18 - Strut Modeling in the Anchorage Zone (The Highest Stresses are at the Strut-Node Interface where the Strut's Area is the Least)

The node failure equation reduces the allowable loads where closely spaced anchors are used and increases the allowable loads where confinement reinforcement is used. For an unconfined anchorage zone with 2"x 6" (10.65 in²) anchors spaced at two anchor widths center-to-center in 4000 psi concrete, the predicted node failure would be 68 kips.

Strut failure was computed in accordance with the "Proposed Post-tensioned Anchorage Zone Provisions for Inclusion in the AASHTO Bridge Specifications"⁴. Compressive stress is checked across the strut cross-section just below its connection with the anchor-node as shown in Figure 2.18. The compressive stress is limited to 70% of the concrete's compressive strength ($0.7f_{ci}$). In the vertical plane, for a strut with a 2:1 inclination ahead of a 2 inch by 6 inch horizontally oriented anchor in 4000 psi concrete, the predicted strut failure prediction is 54 kips.

The predicted failure of the strut-and-tie model for this bridge deck post-tensioned edge anchor would be yielding the

vertical tie, which is reinforcement, at 39 kips. Tie yielding would produce a ductile failure. However, the contribution of concrete tensile stresses could augment this failure load prediction.

Predicted failure loads for the tested anchorage zones are provided in Chapter 5.

Chapter 3 Experimental Program

3.1 General

In order to evaluate the effects of stressing sequence, anchor spacing, and edge distance on post-tensioning anchorage zones in bridge decks, six slabs with a total of 56 anchor pairs were tested. The anchorage zones incorporated monostrand and four-strand anchors, different edge distances and spacings, and a variety of reinforcing details. The specimens were to be loaded to standard post-

ten-
dur

lab

3.2

3.2

dec

*Original photo in
NCHRP 10-29 Final
Report, Fig. 160*

idge
.2)

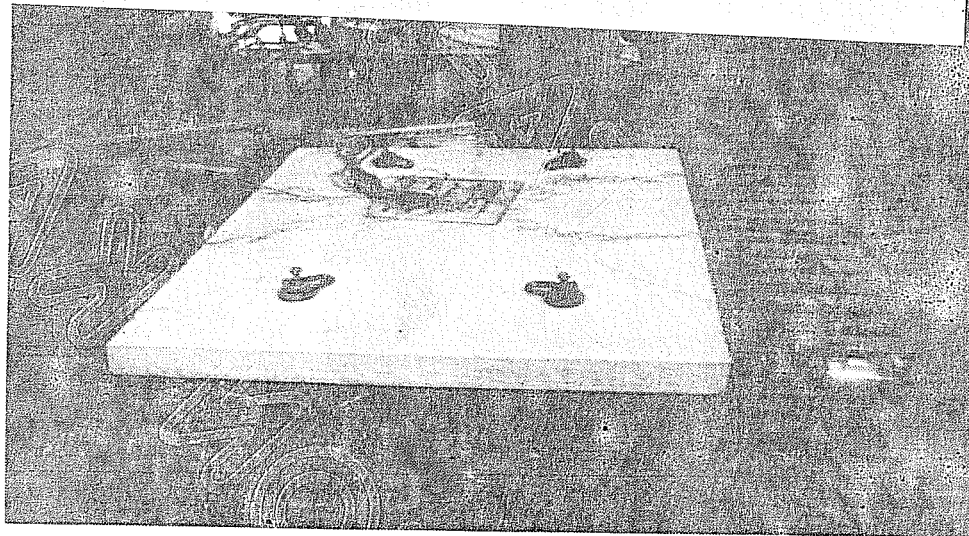


Figure 3.1 - Slab #3 During Testing

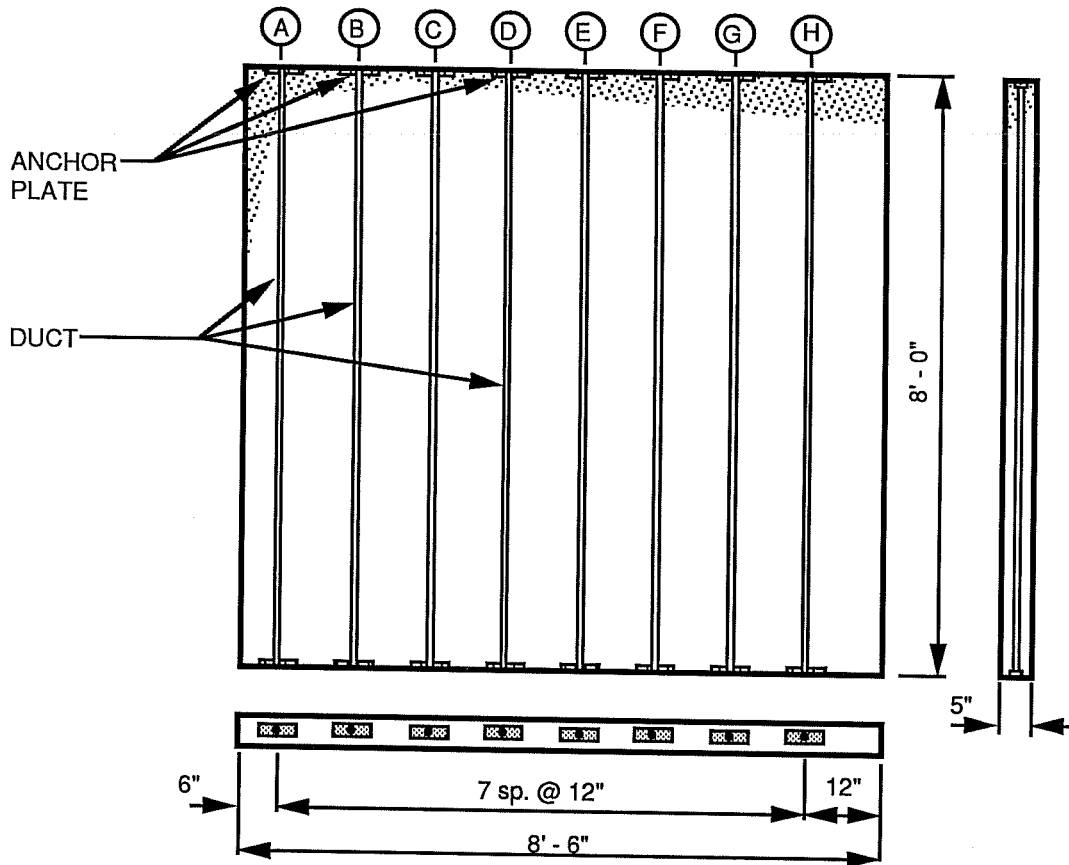


Figure 3.2 - Representative Half-Scale Slab

and the sixth slab was built at full-scale. The slabs incorporated various geometric properties and reinforcing details which are outlined in Table 3.1. The geometric properties were varied. They included the modeling of three different anchor sizes, three different edge distances, inclined tendons, and both initially cracked and initially uncracked anchorage zones. The reinforcing details included the use of back-up bars, hair pins, cross ties, and spirals in the anchorage zone (Figure 3.6).

For detailed plans of each slab's geometry and reinforcement, refer to Chapter 4.

Table 3.1 – Physical Properties of the Experimental Program

Scales

Half-Scale (5 slabs)

Full-Scale (1 slab)

Anchor Types Modeled

4" x 12" Four Strand Anchor (40 Anchor Pairs)

4" x 10" Four Strand Anchor (8 Anchor Pairs)

2" x 5" Mono Strand Anchor (8 Anchor Pairs)

Anchor Orientations

Horizontal (48 Anchor Pairs)

Vertical (8 Anchor Pairs)

Edge Distances

1/2 Plate Width (1 Anchor Pair)

1 Plate Width (9 Anchor Pairs)

2 Plate Width (2 Anchor Pairs)

Tendon Orientation

Perpendicular (48 Anchor Pairs)

Inclined (8 Anchor Pairs)

Slab Condition

Concrete Initially Uncracked (5 Slabs)

Cracks in Anchorage Zone Before Loading
(1 Slab – 3 Anchor Pairs)Reinforcing Details

Unreinforced (20 Anchors)

Horizontal Reinforcing (12 Anchors)

Anchorage Zone Reinforcement

Back-up Bars (6 Anchors)

Hairpins (8 Anchors)

Cross Ties (14 Anchors)

Spiral (8 Anchors)

Hoops (2 Anchors)

Hairpins tied into a Hoop (2 Anchors)

Control Detail (40 Anchors)

Steel electrical conduit was used for the post-tensioning ducts of the slabs. The conduit had 1/16" wall thickness and an inside diameter of either 1" or 1 3/8" depending on the size of the post-tensioning bar used to load the corresponding anchor pair.

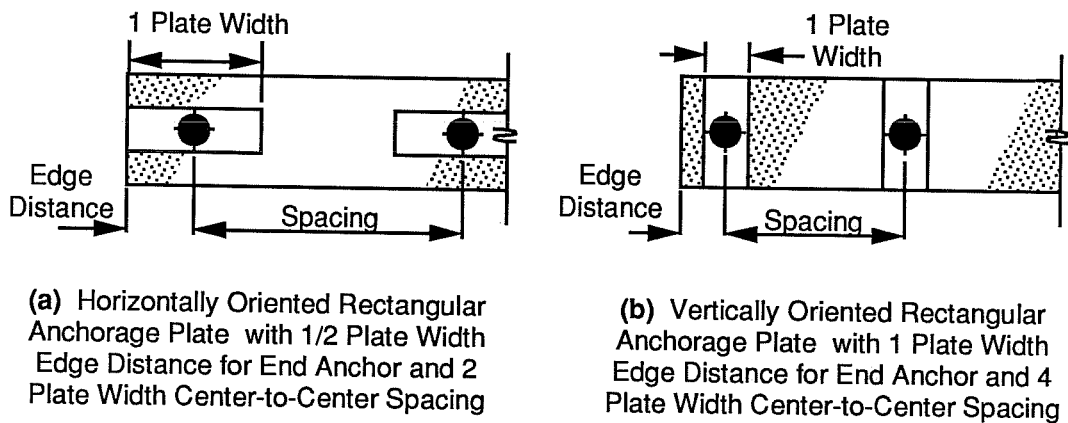


Figure 3.3 - Anchor Orientation, Edge Distance, and Spacing

3.2.2 Anchors and Spacing

Three sizes of rectangular post-tensioning anchor plates were used at two orientations – horizontal and vertical. Anchor spacings and end anchor edge distances were varied (Figure 3.3). 8 of the 56 anchorage zones tested incorporated vertically oriented plates. Anchors were spaced at two or four plate widths center-to-center distance, and the edge distance varied from 1/2 an anchor width to 2 anchor widths.

Steel plates of 2" x 6" x 1/2" and 2" x 5" x 1/2" were used to model commercial anchors. Those dimensions represent both four strand rectangular anchors at half-scale and monostrand anchors at full scale. 48 pairs of the anchorage zones were half-scale four strand anchor models, and eight pairs were monostrand full scale anchorage zones. The vertically oriented anchors modelled four-strand anchors.

All horizontally oriented anchors were spaced at 2 plate widths center to center. The vertically oriented plates were placed at 4 anchor widths center to center. Of the 12 end anchors, 2 had an edge distance of 2 plate widths, and one had an edge distance of

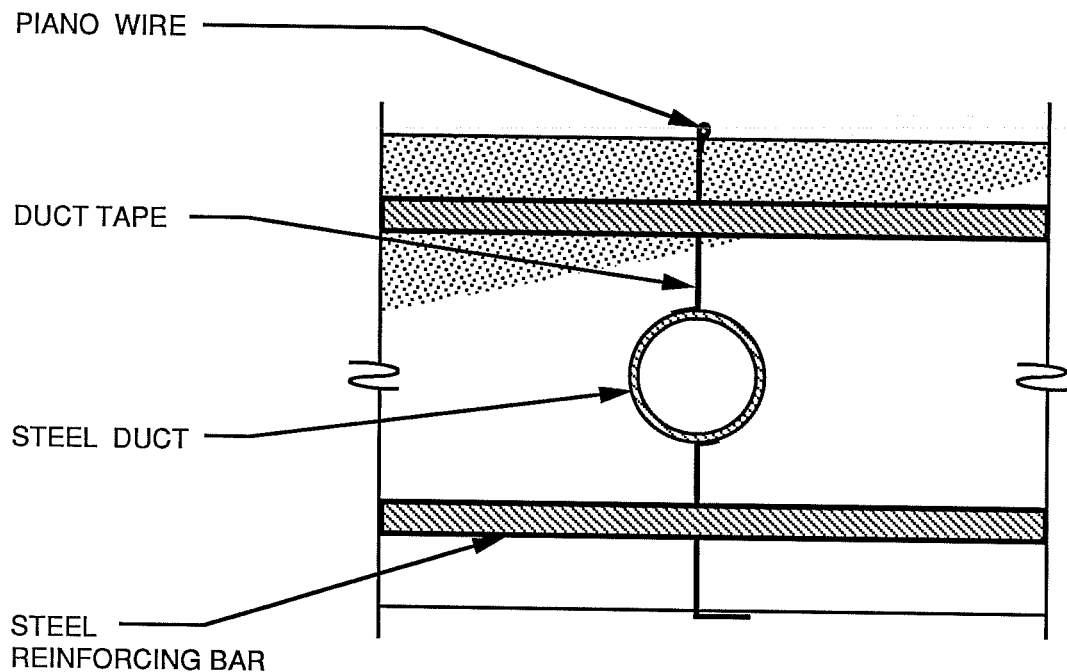


**Figure 3.4 - Pre-Formed Crack in Slab #2
(Anchorage Zones A, C, H)**

1/2 a plate width. The other 9 end anchors had a 1 plate width edge distance.

3.2.3 Preformed Vertical Cracks

In the second slab constructed, cracks were preformed ahead of anchors A, C, & H to negate the effects of concrete tensile strength in the horizontal plane during sequenced stressing. The cracks were formed by affixing duct tape above and below the steel ducts (Figure 3.4). At the top of the slab, the duct tape had been wrapped over taugth piano wire. At the bottom of the slab, the duct tape was affixed to the formwork.

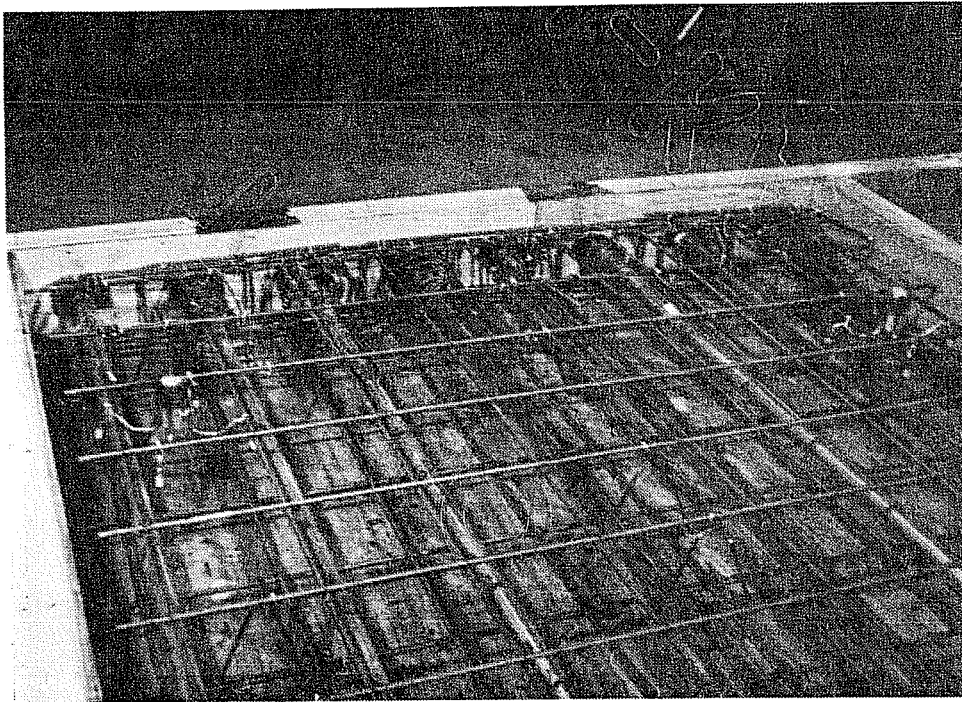


Figure 3.5. Horizontal Steel in Slab #6

3.2.

steel

(Fig

unre

rein

con:

AAS:

(#2

for full scale).

*Original photo in NCHRP
Final Report, Fig. 162*

tal
ads

l -
ure

abs

d by

tion

nter

A variety of anchorage zone reinforcing details were used in fabrication of the slabs (Fig 3.6). The details were picked because they were either common or easily constructed. Some details such as back-up bars, hairpins, and spirals were considered standard

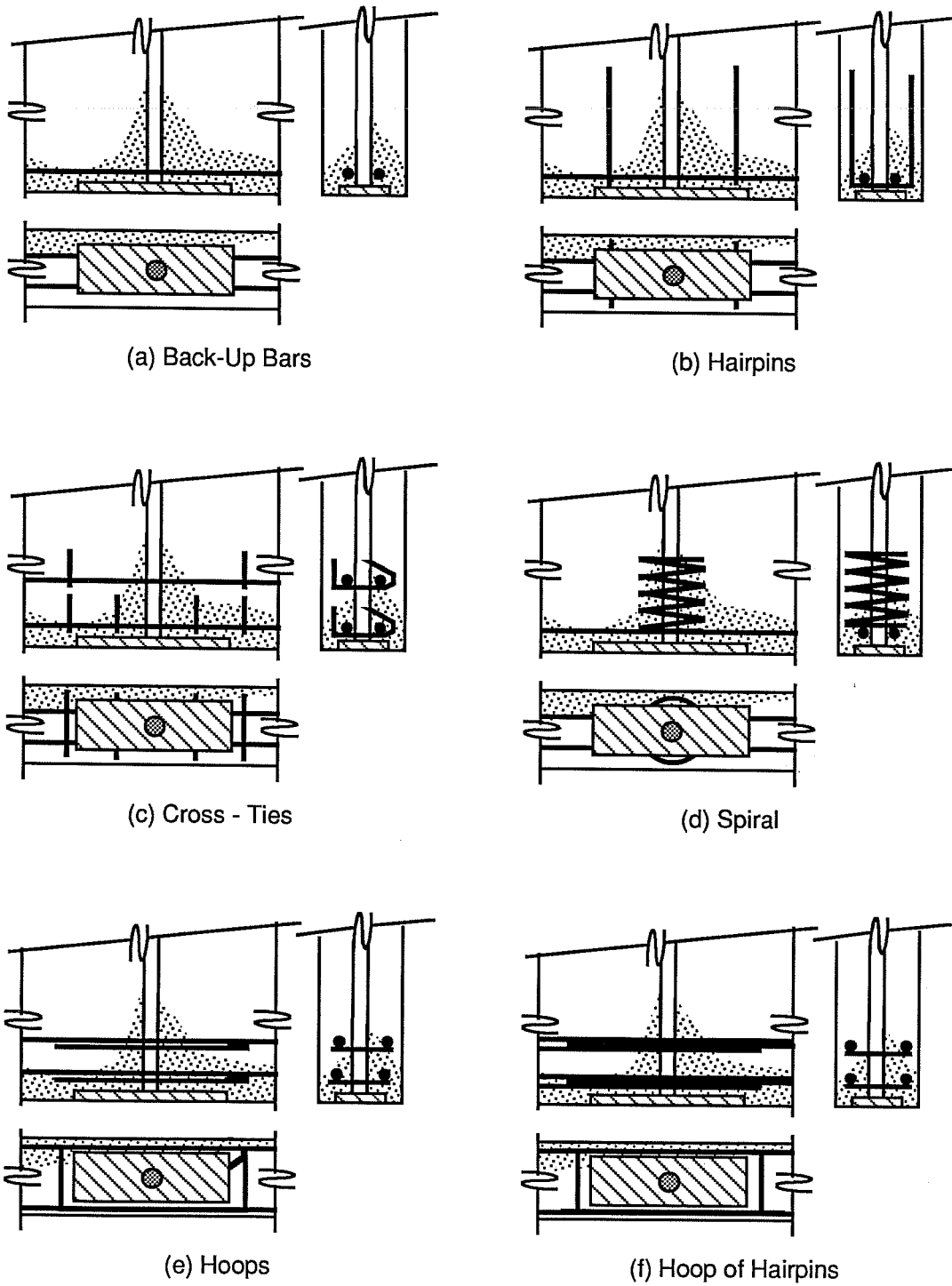


Figure 3.6 - Anchorage Zone Reinforcing Details

anchorage zone reinforcement. Details such as cross ties or a pair of hairpins tied into a hoop were considered easy to construct and efficient anchorage zone reinforcement. Unreinforced anchorage zones were used as a control group for evaluation of anchorage zone reinforcement in general.

Also, each duct had anchorage zones at both ends. To force failure to occur on a desired reinforcing detail, a heavily reinforced control detail, combining a spiral and two hair pins tied into a hoop, was placed at one anchorage zone of each duct (Figure 3.7).

3.3 Instrumentation and Loading Systems

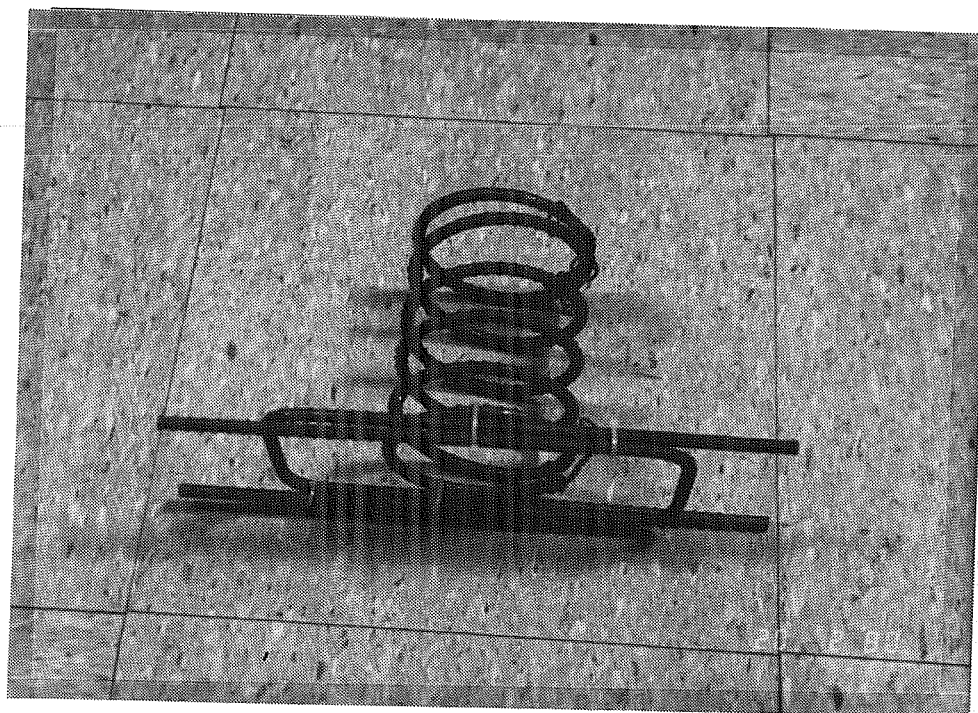
3.3.1 General

During slab testing concrete strains, reinforcing steel strains, cracking loads, and failure loads were recorded. Concrete strains were measured by embedded strain gages. Reinforcement strains were measured with foil strain gages affixed to the reinforcement. Cracking and failure loads were measured with pressure transducers monitoring the hydraulic loading system.

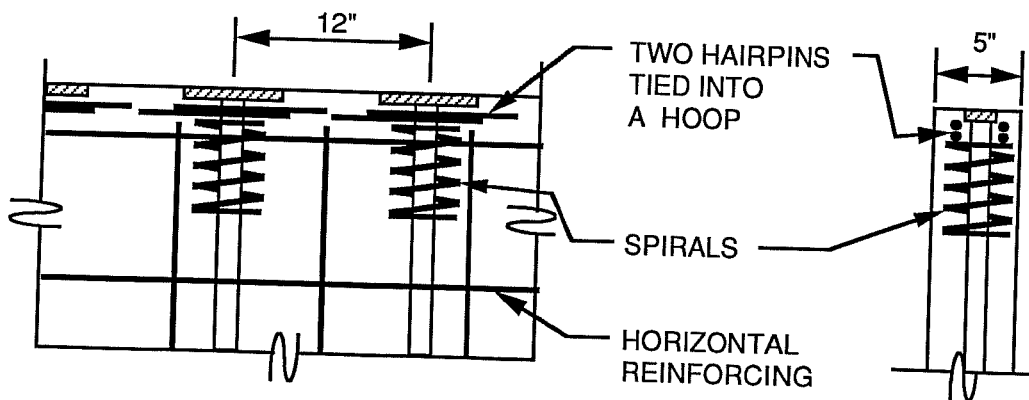
Loading was achieved by tensioning threaded post-tensioning bars or steel strands which were passed through each duct and anchored against each duct's plates. Hydraulic rams tensioned the bars individually emulating jacking forces and seating forces upon each bars corresponding anchors. The anchors were loaded one by one in stressing sequences to produce large horizontal plane stresses in Slabs #1 through #3. After all anchors were loaded to a standard post-tensioning load of 30 kips ($0.70 f_{pu}$), each pair of anchors were loaded until anchorage zone failure occurred.

3.3.2 Embedded Strain Gages

Concrete strains in the unreinforced slabs were measured with embedded strain gages. An embedded strain gage consists of a gaged



(a) Reinforcement Configuration of Control Detail



(b) Diagram of Control Detail

Figure 3.7 - Control Detail (Heavily Reinforced Anchorage Zone)

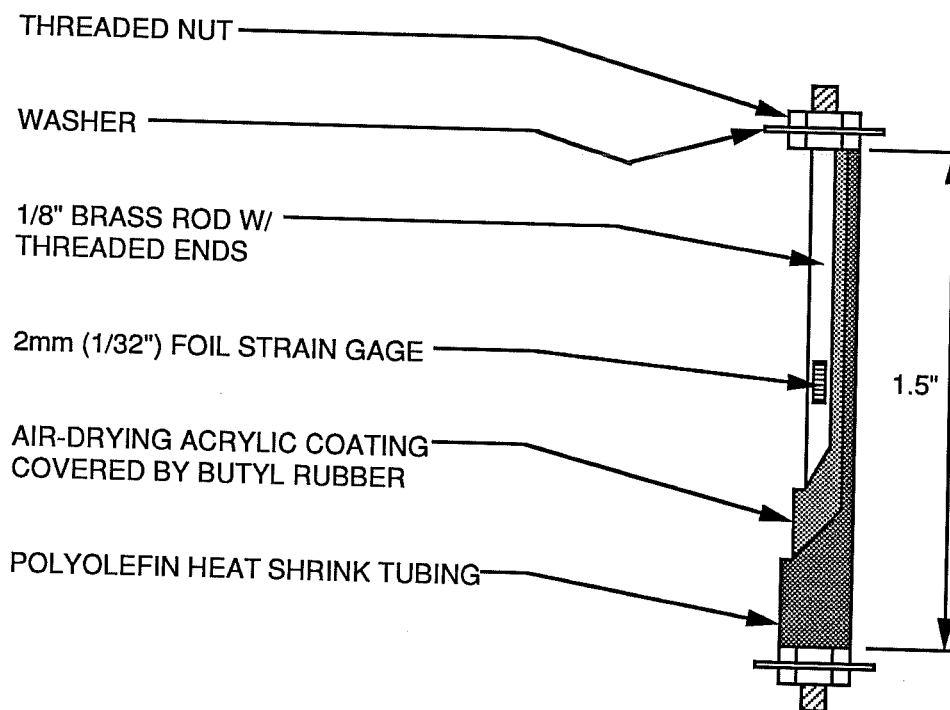


Figure 3.8 - Embedded Strain Gage

brass rod with threaded ends where nuts and washers are attached (Figure 3.8). A foil strain gage is affixed to the brass rod and covered with a water-proof sealant, a tar-like butyl rubber, and a polyolefin heat shrink sheathing.

Embedded strain gages were strung vertically and horizontally in the anchorage zones on piano wires. The locations of the gages are in Chapter 4 and the Appendix A. The gages' strains were recorded by a personal computer data acquisition. Finally, the embedded gage strains were multiplied by the concrete's elastic modulus to obtain the slab's anchorage zone stresses averaged over the gage length of 1.5 inches.

3.3.3 Reinforcement Strain Gages

To monitor reinforcing steel stresses during the loading and failure stages of each anchorage zone, foil strain gages were placed

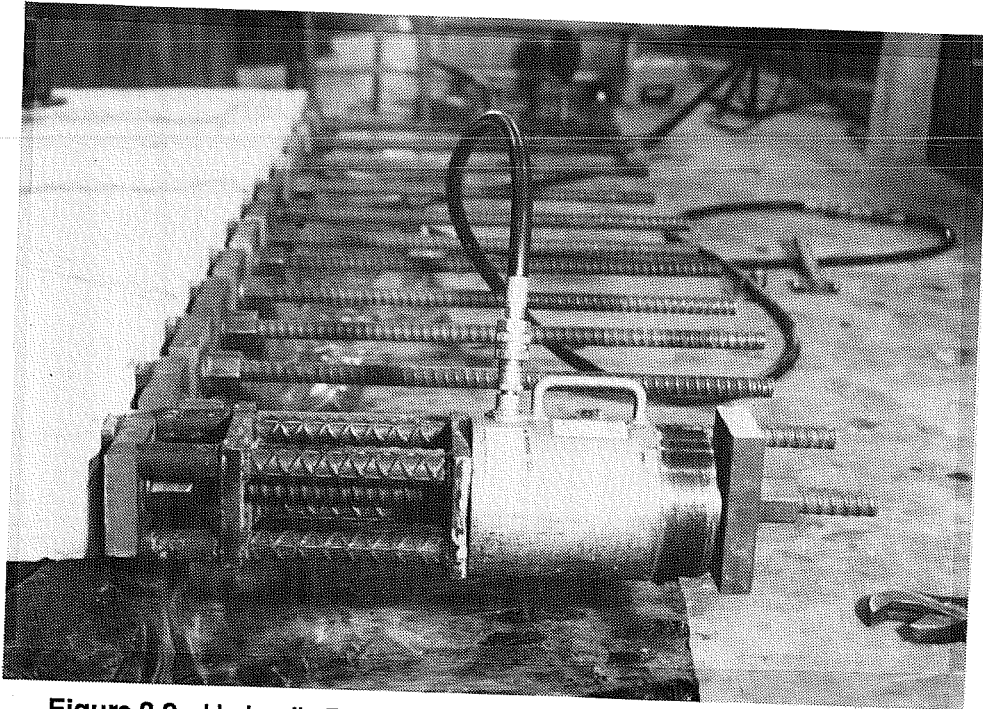


Figure 3.9 - Hydraulic Ram Loading Anchor With Dywidag Threaded Bar

on the slab's reinforcing steel at representative points shown in Chapter 4. The gages were affixed to a smoothed and cleaned section of the reinforcing bar, and then covered with water-proof sealant, butyl-rubber, and a neoprene pad.

Vertical anchorage zone steel, back-up bars, and standard horizontal temperature reinforcement were gaged. The strains were also recorded on a personal computer data acquisition system and stresses were calculated from those strains. The steel stresses were limited to f_y .

3.3.4 Loading Hardware and Process

The anchors were loaded by tensioning threaded prestressing bars against the anchorage plates with a hydraulic ram (Figure 3.9). For some anchorage zones for which the bar's 110 kip capacity was insufficient to cause failure, three 6/10 inch diameter strands (f_y

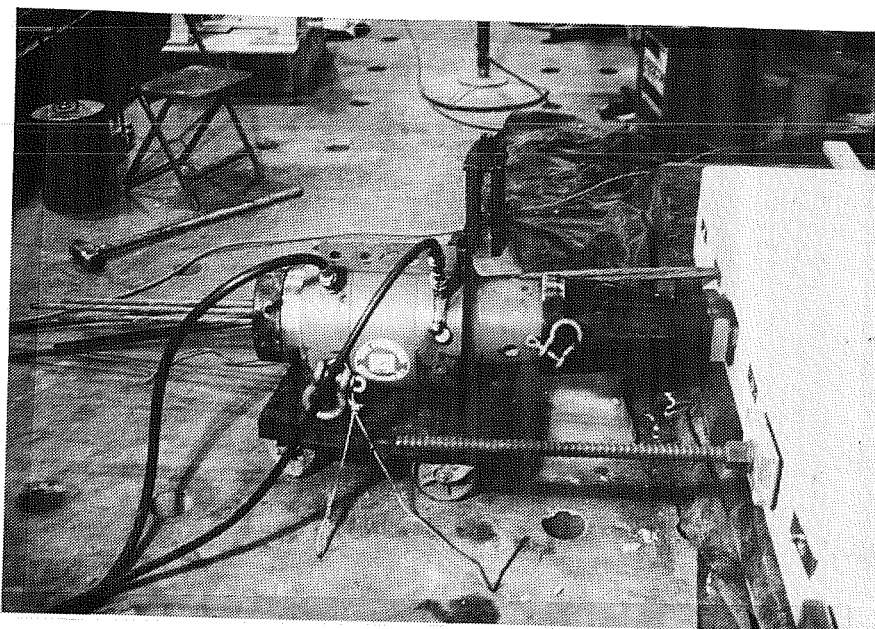


Figure 3.10 - Hydraulic Ram Loading Anchor With Steel Strands

= 220ksi) replaced the bar, and up to 150 kips were applied to the anchors (Figure 3.10). The pressure in the ram was monitored by two pressure transducers. One pressure transducer was read with a strain indicator (Fig 3.11), and the other was read and recorded by the data acquisition system.

The nominal jacking force of a 1/2 inch diameter strand is 35 kips ($0.8f_{pu}$) and the seating force is 30 kips ($0.7f_{pu}$). The full-scale monostrand anchors were loaded with unscaled single 1/2" strand loads. A half-scale model anchor is one fourth the loading area of the actual anchor, and it requires only one fourth the full-scale load which it models. For the half-scale four strand test, a 35 kips jacking force accurately models the full-scale jacking load on that anchor. All anchors in the program were loaded with a 35 kips jacking force. To insure uniform bearing stress ahead of anchorage plates, multiple bearing plates were stacked upon the slab edge anchors.

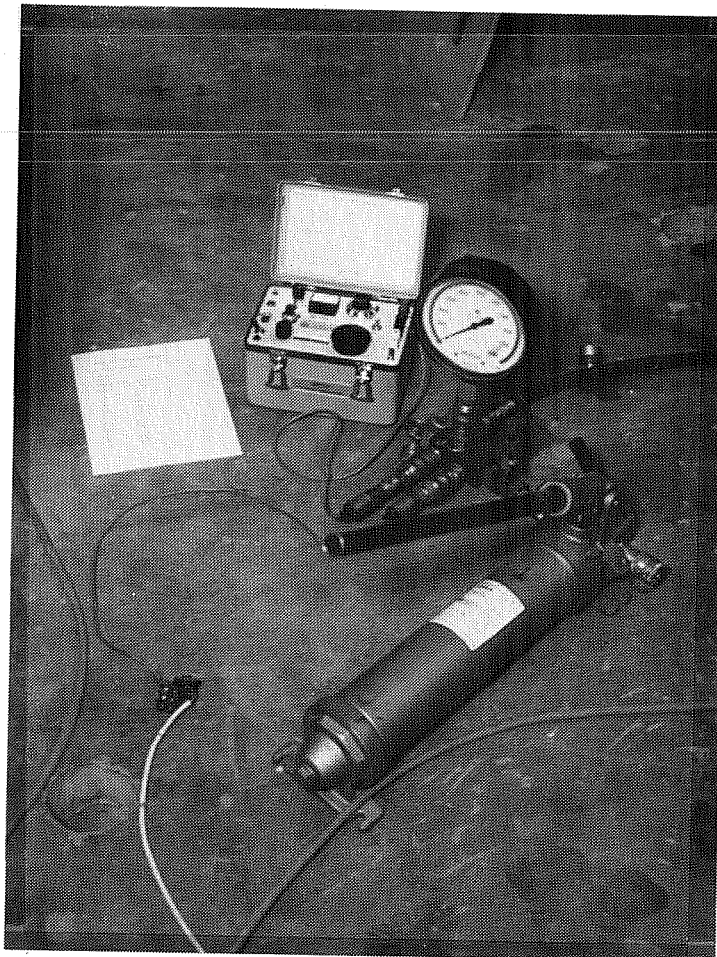


Figure 3.11 - Hydraulic Pump Monitored by Strain Indicator

During testing of the first slab, the anchors were individually loaded to 35 kips and set. During the remaining tests, the anchors were loaded to 35 kips to emulate jacking forces, and then set at 30 kips to emulate seated anchorage forces until all the anchors were loaded to 30 kips. In all the tests, no anchors were loaded to failure until all that slab's anchors had a base post-tensioning load of 30 kips locked onto them.

3.4 Material Tests

3.4.1 General

To evaluate the material quality of the slab anchorage zones, tests were performed on the concrete and the reinforcing steel. Compressive strength and splitting tensile strength tests were performed on test cylinders made with each slab. Tensile stress vs. strain tests were performed on representative reinforcing bars.

3.4.2 Concrete

While casting each slab, test cylinders were cast. On days of testing, three representative cylinders were tested for compressive strength and elastic modulus and three were tested for splitting tensile strength (Table 3.2). The aggregate was Colorado River gravel and sand, and cement was Type I. The maximum gravel diameter was 3/8", and the concrete was cast with a 4" slump. Two different

Table 3.2 - Concrete Strengths of Slabs

SLAB #	f_c' (psi)	f_{sp}' (psi)	E_c (psi)
SLAB 1	3,106	361	3,177,000
SLAB 2	4,635	363	3,881,000
SLAB 3	4,363	325	3,765,000
SLAB 4	3,797	319	3,512,000
SLAB 5	4,555	414	3,847,000
SLAB 6	4,448	386	3,802,000

mixes were used. For Slab 1 the mixture contained 400 lbs. of cement, 1625 lbs. of coarse aggregate, 1619 lbs. of fine aggregate, 275 lbs. of water, and 12 oz. of water reducing add mixture per yd^3 of concrete. For Slabs #2 through #6, the mix contained 470 lbs. of cement, 1625 lbs. of coarse aggregate, 1655 lbs. of fine aggregate, 250 lbs. of water, and 20 oz. of water reducing add mixture per yd^3 of concrete.

3.4.3 Reinforcing Steel

Representative pieces of #2, #3, and welded wire fabric reinforcing bars were tested by affixing foil strain gages to each bar and tensioning it with a universal testing machine. The force is read from the machine while strains were measured with a strain indicator. The stress was computed using the nominal bar area, and elastic modulus and yield points were derived from the stress vs. strain diagram (Figures 3.12 through 3.14). The bars were tensioned until failure to find the ultimate load.

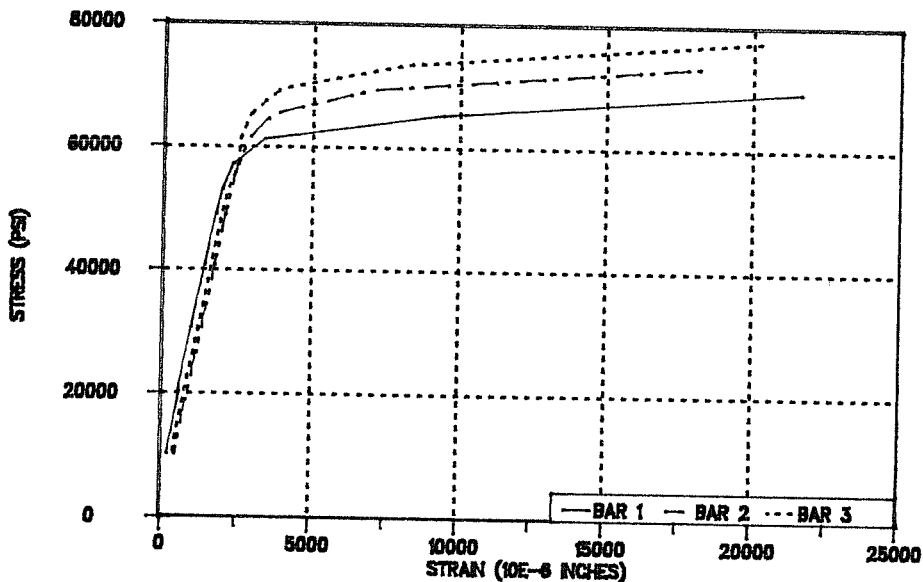


Figure 3.12 - Swedish #2 Reinforcing Bar (6mm)
 Yield Strength = 61,000 psi
 Elastic Modulus = 25,900,000 psi

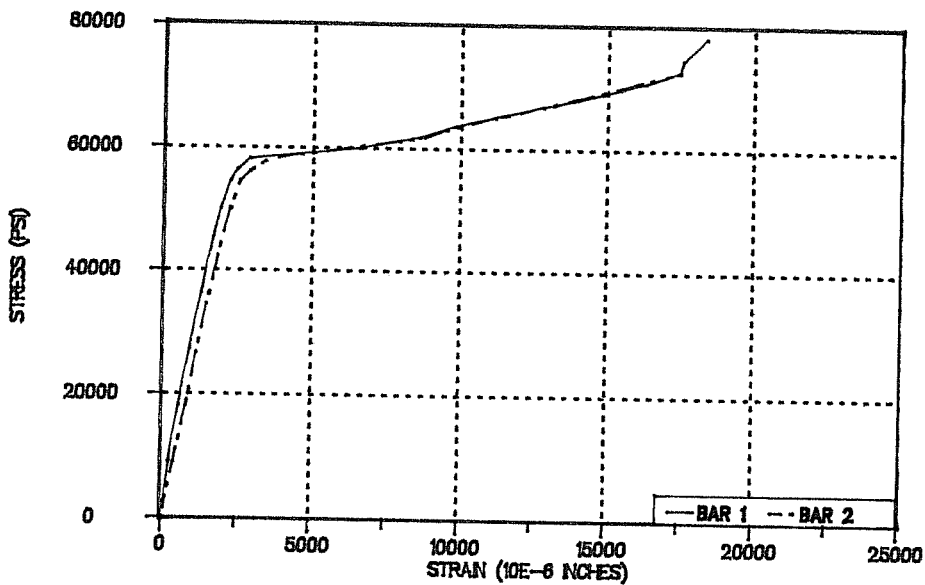


Figure 3.13 - #3 Reinforcing Bars
 Yield Strength = 59,000 psi
 Elastic Modulus = 25,300,000 psi

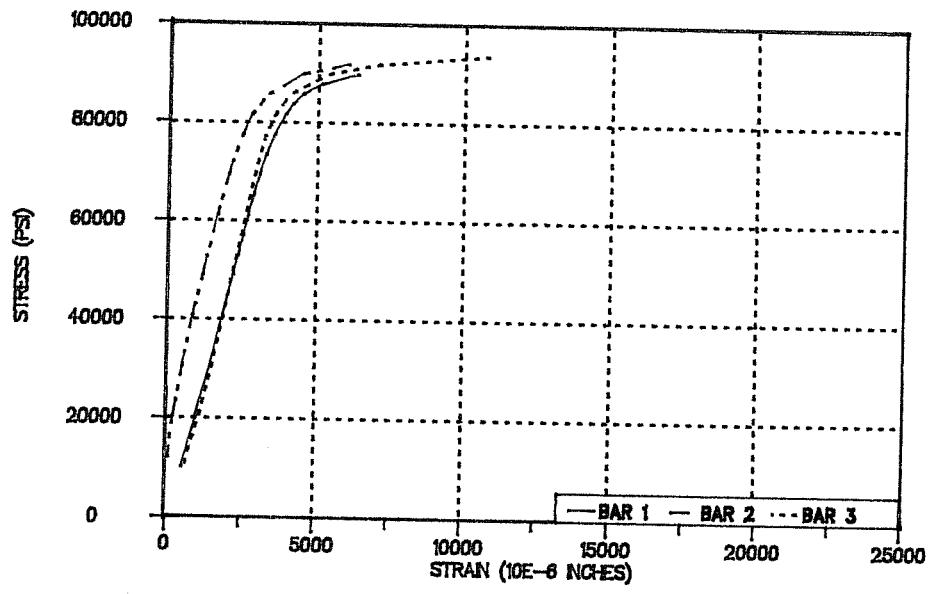


Figure 3.14 - Welded Wire Fabric #2 Reinforcing Bar (6mm)
Yield Strength = 86,000 psi
Elastic Modulus = 26,400,000 psi

Chapter 4 Test Results

4.1 General

As mentioned in Chapter 3, the test program included half-scale models of four strand anchors and full-scale models of mono-strand anchors in 10" bridge decks. Stressing sequence, anchor orientations, anchor spacing, anchor edge distance, and anchorage zone reinforcement were all varied.

Each slab was loaded with scaled representative post-tensioning loads ($0.8f_{pu}$ due to tendon jacking force and $0.7f_{pu}$ immediately after tendon anchorage) on each anchor pair and then loads on individual anchors were increased to failure. Steel reinforcement strains, concrete strains, cracking loads, and anchorage failure loads were measured. The ratio of anchor bearing stress to concrete compressive strength (f_b/f'_c ratio) was calculated for each anchor.

Failures typically burst a semi-circular piece of concrete from either the top, bottom, or top and bottom of the slab at the failed anchor (Figure 4.1). These failures also revealed that a shear cone had developed ahead of the anchor plate during failure (Figure 4.2). For end anchors, bursting cracks were often able to penetrate either the slabs side, or top and bottom (Figure 4.3). For interior anchors, vertical splitting along the tendon occurred infrequently and never before failure. Pre-failure cracking typically extended from the corners of the slab similar to the elevations in Figure 4.1 demonstrating anchor failure.

The first two slabs concentrated primarily on effects of stressing sequence on strains in horizontal and vertical planes, and the final four slabs concentrated primarily on failure testing of anchorage zones. In Slabs #3 through #6, on each anchorage pair, a heavily reinforced anchorage (Figure 3.6) was positioned opposite

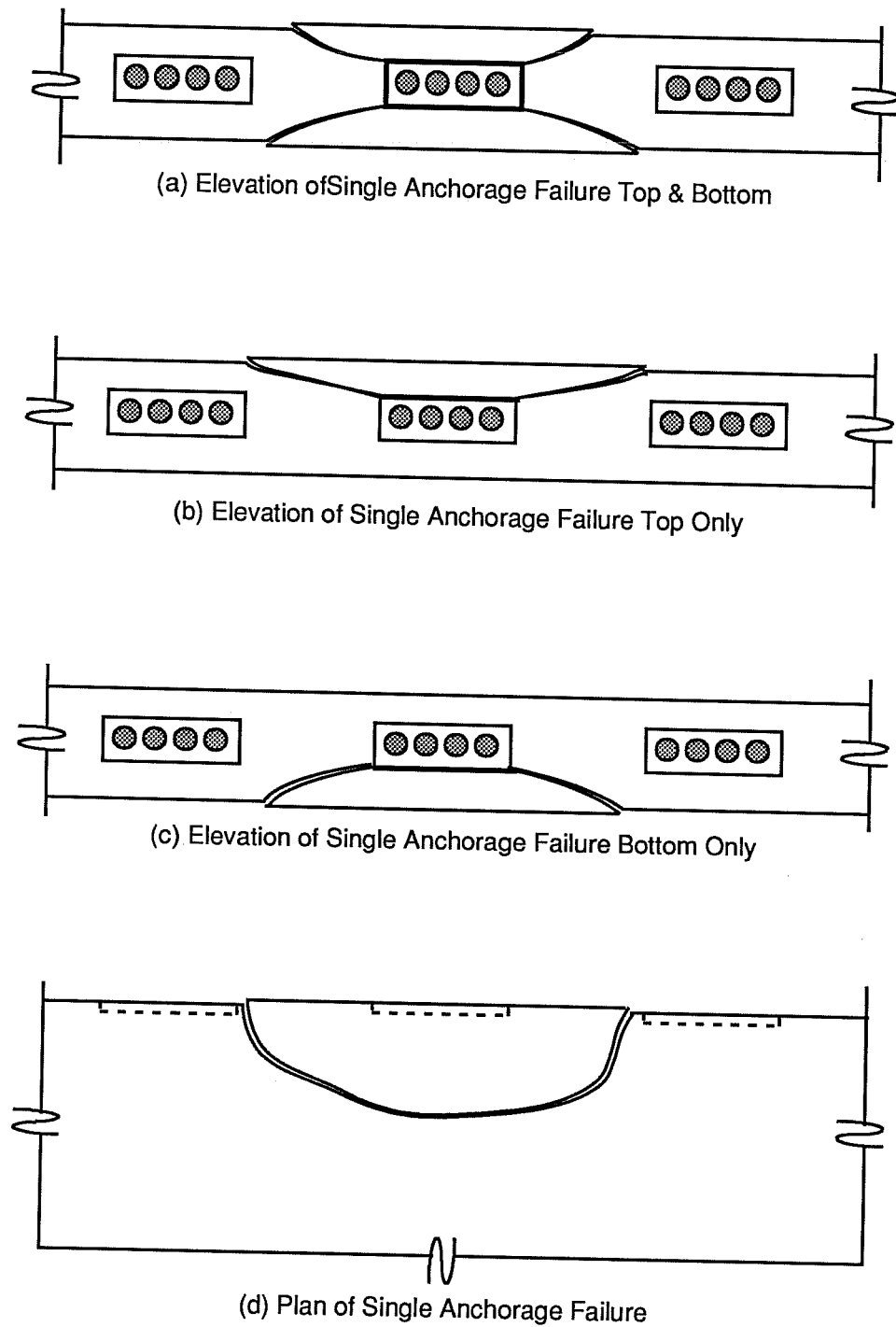


Figure 4.1 - Single Edge Anchorage Failures

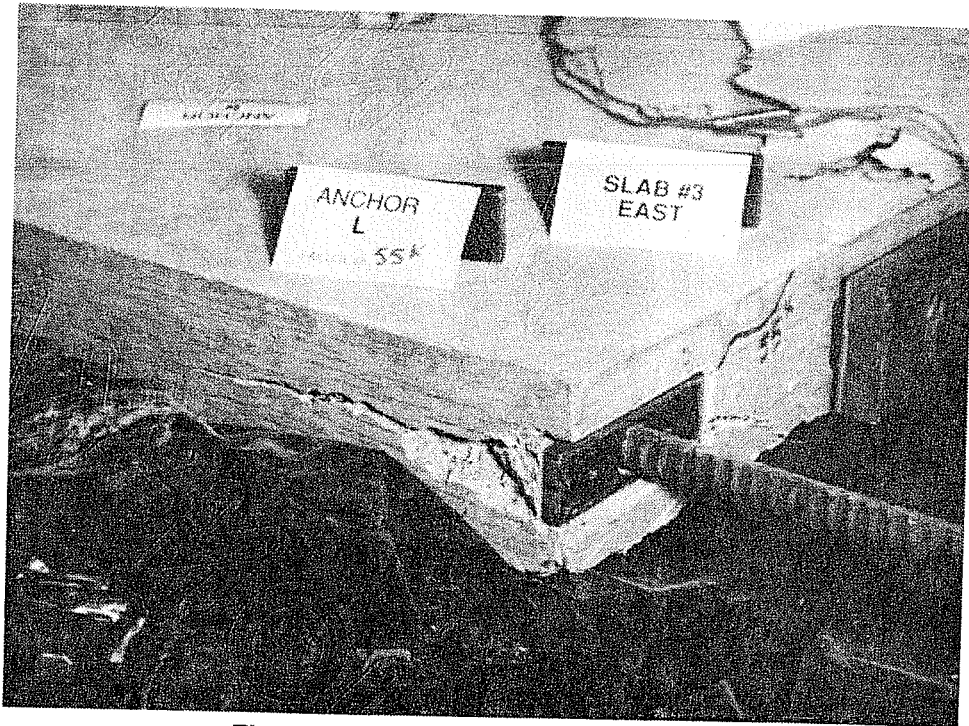


Figure 4.2 - Shear Cone Ahead of Anchor
Slab #3 at Failed Anchor I (back-up bars)

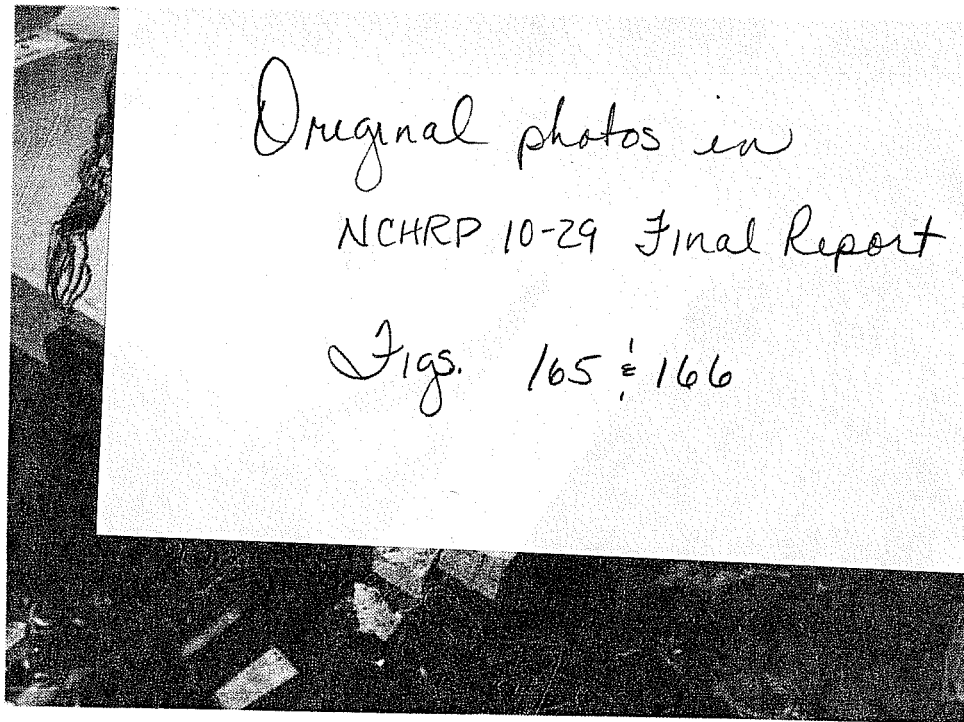


Figure 4.3 - Slab #3 at Failed Anchor A (unreinforced)

from an anchorage zone reinforcing detail which was under investigation. This enabled the slab's anchor failures to be alternated from side to side, and prevented an anchorage zone from being damaged by adjacent failures before it was tested; however, in some cases, the heavily reinforced anchorage failed and the maximum load of the detail being tested was not reached. Failure of the heavily reinforced anchorage was typically effected by damage caused to the anchorage zone by previous adjacent anchorage failure.

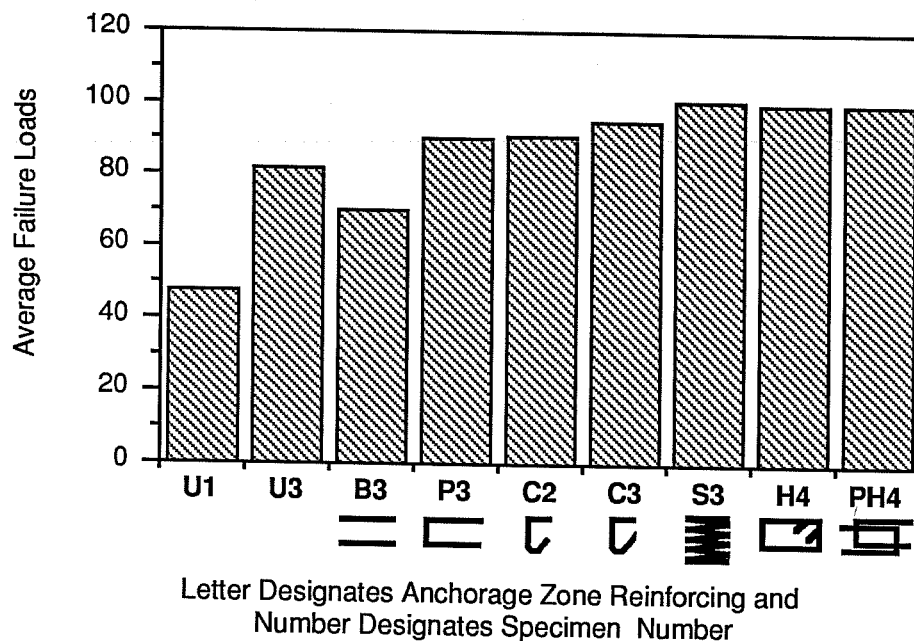
4.2 Half-Scale Four Strand Anchors - Horizontal Orientation

4.2.1 General

Slabs #1 through #4 contained half-scale rectangular four strand anchors with horizontal orientation. These slabs were used to evaluate the effects of stressing sequences on vertical plane and horizontal plane stresses, and the efficiency of anchorage zone reinforcement in post-tensioned bridge decks.

Stressing sequence effects were evaluated from strain measurements of concrete and reinforcing steel in the first three slabs. To more accurately model a bridge deck's horizontal plane geometry, 1 inch diameter steel ducts, which accommodated 5/8 inch diameter threaded bars, were used for most anchor pairs in the first two slabs. The thinner ducts provided a larger critical section for horizontal plane stresses. Only six of those sixteen anchorage pairs had 1 3/8 inch diameter steel ducts, which accommodated 1 inch diameter threaded bars. The larger threaded bars were needed to load an anchor to failure. The larger ducts were placed with all the anchor pairs in Slabs #3 and #4 which were tested to failure at every anchor pair.

Slab #1 had eight anchor pairs and was completely unreinforced as were four anchorage zones in slab #3. The unreinforced anchorage zones were gaged with embedded strain gages. Slab #2 implemented heavy horizontal reinforcing, light horizontal reinforcing, and some

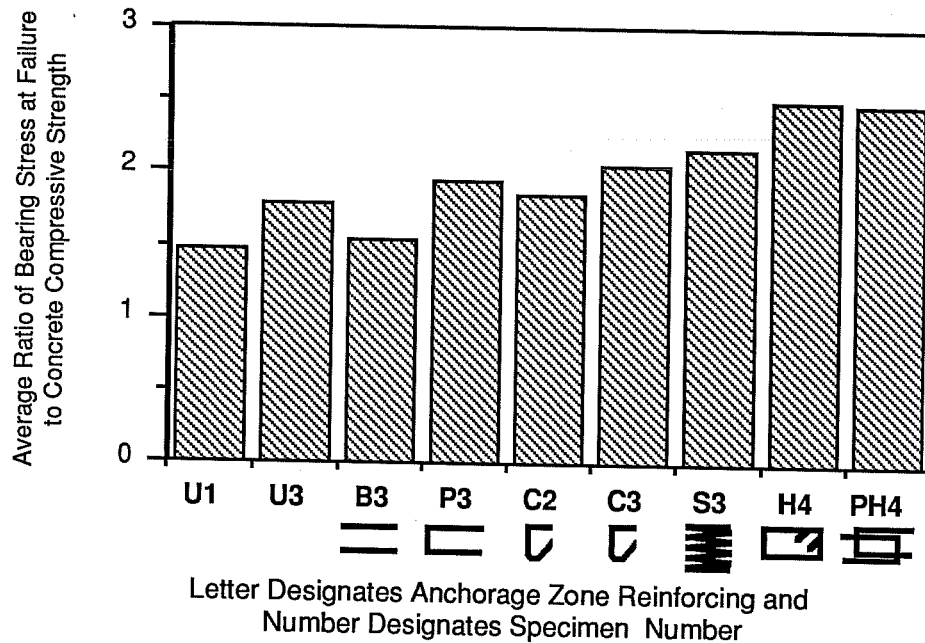


- | | |
|-----------------------------|-----------------------------------|
| U - Unreinforced Anchors | S - Spiral w/Back-up Bars |
| B - Back-up Bars | H - Hoops w/Back-up Bars |
| P - Hairpins w/Back-up Bars | HP - Hairpin Hoops w/Back-up Bars |
| C - Cross Ties | |

Figure 4.4 - Average Failure Loads of Four Strand Horizontally Oriented Anchors at Half-Scale

additional anchorage zone steel. The remaining horizontal four strand anchors in slabs #3 and #4 contained temperature steel and various anchorage zone reinforcement. Back-up bars never gained high stresses before anchorage failure occurred for horizontally oriented four strand anchors.

The failure loads of these anchorage zones are shown in Figure 4.4, and f_b/f'_c ratios are shown in Figure 4.5. Both are given in Table 4.1. The failure loads of anchorage zones reinforced with back-up bars exclusively did not appear to be higher than



- U - Unreinforced Anchors S - Spiral w/Back-up Bars
 B - Back-up Bars H - Hoops w/Back-up Bars
 P - Hairpins w/Back-up Bars HP - Hairpin Hoops w/Back-up Bars
 C - Cross Ties

Figure 4.5 - Average Ratio of Bearing Stress at Failure to Concrete Compressive Strength for Four Strand Horizontally Oriented Anchors at Half-Scale

unreinforced anchorage zones. The anchorage zones with hoop or spiral reinforcing reached the highest f_b/f'_c ratios.

4.2.2 Unreinforced Anchorage Zones

4.2.2.1 General

Both Slab #1 (Figure 4.6) and Slab #3 (Figure 4.7) modeled horizontally oriented four-strand anchors in unreinforced anchorage zones. Strains in the plain concrete of these anchorage zones were measured by embedded strain gages (Figure 3.8) placed vertically and

Table 4.1 - Failure of Four Strand Horizontal Oriented Anchors at Half-Scale

Reinforcement	Slab	Anchor	Failure (kips)	f_b/f'_c (ksi/ksi)
Unreinforced	#1	A	56	1.715
"	"	D	42*	1.286
"	"	H	45*	1.378
		Average	47.7	1.460
Unreinforced	#3	A	75	1.635
"	"	B	80	1.744
"	"	C	80	1.744
"	"	D	90	1.962
		Average	81.25	1.771
Back-Up	#3	K	85	1.853
"	"	L	55	1.199
		Average	70	1.526
Hairpins	#3	E	85	1.853
"	"	F	95	2.071
		Average	90	1.962
Cross Ties	#2	A	75	1.539
"	"	D	102	2.093
"	"	H	95	1.949
		Average	90.7	1.860
Cross Ties	#3	G	90	1.962
"	"	H	100	2.108
		Average	95	1.949
Spiral	#3	I	95	2.071
"	"	J	107	2.332
		Average	101	2.202
Hoops	#4	A	90**	2.254
"	"	B	100	2.505
		Average	100	2.505
Hairpin Hoops	#4	C	100	2.505
"	"	D	100	2.505
		Average	100	2.505

* Eccentricities in Loading System

** Control Detail Failed

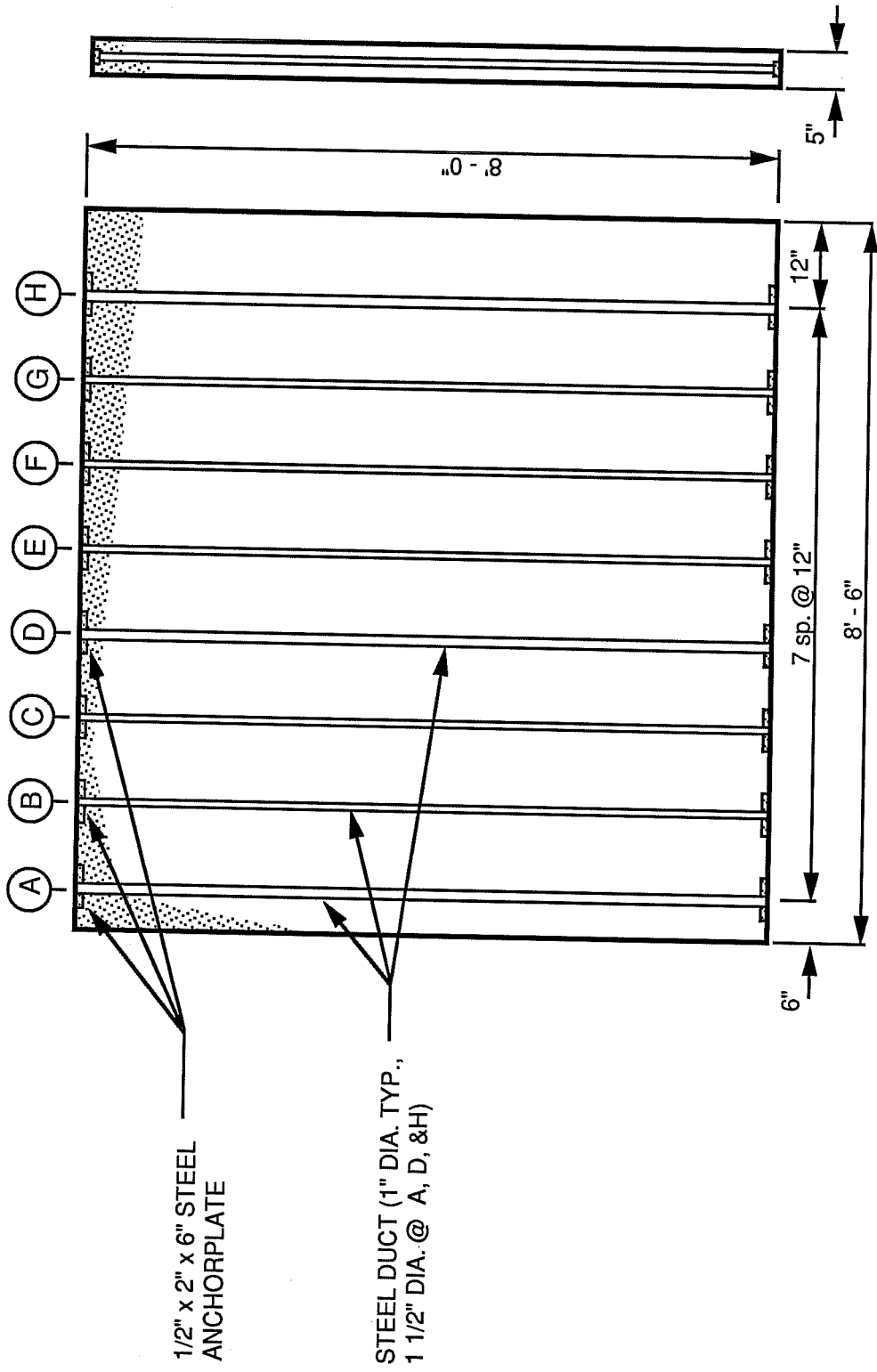


Figure 4.6 - Plan of Slab #1

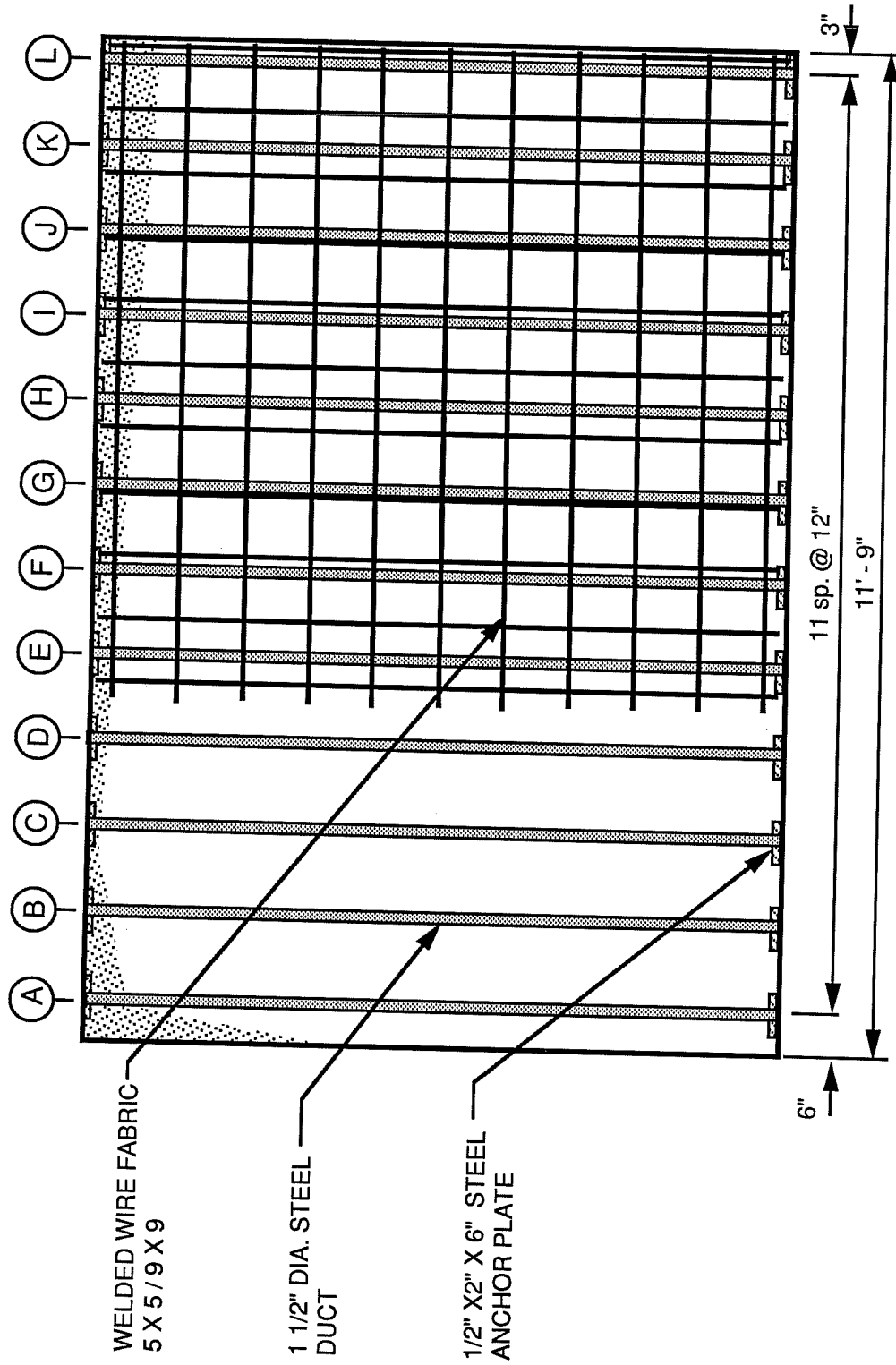


Figure 4.7 - Plan of Slab #3

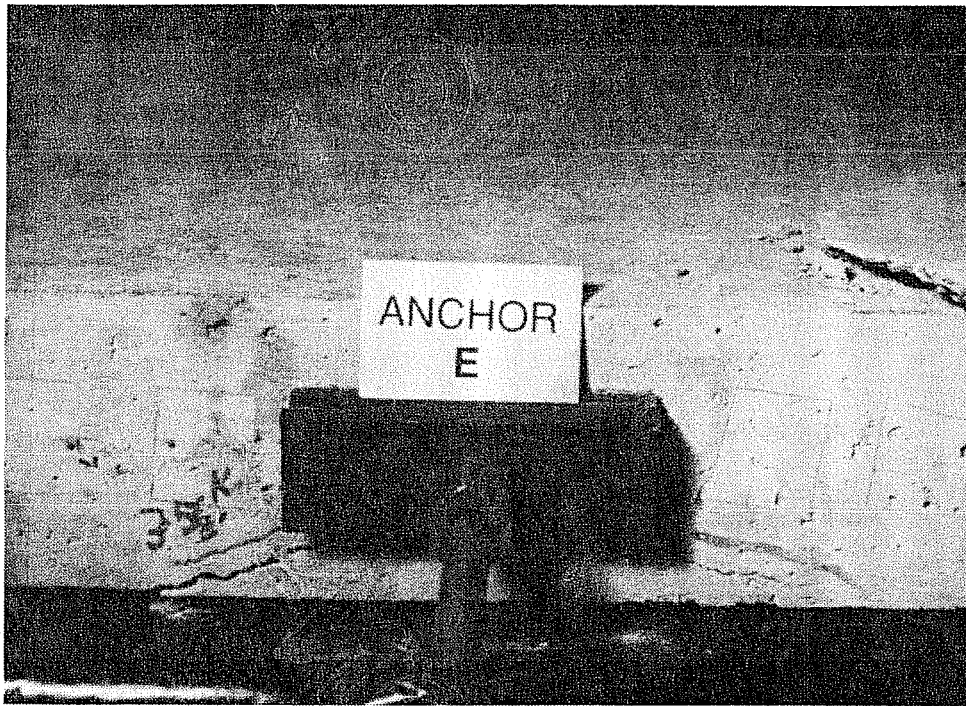


Figure 4.8 - First Cracking at Anchor E of Slab #1

horiz
 the c
 pair:
 sequ
 four
 edge
 While
 exte
 Afte

*Original photo in
 1029 NCHRP Final Report
 Fig. 167*

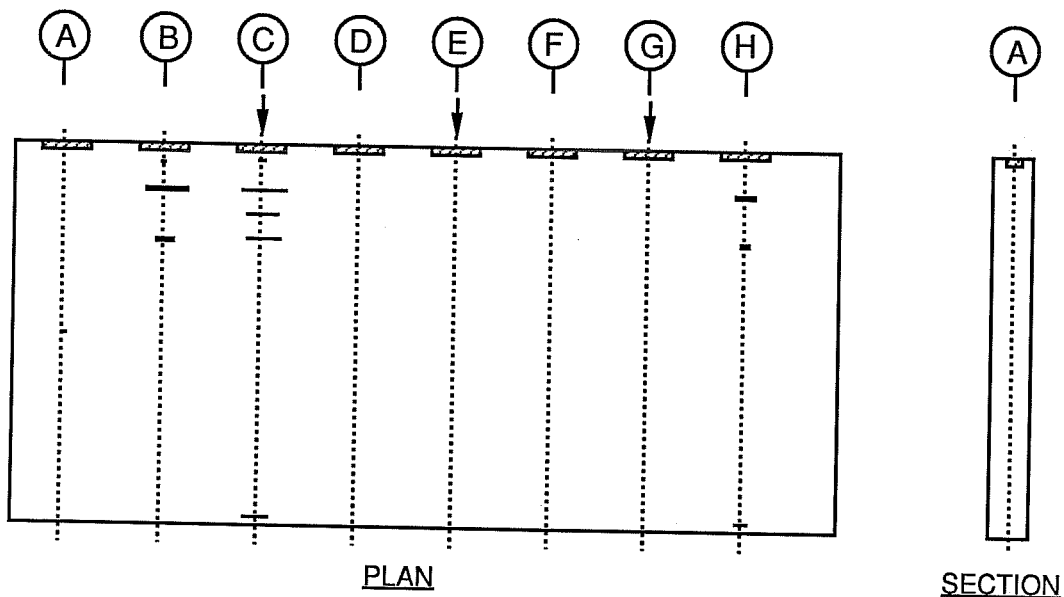
to
 or
 is
 is,
 hor
 ns.
 cks
 8).

4.2

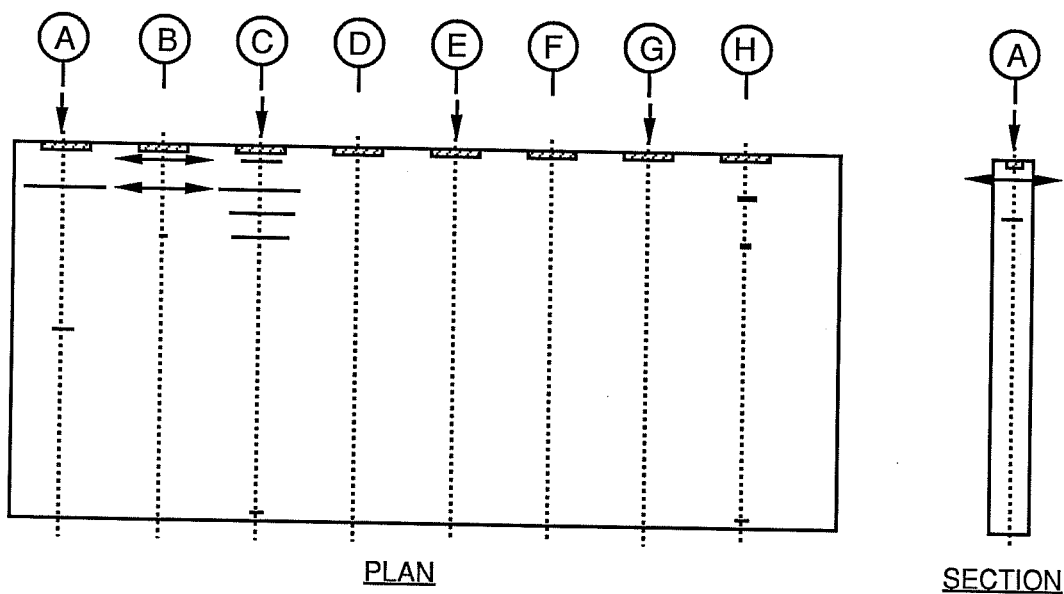
During sequenced stressing of the slabs, bursting and splitting stresses were developed in the horizontal plane, and bursting stresses were developed in the vertical plane. Two stressing sequences were used on Slab #1 and Slab #2. One stressing sequence

loaded every fourth anchor, then every other anchor, and then all anchors. The other stressing sequence stressed the end anchor with the smallest edge distance first, and then adjacent anchors all the way across the slab. Horizontal bursting stresses were highest when every other anchor was loaded including the end anchor with the one plate width edge distance (Figures 4.9 and 4.10). Those figures also demonstrate the magnitude of calculated stresses in the vertical plane under a loaded anchor. Loading the exterior anchor also modified the anchorage zone of Anchor C. The horizontal plane bursting stresses ahead of Anchor C became higher and concentrated closer to the anchor.

For Slab #1, the maximum bursting stress in the plane of the slab (horizontal stresses) was 202 psi (at 6" below anchor A), while loading of an anchor produced a minimum calculated bursting stress perpendicular to the plane of the slab (vertical stresses) of 498 psi (at 3" below anchor A). The measured split cylinder tensile strength of the concrete in Slab #1 was 361 psi. The corresponding calculated bursting stresses for Slab #3 were 146 psi (6" below anchor A) and 353 psi (3" below anchor C). The measured split cylinder strength of the concrete in Slab #3 was 325 psi. Loading of all anchors reduced horizontal stresses ahead of interior Anchor C of Slab #1 (Figures 4.11). No appreciable change was noticed in the working gage ahead of Anchor C in Slab #1 (Figure 4.12). The horizontal bursting stresses created by end anchor loading were similar in magnitude to the bursting stresses created by loading every other anchor (Figure 4.13). Spalling strains were the highest strains produced by sequenced stressing, but they are very localized and commonly regarded as continuity induced strains which are relieved by early micro-cracking and have little effect on anchor failure.



(a) Anchors C, E, & G Loaded to 35k



(b) Anchors A, C, E, & G Loaded to 35k

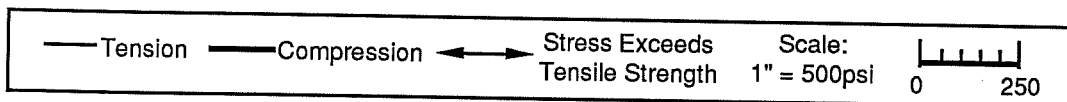
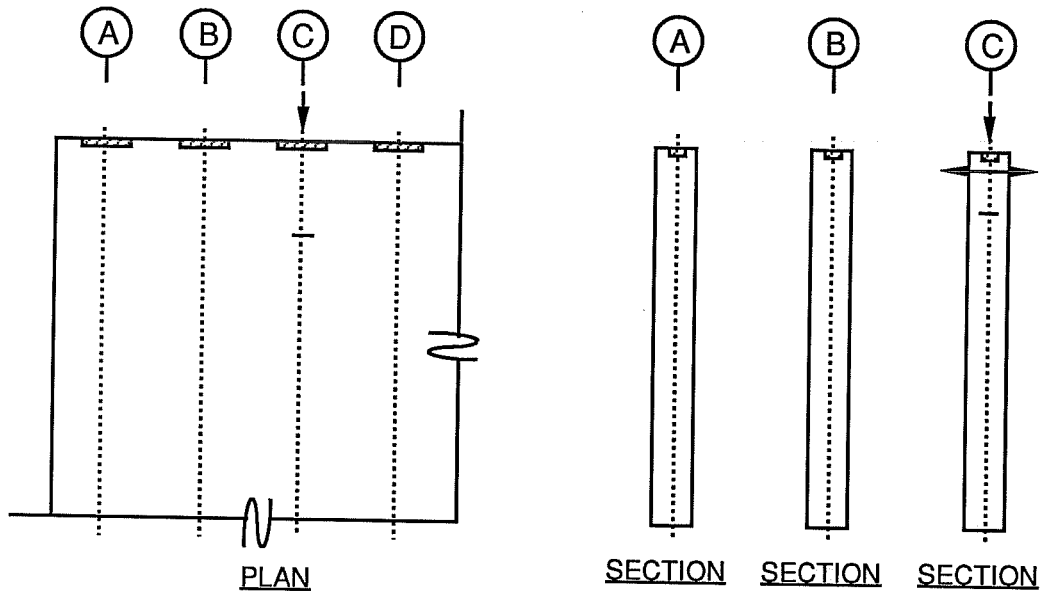
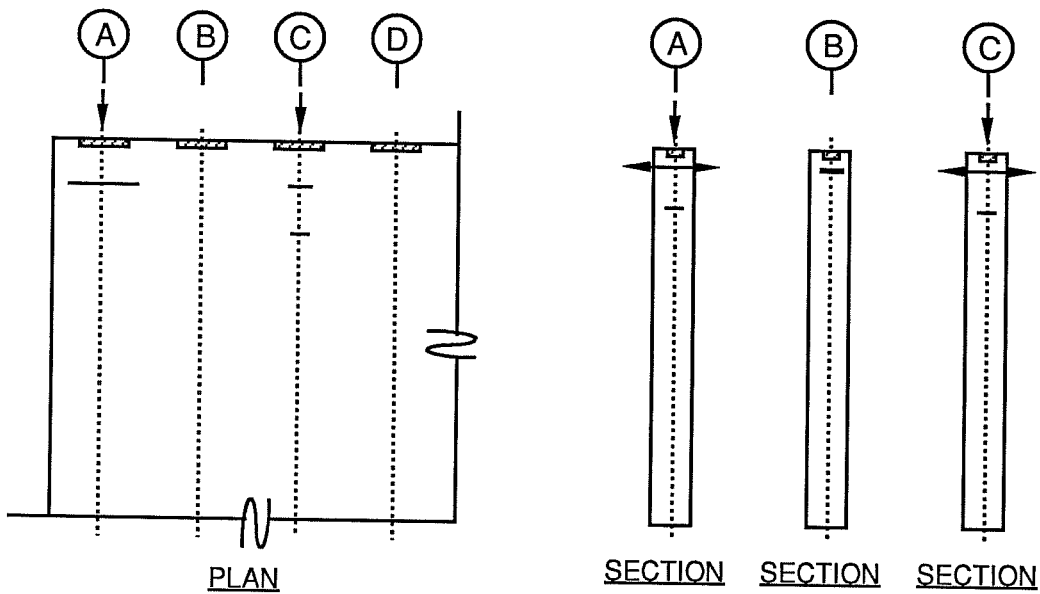


Figure 4.9 - Maximum Calculated Horizontal Bursting Stresses in Slab #1



(a) Anchors C, E, G, J, & K Loaded to 30k



(b) Anchors A, C, E, G, I, & K Loaded to 30k

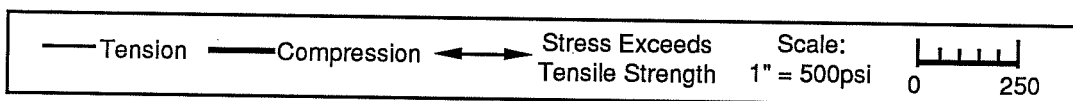
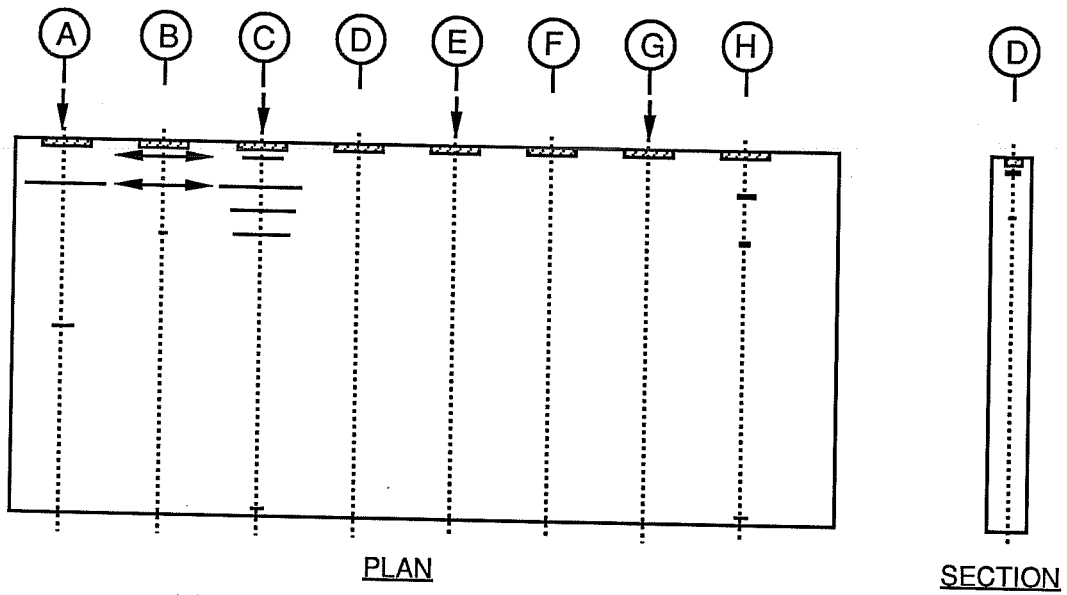
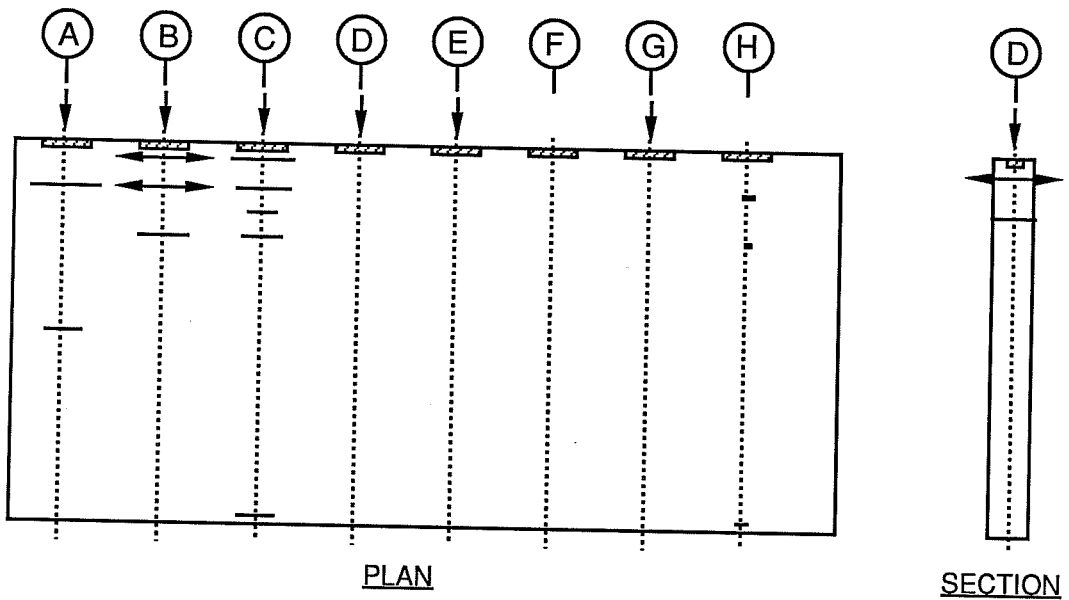


Figure 4.10 - Maximum Calculated Horizontal Bursting Stresses in Slab #3



(a) Anchors A, C, E, & G Loaded to 35k



(b) Anchors A, B, C, D, E, & G Loaded to 35k

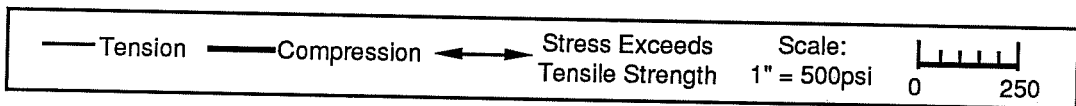
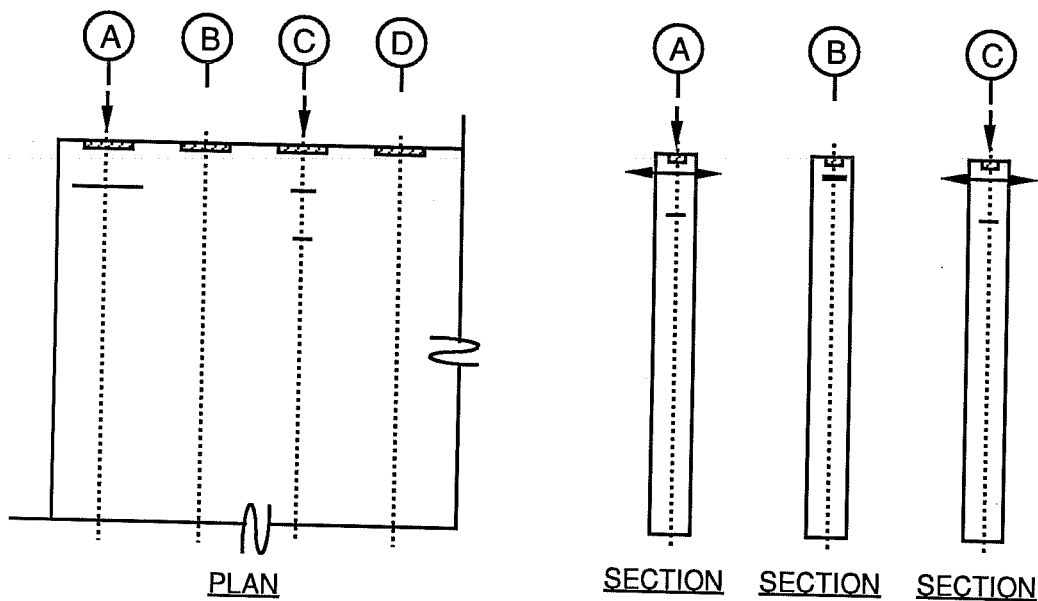
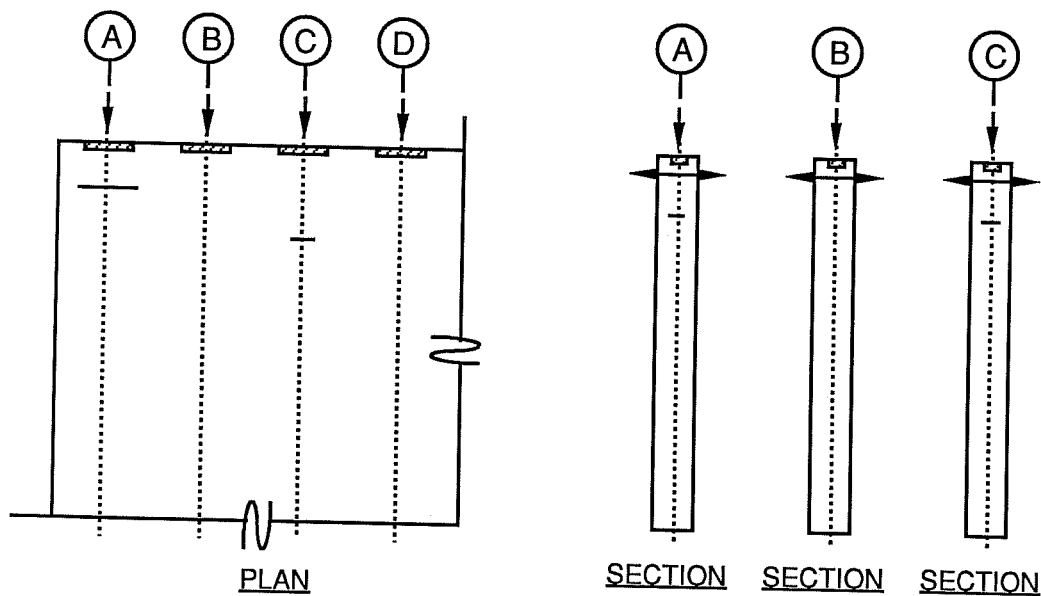


Figure 4.11 - Adjacent Anchor Loading Effects on Calculated Stresses in Slab #1



(a) Anchors A, C, E, G, I, & K Loaded to 30k



(b) Anchors A, B, C, D, E, G, I, & K Loaded to 35k

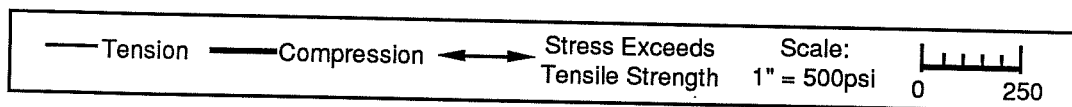


Figure 4.12 - Adjacent Anchor Loading Effects on Calculated Stresses in Slab #3

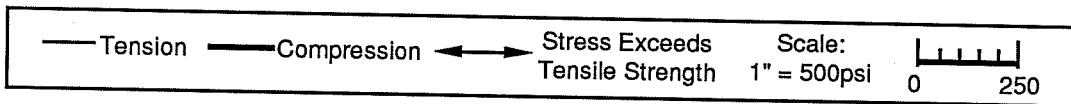
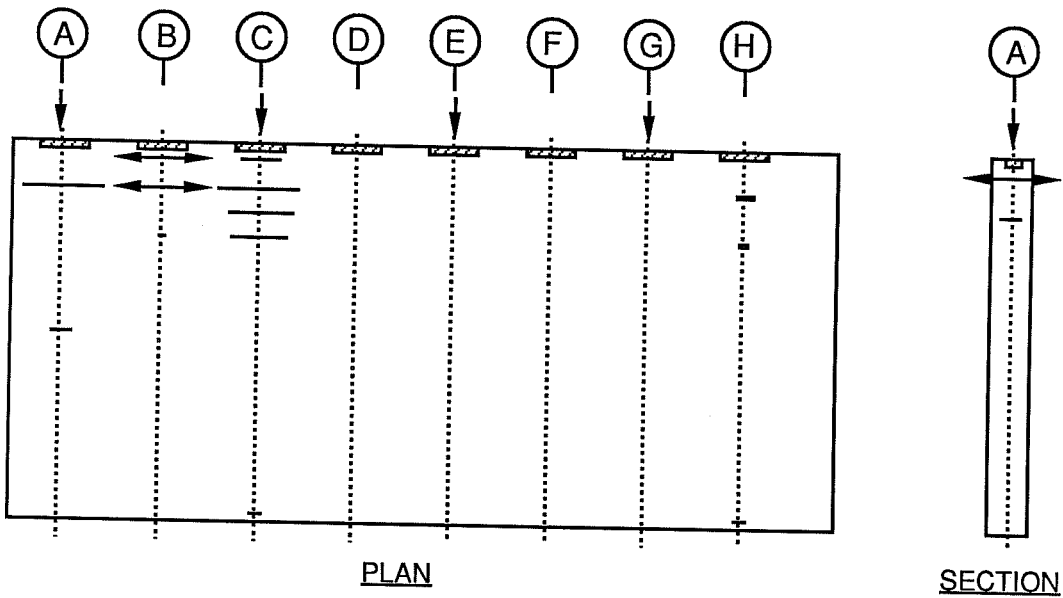
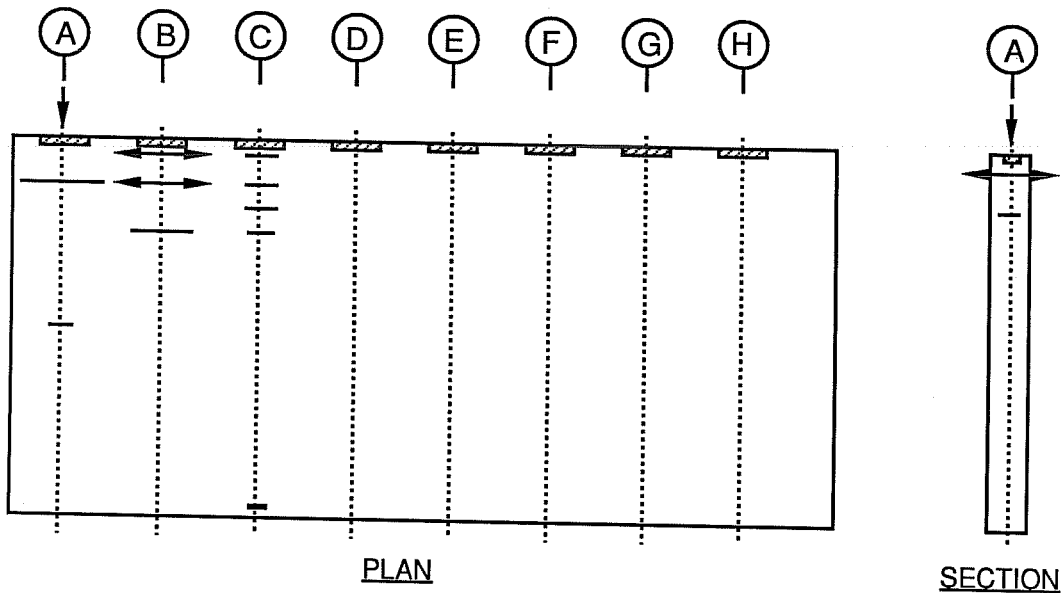


Figure 4.13 - Exterior Anchor Effects on Calculated Stresses in Slab #1

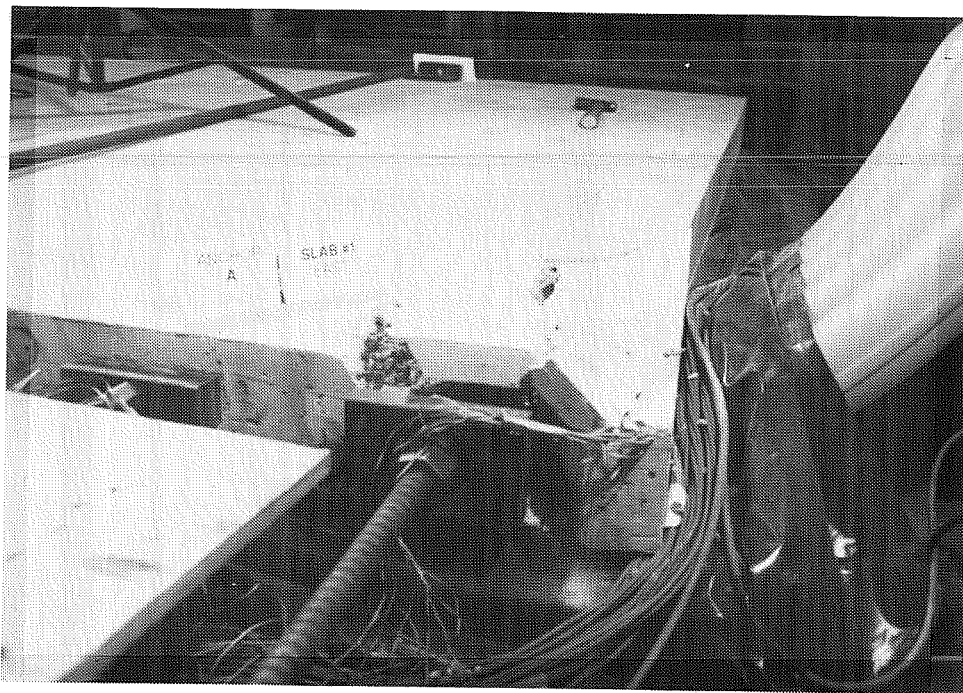


Figure 4.14 - Failed Anchor A in Slab #1

4.2.2.3 Loading to Failure

Slab #1 failed at the A, D, and H anchor pairs. The failure load at anchor A was 56 kips. Difficulties in loading Anchors D and H of the first slab caused severe eccentricities. Anchor pairs D & H failed at loads of 42 kips and 45 kips (average f_b/f'_c ratio of 1.33), respectively, after Anchor H had been previously loaded concentrically to 52 kips. Also the failure loads in the unreinforced anchorage zones of Slab #3 averaged 81.25 kips and the average f_b/f'_c ratio was 1.77. At Anchor A the failure caused a shear cone to develop beneath the bearing plate and it was driven into the slab causing the corner to break away from the slab (Figure 4.14). The unreinforced anchor pairs in Slab #3, which were A, B, C, and D, were also failed. Unreinforced end anchors demonstrated the same failure characteristics in Slab #3 (Figure 4.3) as in Slab #1. Considering only the Anchor A failure of Slab #1 and the four

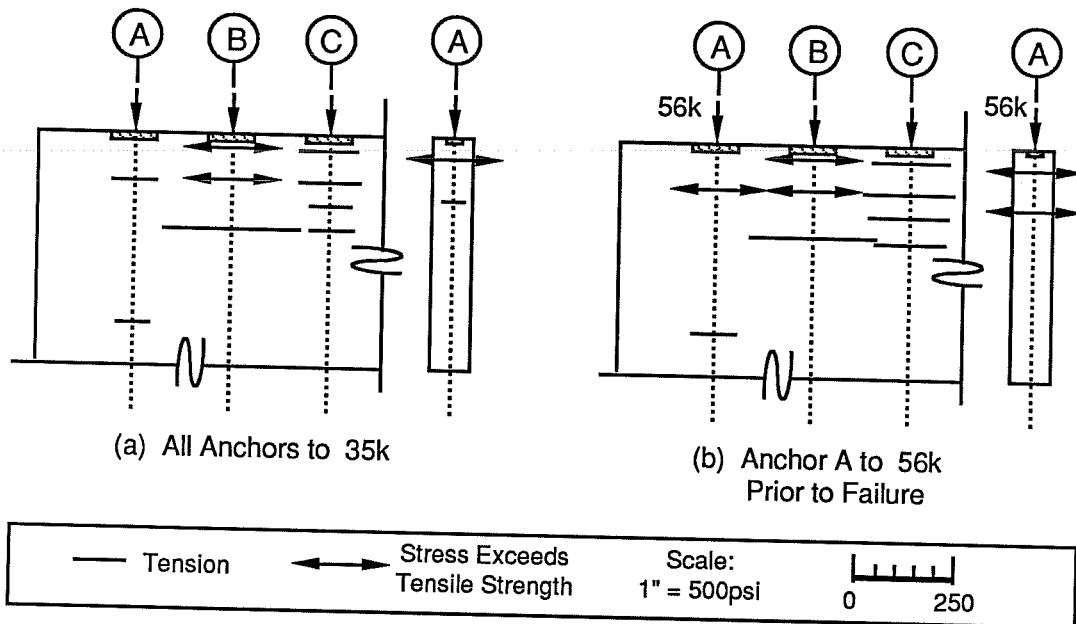


Figure 4.15 - Slab #1 Failure at Anchor A

anchor failures in Slab #3, the average f_b/f'_c ratio was 1.76 for the unreinforced anchorage zones.

Figures 4.15 through 4.18 display the increase of stresses in the unreinforced anchorage zones as they approached failure. The vertical bursting stresses are the largest. Both the failure geometry (Figure 4.1) and the vertical embedded strain gage readings under loaded anchors indicate that vertical plane bursting stresses have the greatest effect on anchorage zone failure for bridge deck edge anchors.

4.2.3 Anchorage Zones with Horizontal Steel

4.2.3.1 General

Bridge deck edge anchorages fail due to vertical bursting stresses before horizontal stresses crack the concrete, and therefore, the horizontal reinforcing bars do not develop

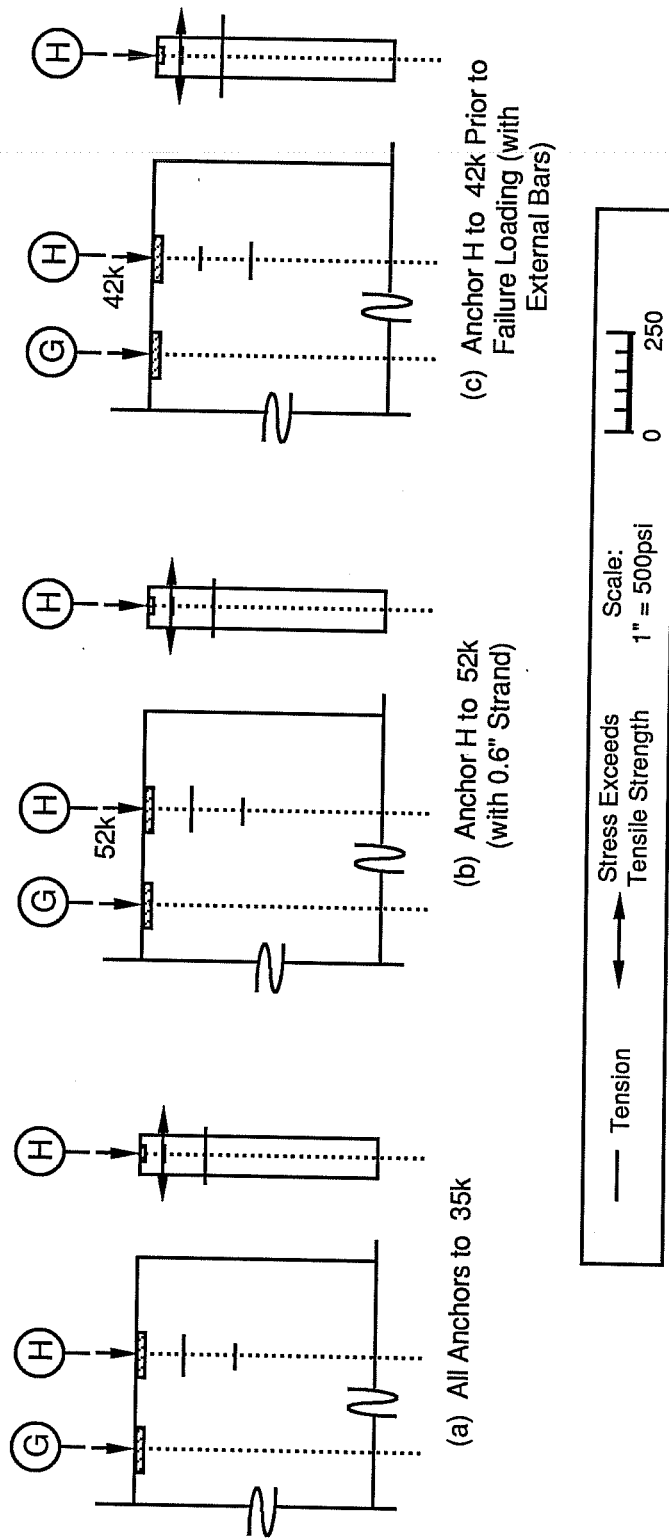
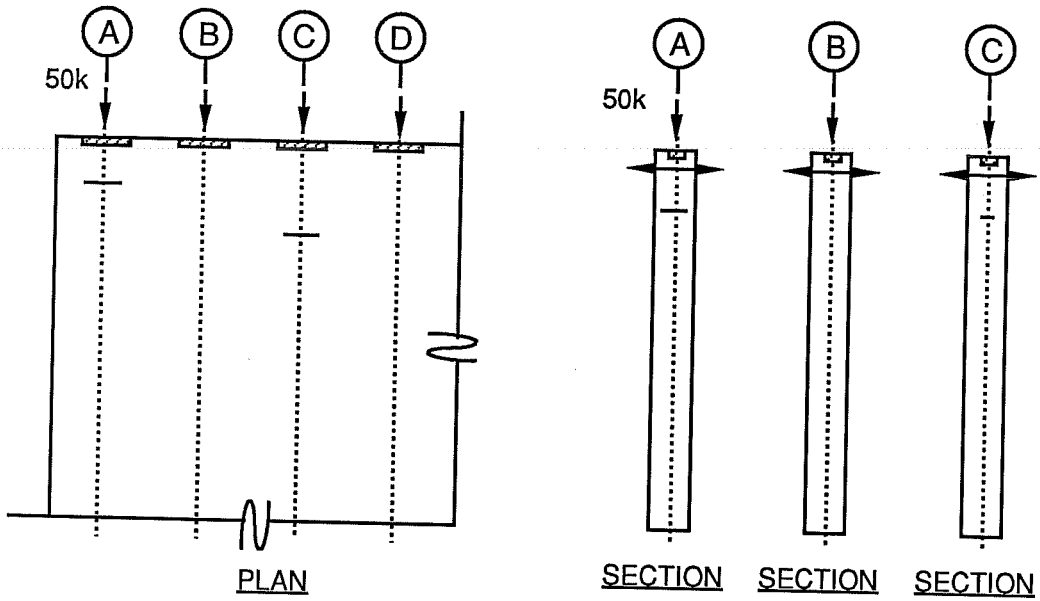
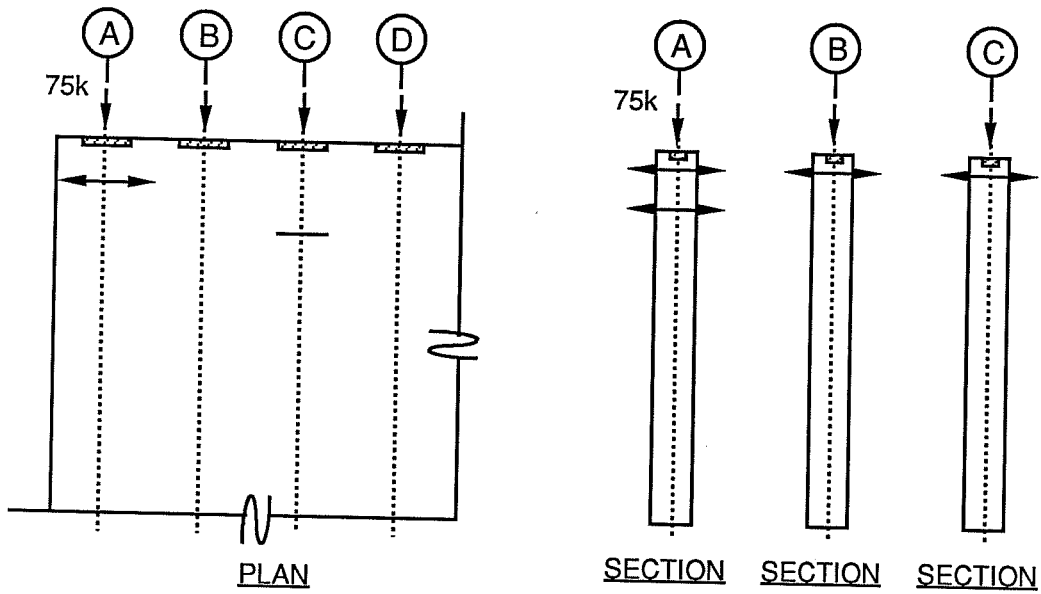


Figure 4.16 - Slab #1 Failure at Anchor H



(a) Anchor A Loaded to 50k and All Others Loaded to 35k



(b) Anchor A Loaded to 75k All Other Anchors Loaded to 35k
Anchor A Failed at 80k

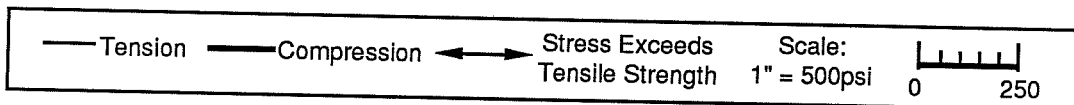
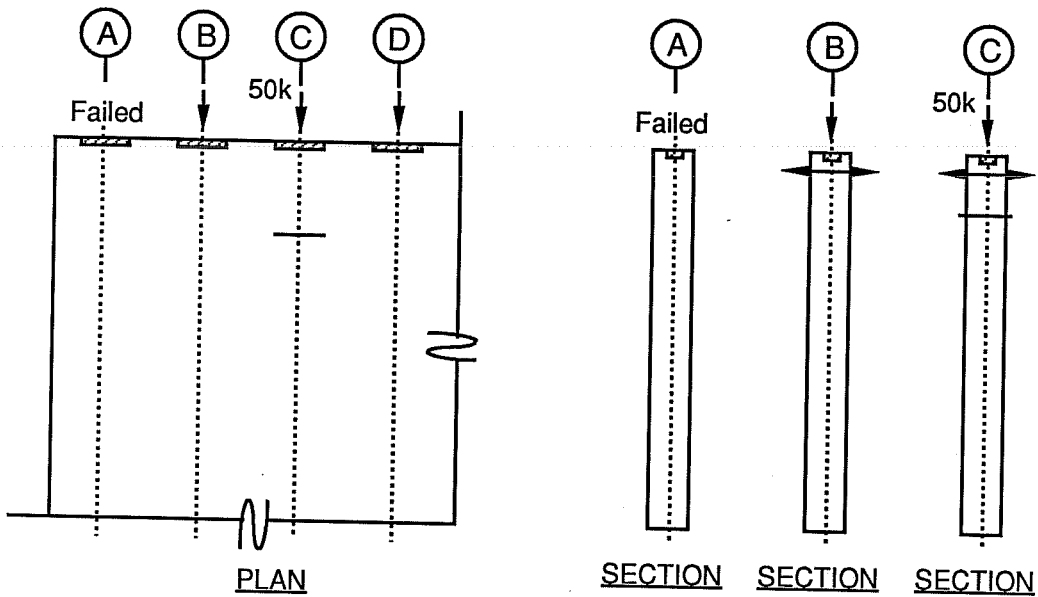
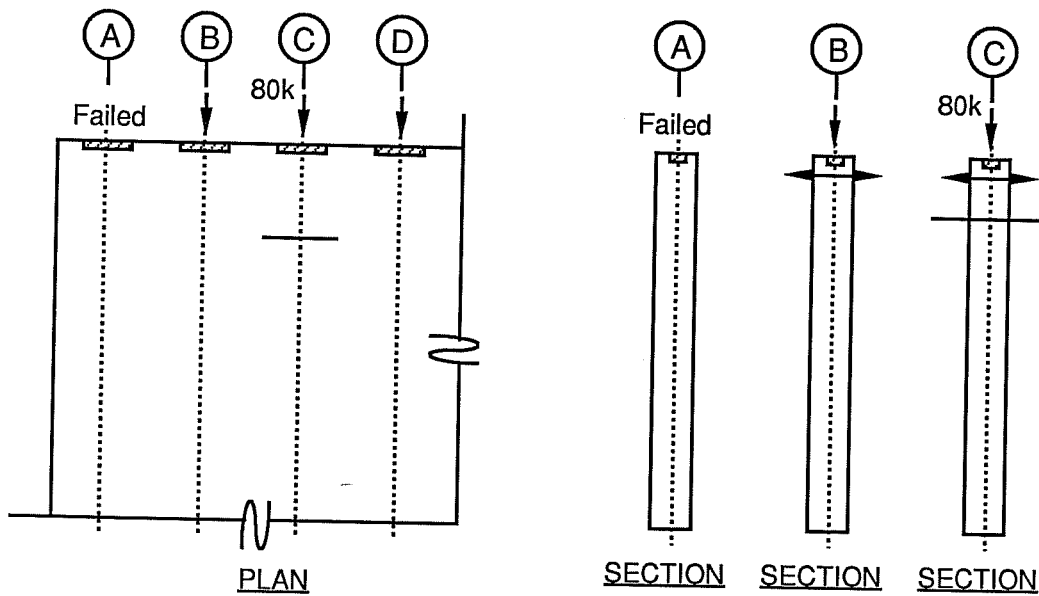


Figure 4.17 - Slab #3 Failure at Anchor A



(a) Anchor C Loaded to 50k and All Other Anchors Loaded to 35k



(b) Anchor A Loaded to 80k & All Other Anchors Loaded to 35k
Anchor C Failed at 80k

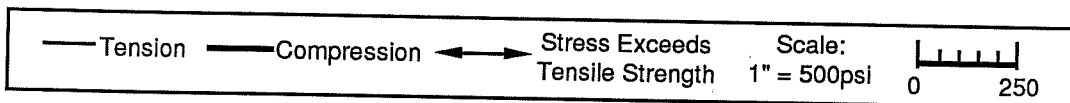


Figure 4.18 - Slab #3 Failure at Anchor C

significant strains before the concrete is cracked. To simulate cracking due to other than load effects in Slab #2 (Figure 4.19), the horizontal steel passed through preformed vertical cracks which divided six separate anchorage zones into two halves each along their ducts (Figures 3.4).

The horizontal steel required by AASHTO in a bridge deck to prevent deterioration due to temperature changes is referred to as temperature steel, and it is $0.25 \text{ in}^2/\text{linear ft}$ of slab/face. That corresponds with $0.0625 \text{ in}^2/\text{ft}$ at half-scale. Two steel reinforcement ratios were used in Slab #2 (Figure 4.19) - #3 bars at 10" center to center spacing on the West side ($0.13 \text{ in}^2/\text{ft}$, double temperature steel) and #2 bars at 14" center to center spacing on the East side ($0.042 \text{ in}^2/\text{ft}$, 64% of temperature steel).

4.2.3.2 Effects of Stressing Sequence

The highest stress created in any of the horizontal reinforcement during initial loading to normal service load conditions was 19.6 ksi in the #2 bar located 6" ahead of Anchor A and across a pre-formed crack. This maximum reinforcement stress was created, as in the unreinforced slabs, under the end anchor when every second anchor was stressed across the slab (Figure 4.20). As in the unreinforced anchorage zones, the calculated bursting stress ahead of interior Anchor C was reduced when all the anchors became loaded (Figure 4.21). The vertical reinforcement did not indicate high stresses because of the concrete's tensile capacity in the uncracked vertical plane.

4.2.3.3 Loading to Failure

Three of the eight anchors in Slab #2 were loaded to failure and those anchors had cross ties for anchorage zone reinforcement (Figure 4.22). Anchor A was an end anchor with a 1 plate width edge distance, and it failed at 75 kips. Anchor D was an interior anchor

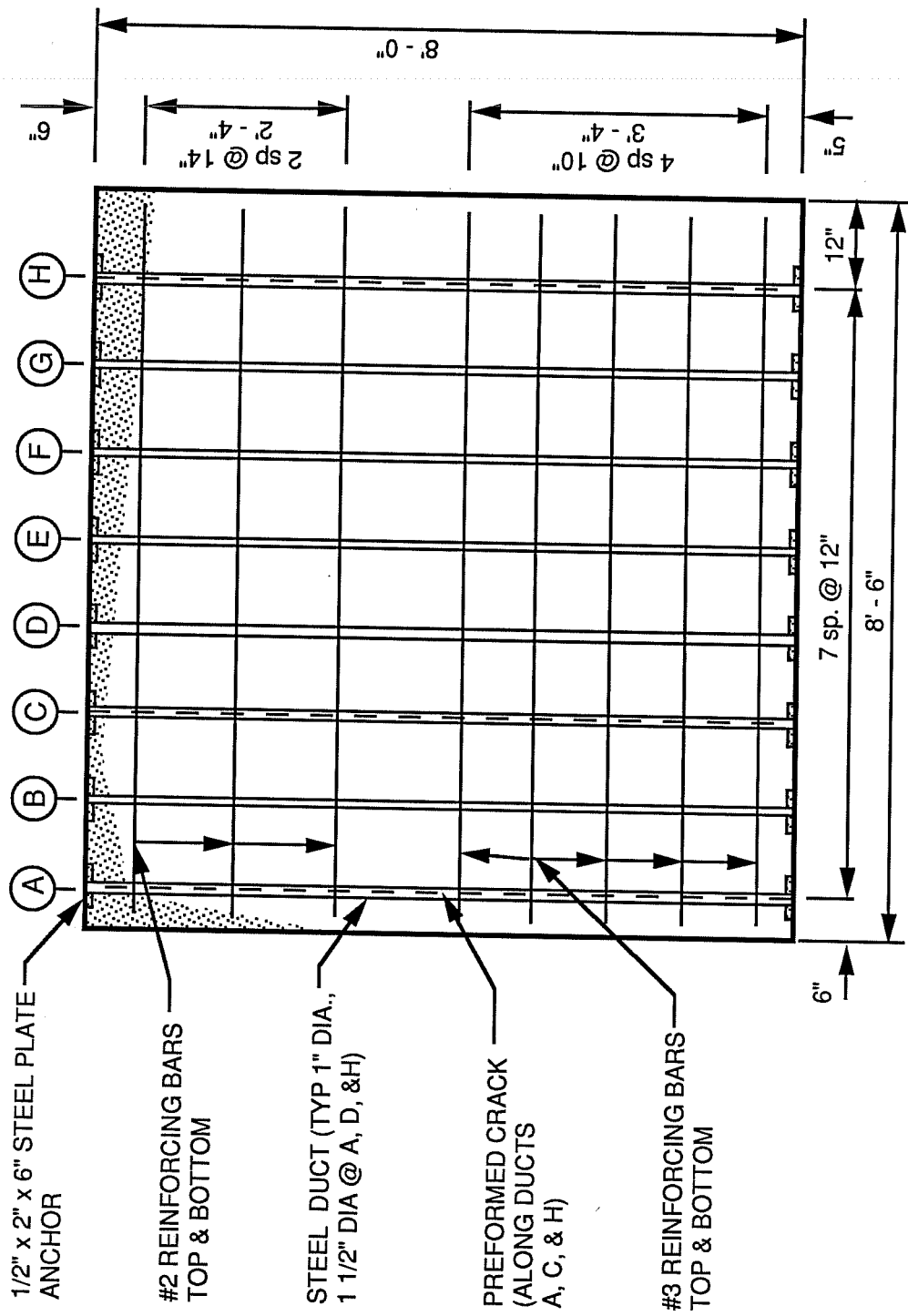
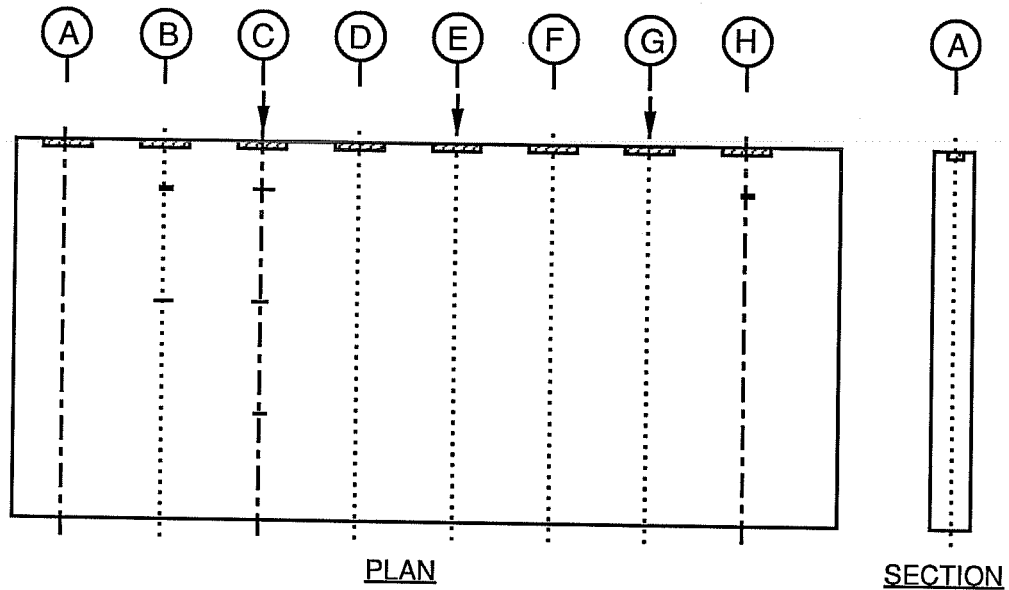
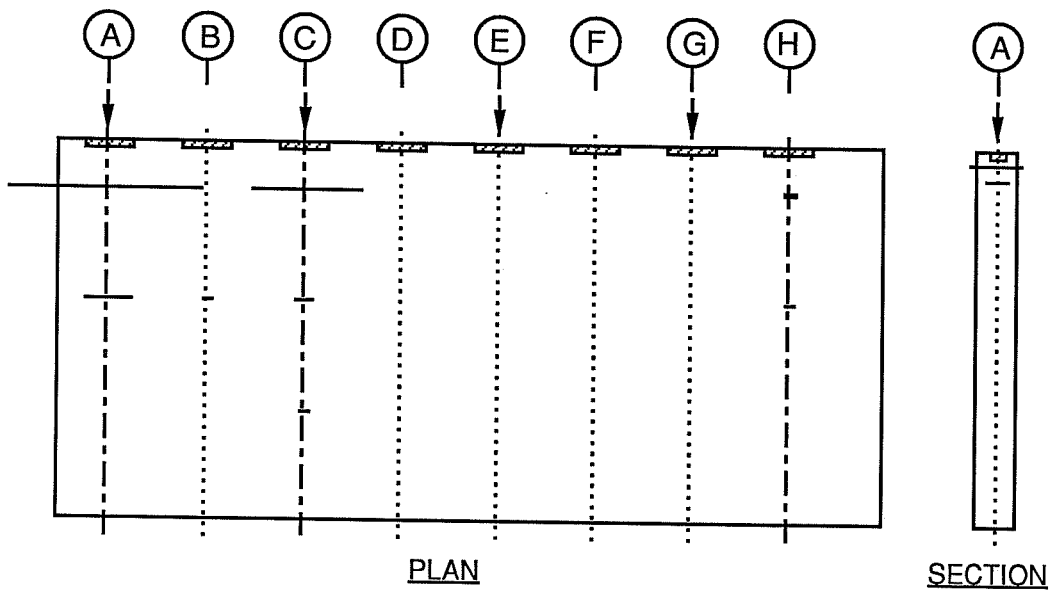


Figure 4.19 - Plan of Slab #2



(a) Anchors C,E, & G Loaded to 30k



(b) Anchors A,C,E, & G Loaded to 30k

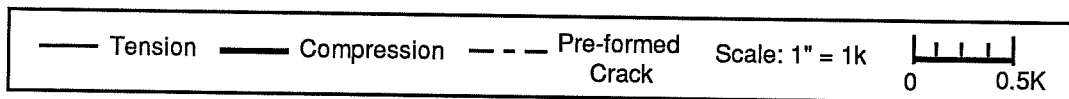
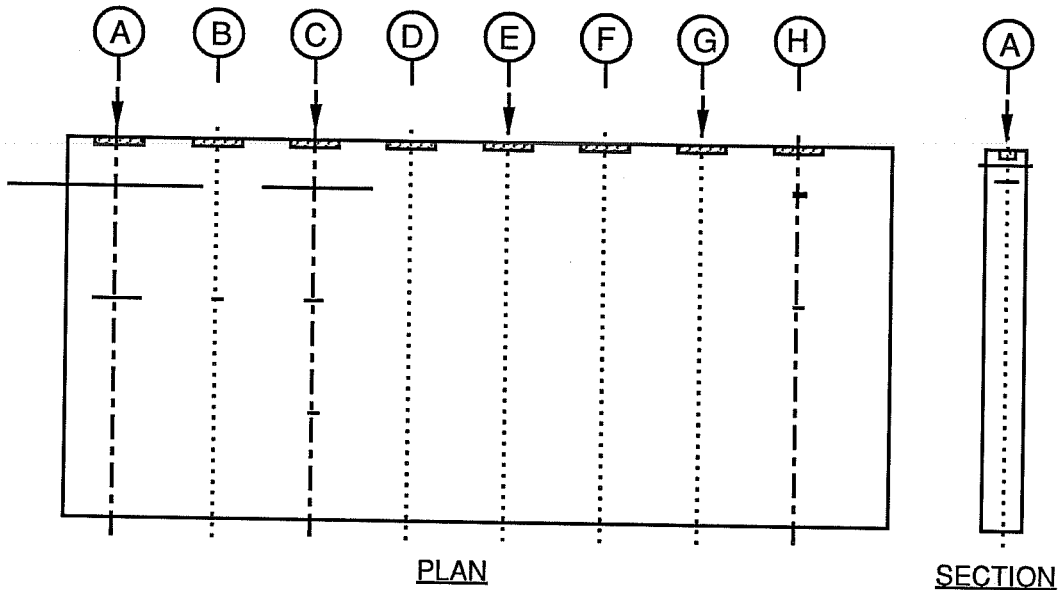
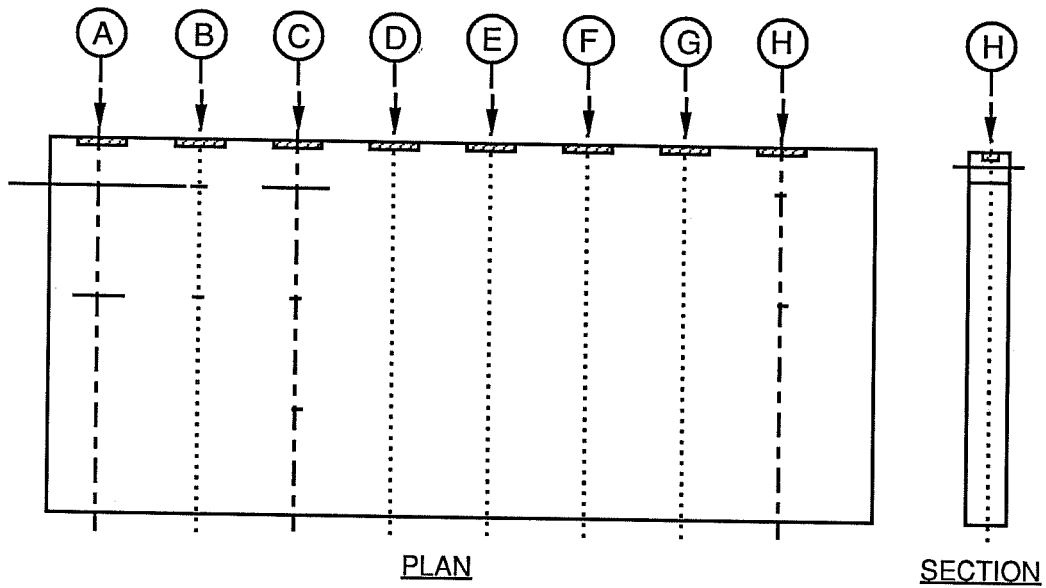


Figure 4.20 - Maximum Calculated Force in #2 Reinforcing Bars of Slab #2
(Yield Point for # 2 Steel Bar is 3.28k)



(a) Anchors A,C,E, & G Loaded to 30k



(b) All Anchors Loaded to 30k

— Tension	— Compression	- - - Pre-formed Crack	Scale: 1" = 1k	0 0.5K
-----------	---------------	------------------------	----------------	--------

Figure 4.21 - Adjacent Anchor Loading Effects on Calculated Forces in Slab #2 (yield point for # 2 steel bar is 3.28k)

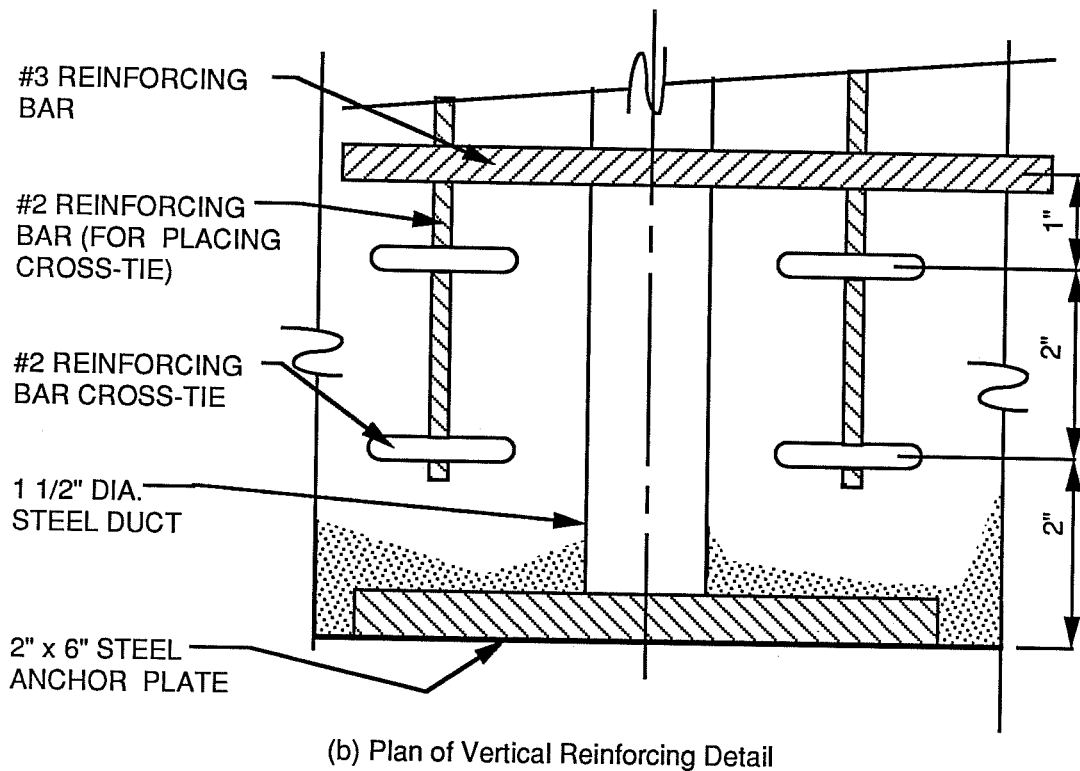
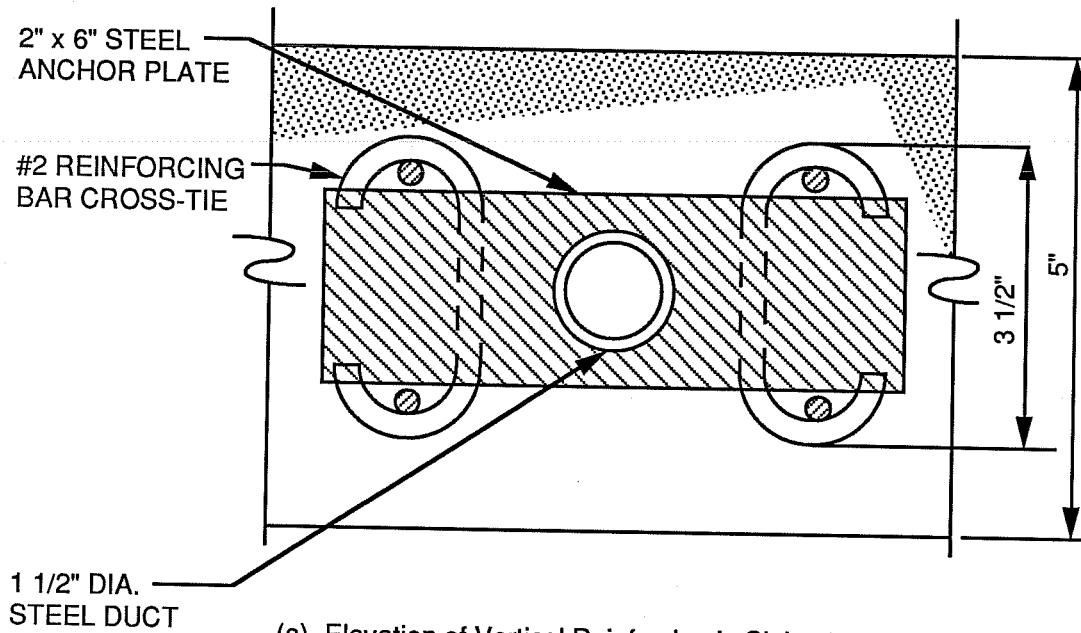


Figure 4.22 - Reinforcing Detail in Slab #2

which failed at 102 kips. Anchor H was also an end anchor with an edge distance of 2 plate widths, and it failed at 95 kips. The average f_b/f'_c ratio was 1.86 for these horizontally reinforced anchorage zones with cross ties.

During loading, cracks extended to the surface ahead of Anchor A East along the preformed crack beginning at 25 kips and extending in stages until failure (Figure 4.23). Crack opening along the preformed crack also occurred at Anchor A West and Anchor H West.

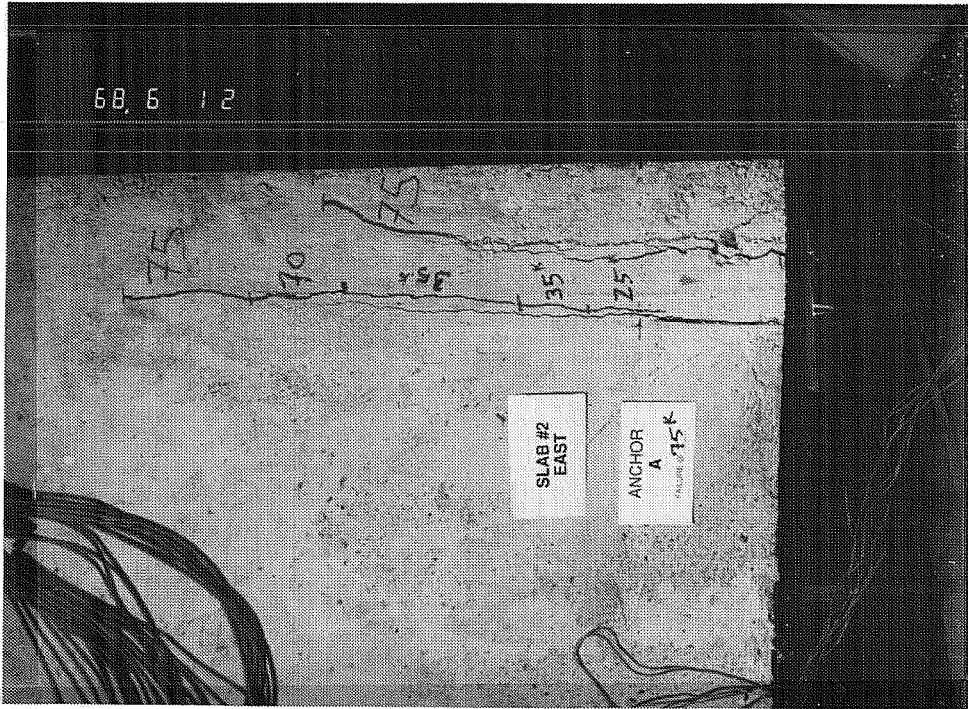
Figures 4.24 through 4.26 illustrate the reinforcement stresses in Slab #2 as its anchorages were taken to failure. Anchorages A and D failed on the lightly horizontally reinforced end and anchorage H failed on the heavily reinforced end. Horizontal reinforcing has no definite effect on failure loads. The initial vertical reinforcement stresses were lower than the horizontal reinforcement stresses because concrete tensile strength carried some of the vertical plane stresses, while the horizontal reinforcement carried all of the horizontal plane stresses across the preformed cracks. The final vertical reinforcement stresses were higher due to internal concrete cracking. The failure geometry of Anchors A and H did not exhibit any characteristics which could be attributed to the preformed cracks.

4.2.4 Detail B - Back-Up Bars

Slab #3 (Figure 4.7) included back-up bars as additional horizontal anchorage zone reinforcement ahead of Anchors K and L which as shown in Figure 4.27. The back-up bars did not yield or reach high stresses during loading of the anchors. Anchorage K failed at 85 kips and anchorage L, which was an end anchor with a half plate edge distance, failed at 55 kips. In failure, Anchor L formed a shear cone ahead of the anchor, which is shown in Figure 4.2, and split the top and bottom of the slab apart.

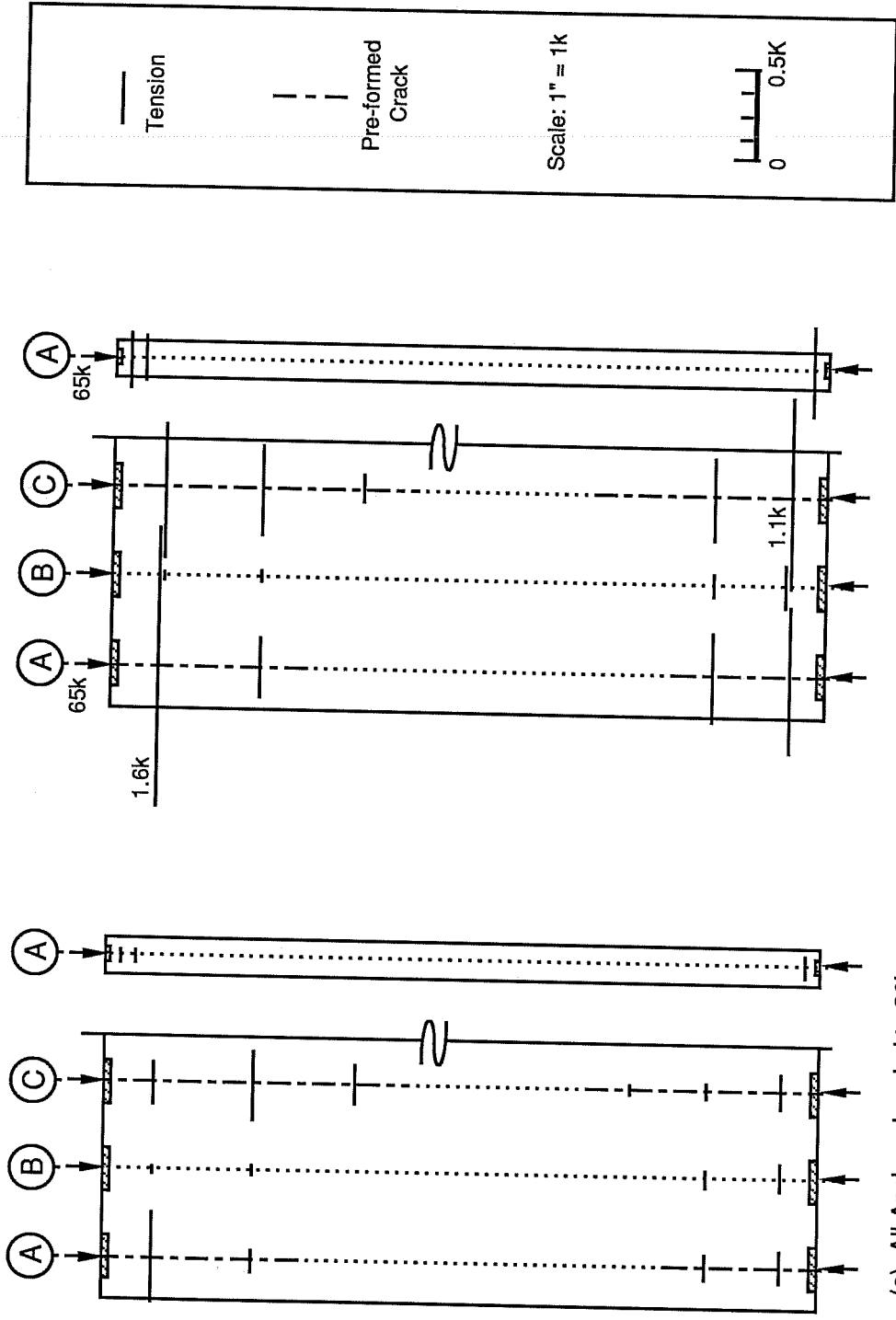


(a) Cracking Began at 25 Kips.



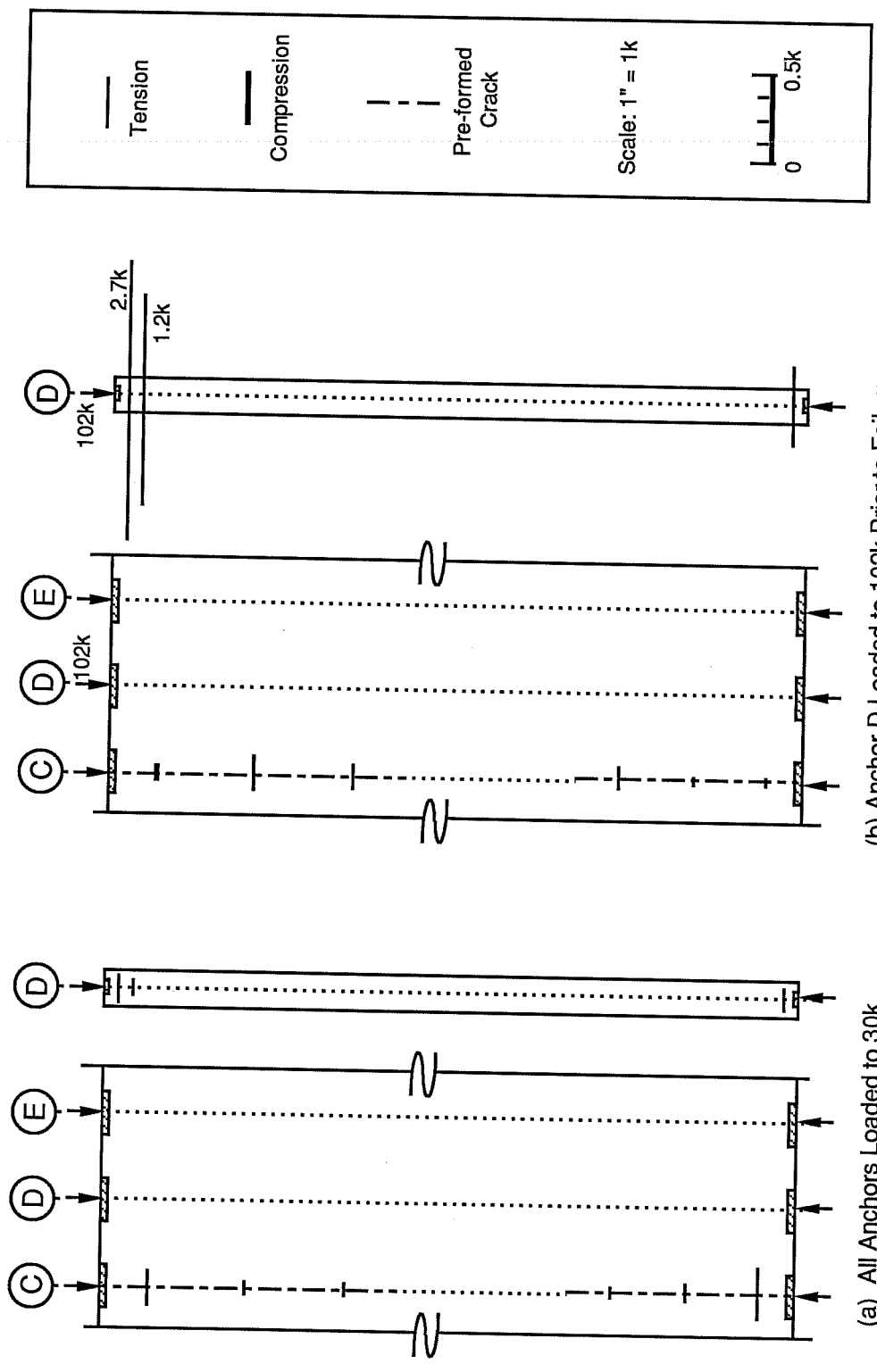
(b) Cracking Extended with Loading Until Failure

Figure 4.23 - Cracking Along the Preformed Crack



(a) All Anchors Loaded to 30k (b) Anchor A Loaded to 65k Prior to Failure

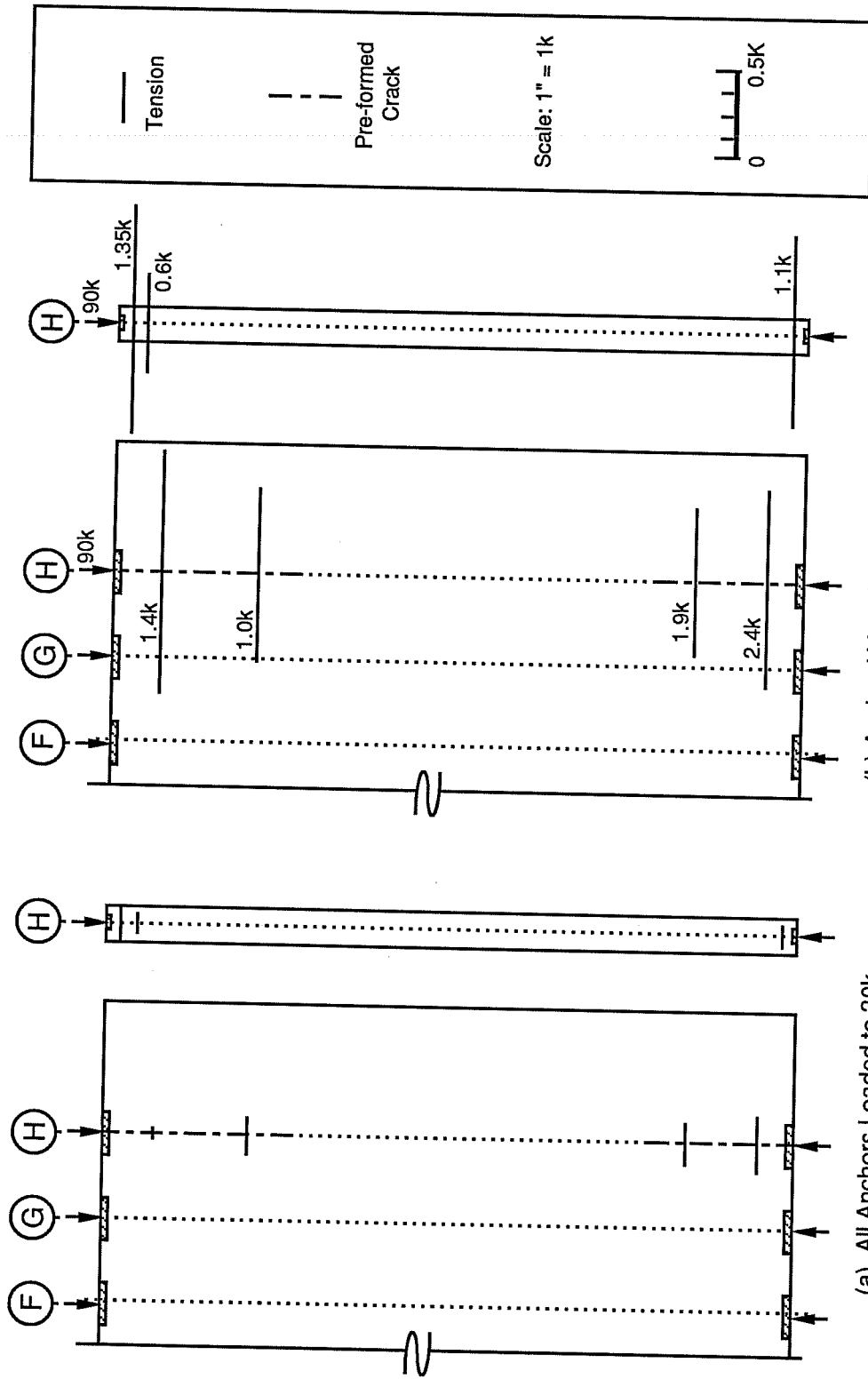
Figure 4.24 - Slab #2 Failure at Anchor A



(b) Anchor D Loaded to 102k Prior to Failure

(a) All Anchors Loaded to 30k

Figure 4.25 - Slab #2 Failure at Anchor D



(a) All Anchors Loaded to 30k
(b) Anchor H Loaded to 90k Prior to Failure

Figure 4.26 - Slab #2 Failure at Anchor H

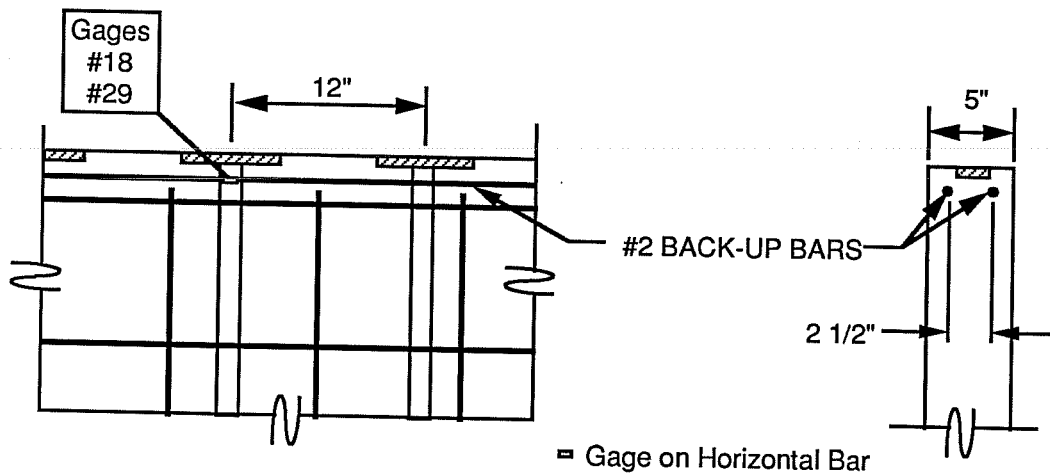


Figure 4.27 - Slab #3 Detail @ Anchors K & L
Back-up Bars with Gages

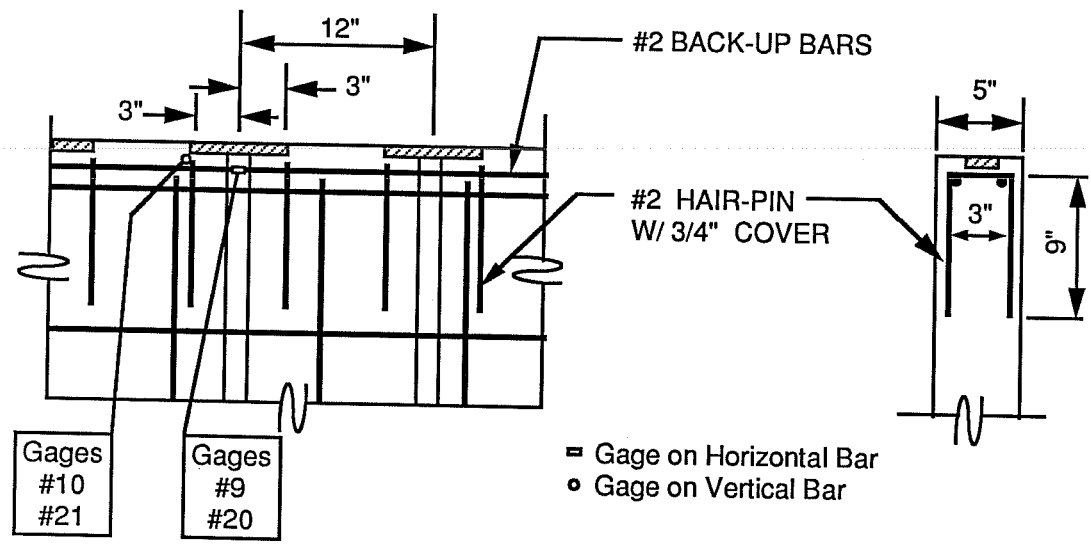
4.2.5 Detail P - Hairpins and Back-Up Bars

Figure 4.28 shows the stresses in the hairpins used as vertical anchorage zone reinforcement ahead of Anchors E and F in Slab #3. The largest increase in stress was at an anchor load of 80 kips. This indicates internal cracking in the anchorage zone. The back-up bars did not exceed stresses of 5 ksi during anchor loading.

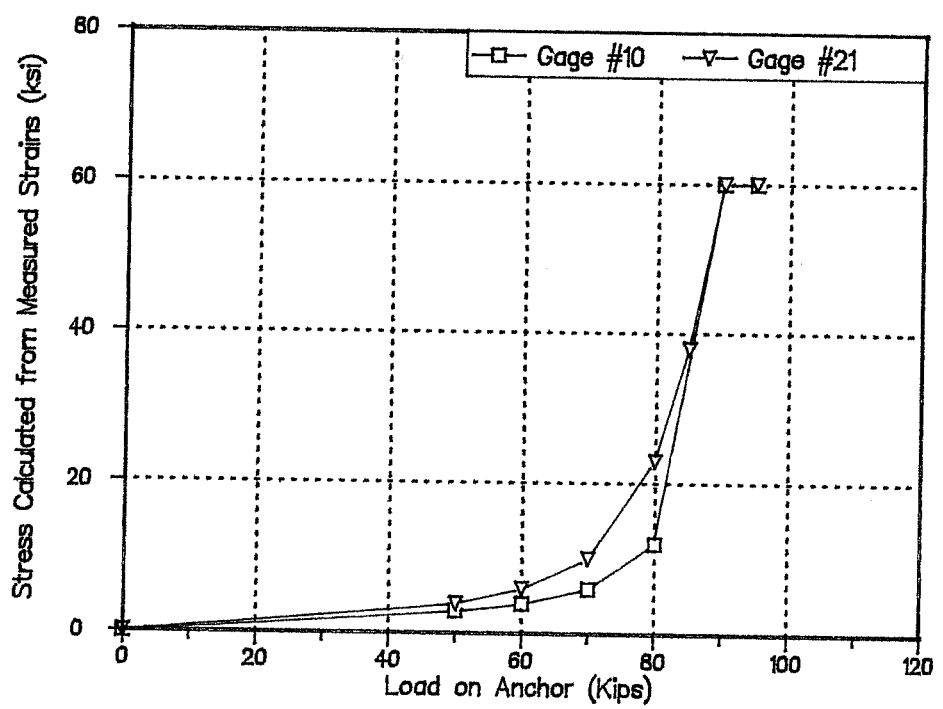
4.2.6 Detail C - Cross Ties and Back-Up Bars

Figure 4.29 shows the stresses in the cross ties used as vertical anchorage zone reinforcement ahead of Anchors G and H in Slab #3. As with the hairpins, the cross ties greatly increased in stress at around an 80 kip anchor load. The cross ties placed 12'' ahead of the anchor and the back-up bars did not carry much stress prior to failure. Figure 4.30 shows the failure geometry of Anchor H.

Section 4.2.3 discusses the performance of the cross-ties in Slab #2.

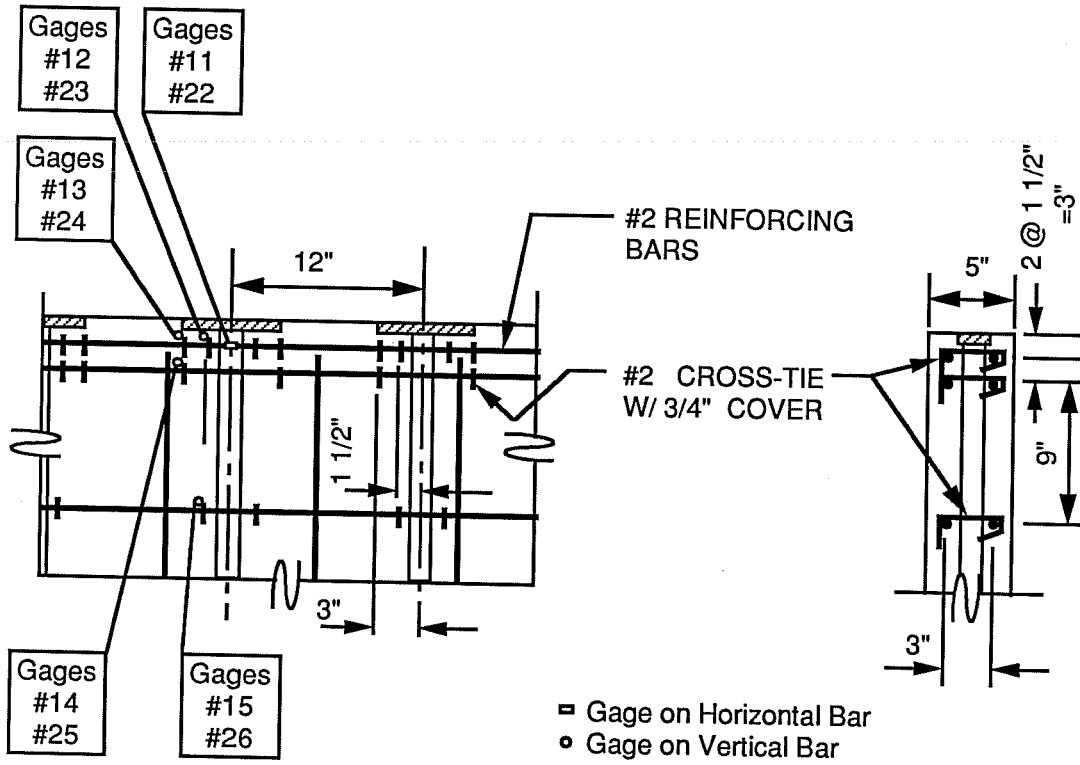


(a) Back-up Bars and Hair Pins @ Anchors E & F

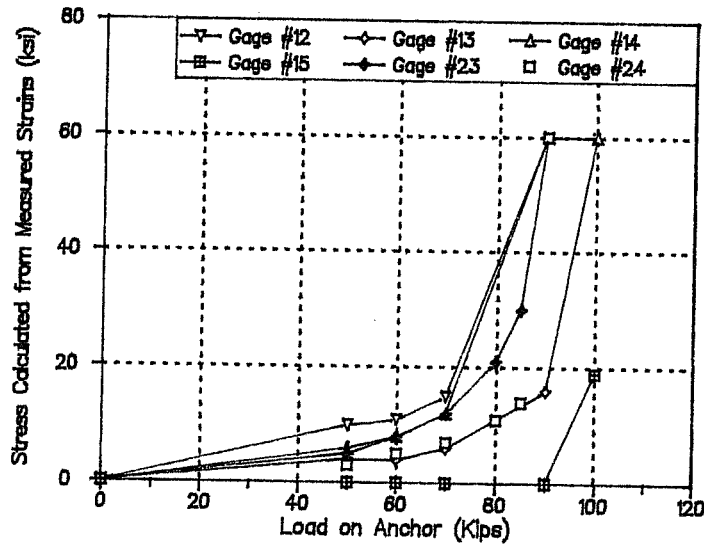


(b) Bar Stresses During Anchor Loading

Figure 4.28 - Slab #3 Hairpin Detail

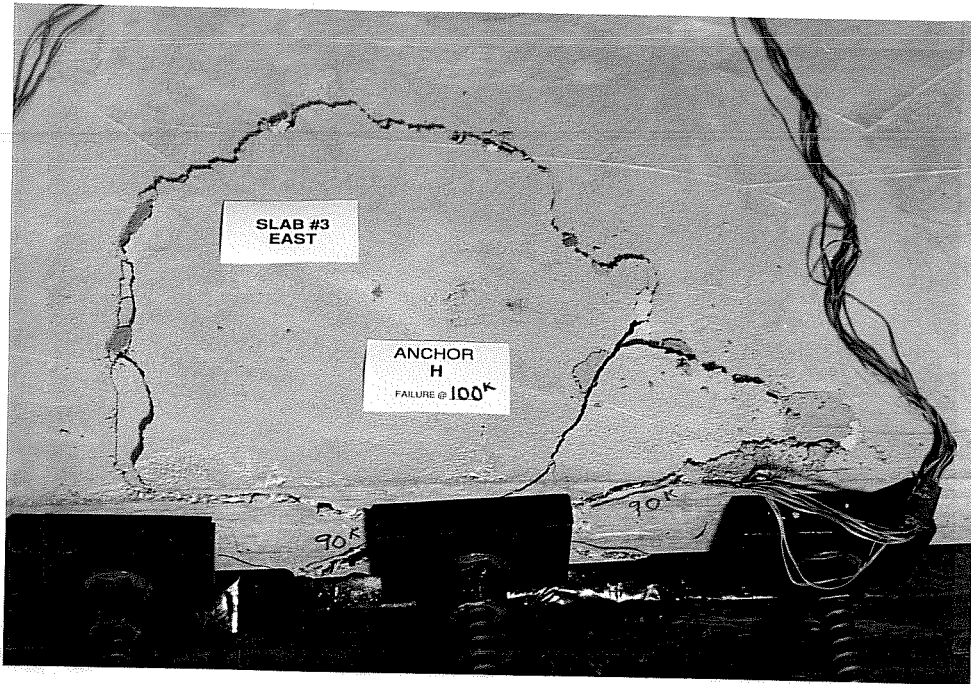


(a) Cross Ties @ Anchors G & H

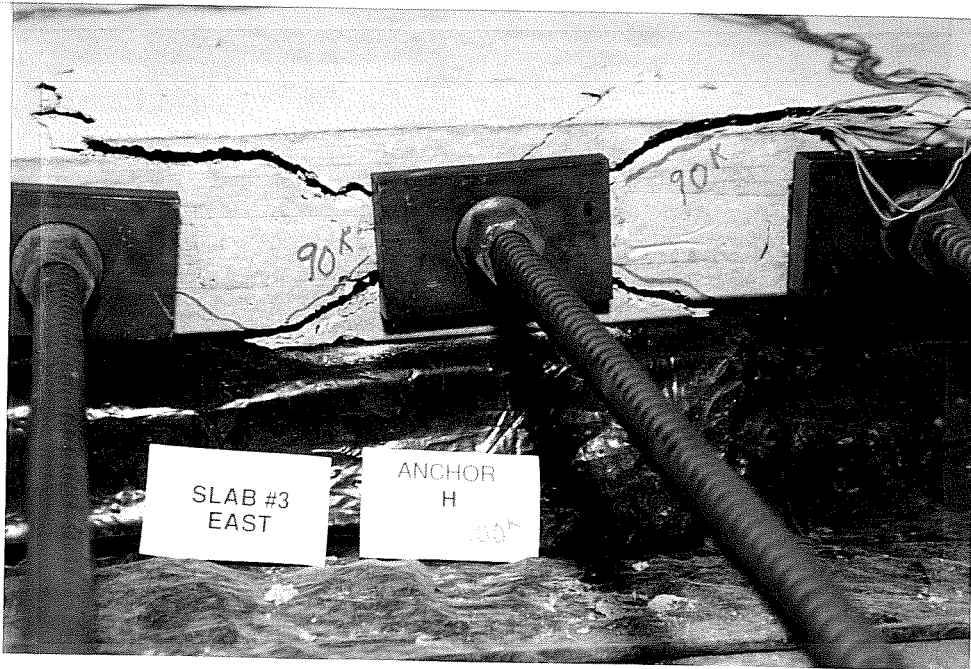


(b) Bar Stresses During Anchor Loading

Figure 4.29 - Slab #3 Cross Ties Detail



(a) Top View



(b) Edge View

Figure 4.30 - Failure in Slab #3 at Anchor H

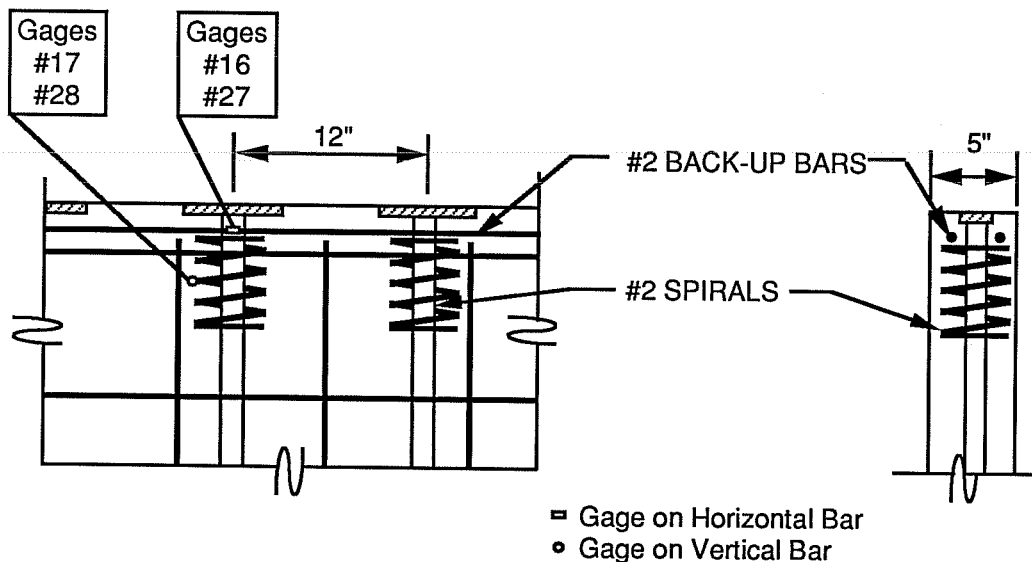


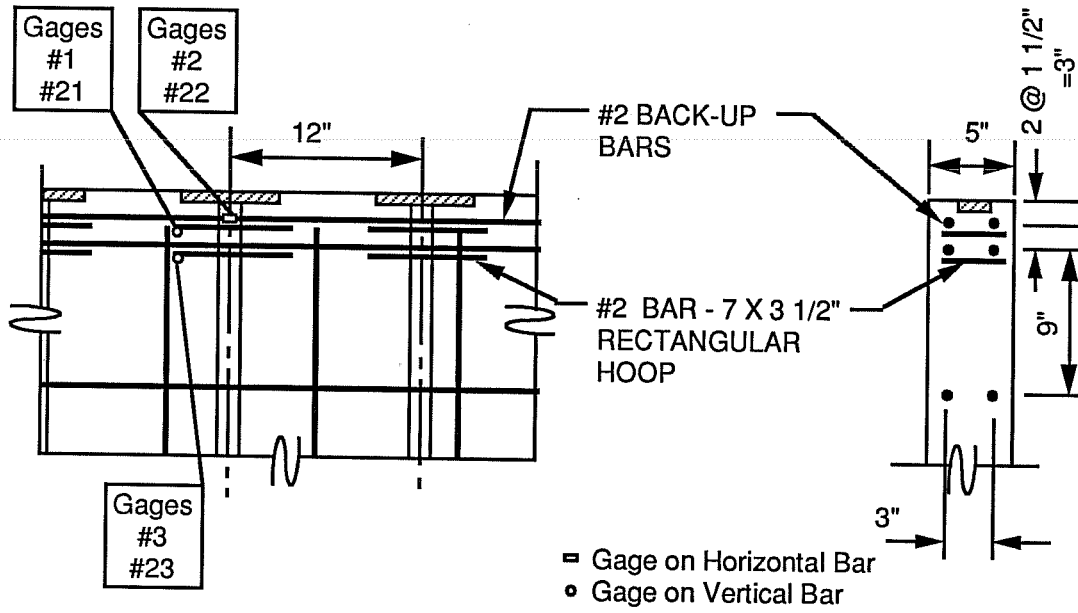
Figure 4.31 - Slab #3 Spiral Detail @ Anchors I & J

4.2.7 Detail S - Spiral and Back-Up Bars

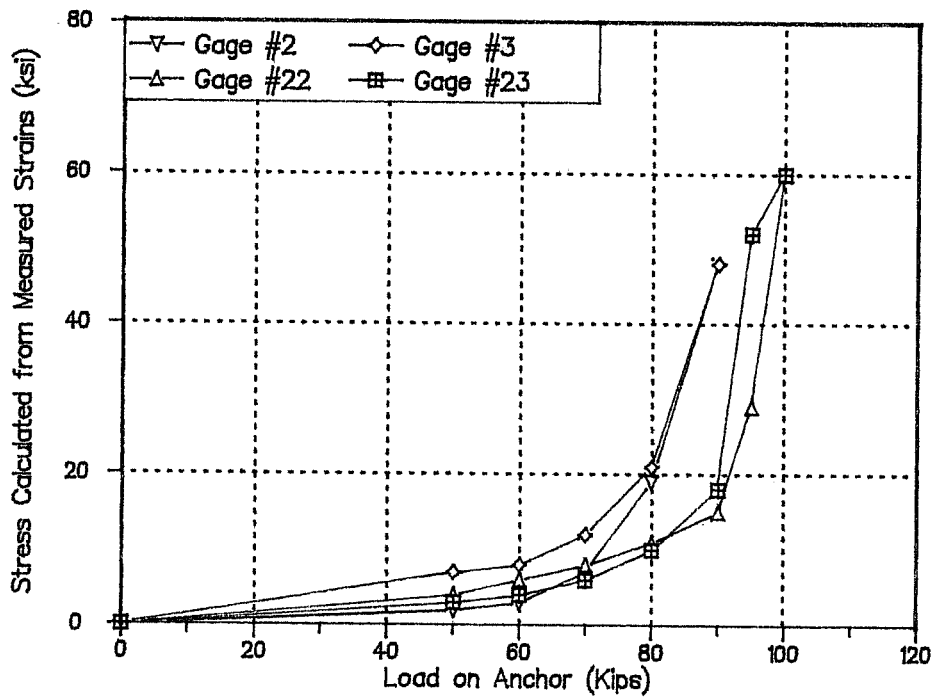
Figure 4.31 shows the spiral used as vertical anchorage zone reinforcement ahead of Anchors I and J in Slab #3. Neither the spiral reinforcement nor the back-up bars appeared to reach yield before anchor failure and gage destruction.

4.2.8 Detail H - Hoops and Back-Up Bars

Figure 4.32 shows the stresses in the hoops used as vertical anchorage zone reinforcement ahead of Anchors A and B in Slab #4 (Figure 4.33). At anchor pair A the control detail failed at 90 kips because the steel reinforcement had been moved during casting and had insufficient concrete cover. The other anchor failed at the hoop detail at 100 kips. During loading, the two hoops of a detail gained stress simultaneously. Both details also seemed to increase in the rate of reinforcement stress per load at a specific load. The load was 80 kips for Anchor A and 90 kips for Anchor B. Anchor A was an end anchor.



(a) Hoops @ Anchors A & B



(b) Bar Stresses During Anchor Loading

Figure 4.32 - Slab #4 Hoops Detail

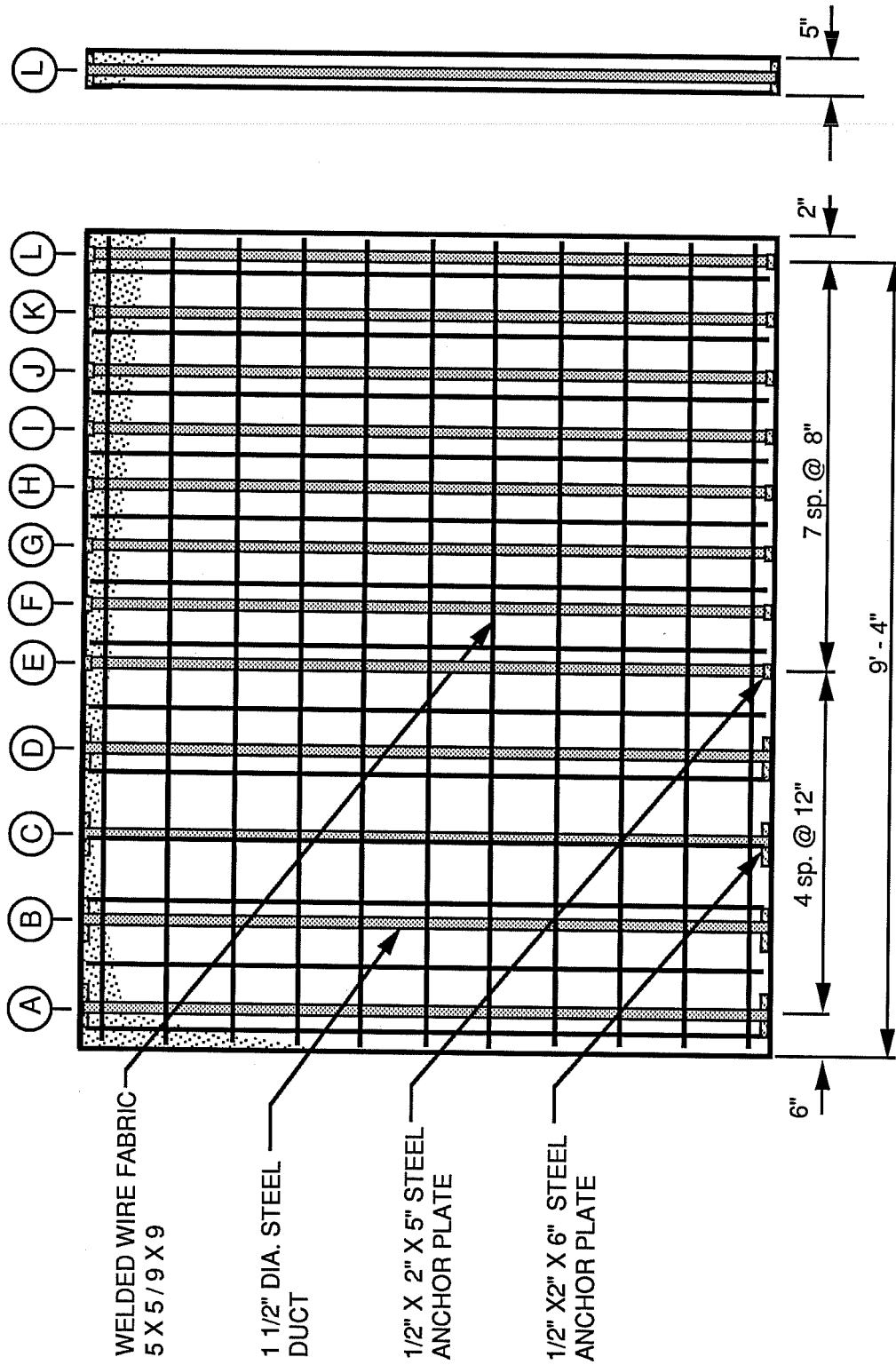


Figure 4.33 - Plan of Slab #4

4.2.9 Detail HP - Hairpin Hoops and Back-Up Bars

Figure 4.34 shows the stresses in the hoops made with two hairpins used as vertical anchorage zone reinforcement ahead of Anchors A and B in Slab #4. These hairpins were easy to install as hoops after the ducts had been placed. The increase of stress for these gages occurred with loads from 80 to 90 kips on the anchor.

4.2.10 Control Detail

The control detail (Figure 3.7), consisting of a hoop made with two hairpins and a spiral, withstood all loading in the four strand horizontally oriented anchor series except at Anchor A of Slab #4, which contained a fabrication defect and failed at 90 kips.

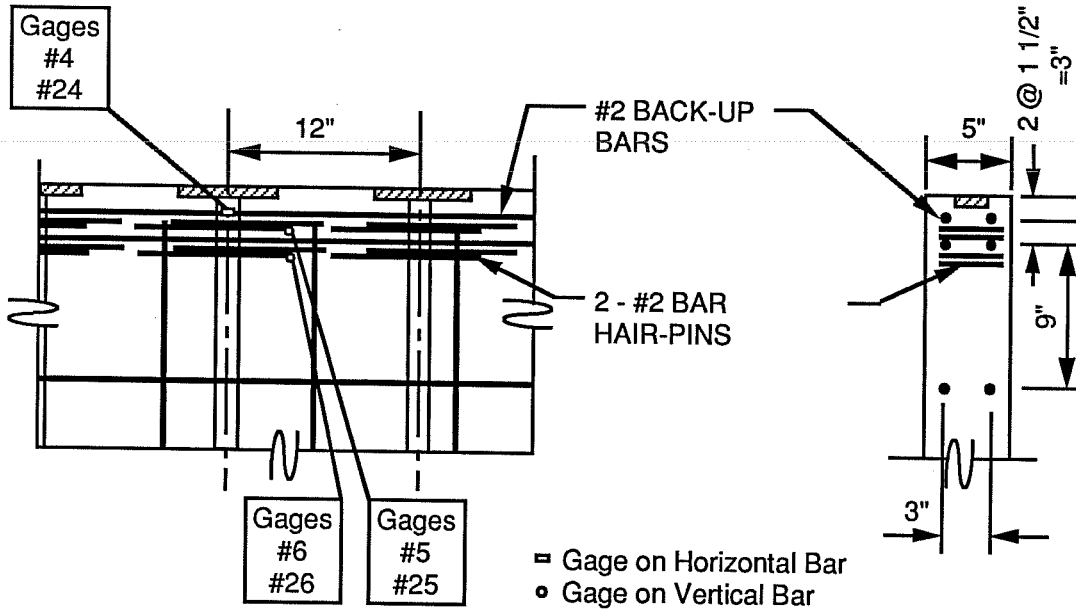
4.3 Half-Scale Four Strand Anchors - Vertical Orientation

4.3.1 General

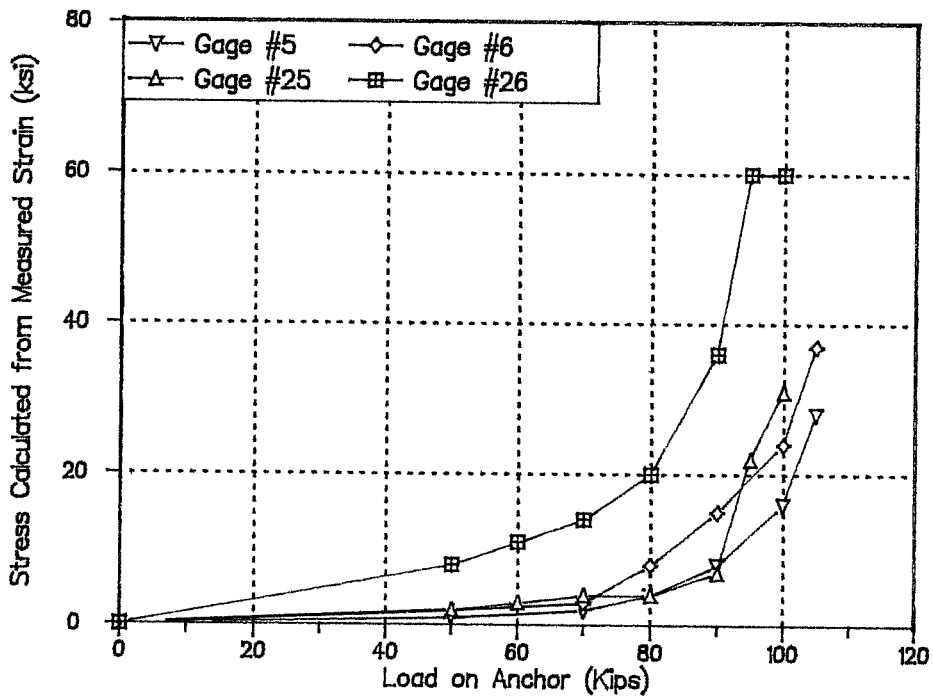
Slab #4 had eight vertically oriented four-strand anchor pairs spaced four plate widths apart center to center (Figure 4.33). The failures of these anchorages were used to evaluate effects of vertically oriented anchors on failure geometry and anchorage zone reinforcing efficiency. Figure 4.35 shows the failed anchor J. The semi-circular bursting region is much more confined for the vertically oriented anchor than for the horizontally oriented anchor shown in Figure 4.1. The failure loads and f_b/f'_c ratios for these anchors are shown in Figures 4.36 and 4.37, respectively, and in Table 4.2.

Unlike the horizontally oriented anchor specimens, the vertically oriented anchor specimens demonstrated high stresses in the back-up bars due to anchor loading.

The hairpins and the spirals were the most effective reinforcement. They average failure loads for both reinforcement types were 92.5 kips and the average f_b/f'_c ratio was 1.90.



(A) Double Hairpins @ Anchors C & D



(b) Bar Stresses During Anchor Loading

Figure 4.34 - Slab #4 Double Hairpins Detail

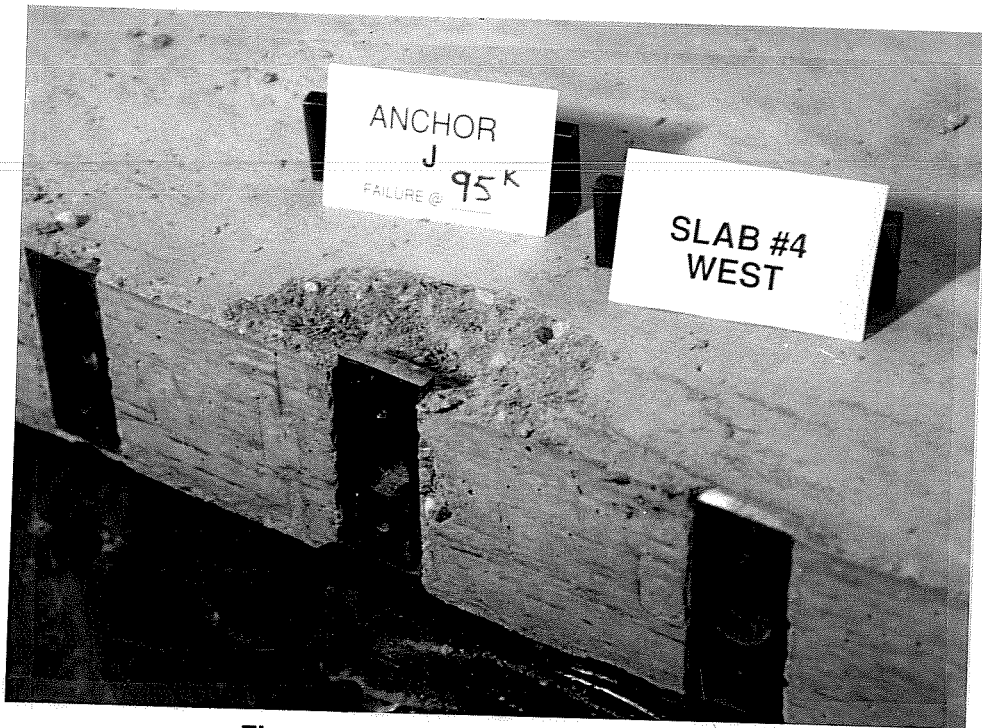
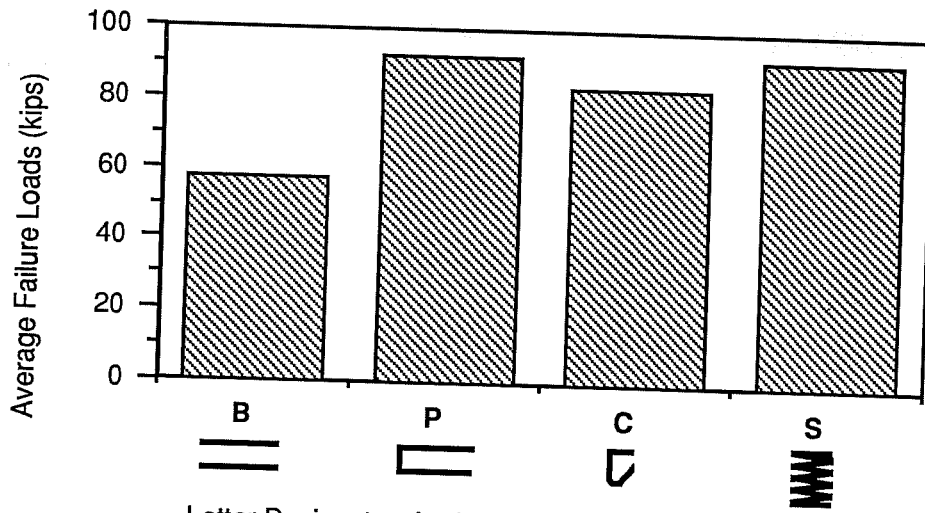


Figure 4.35 - Failed Anchor J in Slab #4



- B - Back-up Bars
- P - Hairpins w/Back-up Bars
- C - Cross Ties w/Back-up Bars
- S - Spiral w/Back-up Bars

Figure 4.36 - Average Failure Loads for Four Strand Vertically Oriented Anchors at Half-Scale

4.3.2 Detail B - Back-up Bars

Figure 4.38 shows the stress in a back-up bar used as horizontal anchorage zone reinforcement in Slab #4 at Anchor K. Anchor L, an end anchor, was also reinforced with only back-up bars, but its gage was destroyed prior to testing. The gaged back-up bar went through a large increase in stress as the load passed 60 kips. Anchor K failed at 70 kips.

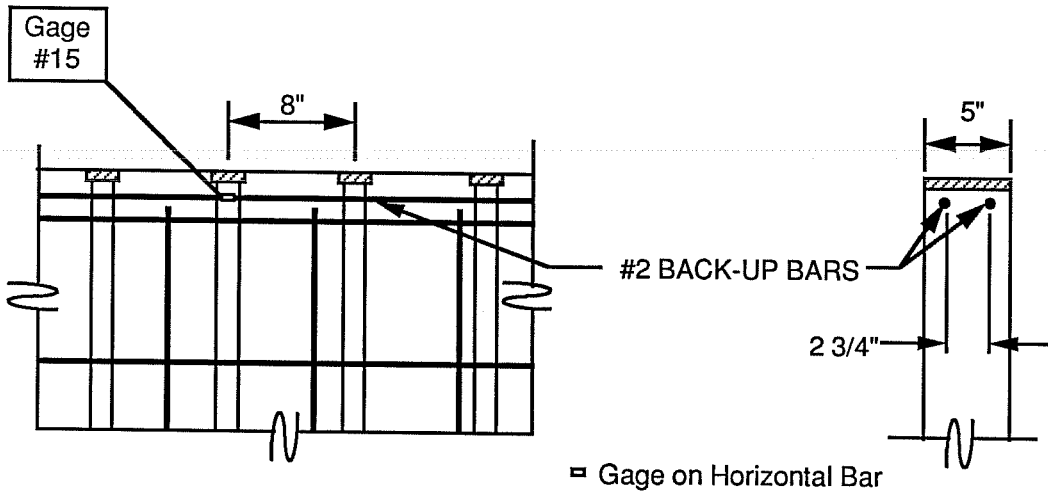
Anchor L was an end anchor with a 1 plate width (2") edge distance and failed at 45 kips (Figure 4.39). This was the only failure to demonstrate splitting of the horizontal plane during failure rather than splitting of the vertical plane. Comparison of Figure 4.2 to Figure 4.39 exhibits this difference.

4.3.3 Detail P - Hairpins and Back-Up Bars

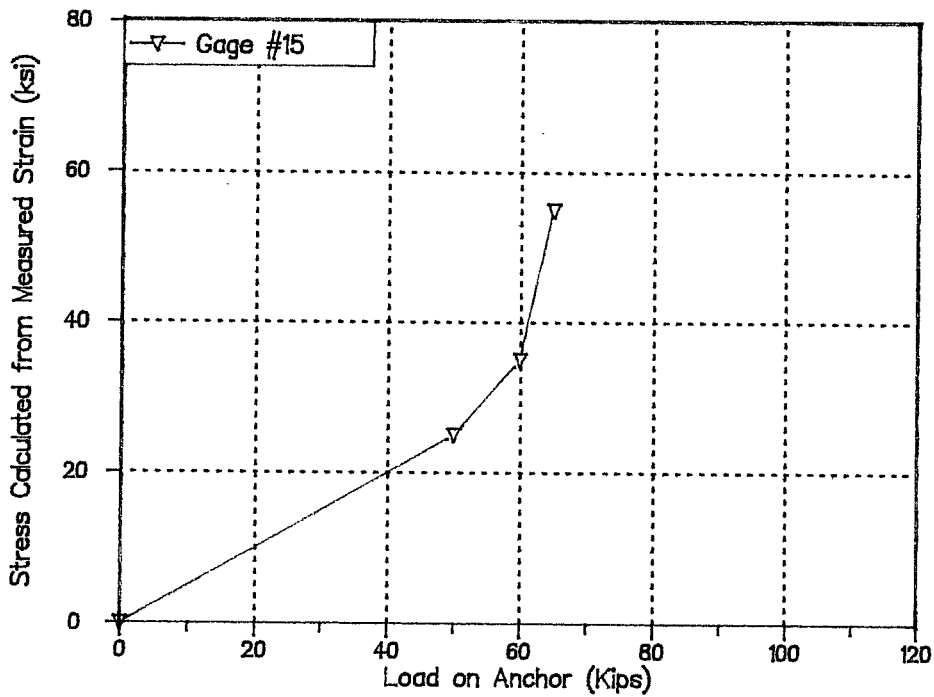
Figure 4.40 shows the stresses in the hairpins and back-up bars used in Slab #4 as anchorage zone reinforcement at Anchors E and F. The hairpins did increase in stress during anchor loading but did not reach the range of yielding, and neither did the one gaged back-up bar. The failure at Anchor F was at the control detail anchorage zone which was damaged by adjacent anchor failure; thus, 95 kips was actually less than the failure load for the hairpins and back-up bars detail.

4.3.4 Detail C - Cross Ties and Back-Up Bars

Figure 4.41 shows the cross ties and back-up bars used in Slab #4 as anchorage zone reinforcement at Anchorages G and H. A back-up bar ahead of Anchor G is the only bar that reached yield during loading and failure of these two anchorage zones. Yielding occurred around 70 kips.



(a) Back-up Bars @ Anchors K & L



(b) Bar Stresses During Anchor Loading

Figure 4.38 - Slab #4 Back-up Bars Detail

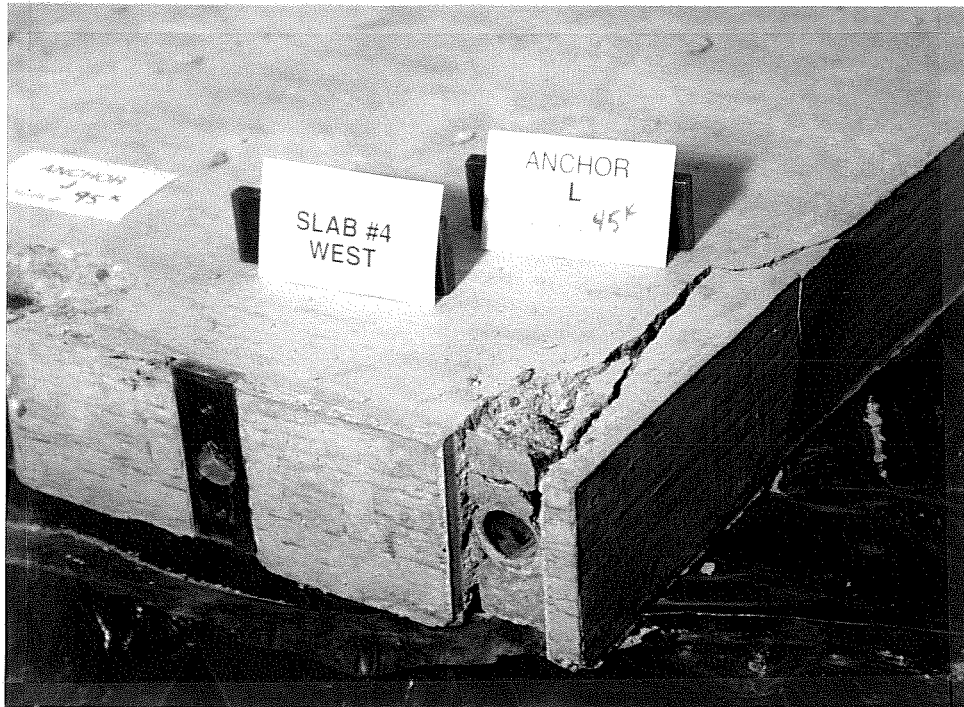
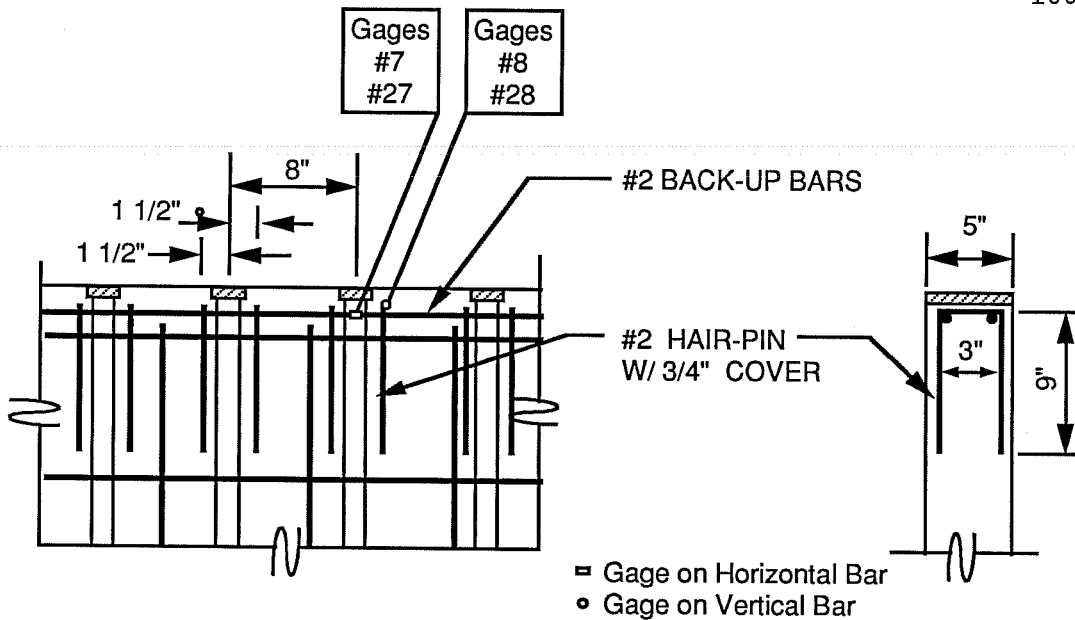
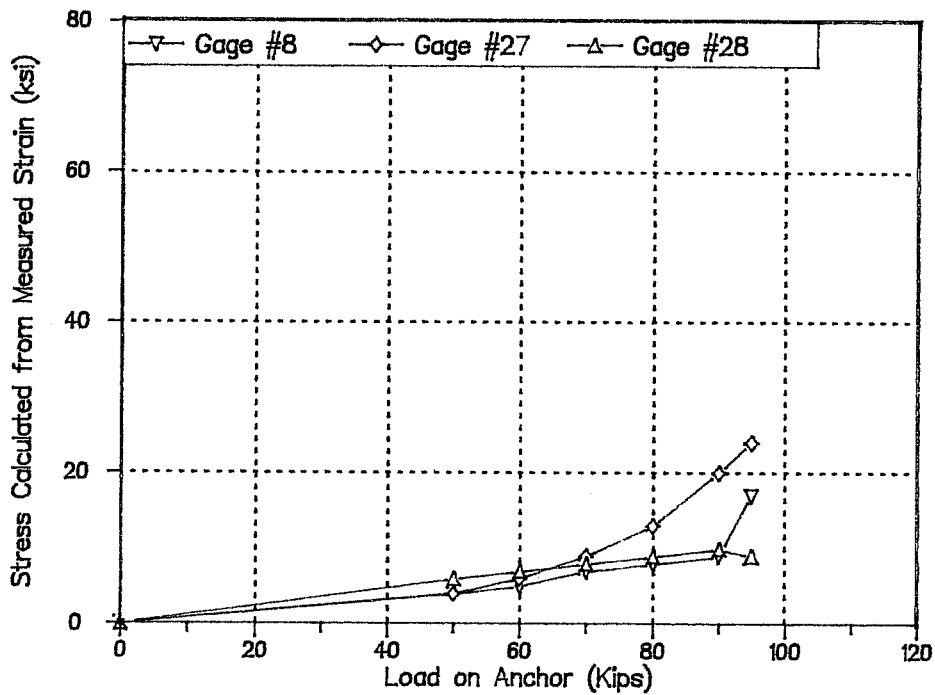


Figure 4.39 - Failed End Anchor L in Slab #4

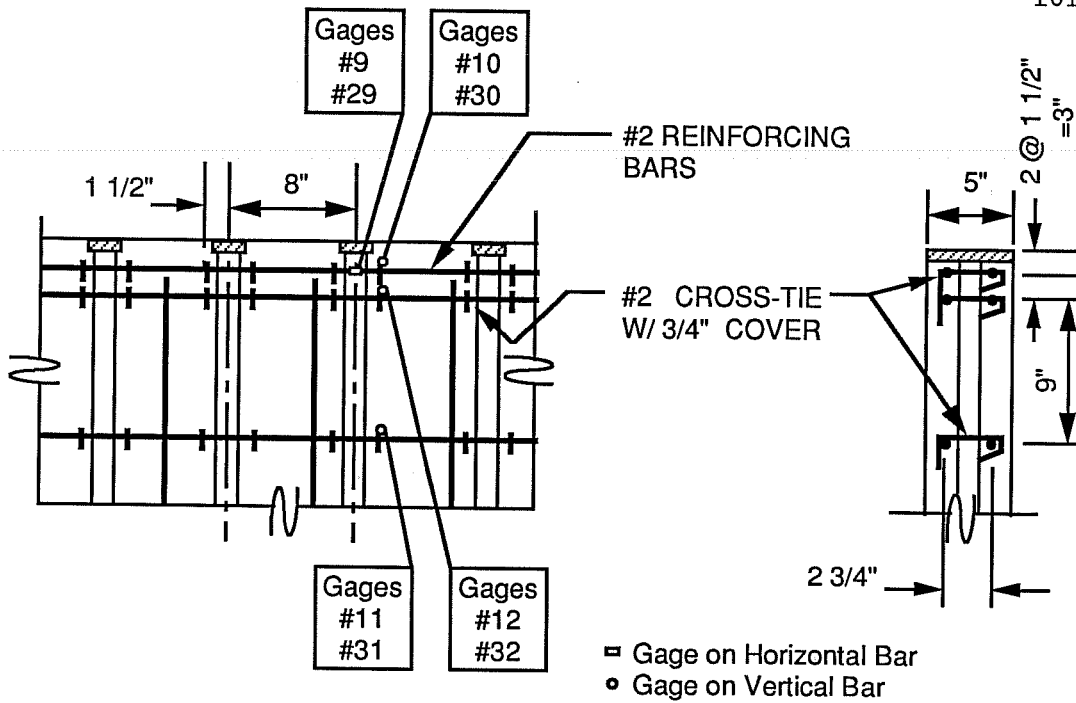


(a) Hairpins @ Anchors E & F

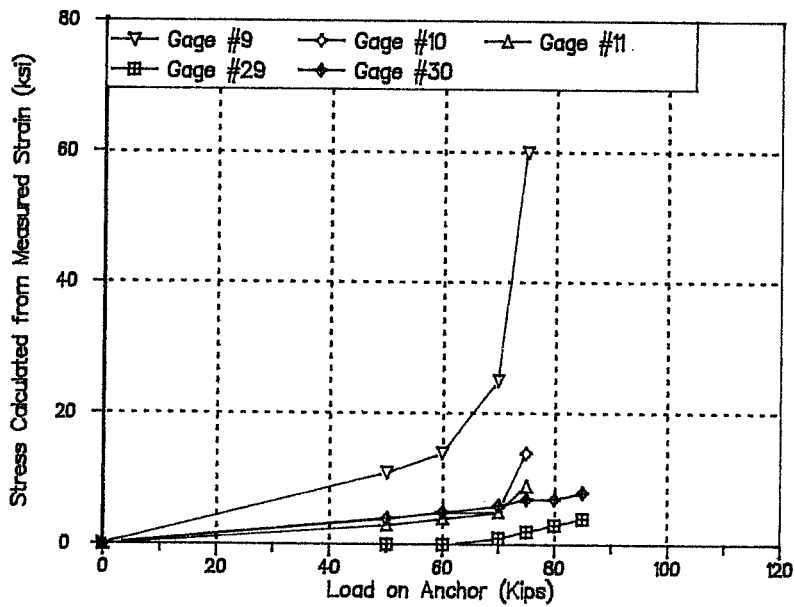


(b) Bar Stresses During Loading

Figure 4.40 - Slab #4 Hairpin Detail



(a) Cross Ties @ Anchors G & H



(b) Bar Stresses During Anchor Loading

Figure 4.41 - Slab #4 Cross Ties Detail

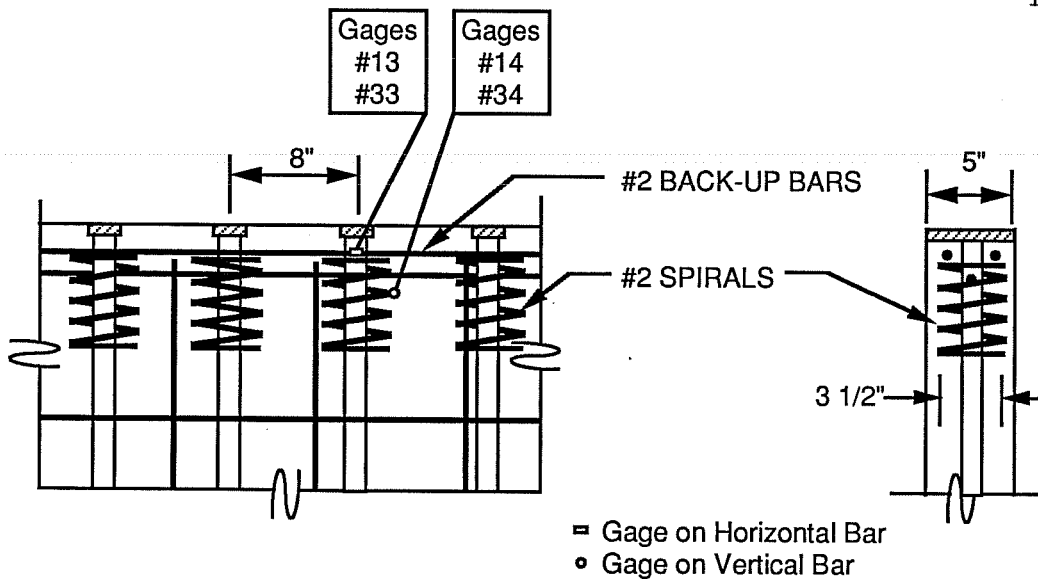


Figure 4.42 - Slab #3 Spiral Detail @ Anchors I & J

4.3.5 Detail S - Spiral

Figure 4.42 shows the spirals and cross-ties used as anchorage zone reinforcement in slab #4 at anchorages I and J. The stresses in the reinforcing did not reach critical levels prior to failure. The failure geometry was typical as shown in Figure 4.37.

4.3.6 Control Detail

The control detail (Figure 3.7), which consisted of two hairpins tied into a hoop and a spiral, withstood all loading applied to vertically oriented anchors except at Anchor F of Slab #4. At that anchor the control detail anchorage zone had been damaged by the failures of the adjacent anchors and failed at 90 kips.

4.4 Half-Scale Four Strand Anchors With Inclined Tendons

4.4.1 General

Inclined tendons were placed in Slab #5 (Figure 4.43) with eight half-scale horizontally oriented four strand anchor pairs. In general, these anchors carried higher loads relative to their concrete compressive strength. Figures 4.44 and 4.45 and Table 4.3 show the failure loads and f_b/f'_c ratios of the eight anchor pairs. During all failures, the extended ridge of the inclined anchorage zone was separated from the slab (Figure 4.46).

Back-up bars were not used in this specimen because they obviously could not be placed ahead of the anchors along the slab's jagged edge. The slab horizontal reinforcement was placed as close to the anchors as possible while still maintaining a 3/4" concrete cover.

4.4.2 Horizontal Anchorage Zone Reinforcement

Figure 4.47 shows the stresses in the horizontal reinforcement used as anchorage zone reinforcement at Anchorages G and H in Slab 5. Anchorage H was an end anchor and failed at 110 kips while the interior Anchor G failed at 105 kips. The stress in the reinforcing bars picked up dramatically immediately prior to failure, but no stress was measured above 20 ksi before failure, and the failure did not cause the slab to split along the tendon and across the reinforcement prior to failure.

4.4.3 Detail P - Hairpins

Figure 4.48 shows the stresses measured in the hairpins that were used as vertical anchorage zone reinforcement at anchorages A and B in Slab #5. Anchorage A was an end anchor and failed at a level of 95 kips. Anchorage B failed at 110 kips. In both anchorages, the stress in the hairpins rose gradually with the load,

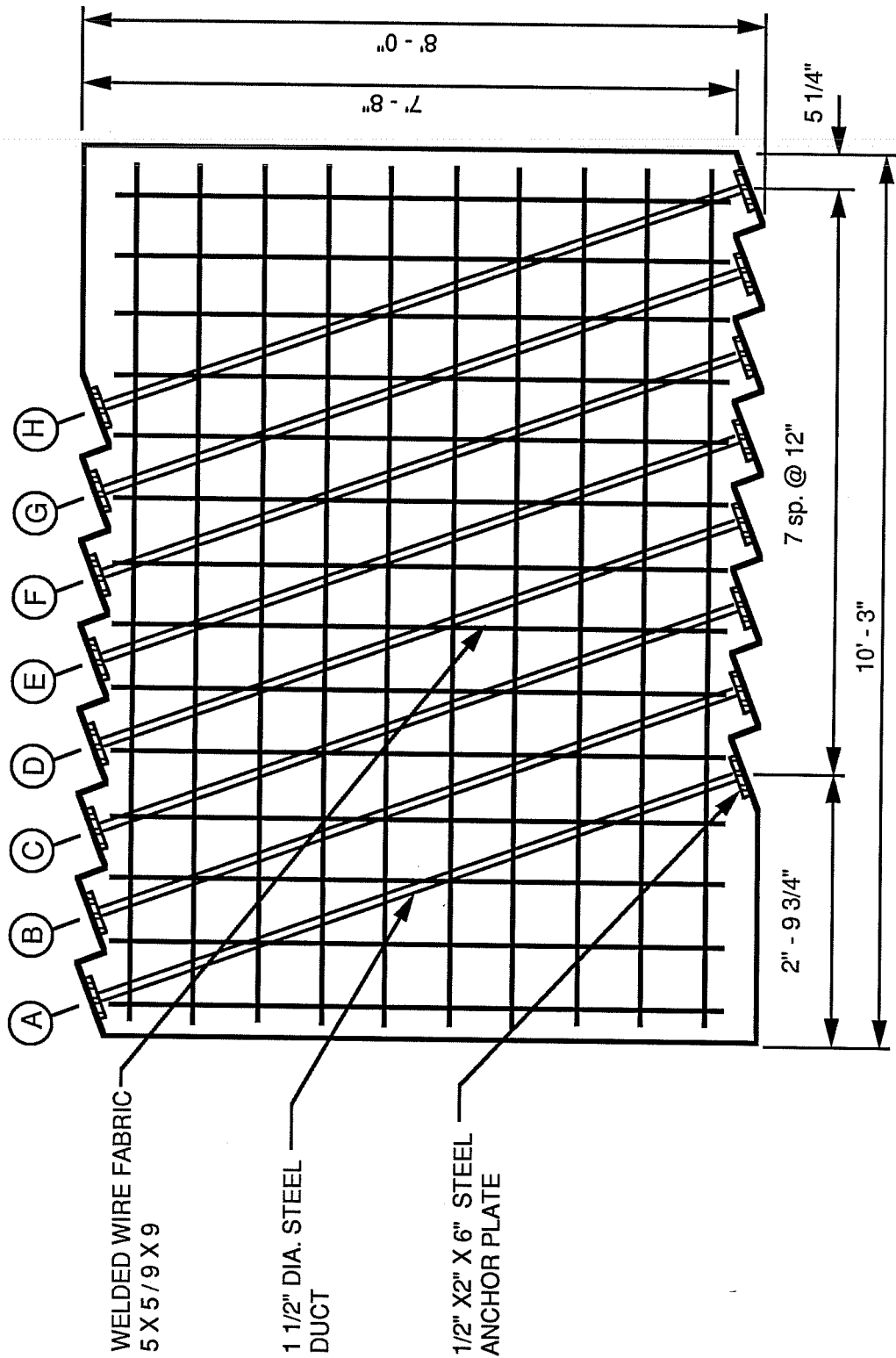
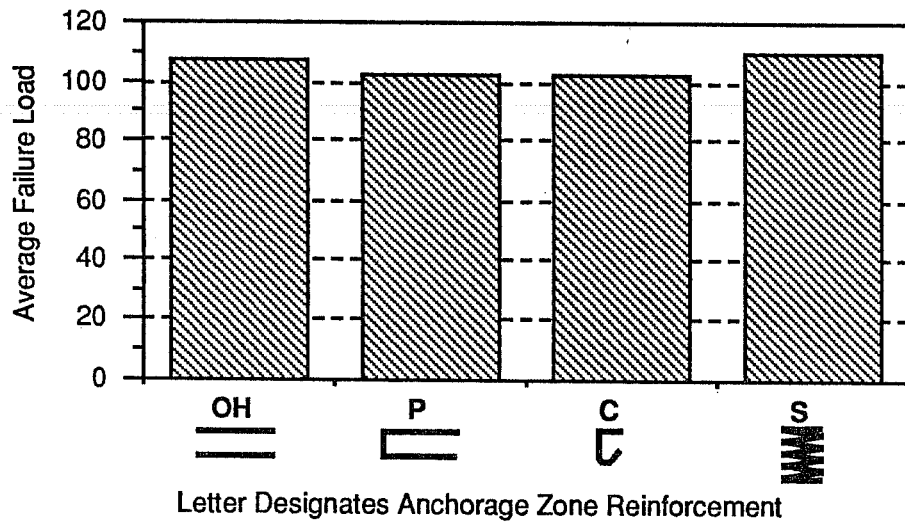
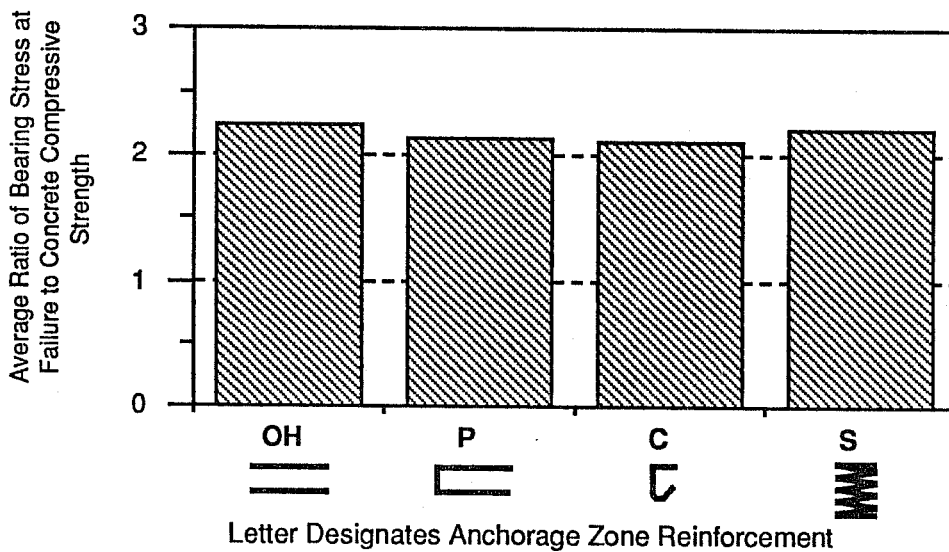


Figure 4.43 - Plan of Slab #5 - 20 Degree Inclined Ducts



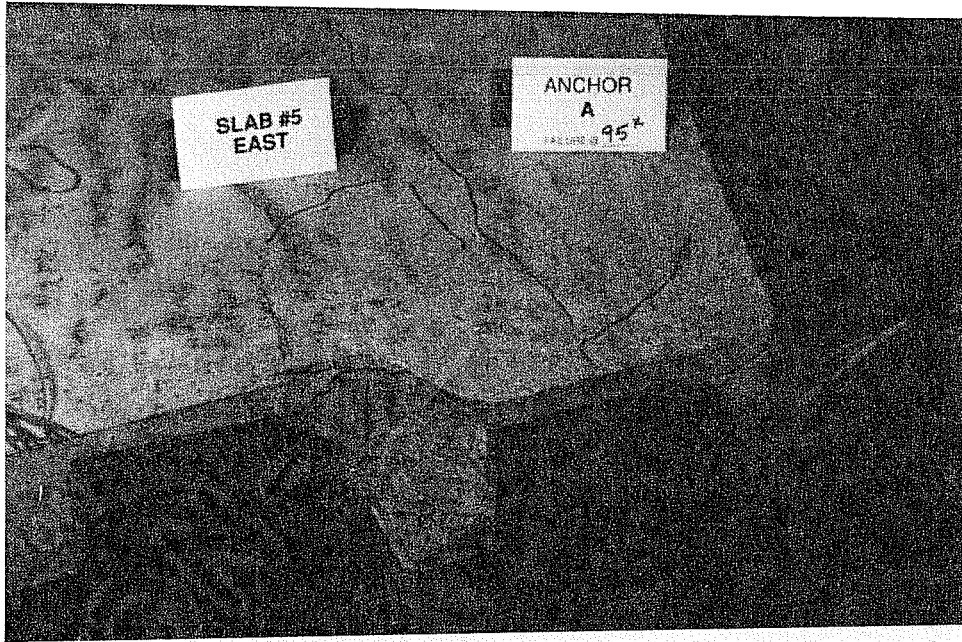
- OH - Horizontal Reinforcement Only C - Cross Ties w/Back-up Bars
 P - Hairpins w/Back-up Bars S - Spiral w/Back-up Bars

Figure 4.44 - Average Failure Loads for Horizontal Anchors with Inclined Tendons



- OH - Horizontal Reinforcement Only C - Cross Ties w/Back-up Bars
 P - Hairpins w/Back-up Bars S - Spiral w/Back-up Bars

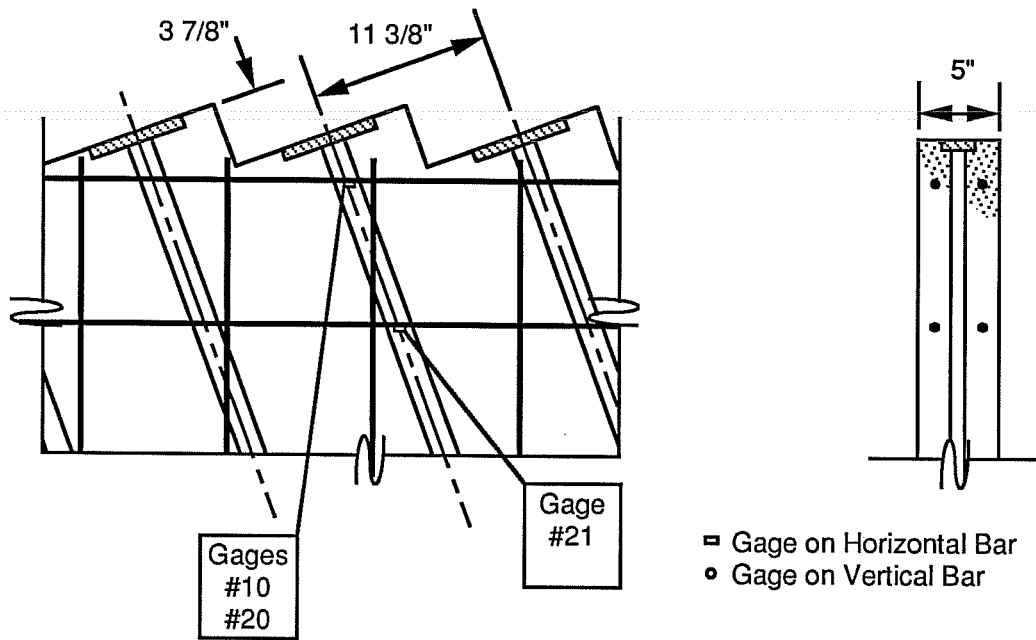
Figure 4.45 - Average Ratio of Bearing Stress at Failure to Concrete Compressive Strength for Horizontal Anchors with Inclined Tendons



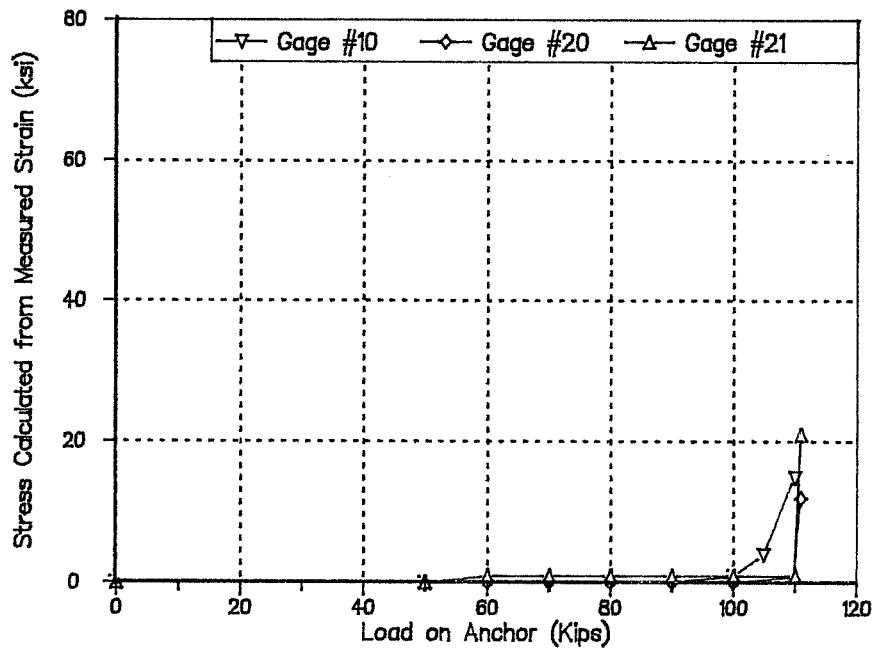
Original photo in
NCHRP 10-29 Final Report
Fig. 174

		100	2.088
"	D	105	2.192
	Average	102.5	2.140
Spiral	E	110	2.297
"	F	105*	2.192
	Average	110	2.297

* Control Detail Failed

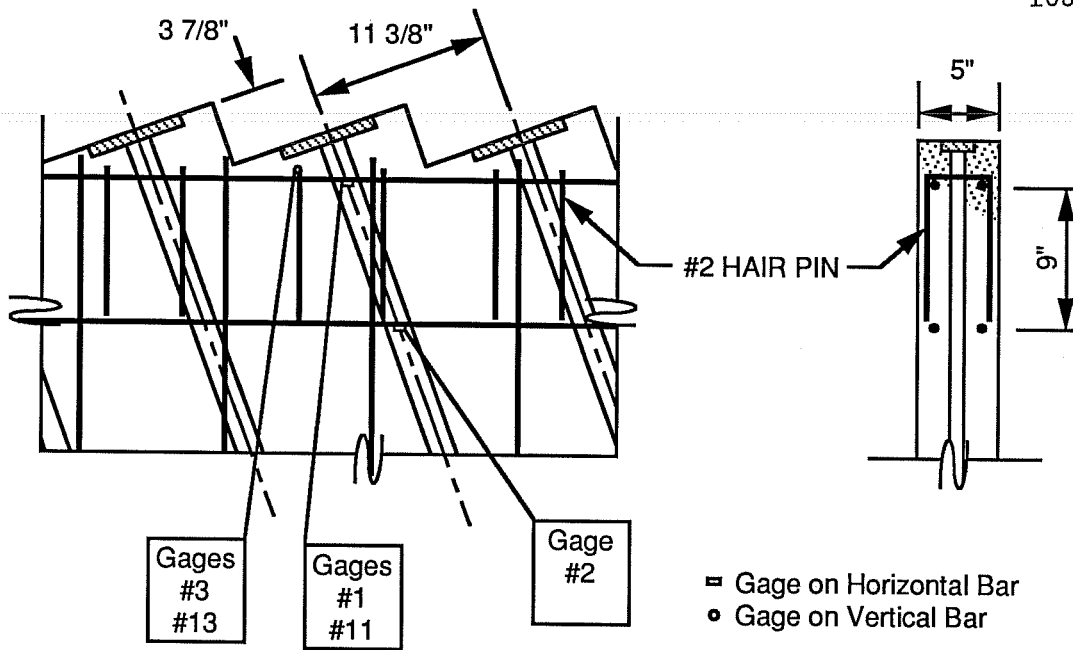


(a) Slab #5 Horizontal Reinforcing Detail @ Anchors G & H

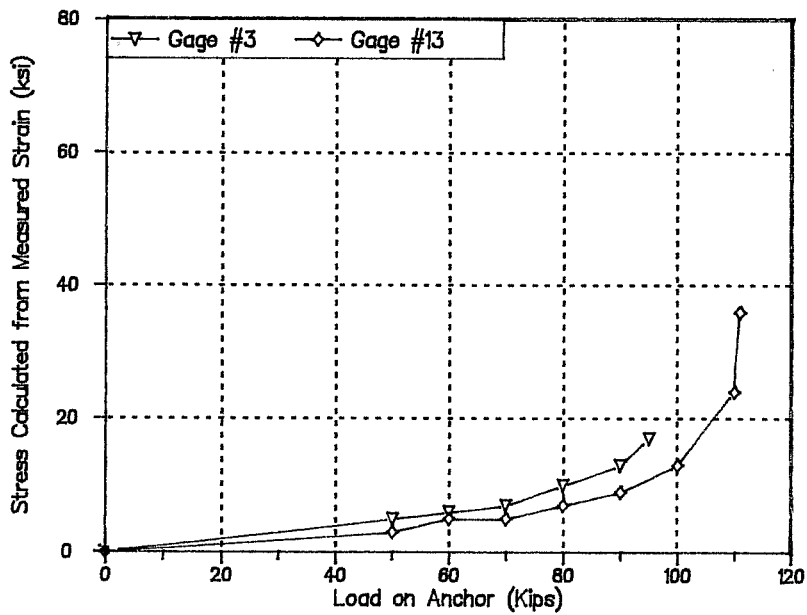


(b) Bar Stresses During Anchor Loading

Figure 4.47 - Slab #5 Horizontal Reinforcing Detail



(a) Slab #5 Hairpins @ Anchors A & B



(b) Bar Stresses During Anchor Loading

Figure 4.48 - Slab #5 Hairpin Detail

and the rate of stress per load increased prior to failure; however, only the stress in the hairpin ahead of Anchor B (Gage #13) surpassed 20 ksi. The horizontal reinforcement did not increase beyond 2 ksi prior to failure.

4.4.4 Detail C - Cross Ties

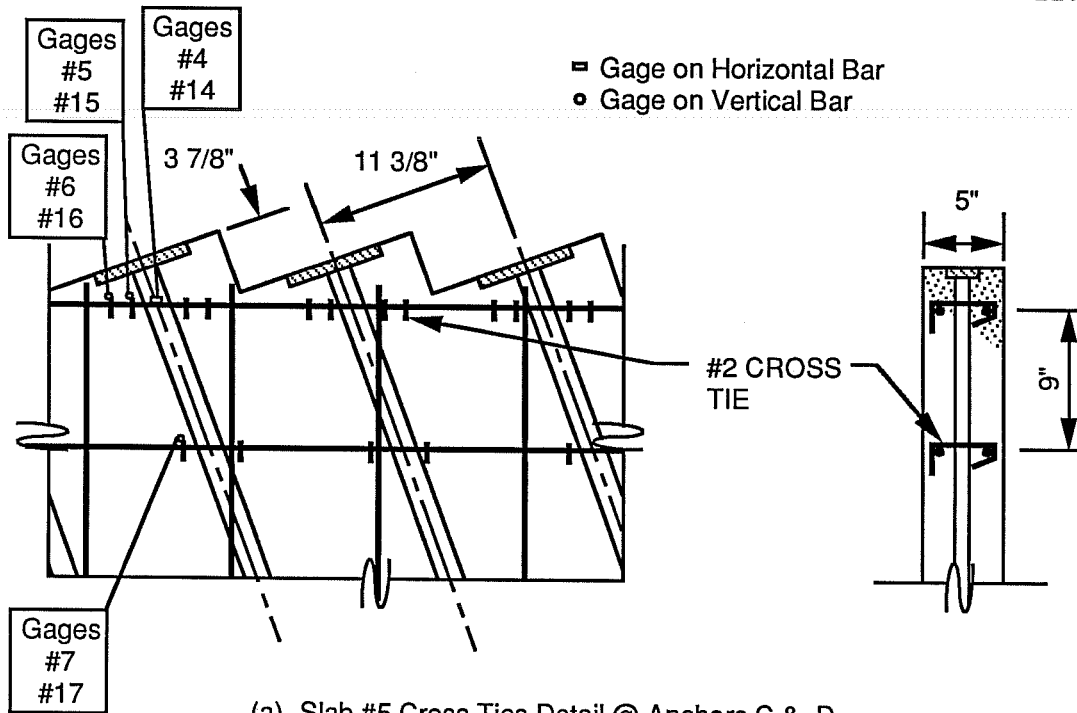
Figure 4.49 shows the stresses in the cross ties that were used as vertical anchorage zone reinforcement at Anchorages C and D in Slab #5. The cross-ties increased in stress as load increased, but never exceeded 20 ksi. The stress in the cross-ties 12" ahead of anchor gained less than 5 ksi stress prior to failure.

4.4.5 Detail S - Spiral

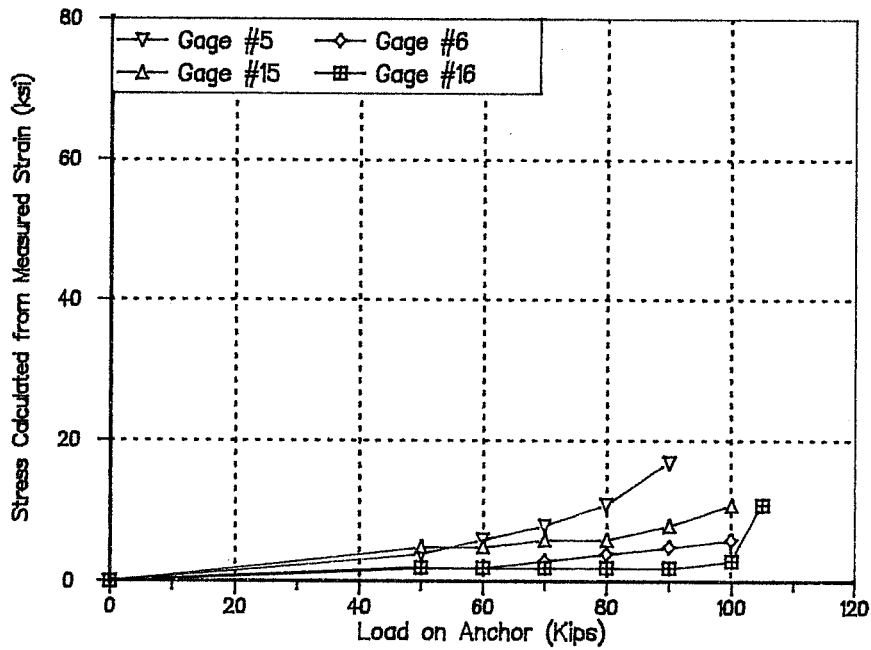
Figure 4.50 shows the stress in the spirals which were used as anchorage zone reinforcement at anchorages E and F in Slab #5. Spiral stresses increased linearly with the increase in load but never surpassed 15 ksi prior to failure. Horizontal reinforcement stresses remained below 2 ksi prior to failure. The anchorages were originally loaded twice with the threaded bars, as described in Chapter Three, to 110 kips without failure, and then the anchorages were loaded with strands, also described in Chapter Three, and failed at 110 and 105 kips, possibly due to small eccentricities in the loading system. The control detail anchorage zone failed at the F anchor pair where there was anchorage zone damage from adjacent anchor failure and possible eccentricities in the loading system.

4.4.6 Control Detail

The control detail (Figure 3.7) withstood all loading in the inclined tendon horizontally oriented four strand anchor series except along tendon F where damage to the anchorage zone and

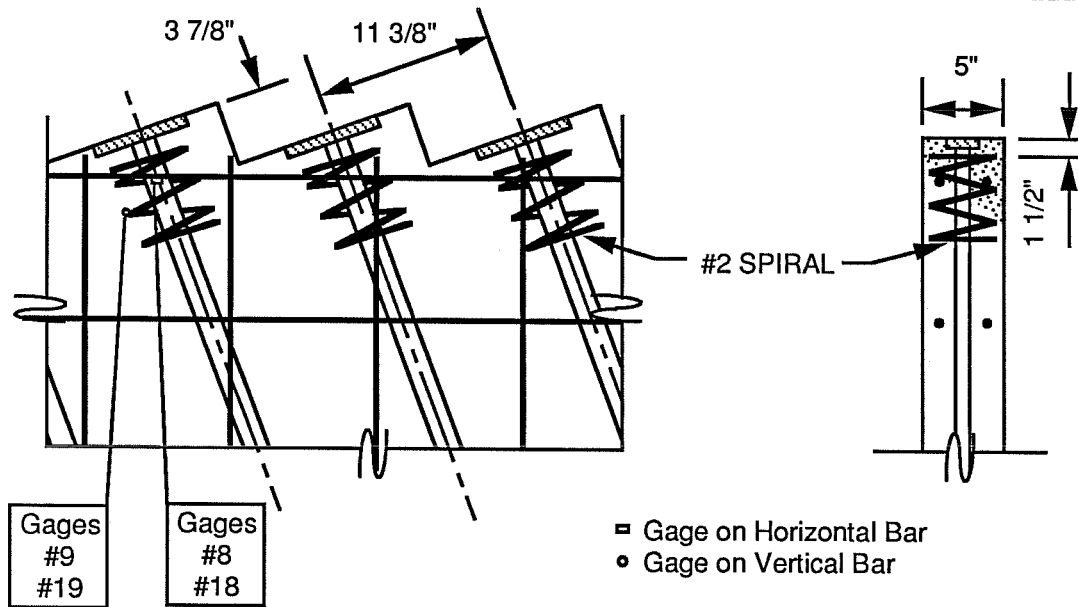


(a) Slab #5 Cross Ties Detail @ Anchors C & D

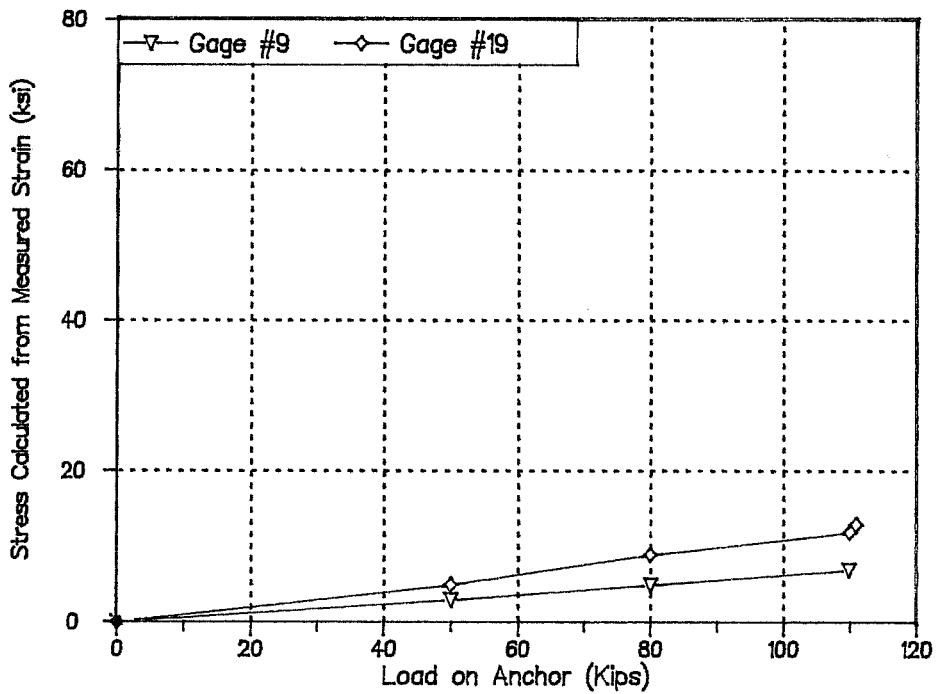


(b) Bar Stresses During Anchor Loading

Figure 4.49 - Slab #5 Cross Ties Details



(a) Slab #5 Spiral Detail @ Anchors E & F



(b) Bar Stresses During Loading

Figure 4.50 - Slab #5 Spiral Details

possible small eccentricities in the loading prompted the anchorage failure.

4.5 Full-Scale Monostrand Anchors

4.5.1 General

Slab #6 (Figure 4.51) had eight horizontally oriented monostrand anchor pairs spaced four plate widths apart center to center. The failures of these anchorages were used to evaluate effects of monostrand anchors on failure geometry and anchorage zone reinforcing efficiency. Figure 4.52 shows the failed Anchor B which occurred under a 145 kip load, which is 4.14 times the maximum jacking force ($0.8f_{pu}$) that would ordinarily be applied to a monostrand anchor for a 1/2 inch strand ($f_b/f'_c = 3.96$). For this failure, the horizontal crack is not localized. The failure loads and f_b/f'_c ratios for all of the anchors are shown in Figures 4.53 and 4.54, respectively, and in Table 4.4.

The anchorage zones reinforced with a spiral could not be failed with the maximum capacity of the loading equipment, 150 kips. The control detail failed along two tendons where the anchorage zone had been damaged by prior adjacent anchor failures.

4.5.2 Detail B - Back-up Bars

Figure 4.55 shows the back-up bars used as horizontal anchorage zone reinforcement at anchorages G and H in Slab #6. The back-up bars did not attain more than 6 ksi of stress prior to failure. The end anchorages at H failed at 95 kips. The failure of Anchor H produced cracks around the control detail anchorage zone of tendon G, and the Anchor G control detail failed at 125 kips.

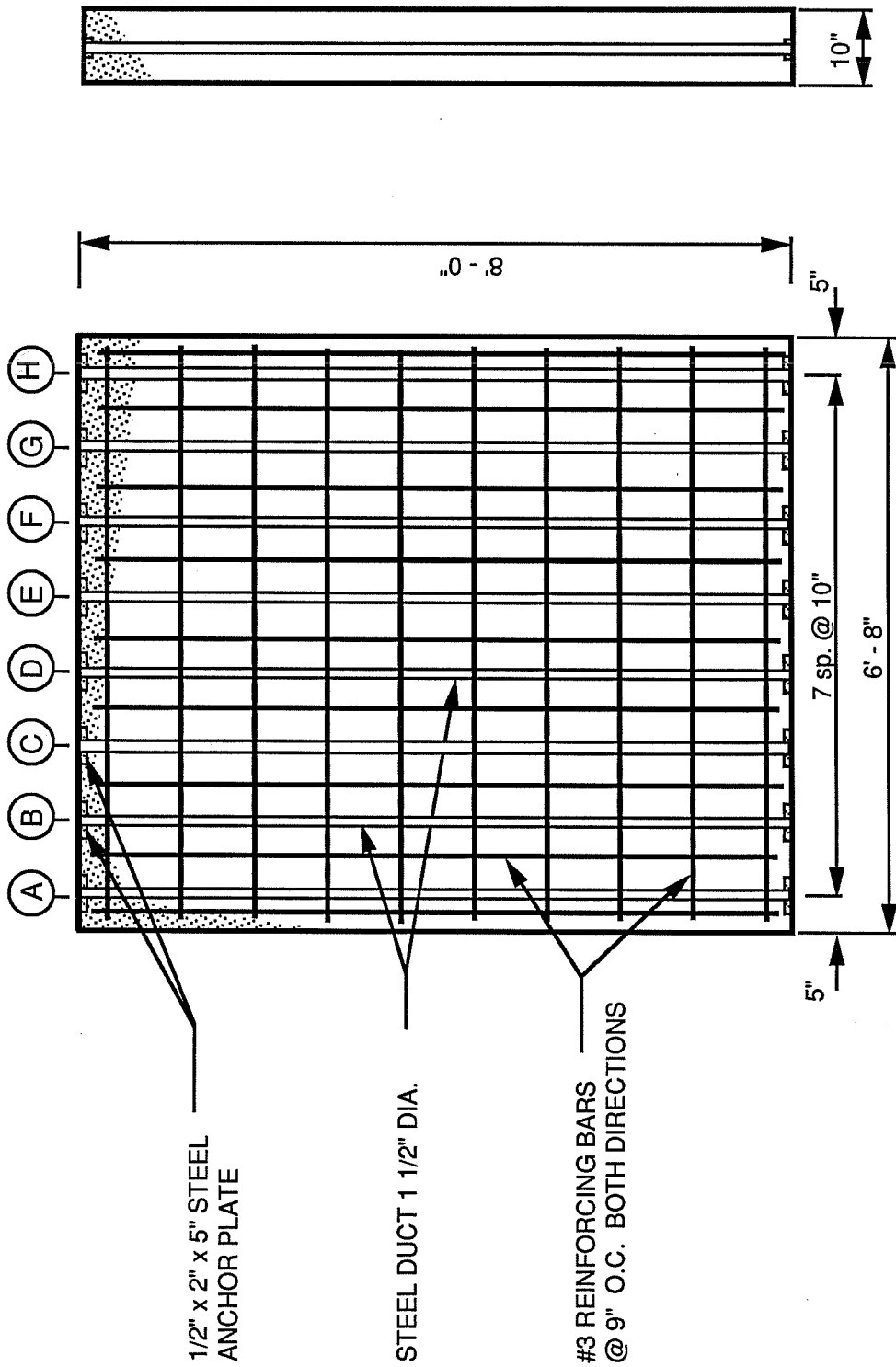


Figure 4.51 - Plan of Slab #6 - Full Scale Monostrand Anchors



Figure 4.8 - Relationship between Average FAL in Canada and Average FAL in the United States

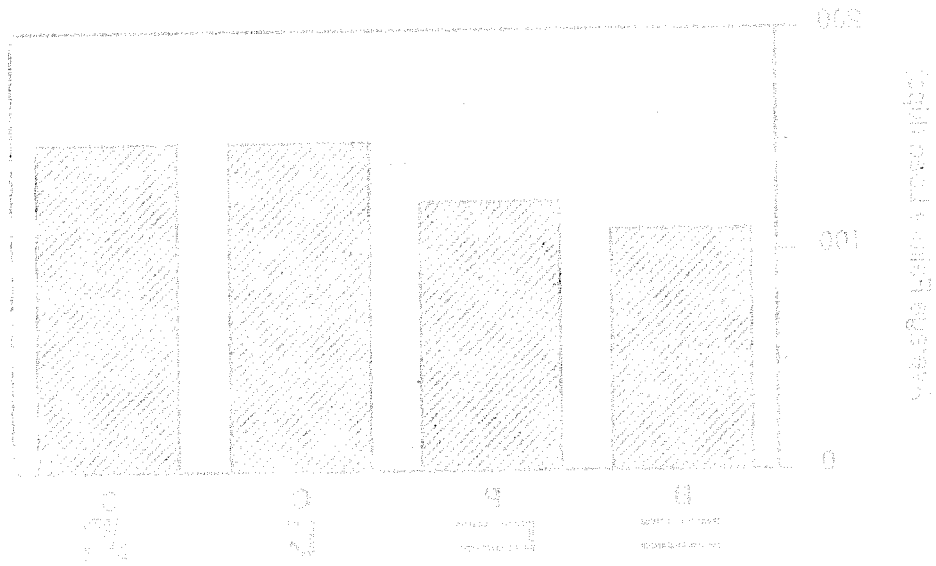


Figure 4.9 - Average FAL in Canada by Treatment and Average FAL in the United States by Treatment

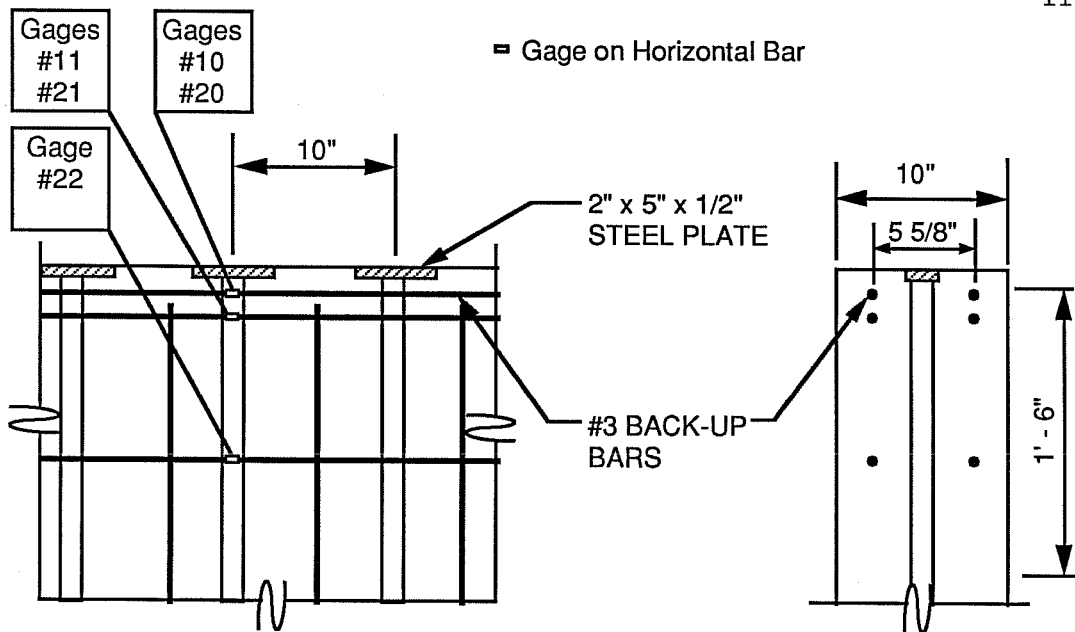
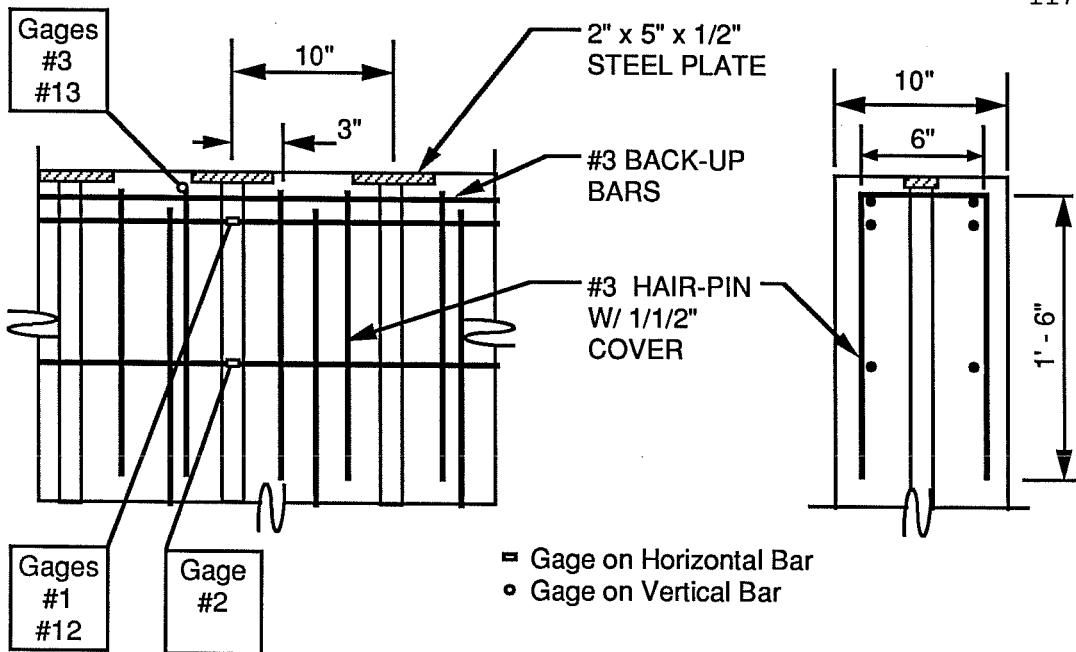


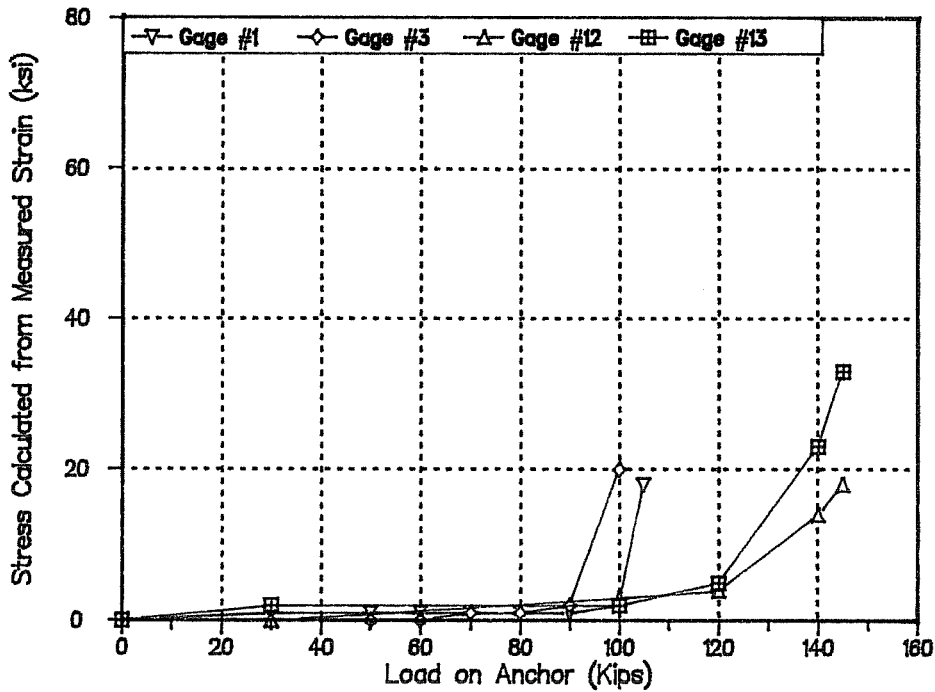
Figure 4.55 - Slab #6 Back-up Bars Detail @ Anchors K & L

4.5.3 Detail P - Hairpins and Back-Up Bars

Figure 4.56 shows the stress in the hairpins and back-up bars used as anchorage zone reinforcement at Anchors A and B in Slab #6. The hairpin ahead of end anchorage A, gaged with Gage #3, began large increases in stress as the anchor load exceeded 90 kips. Ahead of Anchor B, the hairpin gaged with Gage #13, began large increases in stress beyond 120 kips. Anchor A failed at 100 kips, while the interior anchor failed at 145 kips. The failure of Anchor B is shown in Figure 4.52. During the anchor's failure, the long horizontal crack broke the previously uncracked anchorage zone adjacent to it and produced a crack running down the side of the slab.



(a) Hairpins @ Anchors E & F



(b) Bar Stresses During Anchor Loading

Figure 4.56 - Slab #6 Hairpin Detail

4.5.4 Detail C - Cross Ties and Back-Up Bars

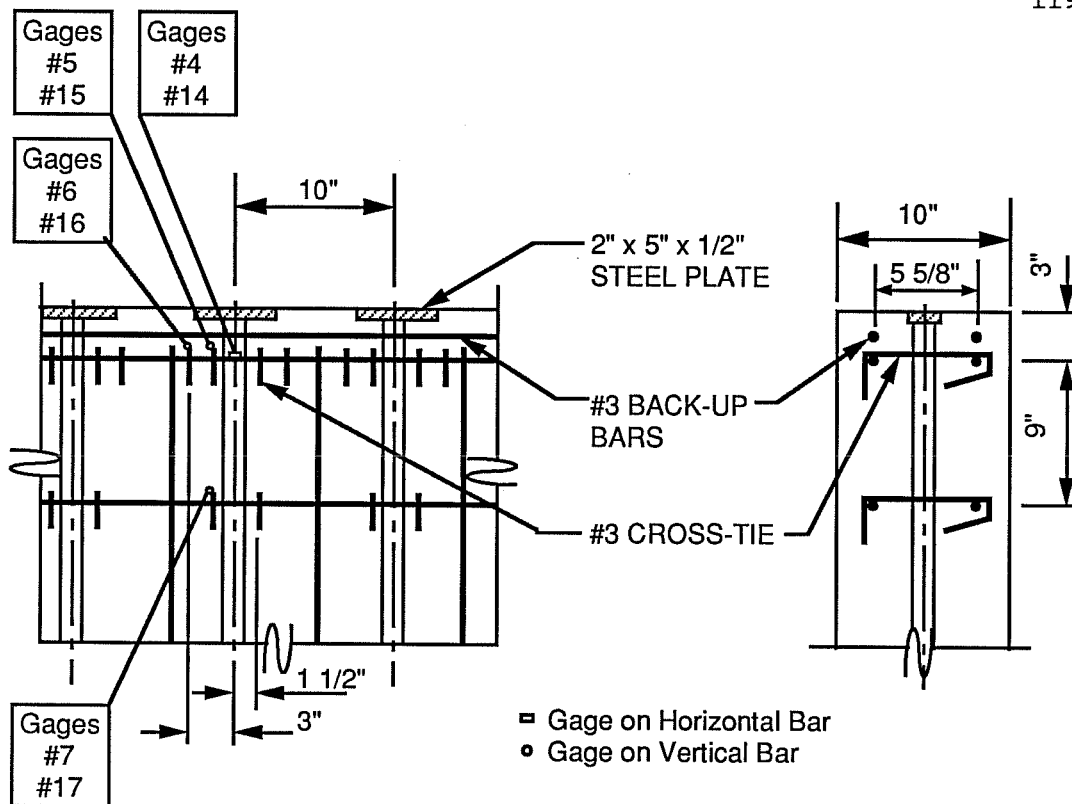
Figure 4.57 shows the stress in the cross ties and back-up bars used as anchorage zone reinforcement at Anchorages C and D in Slab #6. There was a slight increase in the rate of stress during loading beyond 140 kips. Ahead of Anchor C, a back-up bar, which was gaged with Gage #4, was stressed to yield during loading. Similar to Anchor B, the failure of Anchor C created a long horizontal crack. That long horizontal crack extended into adjacent anchorage zones and contributed to the failure of the neighboring control detail at Anchor D at 150 kips.

4.5.5 Detail S - Spiral and Back-Up Bars

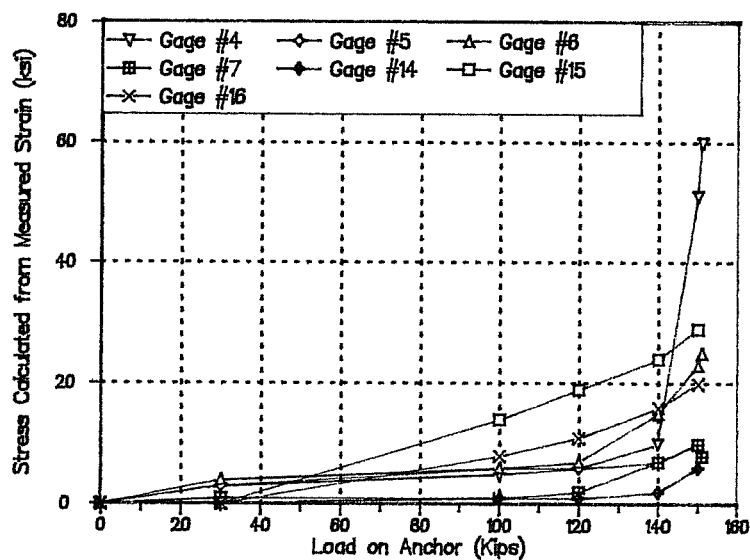
Figure 4.58 shows stress in the spirals and back-up bars used as anchorage zone reinforcement at anchorages E and F in Slab #6. Both anchorages were loaded to 150 kips, but failure was not achieved. The measured stress in the reinforcement never surpassed 10 ksi.

4.5.6 Control Detail

The control detail (Figure 3.7) was modified in this full-scale model to twice the outer dimensions and it was made of #3 reinforcing bars instead of #2. In the full-scale horizontally oriented monostrand anchors series, the control detail failed along tendons D and G because of damage to the anchorage zone due to prior adjacent anchor failures.



(a) Cross Ties @ Anchors C & D



(b) Bar Stresses During Anchor Loading

Figure 4.57 - Slab #6 Cross Ties Detail

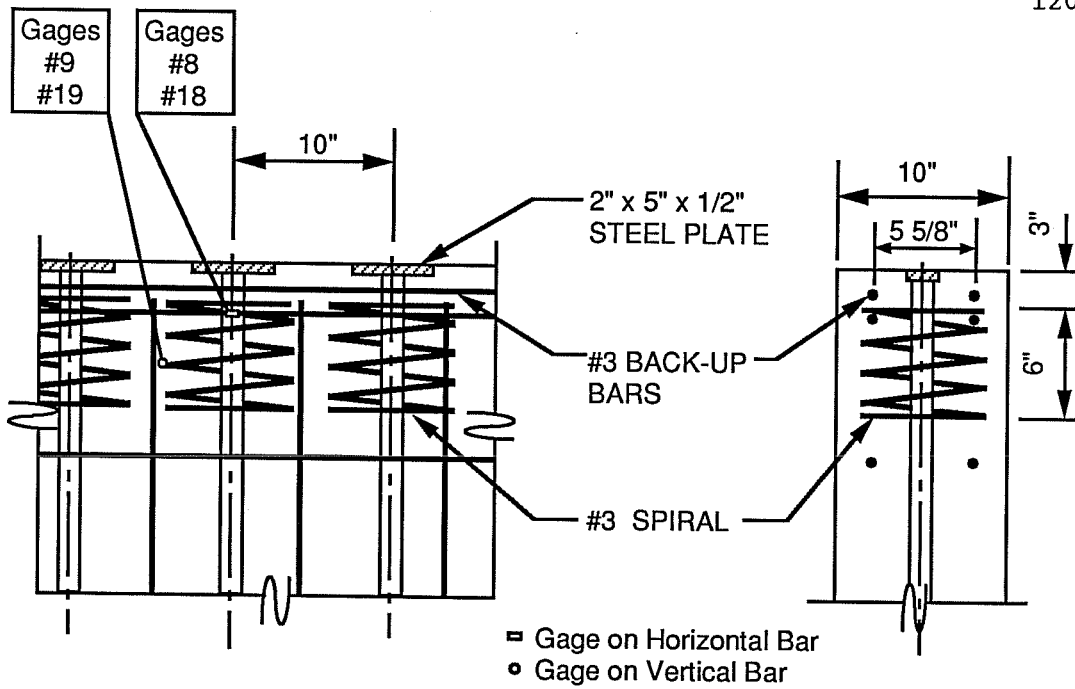


Figure 4.58 - Slab #6 Spiral Detail @ Anchors E & F

Chapter 5 Comparison and Discussion of Test Results

5.1 General

Based on the test results reported in Chapter 4, bridge deck post-tensioning anchorage zones examined were generally strong enough to withstand the tendon jacking force ($0.8f_{pu}$) of typical monostrand and multi-strand slab anchorage devices. However, exterior anchors with small edge distances could be an exception. Analytical and physical experiments were performed to evaluate the strength of slab anchorage zones with regard to anchor spacing, exterior anchor edge distance, anchor orientation, tendon inclination, anchor type, and anchorage zone reinforcement. The analytical program included linear-elastic finite element analysis and strut-and-tie modeling (Chapter 2). The physical experimental program consisted of the construction and testing of six slabs each containing eight to twelve anchor pairs (Chapters 3 and 4).

The effects of geometric and reinforcing variations on anchorage zone strength can be evaluated primarily through the comparison of failure loads or more meaningfully, the ratio of the anchorage bearing stress at failure to the concrete compressive strength at the time of tendon stressing and failure (f_b/f'_c). The f_b/f'_c ratio is used to compare anchor failures from different slabs or with different anchor plates. The analytical approaches, finite element analysis and strut-and-tie modeling, were evaluated by comparing predicted results to physical test results. Two criteria were used to evaluate the analytical procedures.

- 1) Concrete strains in the bridge deck anchorage zone were measured during tendon stressing and compared to finite element predictions.

- 2) Failure loads were compared to both the strut-and-tie model critical component and to the finite element failure predictions.

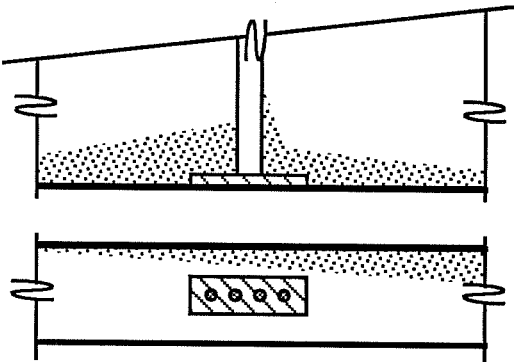
These evaluations and the general performance of the various anchorage configurations were used as the basis for recommendations for the analysis and design of anchorage zones of post-tensioned bridge deck edge anchors.

5.2 Evaluation of Anchorages - Geometric, Tendon Stressing Sequence, and Reinforcement Effects

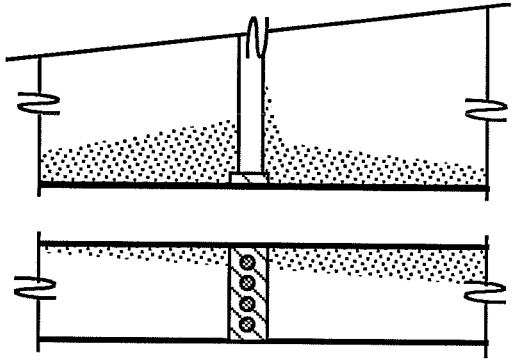
5.2.1 General

The geometric anchor properties which were varied in the experimental program were the edge distance of exterior anchors, the anchor spacing, the anchor orientation, the anchor type, and the tendon inclination (Figure 5.1). 48 of the 56 anchor pairs modelled four-strand anchors in a 10 inch thick bridge deck and were tested at half-scale. The other anchor pairs were monostrand anchors in a 10 inch thick bridge deck at full-scale, which can also be considered as half-scale models of four-strand anchors with larger concrete cover. Anchorage zone reinforcement was varied to include back-up bars, hairpins, cross ties, spirals, hoops, and hairpin hoops (Figure 5.2). Anchorage zones with similar reinforcing were loaded to failure with and without loads on adjacent anchors to examine the effects of anchor spacing on failure loads. Exterior anchorage failure loads were compared to failure loads of similarly reinforced interior anchorages to examine differences in failure loads between exterior and interior anchors.

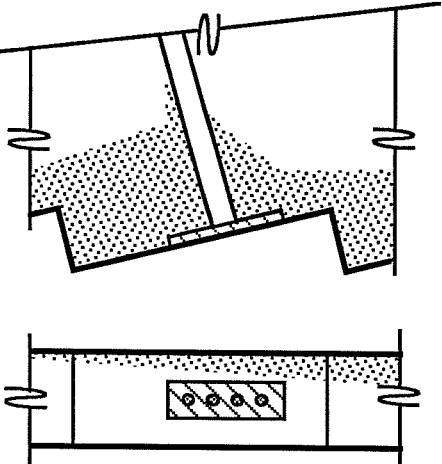
The examination of horizontally oriented four-strand anchors included the acquisition and analysis of horizontal plane and vertical plane concrete strains during the application of a tendon stressing sequence. Various tendon stressing sequences were used to



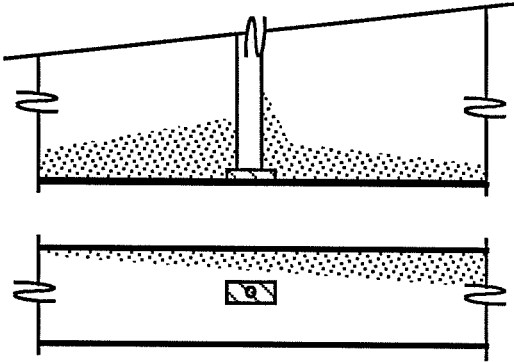
(a) Horizontal Four-strand Anchor in a 10" Thick Bridge Deck



(b) Vertical Four-strand Anchor in a 10" Thick Bridge Deck



(c) Horizontal Four-strand Anchor with Inclined Tendons in a 10" Thick Bridge Deck



(d) Horizontal Monostrand Anchor in a 10" Thick Bridge Deck

Figure 5.1 - Four Tested Anchor Arrangements

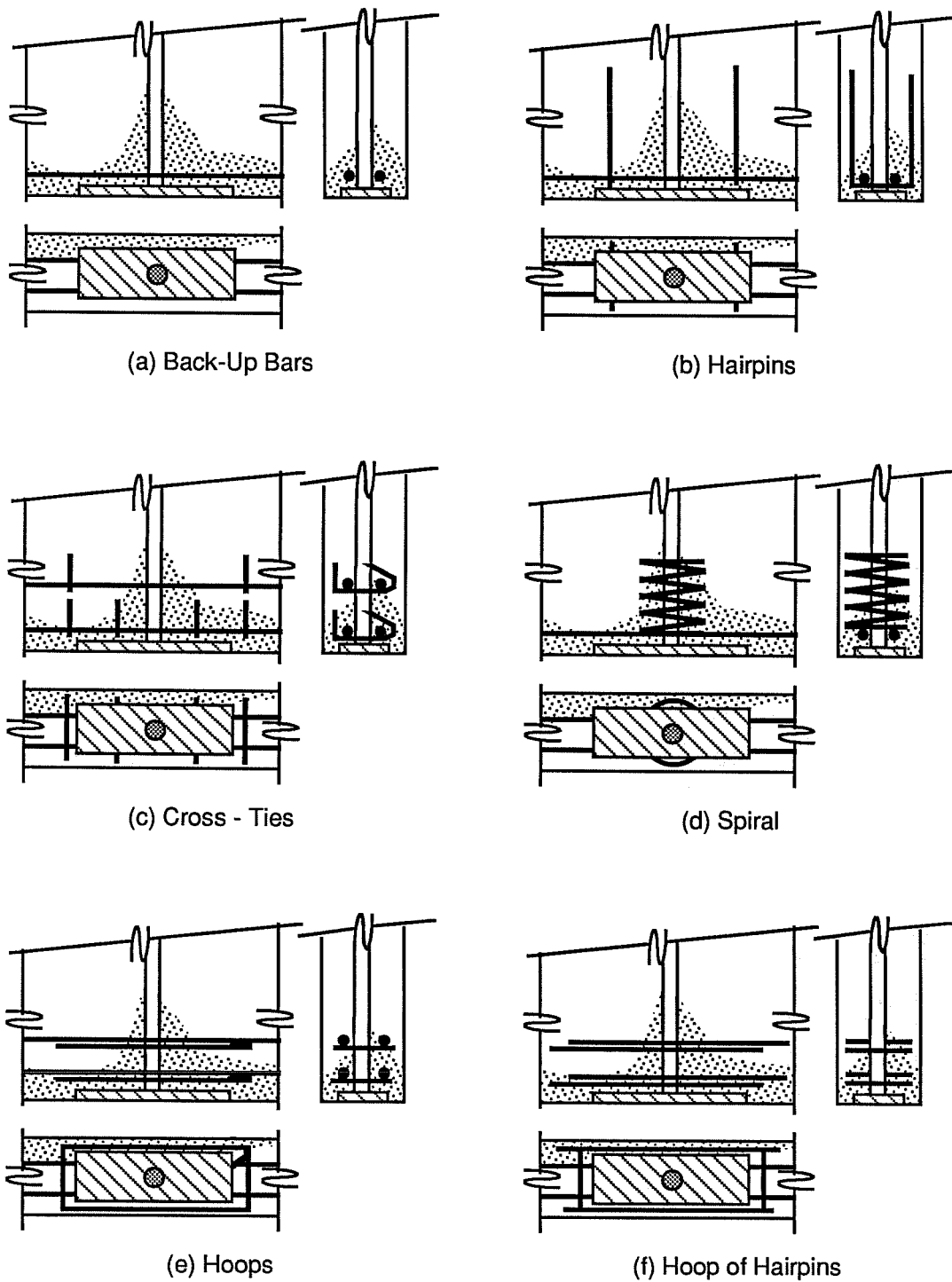
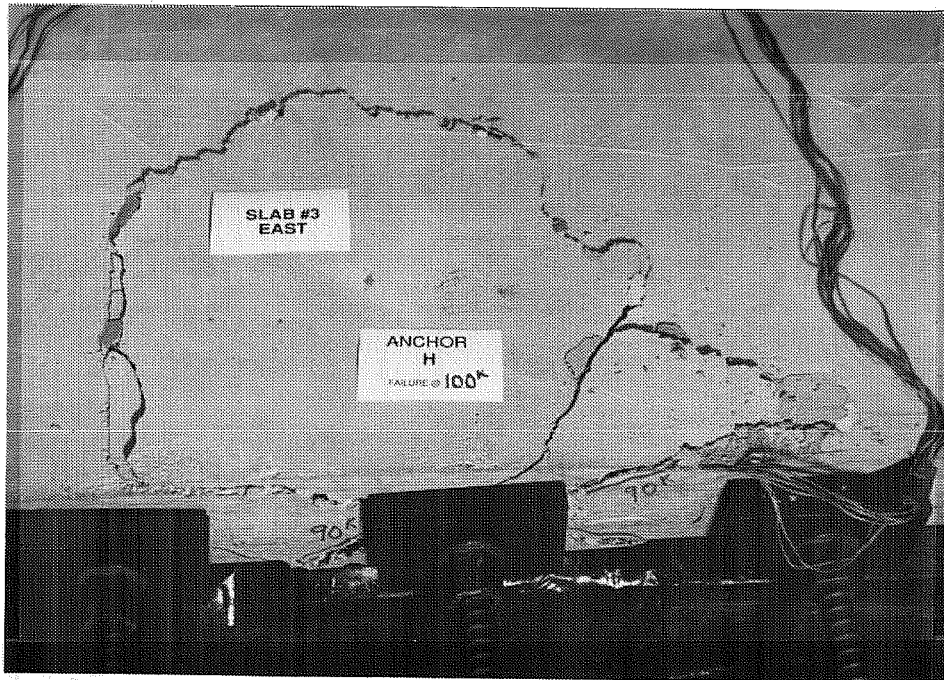


Figure 5.2 - Anchorage Zone Reinforcing Details

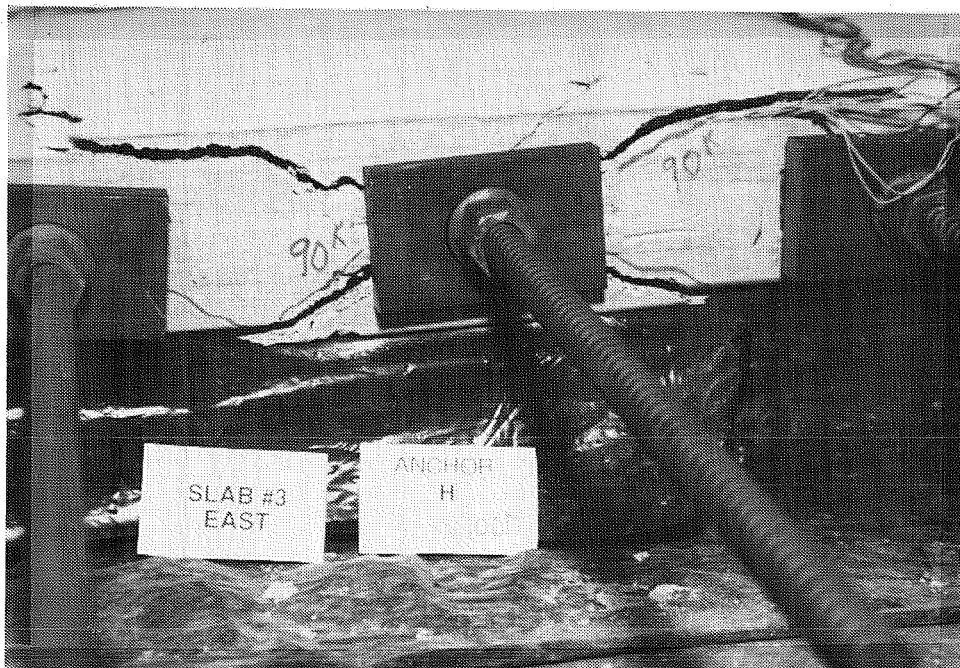
load the anchors of Slabs #1 and #3 to transfer ($0.8f_{pu}$) and service ($0.7f_{pu}$) load levels before anchors were then loaded until failure. The acquired stressing sequence strains were also used to examine the effects of anchor spacing on internal concrete strains.

5.2.2 Exterior Anchors and Edge Distance

Twelve exterior anchors were tested in the six slabs. Comparing anchorage zones in the same slab with the same anchor type, orientation, center-to-center spacing, and reinforcing, exterior anchors failed at an average of 88% of the failure loads of interior anchors. Exterior anchors with small edge distances failed at significantly lower loads. Four anchors with edge distances that were less than the slab thickness failed at an average of 68% of the failure loads of similar interior anchors. Horizontally oriented anchors failed with destruction (splitting, crushing, or spalling) in the vertical plane (Figure 5.3) regardless of whether they were interior or exterior anchors. The tested anchorage zones often combined the general zone and the local zone in virtually the same region. The destruction typically involved concrete crushing ahead of the anchor plate and separation of the confining concrete from the anchor within the local zone. Therefore, it is assumed that these failures were local zone failures. The vertically oriented exterior anchor produced vertical plane splitting (Figure 5.4b) while the interior vertically oriented anchor failures appeared to be basically bearing failures (Figure 5.4a). The splitting produced ahead of the anchor plate during the exterior anchor failure extended away from the anchor and included what is considered the general zone indicating a general zone failure. Consequently, the vertical oriented exterior anchor was also the weakest in comparison to its similar orientation interior anchor. It was 36% weaker. Notice the diagonal cracks which extend from the anchor plate's corners as shown in Figure 5.3, they indicate that the loading

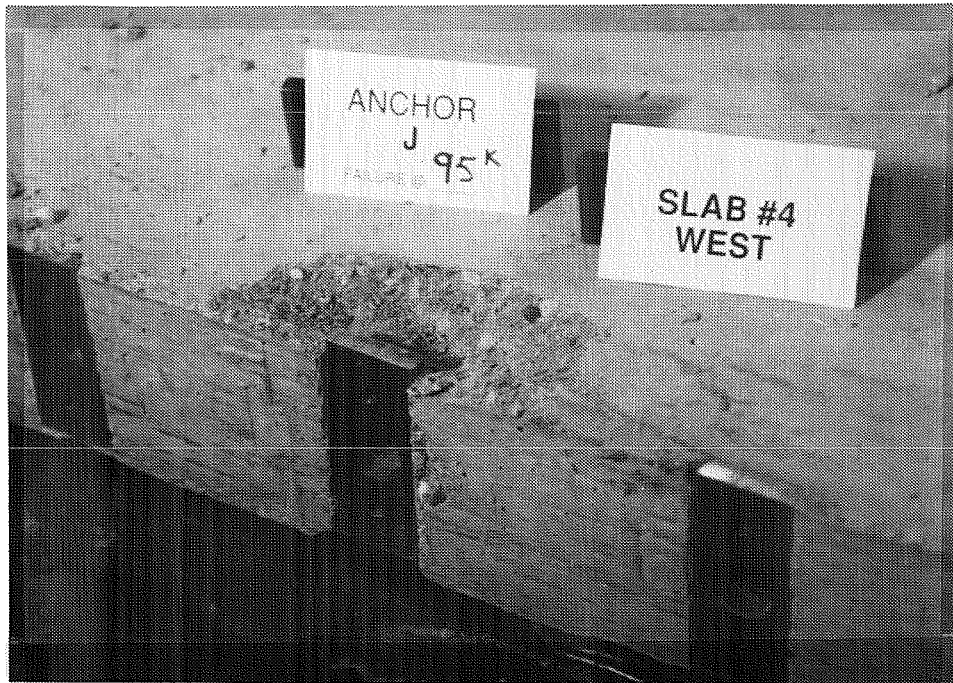


(a) Top View

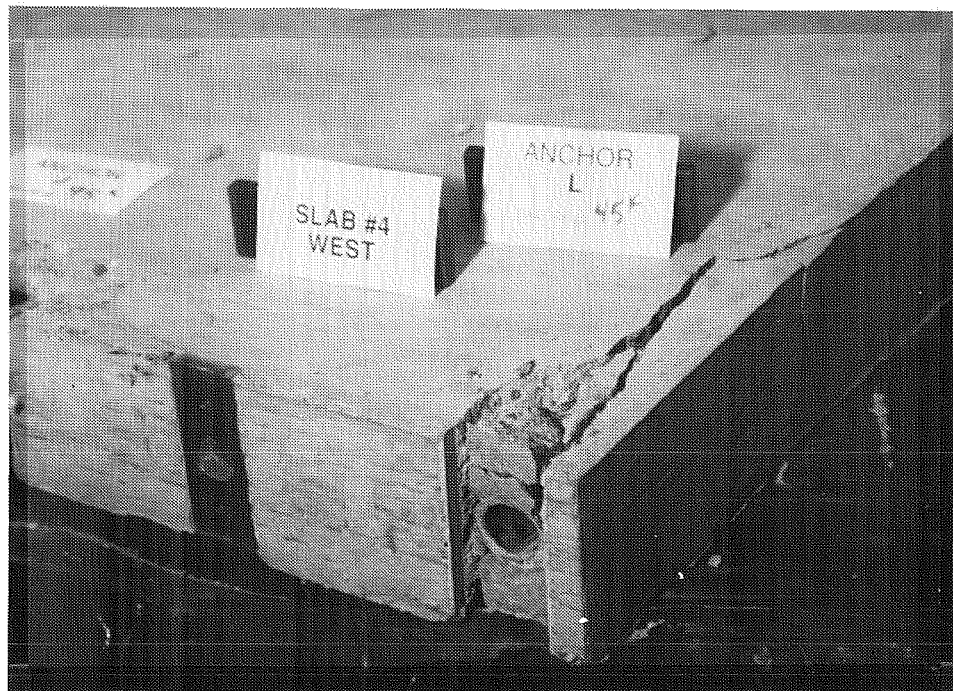


(b) Edge View

Figure 5.3 - Failure of Modelled Horizontally Oriented Four-strand Anchor

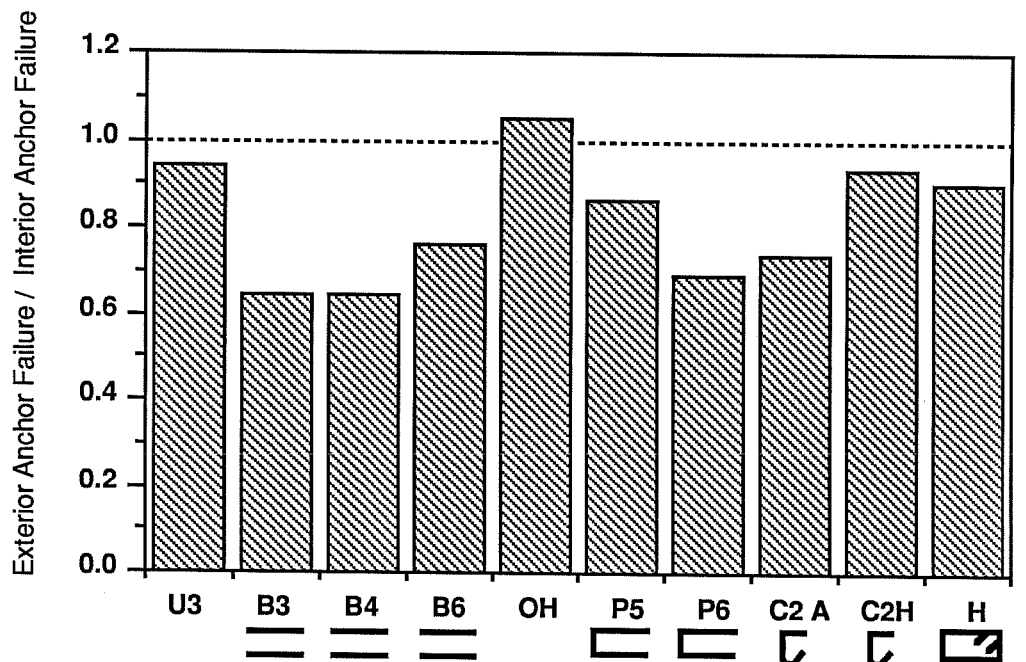


(a) Failed Interior Anchor with Spiral Reinforcing



(b) Failed Exterior Anchor with Back-up Bars as Reinforcing

Figure 5.4- Failures of Modelled Vertically Oriented Four-Strand Anchors



First Letter Designates Anchorage Zone Reinforcing, Number Indicates Specimen Number, and Second Letter Indicates Anchor When Necessary

- | | |
|----------------------------------|-----------------------------|
| U - Unreinforced Anchors | P - Hairpins w/Back-up Bars |
| B - Back-up Bars | C - Cross Ties |
| OH - Horizontal Reinforcing Only | H - Hoops w/Back-up Bars |

Figure 5.5 - Ratio of Exterior Anchor Failure Loads to Similar Reinforced Interior Anchor Failure Loads

corners as shown in Figure 5.3, they indicate that the loading system provided a uniform bearing stress ahead of the anchor plate.

Figure 5.5 and Table 5.1 compare the failure loads of all of the similar exterior and interior anchors. The only exterior anchor which failed at a load which was higher or equal to that of an interior anchor (excluding the eccentrically loaded anchors of Slab #1) was the horizontally reinforced anchorage with inclined tendons.

Table 5.1 - Exterior Anchor Failures (Edge Distance as a Factor of Anchor Width)

Reinforcement	Edge Distance	Slab	Anch. Failure	Failure (kips)	% of Int. Anch. Load
Unreinforced	1 (6")	#1	A	56	133
"	2 (12")	"	H	45*	107*
"	7 (42")	"	D	42*	100*
"	1 (6")	#3	A	75	94
"	5 (30")	"	C	80	100
Back-Up	1/2 (3")	#3	L	55	65
"	3/2 (9")	"	K	85	100
"	1 (2")	#4	L	45	64
"	5 (10")	"	K	70	100
"	1 (5")	#6	H	95	76
"	3 (15")	"	G	125**	100**
Horizontal Only	1 (5")	#5	H	110	105
"	7 (34")	"	G	105	100
Hairpins	1 (5")	#5	A	95	86
"	7 (34")	"	B	110	100
"	1 (10")	#6	H	100	69
"	3 (15")	"	G	145	100
Cross Ties	1 (6")	#2	A	75	74
"	2 (12")	"	H	95	93
"	7 (42")	"	D	102	100
Hoops	1 (6")	#4	A	90**	90**
"	3 (18")	"	B	100	100

* Eccentricities in Loading System

** Control Detail Failed

Only the horizontal oriented anchors had unreinforced anchorage zones and they were not conclusively weaker than interior ones. Two unreinforced anchorage zones from Slab #1 were assumed

to have failed due to eccentric loading and their failure loads can not be directly compared with others. The interior unreinforced anchorage zones in the Slab #3 had an average 6% increase in the failure load when compared with the exterior anchor.

A horizontal orientation, a vertical orientation, and a monostrand exterior anchor were reinforced with back-up bars. The average failure load for these three exterior anchors was 68% of the average failure load of interior anchors reinforced with back-up bars. However, all of these anchors had edge distances of less than the slab thickness. Reinforcing and edge distance effects are combined. Back-up bars, because they are horizontal, resist vertical splitting most efficiently. Only the vertical oriented exterior anchor's failure indicated that vertical splitting was critical in the anchorage zone failure. This anchor also had the lowest failure load for a concentric load.

A monostrand exterior anchor and a four-strand exterior anchor with an inclined tendon were reinforced with hairpins. The average failure load of these exterior anchors was 78% of the similar interior anchors' average failure load. However, the monostrand exterior anchor had an edge distance of less than the slab thickness and failed at 69% of the interior anchor load. The inclined tendon exterior anchorage zone with hairpins failed at 86% of the interior anchorage zone failure load, but it is more interesting that the other inclined tendon exterior anchorage zone with only horizontal slab reinforcing failed at a load 5% higher than the similarly reinforced interior anchorage zone. Exterior anchor effects were less for anchorage zones with inclined tendons.

One horizontal oriented exterior anchorage was reinforced with hoops and failed at 90% of the comparable interior anchor failure load. However, this failure was due to a local failure in the control detail due to a construction error; nevertheless, even with this artificial constraint, the hoop performed better than the

exterior anchors with back-up bars or hairpins in any configuration. Possibly more important is the fact that this failure was the only control detail failure for an exterior anchorage. Thus, the control detail confines exterior anchorage zones well.

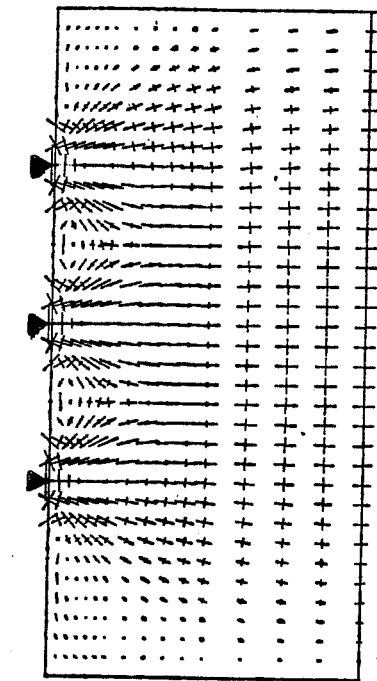
Overall, it is apparent that edge distances of less than the slab thickness significantly reduce the strength of the exterior anchorage zone and that for these anchorages, confining reinforcement such as spirals and hoops are effective in strengthening the anchorage zone.

5.2.3 Anchor Spacing and Stressing Sequence

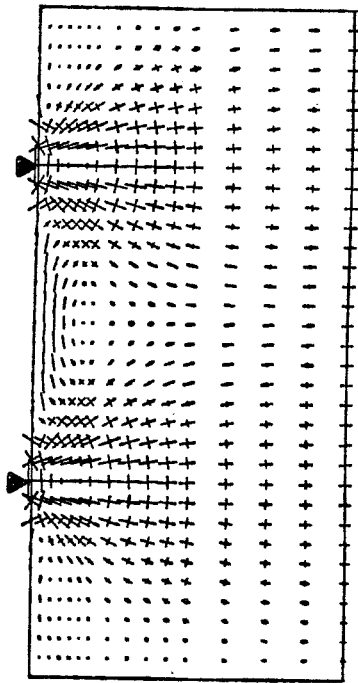
The effects of anchor spacing and stressing sequence are slight on horizontal plane strains, but as shown by Sanders, Breen and Duncan¹³ the reduced effective area of closely spaced anchors can reduce the anchorage zone strength of individual anchors.

In the experimental program, horizontal and vertical plane stresses in plain concrete were calculated from gage strain readings acquired from Slab #1 and Slab #3 during sequenced loading of the anchors to service loads. Horizontal and vertical reinforcement stresses were calculated from gage readings acquired from Slab #2 during sequenced anchor loading. Two tendon stressing sequences were used. All three slabs were loaded by first stressing alternating tendons (loading every other anchorage) to transfer and service load levels ($0.8f_{pu}$ and $0.7f_{pu}$, respectively). The first two specimens were also loaded by first stressing an exterior tendon and then stressing each directly adjacent tendon from one end of the slab. The second sequence was intended to represent the worst possible tendon stressing sequence.

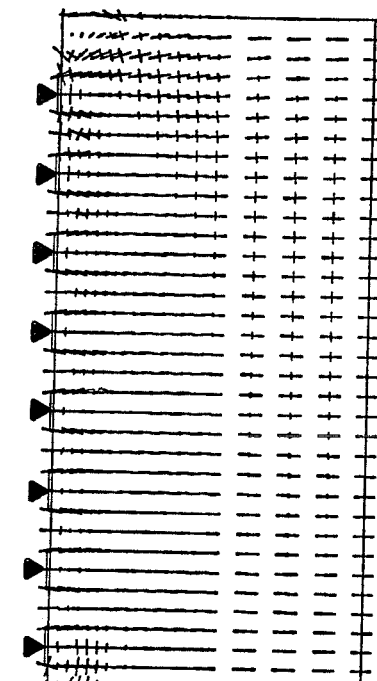
The general patterns of the finite element generated principal stress distributions are repeated in Figure 5.6. They are similar to the concrete and reinforcement strain distributions measured during sequenced tendon stressing. As shown in Figure 5.7, the



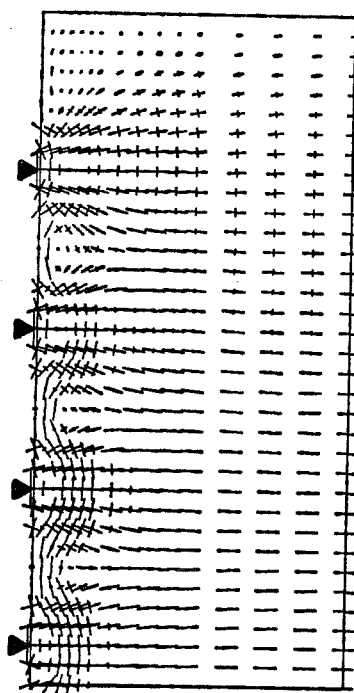
(a) Load on Two Distant Anchors



(b) Load on Three Anchors

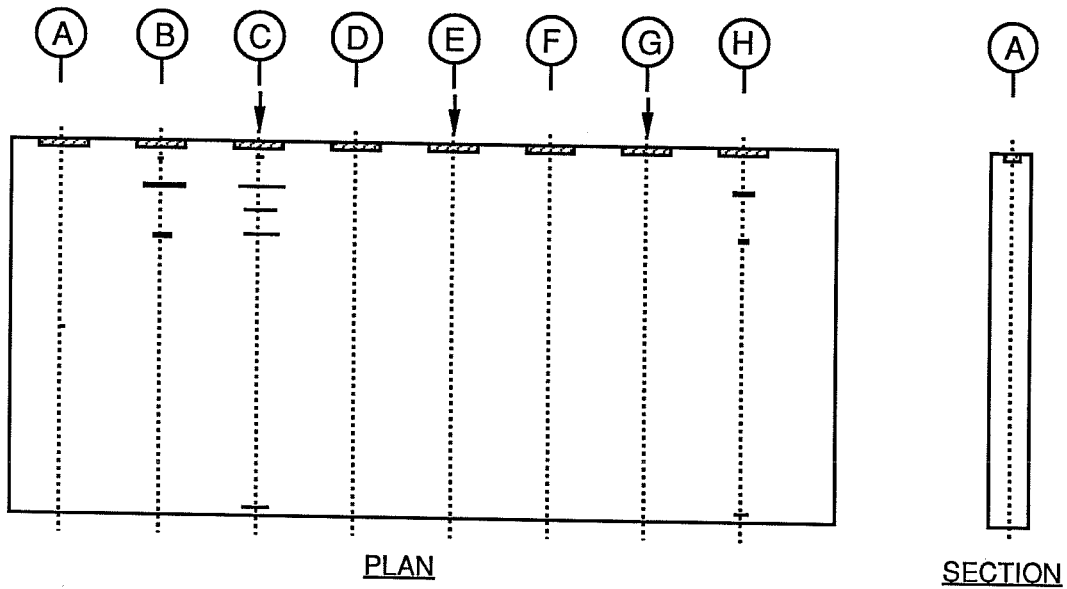


(c) Load on Alternate Anchors

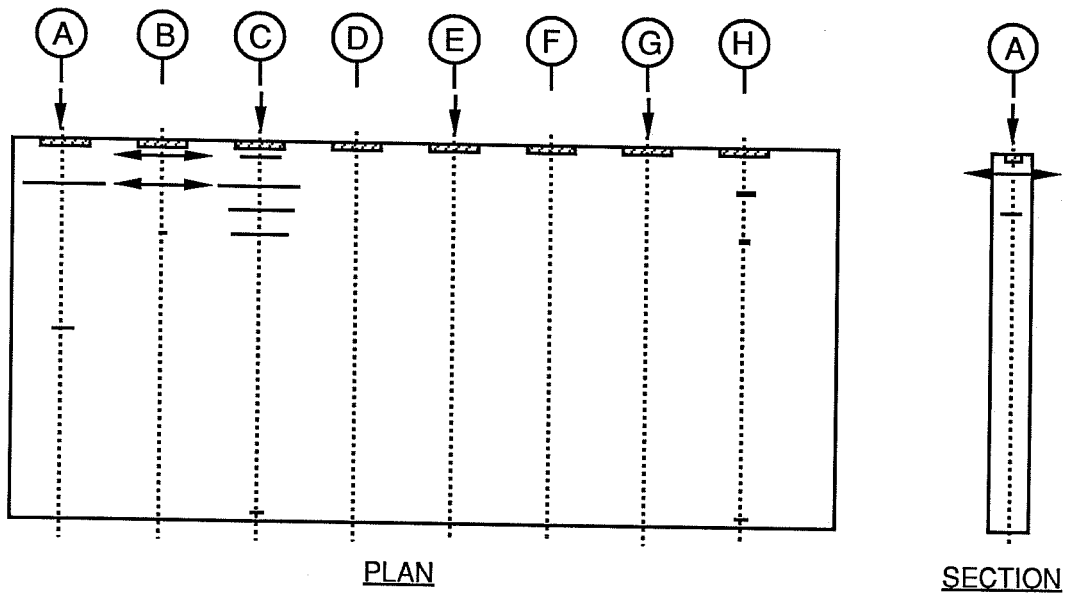


(d) Load on All Anchors

Figure 5.6 - Horizontal Plane Principal Stresses During Stressing Sequence



(a) Anchors C, E, &G Loaded to 35k



(b) Anchors A, C, E, & G Loaded to 35k

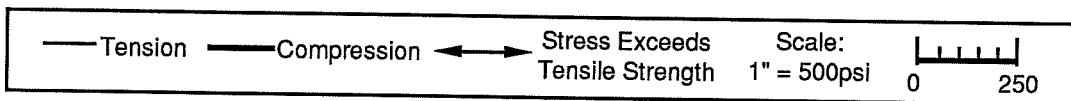
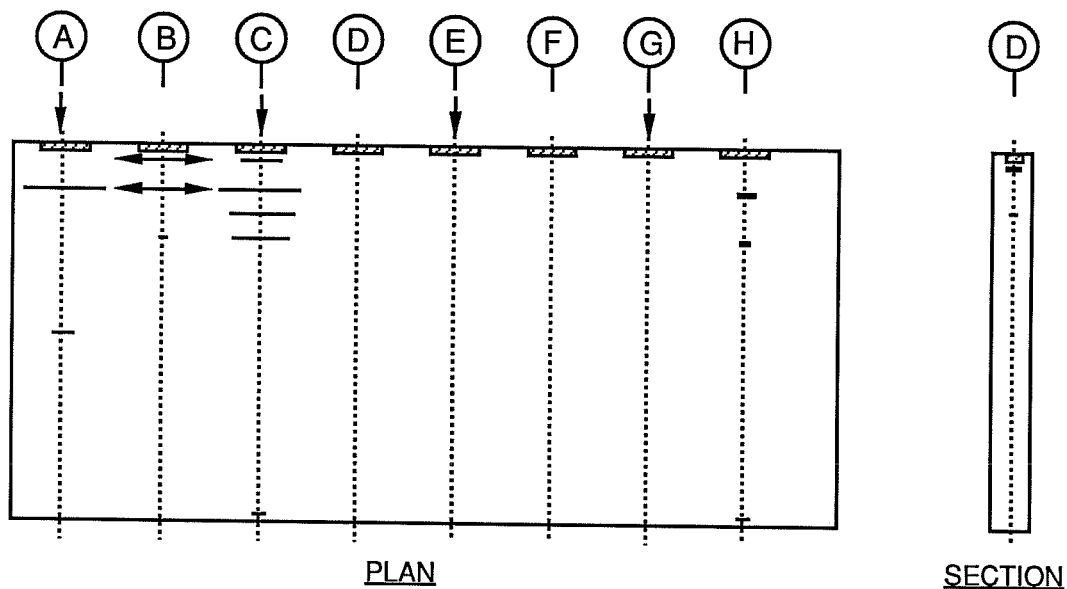


Figure 5.7 - Bursting Stress Distribution in Slab #1

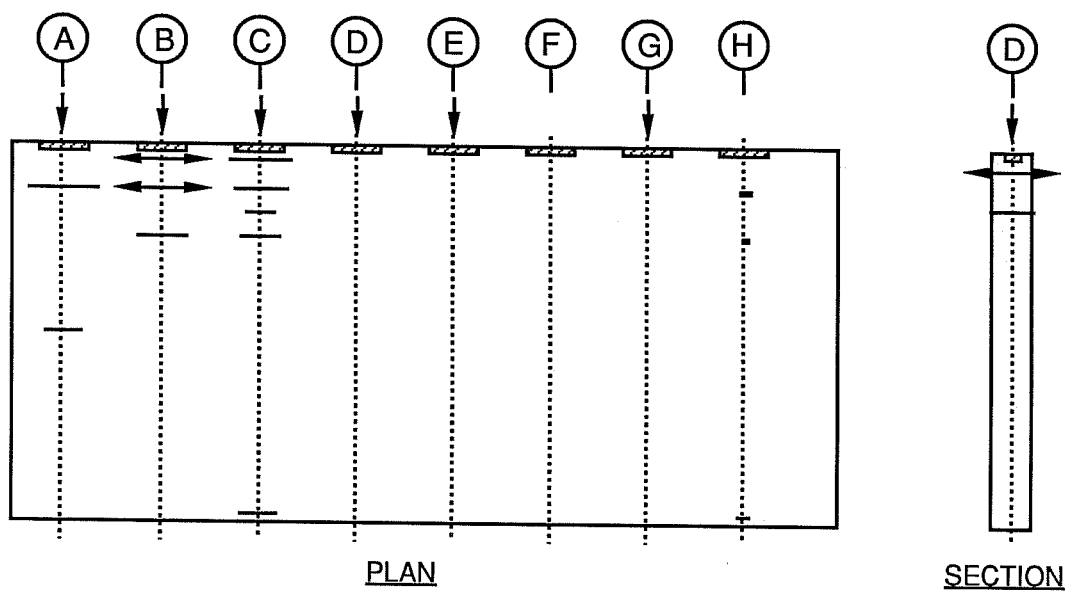
loading of alternate unreinforced anchors including an exterior anchor with a small edge distance causes the interior Anchor C to develop larger bursting stresses. These are concentrated close to the bearing plate and are similar to those shown in Figure 5.6c. The same behavior was demonstrated by the reinforced Slab #2 (Figure 4.20). Loading the exterior anchor changed the smallest edge distance of the loaded anchors, but it did not change the anchor-to-anchor spacing. Horizontal plane stresses are affected mainly by the exterior anchor edge distance. In addition, the loading of adjacent anchors, which is shown in Figure 5.8 (Figure 4.21 for reinforced), significantly reduces the interior anchor horizontal plane bursting stresses but has less effect on exterior anchor horizontal bursting stresses.

All of these cases indicate that the calculated vertical plane bursting stresses due to loading a single anchor are higher than the calculated horizontal plane bursting stresses due to any stressing sequence. Furthermore, Slab #2 was reinforced across pre-formed cracks in the anchorage zones with less horizontal reinforcement than the minimum temperature reinforcement allowed by AASHTO¹ for bridge decks. While carrying the horizontal tensile forces due to anchor transfer and service loads, the light horizontal reinforcement reached only one-third of its yield strength (20 ksi/60 ksi); therefore, the AASHTO minimum reinforcement placed in bridge decks is sufficient to carry horizontal plane bursting forces in edge anchorage zones.

Table 5.2 and Figure 5.9 show the ratios of interior anchor failure loads accompanied by service level stressing loads on adjacent anchors to the failure loads of interior anchors without adjacent loads. Six anchorages failed at loads an average of 9.3% higher than failure loads obtained without service loads on adjacent anchors, three anchors failed at the same load level, and two



(a) Anchors A, C, E, & G Loaded to 35k



(b) Anchors A, B, C, D, E, & G Loaded to 35k

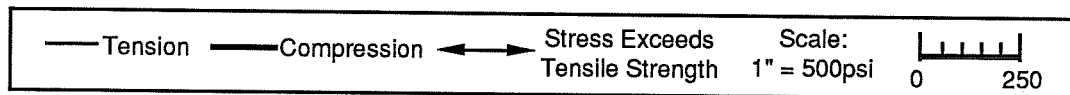
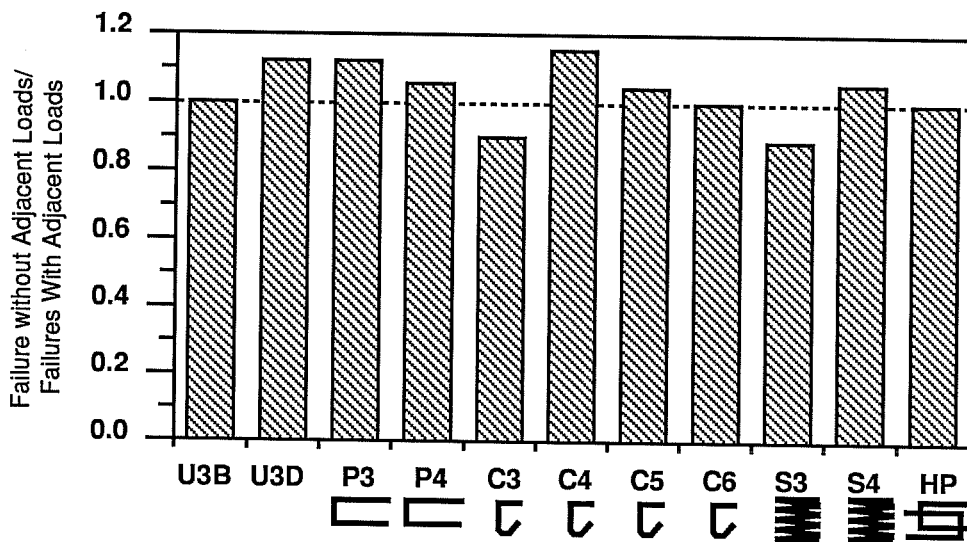


Figure 5.8 - Effects of Adjacent Anchor Loading Calculated Stresses in Slab #1

Table 5.2 - Anchor Failures for Interior Anchors with and without Adjacent Loads

Reinforcement	Adjacent Loads	Slab	Anch. Failure	Failure (kips)	% of Adj. Load Fail
Unreinforced	Yes	#3	C	80	100
"	No	"	B	80	100
"	"	"	D	90	113
Hairpins	Yes	#3	E	85	100
"	No	"	F	95	112
"	Yes	#4	E	90	100
"	No	"	F	95	105
Cross Ties	Yes	#3	H	100	100
"	No	"	G	90	90
"	Yes	#4	G	78	100
"	No	"	H	90	115
"	Yes	#5	C	100	100
"	No	"	D	105	105
"	Yes	#6	C	150	100
"	No	"	D	150*	100*
Spiral	Yes	#3	J	107	100
"	No	"	I	95	89
"	Yes	#4	I	90	100
"	No	"	J	95	105
Hairpin Hoop	Yes	#4	C	100	100
"	No	"	D	100	100

* Control Detail Failed



First Letter Designates Anchorage Zone Reinforcement, Numbers Designate Specimen Number, and Second Letter Designates Anchor When Necessary

- | | |
|--------------------------------------|--|
| U - Unreinforced Anchors | S - Spiral w/Back-up Bars |
| P - Hairpins w/Back-up Bars | HP - Hairpin Hoops w/Back-up Bars |
| C - Cross Ties w/Back-up Bars | |

Figure 5.9 - Ratio of Failure Loads of Anchors without Adjacent Anchor Loads to Failure Loads of Anchors with Adjacent Anchor Loads

anchors had failure loads 11.9% lower than failure loads obtained without service loads on adjacent anchors.

5.2.4 Effects of Anchor Orientation, Anchor Type and Tendon Inclination on Failure

The control group for the bridge deck edge anchors tested was the series of horizontally oriented four-strand anchors modeled at half-scale. From this group three main geometric variations were examined. Anchor orientation was changed, the post-tensioning tendons were inclined, and monostrand anchors replaced the four-strand. Within those groups three standard reinforcing details were

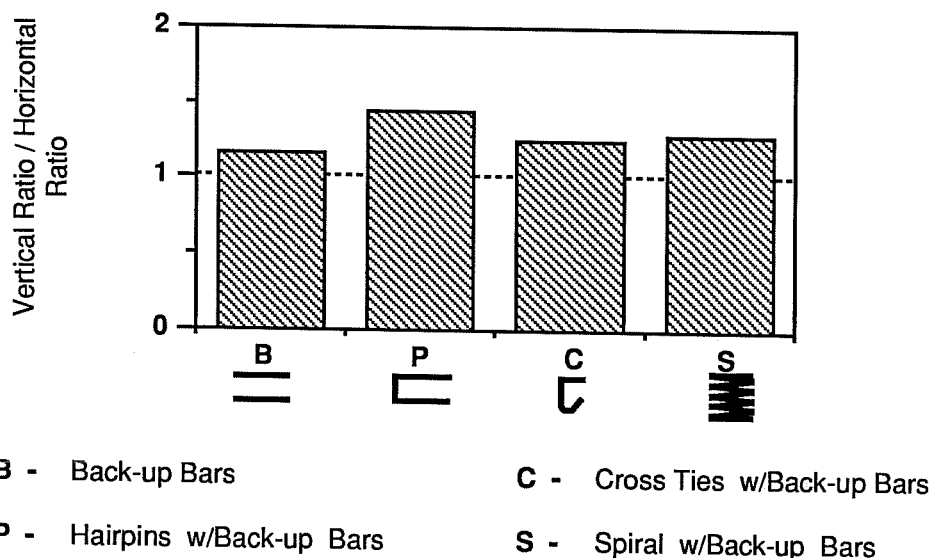


Figure 5.10 - Ratio of Vertically Oriented Anchor to Horizontally Oriented Anchor (Bearing Stress at Failure over Concrete Compressive Strength)

maintained - hairpins, cross ties and spirals. Back-up bars were placed in all but the inclined tendon specimen which had anchorage zones with only horizontal temperature reinforcement.

The vertically oriented anchors had an average f_b/f'_c ratio which was 131% of the similarly reinforced horizontally oriented anchors average ratio. However, if effective bearing areas are considered for the two anchors, the f_b/f'_c ratio of the vertical anchors becomes 262% of the horizontal anchors' ratio. Figure 5.10 shows the ratio of the average f_b/f'_c ratios for horizontal and vertical oriented anchors by reinforcement type, without considering effective areas.

The effective bearing area is considered the maximum concentric and geometrically similar portion of the concrete bearing surface. Only the vertical four-strand anchors had an effective bearing area which was proportionally different from the horizontally oriented four-strand anchors (Figure 5.11). The

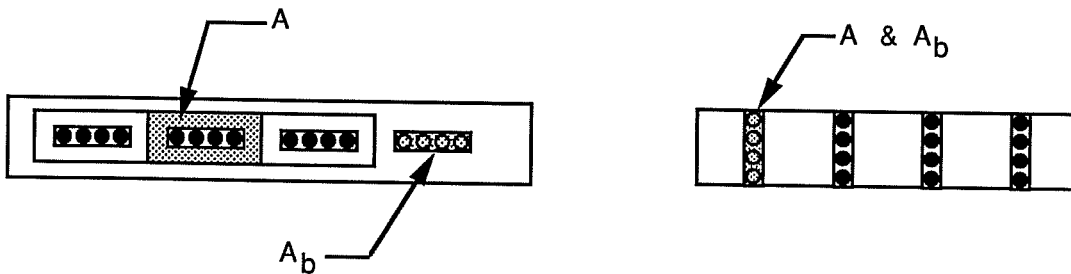


Figure 5.11 - Maximum Area of the Portion of the Concrete Surface that is Geometrically Similar to and Concentric with the Area of the Anchorage

effective bearing area of an anchor allows the bearing stress of a loaded anchor to be raised by assuming it is spread over a larger area. The anchor area can be multiplied by the following factor to produce a modified bearing area and thus a new bearing stress (f_b). The factor is:

$$\sqrt{\frac{A}{A_b}}$$

A = maximum area of the portion of the concrete anchorage surface that is geometrically similar to and concentric with the area of the anchorage (Figure 5.4)

A_b = bearing area of the anchorage

The geometrically similar concentric surface area is the anchor area for the vertical anchors and 48 in^2 (4 times the anchor's area) for the horizontally oriented anchors. The modified horizontally oriented anchor bearing area is twice the actual anchor area so that the bearing stress (f_b) can be divided by two. Figure 5.12 shows

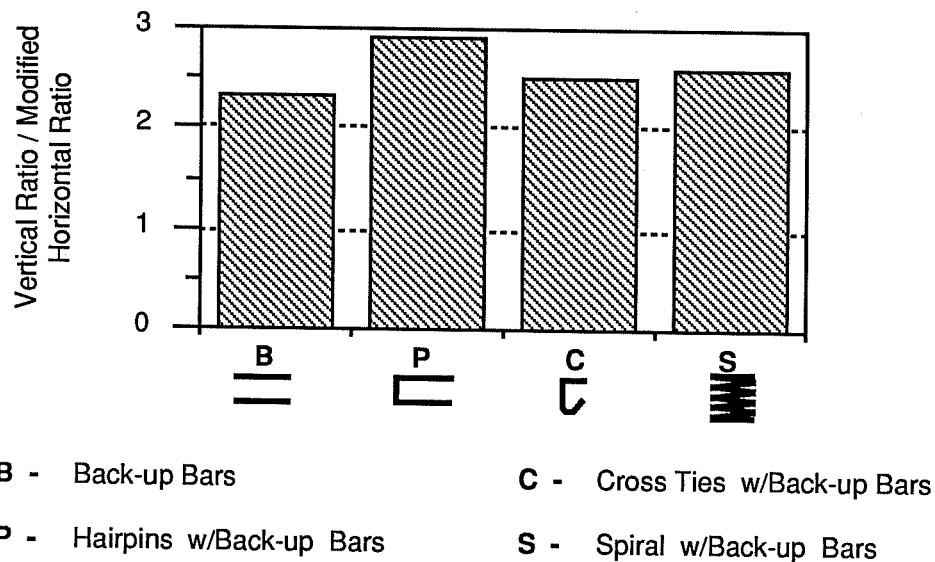


Figure 5.12 - Ratio of Vertically Oriented Anchor to Modified Horizontally Oriented Anchor (Bearing Stress at Failure over Concrete Compressive Strength)

the comparison of the average modified f_b/f'_c ratios for the vertical oriented anchors to the similarly reinforced horizontally oriented anchors.

The system for modifying the bearing area is inexact for the extreme case of the vertical anchors with no edge cover, but it is conservative. For the monostrand anchorages the modification of the bearing area was also probably inexact but conservative.

The average f_b/f'_c ratios for the monostrand anchors were 183% of that for the similarly reinforced four-strand horizontal anchors. Figure 5.13 shows the ratio of the monostrand anchors average f_b/f'_c ratios to that of the four-strand anchors (note that the spiral reinforced monostrand anchorage zones sustained the maximum force of the loading system without failure). Another possibility for the difference in average f_b/f'_c ratios is the difference in the failure modes of the anchorage zones. Horizontal four-strand anchors produced combined splitting and bearing failure around the anchor. Vertical interior anchors failed with very localized

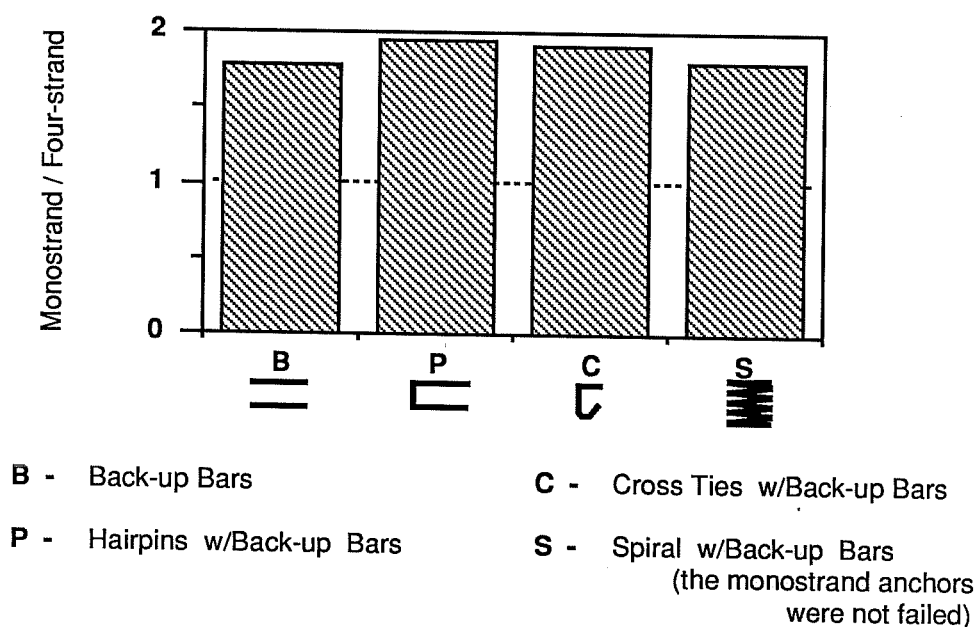


Figure 5.13 - Ratio of Monostrand Anchor to Four-strand Anchor (Bearing Stress at Failure over Concrete Compressive Strength)

spalling and crushing of the concrete directly ahead of the anchor. The failure of the monostrand anchorage zones produced horizontal plane cracking (Figure 5.14) which extended away from the anchor and included what is considered to be the general zone. These failures indicate that the vertical bursting stresses had the greatest significance in the monostrand anchorage zones and the least significance in the anchorage zones with vertically oriented four-strand anchors. Bearing stress may be a bad comparison for anchors which do not fail in bearing.

In these tests, the loading system modeled uniformly distributed post-tensioning loads ahead of the anchorage plates. However, that can be unrealistic for an actual anchor. If the stiffness of a standard monostrand anchor (Figure 1.3) is calculated according to Roberts¹¹, which concurs with the proposed AASHTO anchorage zone provisions², the monostrand anchor does not have sufficient stiffness to evenly distribute the post-tensioning

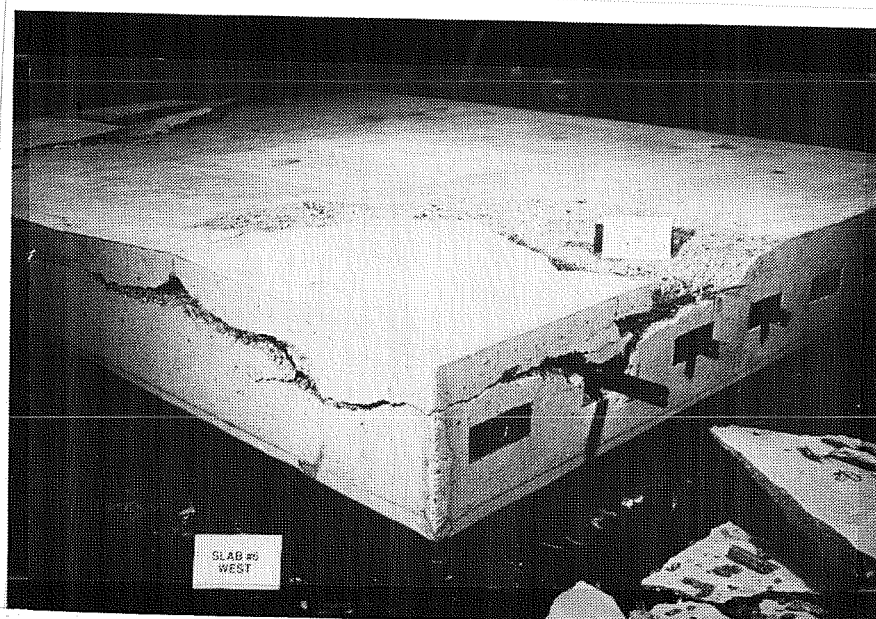


Figure 5.14 - Vertical Splitting at Failed Anchor B in Slab #6

transfer and service loads of one strand to the concrete. A local zone test² would have to be used to evaluate this anchors performance in the field. In contrast, the four-strand anchors are assumed to have sufficient stiffness to carry transfer and service loads.

The inclined tendon four-strand anchorage results were very similar to the horizontally oriented four-strand anchorage results. Figure 5.15 shows the ratio of the average f_b/f'_c ratios for the inclined and perpendicular tendon anchorage zones. The two anchorage zones with inclined tendons which exhibited vastly different failure loads had only horizontal reinforcement and their f_b/f'_c ratio was 147% of the perpendicular tendon anchorage zones reinforced with back-up bars. The other six inclined tendon anchorages also failed at higher f_b/f'_c ratios, but only by an average of 6% higher.

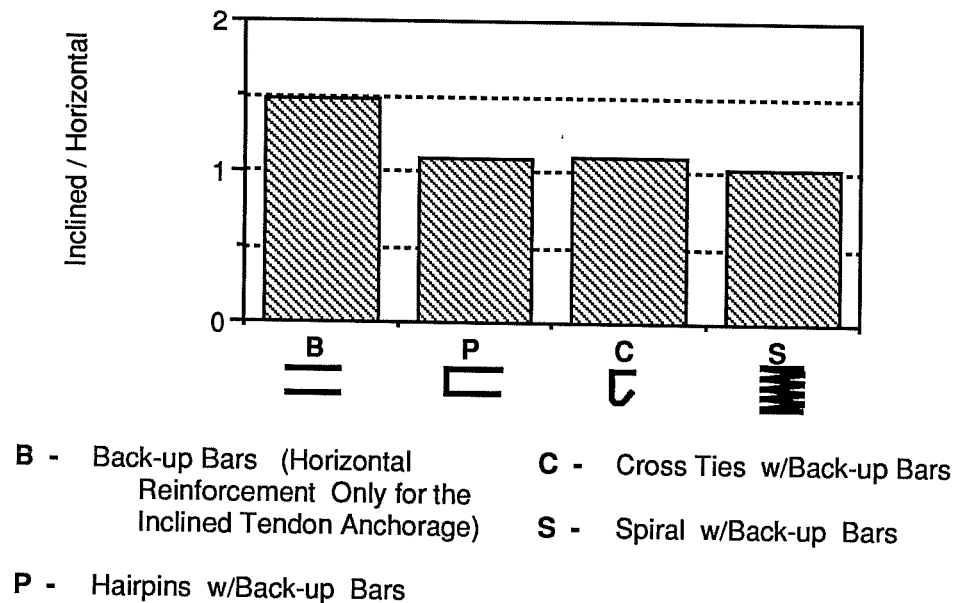


Figure 5.15 - Ratio of Inclined Tendon Anchor to Perpendicular Tendon Anchor (Bearing Stress at Failure over Concrete Compressive Strength)

As noted in Section 5.2.2, the horizontally reinforced exterior anchor with inclined tendons was the only exterior anchor to fail at a load higher than the load at which the interior anchor failed. It is possible that the edge distance has less of an effect on anchorage zones with inclined tendons. The anchorage zones along the stepped edge of an inclined tendon slab (Figure 4.43) are also more isolated than the adjacent anchorage zones along the straight edge of a bridge deck without inclined tendons.

5.2.5 Evaluation of Anchorage Zone Reinforcing Details

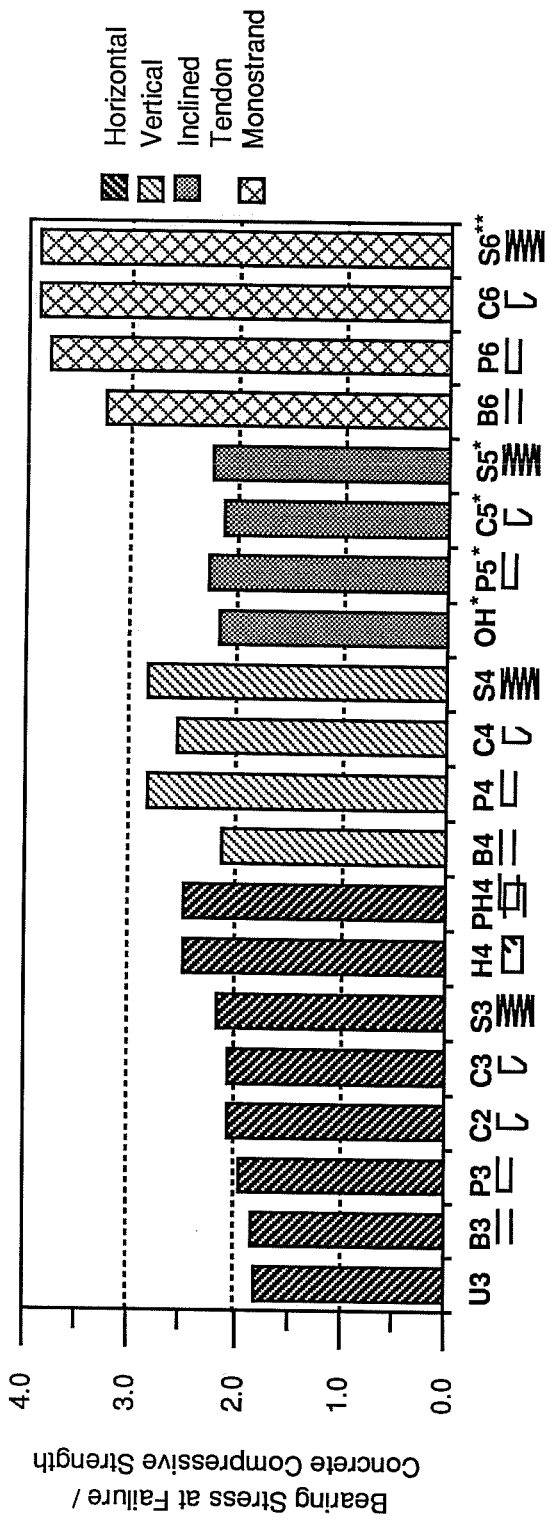
All of the anchors, even unreinforced, withstood loads in excess of their expected maximum field stressing loads, which was 35 kips for tendon force transfer loading ($0.8f_{pu}$) for all the tested anchors considering scale effects. The weakest anchorage group was the vertically oriented four-strand anchors which failed at an

average of 81.6 kips, which is 2.3 times the realistic maximum load of a half-scale four-strand anchorage. Vertical reinforcing generally reached high stresses ahead of horizontally oriented anchors, and horizontal reinforcing generally reached high stresses ahead of vertically oriented anchors. However, only a few failures produced anchorage zone splitting which indicate critical tensile forces. Exterior anchors and the monostrand anchors produced splitting.

Figure 5.16 and Tables 4.1 through 4.4 show the average f_b/f'_c ratios of interior anchors by group and reinforcement. As covered in Chapter 4, spiral anchorage reinforcement was consistently effective in sustaining high loads without reaching high stresses. The consistently low level of stresses indicates that the spiral acts as confining reinforcement which stiffens the anchorage zone until the local zone fails due to bearing stresses. The hairpin, cross tie, hoop, and hairpin hoop reinforcement ahead of horizontal anchorages all reached high stresses and most yielded during loading of the anchorage.

Spirals, hoops, and hairpin hoops had the highest average f_b/f'_c ratios ahead of horizontal four-strand anchors. However, unlike the spiral, the hoop and hairpin hoop reinforcement reached high stresses approaching failure which indicates a reaction to vertical plane stresses rather than just confinement of the local zone.

The vertical interior anchor with only back-up bars was much weaker than vertical interior anchors containing vertical reinforcement. These anchors exhibited bearing failures (Figure 5.4b) and apparently benefitted from the anchorage zone confinement provided by the vertical reinforcement. The hairpin, cross tie, and spiral reinforced vertical interior anchors had an average f_b/f'_c ratio of 2.73, and the back-up bar reinforced interior anchor's ratio was 2.13.



Letter Designates Anchorage Zone Reinforcement and Number Designates Specimen Number

- U - Unreinforced Anchors
 - B - Back-up Bars
 - P - Hairpins w/Back-up Bars
 - C - Cross Ties w/Back-up Bars
 - S - Spiral w/Back-up Bars
 - H - Hoops w/Back-up Bars
 - HP - Hairpin Hoops w/Back-up Bars
 - OH - Horizontal Reinforcing Only
- * These Anchorage Zones did not include Back-up Bars as Reinforcement
- ** The Spiral Reinforced Monostrand Anchors were not failed at the Highest Applicable Load.

Figure 5.16 - Ratio of Bearing Stress to Concrete Compressive Strength for Horizontal Four-strand, Vertical Four-strand, Horizontal Four-strand with Inclined Tendons, and Monostrand Anchors

In contrast to the interior anchor failures, the exterior vertical anchor failure produced primarily horizontal plane splitting (Figure 5.4) and failed with a f_b/f'_c ratio of 1.37. Although the back-up bars reached high stresses ahead of all of the vertical anchorages, they spanned the crack which caused the failure in this case and play an obvious role in resisting the failure. For the case of the vertical exterior anchor with a small edge distance, the horizontal plane bursting stresses are critical and the horizontal reinforcement should also be critical.

The inclined tendon anchorage zones produced similar failure loads regardless of reinforcement ranging from 95 kips to 110; it should be noted, however, that the spiral reinforced anchorage zones withstood 110 kip loads without failure (f_b/f'_c ratio was 2.297) then failed at lower anchor loads due to what was considered to be eccentric loading. The average f_b/f'_c ratio for the other six anchors was 2.15. The strength of the anchorage zones in this specimen were apparently unaffected by most reinforcing. The concrete tensile strength may have been sufficient to carry loads which were beyond the capacity of all but the spiral reinforcement.

The full-scale spirally reinforced monostrand anchorage zones withstood a 150 kip load and f_b/f'_c ratio of to 3.90. A monostrand anchor is typically loaded with 35 kips at transfer loading ($0.8f_{pu}$) with a 1/2 inch strand. The anchorages reinforced with cross ties both failed at a load of 150 kips. The tendon with the back-up bar reinforced monostrand interior anchorage failed at the control detail, and the interior anchorage zone reinforced with hairpins and back-up bars failed at 145 kips; therefore, hairpins and back-up bars as monostrand anchorage zone reinforcement are not conclusively worse than cross ties even though they failed in this test at lower loads. The horizontal monostrand failures produced vertical splitting ahead of the anchors which indicates critical vertical stresses, but the failure loads of five of the monostrand anchors

exceeded four times the expected anchor loading of a monostrand anchor.

5.3 Evaluation of Finite Element Analysis Predictions

The linear-elastic finite element analysis of the four-strand horizontally oriented anchors (Section 2.2) estimated that 249 psi of vertical plane bursting stress and a 1404 psi local-general zone bearing stress is ahead of a half-scale horizontal four-strand anchor with a load of 35 kips applied to the anchor. The splitting tensile strength and compressive cylinder strength of the concrete was measured (Section 3.4.2) for each slab. The first cracking load was calculated as the load which would create an estimated vertical plane bursting stress equal to the slab's concrete splitting tensile strength.

The estimated first cracking anchor loads for the horizontally oriented four-strand anchors are in Table 5.3. However, pre-failure visible cracking loads were infrequent for edge anchors, and the first cracking loads predicted by the finite element analysis were in general much lower than the anchorage failure loads. The unreinforced anchorage zone failures of Slab #3 were an average of 77% above the first cracking loads predicted by the finite element analysis. It is unlikely that the first cracking load would match the ultimate failure load of even an unreinforced anchorage zone because the capacity of an anchor may increase after internal cracking as illustrated in Figure 2.17 due to redistribution of concrete tensile strength. As the crack extends ahead of the anchor, the bursting stresses move lower in the section where the plain concrete can carry higher anchor loads with lower tensile stresses. Furthermore, the cracking predicted by the finite element analysis is in the vertical plane, along the tendon, and within the specimen; therefore, it is not visible cracking. When visible

Table 5.3 - Finite Element Predicted Anchor Failure Loads and Actual Failure Loads

Reinforcement	Slab	Anch.	Predicted Cracking (kips)	Predicted Failure (kips)	Actual Failure (kips)
Unreinforced	#3	A	46	51	75
"	"	B	46	51	80
"	"	C	46	51	80
"	"	D	46	51	90
Back-Up	#3	K	46	51	85
"	"	L	46	51	55
Horizontal	#5	G	58	54	105
"	"	H	58	54	110
Hairpins	#3	E	46	74	85
"	"	F	46	74	95
"	#5	A	58	77	95
"	"	B	58	77	110
Cross Ties	#2	A	51	87	75
"	"	H	51	87	95
"	"	D	51	87	102
"	#3	G	46	82	90
"	"	H	46	82	100
"	#5	C	58	77	100
"	"	D	58	77	105
Spiral	#3	I	46	82	95
"	"	J	46	82	107
"	#5	E	58	85	110
"	"	F	58	85*	105*
Hoops	#4	A	45	71*	90*
"	"	B	45	71	100
Hairpin Hoops	#4	C	45	71	100
"	"	D	45	71	100

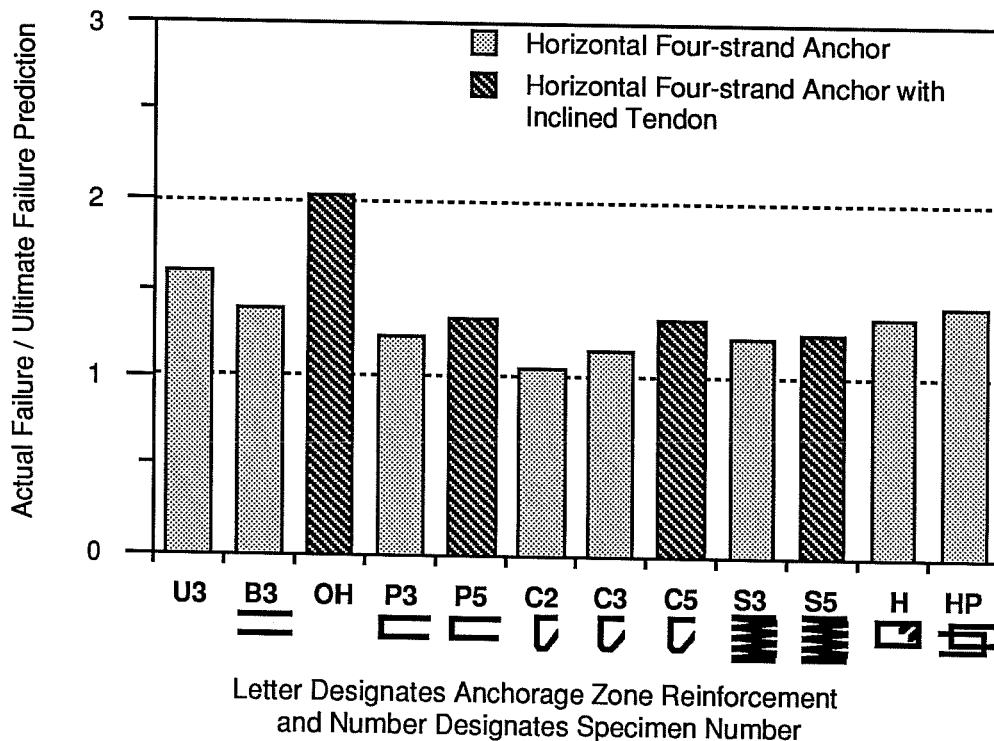
* Control Detail Failed

cracking did occur, it generally extended diagonally from the corners of the anchorage plate to the slabs top and bottom (Figures 4.1 and 4.8).

The failure loads of anchorages were compared to predictions made from the finite element analysis based on the calculated bearing stress at the interface between the local zone and the general zone. The calculated bearing stress at the interface was limited to 75% of the concrete's compressive strength ($0.75f'_c$). The vertical finite element model calculated the highest stresses, and the depth of the local zone was chosen to be 2 inches (the plate width) for unreinforced and back-up bar reinforced anchorages, 4 inches for anchorages with one layer of vertical reinforcement ahead of the anchor, and 6" for anchorages with local zones confined with spirals or two layers of vertical reinforcement ahead of the anchor.

Figure 5.17 shows the ratio of actual failure loads to finite element predicted failure loads for horizontal oriented four-strand anchors with and without inclined tendons. Table 5.3 lists both the predicted failure loads and actual failure loads. The predictions were fairly accurate and always conservative. The average ratio of actual to predicted failure load was 137 %.

The least accurate predictions were for the anchors lacking vertical reinforcement. This inaccuracy is probably related to the inaccuracy in picking the depth of the local zone. Figure 5.18 shows the sensitivity of the finite element analysis' maximum compressive stress ahead of an anchor to variation in the depth at which the compressive stress is checked. Within the first four inches ahead of the anchor (a 2 inch plate in a 5 inch slab), the stresses become relatively uniform, but at a depth of 2 inches, the maximum predicted stress is predicted as 150% of the uniform stress distribution.



- Letter Designates Anchorage Zone Reinforcement and Number Designates Specimen Number
- | | |
|----------------------------------|-----------------------------------|
| U - Unreinforced Anchors | C - Cross Ties |
| B - Back-up Bars | S - Spiral w/Back-up Bars |
| OH - Horizontal Reinforcing Only | H - Hoops w/Back-up Bars |
| P - Hairpins w/Back-up Bars | HP - Hairpin Hoops w/Back-up Bars |

Figure 5.17 - Ratio of Actual Average Anchor Failure Loads to Predicted Failure Loads from Finite Element Analysis

5.4 Evaluation of Strut-and-tie Model Predictions

5.4.1 General

The strut-and-tie model predicts failures by comparing the model's strut, tie, and node strength to the forces that each component will be subjected to during loading. The calculation of strut-and-tie failure load predictions is presented in Section 2.3.4. The vertical plane strut-and-tie model controlled all of the horizontally oriented anchor failure predictions and the horizontal

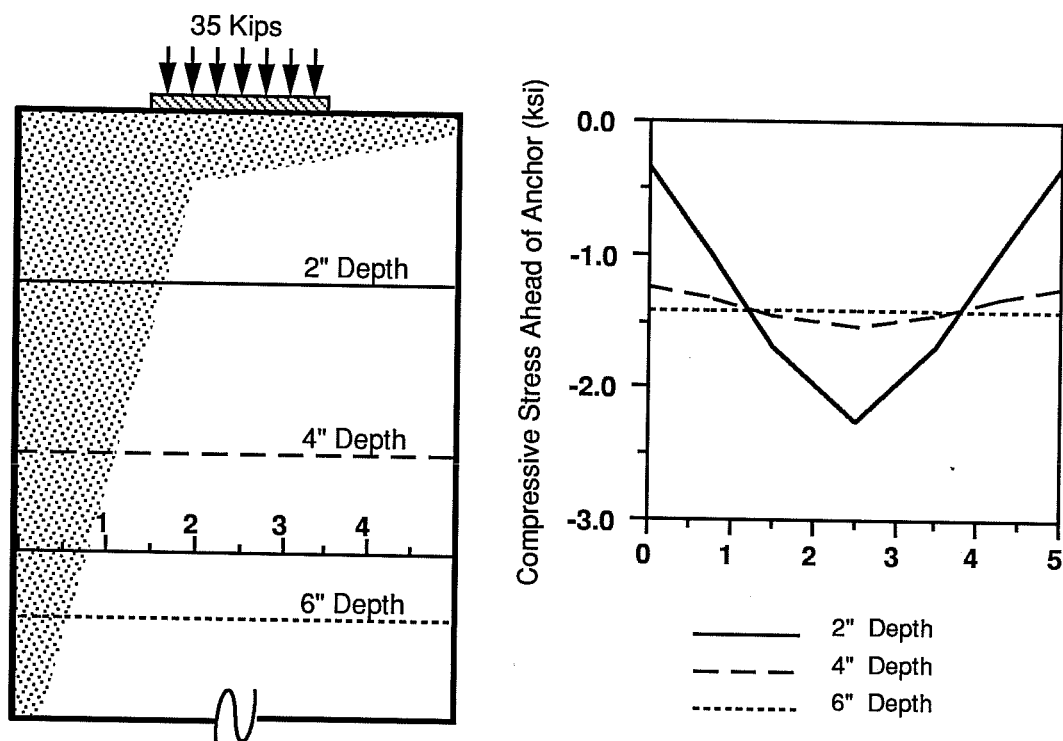


Figure 5.18 - Finite Element Generated Bearing Stresses Ahead of Edge Anchor

plane strut-and-tie model controlled the vertically oriented anchor predictions. Tension forces carried by the plain concrete (Sections 2.3.4) caused the accuracy of tie failure predictions to be very inconsistent, particularly for hairpin, back-up bar reinforced, or unreinforced anchorages which are assumed to have little or no tie load capacity. Predictions of node and strut failures should provide more consistent results in cases where node or strut failure controls. Failures were very localized and often seemed to involve concrete crushing directly ahead of the anchor, which would indicate that the strut-and tie model failed at the node-strut connection or node-anchor plate connection directly ahead of the anchor plate. Those failures could be considered local zone failures. The vertically oriented exterior anchor failure (Figure 5.4b) and the

Table 5.4 - Average Strut and Tie Predicted Anchor Failure Loads for Various Anchors

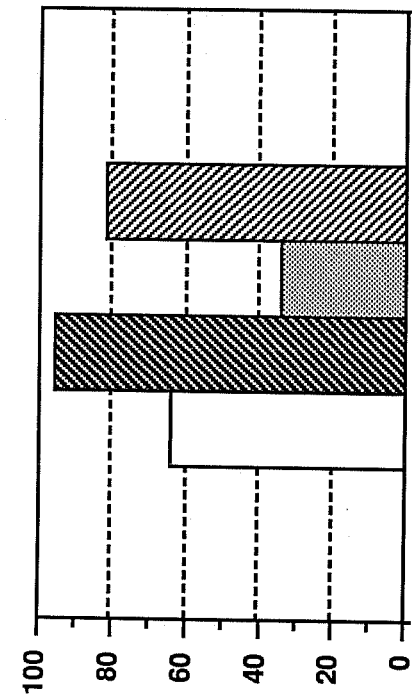
Anchor Description	Strut-and-Tie Predicted Component Failures (Kips)			Actual Failure (Kips)
	Strut	Tie*	Node	
Horizontal Four-Strand	85	58*	74	89
Vertical Four Strand	64	96	34	82
Horizontal Four-Strand Inclined	77	72*	77	105
Horizontal Monostrand	122	124*	73	133**

* Tie strengths which were far less than actual failure loads (10% or less) were excluded from these averages because no method was used to estimate concrete-tie strength. These cases were typically back-up bars and hairpins.

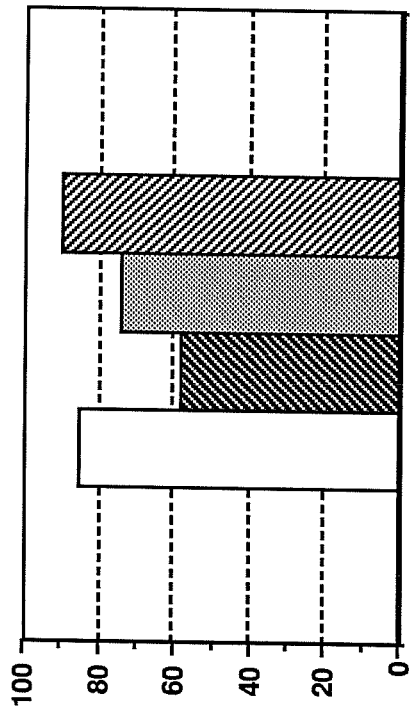
** The spiral reinforced monostrand anchorage zones were never failed. This number is a lower bound.

monostrand anchors (Figure 5.14) produced slab splitting which extended ahead of the anchor across assumed tie locations. This suggests that failure was due to bursting tie forces rather than concrete crushing at the anchor-node-strut interface, and these failures could be considered a general zone failure.

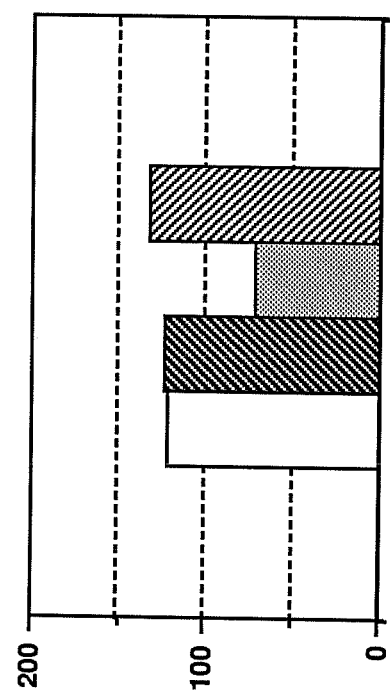
Table 5.4 and Figure 5.19 show the actual failure loads and the predicted component strut-and-tie anchorage failure loads for the tested anchorage group. The model is conservative whenever the actual failure load level is higher than the lowest predicted component failure load level. For anchorages with horizontally oriented anchors with no vertical reinforcement or hairpins, tie failure predictions were excluded because concrete tensile strength



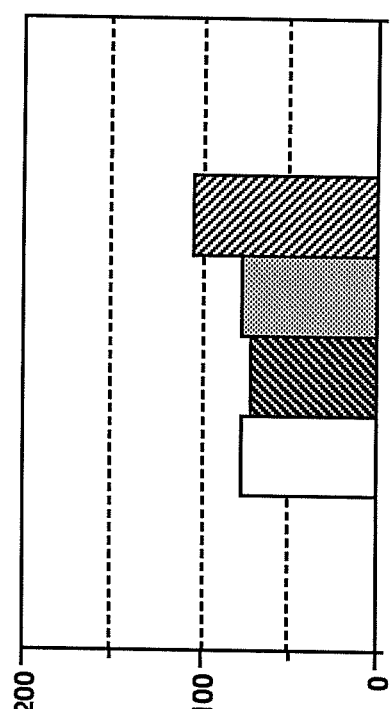
(a) Horizontal Four-Strand Anchors (Excluding the Back-Up Bar & Hairpin Tie Failure Predictions)



(b) Vertical Four-Strand Anchors (Excluding the Exterior Anchor Tie Failure Predictions)



(c) Anchors with Inclined Tendons (Cross Tie and Spiral Tie Failure Predictions Only)



(d) Monostrand Anchors (Cross Tie and Spiral Tie Failure Predictions Only)

Strut
 Tie
 Node
 Actual Failure

Figure 5.19 - Predicted Strut-and-Tie Component Failure Loads and Actual Failure Loads for Various Anchor Types, Anchor Orientations, and Tendon Inclination

withstood tie forces which allowed the anchor to carry 10 or more times the predicted tie failure anchor loads.

In general, the strut-and-tie models' failure load predictions were most accurate for the horizontally oriented four-strand anchors with and without inclined tendons. Tie failure predictions were most accurate overall because the strut and node failure loads were conservative for the vertically oriented anchors and the monostrand anchors. However, the failure geometry of the interior vertical anchors does not indicate that the anchorage zone failure included tie component failure.

Figures 5.20 through 5.23 and Tables 5.4 through 5.7 show the actual failure loads and the predicted component failure loads for the tested anchorage zone reinforcements in each anchorage type.

5.4.2 Strut Failure Predictions

The strut failure predictions should be the most accurate overall predictions of anchorage failure loads. The calculated strut and node failure loads should provide the most accurate predictions of failure because the failure geometry of most of the four-strand anchors indicated bearing and compression failures ahead of the anchor, rather than splitting due to bursting stresses across reinforcement. The horizontally oriented four-strand anchors had an average ratio of actual failure loads to predicted node failure load of 1.08, and the ratio was 1.37 for the anchors with inclined tendons.

The ratio of the actual failure load to the predicted tie failure load for the anchors with inclined tendons was 1.20 which is more accurate, but that value does not include the anchors with hairpins or only horizontal reinforcement which had similar failure loads to the other anchorage zones but much lower predicted tie strengths. The similar failure loads indicate that concrete tensile strength

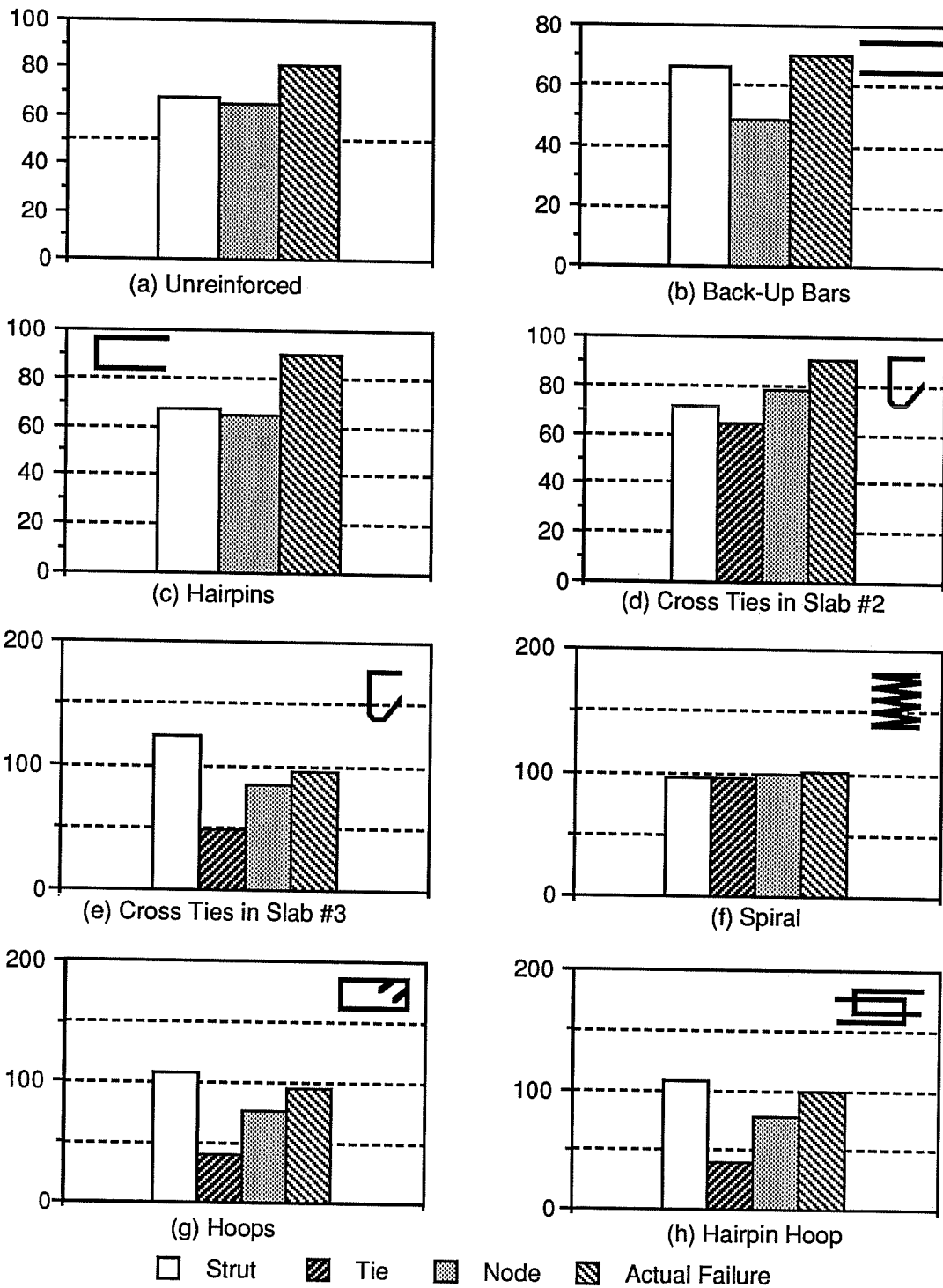


Figure 5.20 - Predicted Strut-and-Tie Component Failure Loads and Actual Failure Loads for Horizontal Oriented Four-strand Anchors (kips)

Table 5.5 - Strut and Tie Predicted Anchor Failure Loads
for Horizontally Oriented Anchors

Reinforcement	Slab & Anchor		Strut-and-Tie Predicted			Actual Failure (Kips)
			Component Failures (Kips)			
			Strut	Tie	Node	
Unreinforced	#3	A	67	0	<u>65</u>	75
"	"	B	67	0	<u>65</u>	80
"	"	C	67	0	<u>65</u>	80
"	"	D	67	0	<u>65</u>	90
Back-Up	#3	K	67	0	<u>65</u>	85
"	"	L	66	0	<u>33</u>	55
Hairpins	#3	E	67	8	<u>65</u>	85
"	"	F	67	8	<u>65</u>	95
Cross Ties	#2	A	71	<u>64</u>	69	75
"	"	D	71	<u>64</u>	69	102
"	"	H	71	<u>64</u>	69	95
"	#3	G	123	<u>48</u>	85	90
"	"	H	123	<u>48</u>	85	100
Spiral	#3	I	<u>95</u>	96	100	95
"	"	J	<u>95</u>	96	100	107
Hoops	#4	A	107	<u>40</u>	77	90*
"	"	B	107	<u>40</u>	77	100
Hairpin Hoops	#4	C	107	<u>40</u>	77	100
"	"	D	107	<u>40</u>	77	100

* Control Detail Failed

had a large effect on the tie strength and the accuracy of the predicted tie failure is purely coincidental.

5.4.3 Node Failure Prediction

Node failure was predicted with the equation for the allowable anchor load provided in Section 2.3.4. The anchorage zone reinforcement was considered confinement reinforcement only when

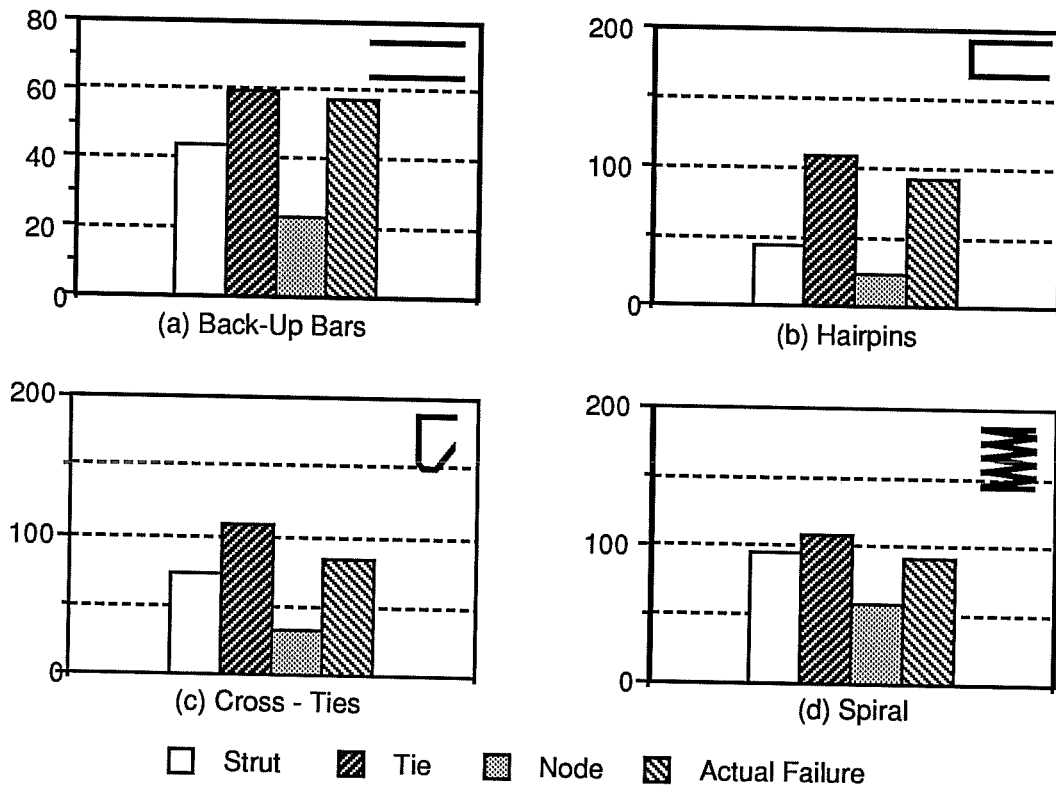


Figure 5.21 - Predicted Strut-and-Tie Component Failure Loads and Actual Failure Loads for Vertical Oriented Four-strand Anchors (kips)

Table 5.6 - Strut and Tie Predicted Anchor Failure Loads for Vertical Oriented Four-strand Anchors

Reinforcement	Slab & Anchor		Strut-and-Tie Predicted Component Failures (Kips)			Actual Failure (Kips)
			Strut	Tie	Node	
			Back-Up	#4	K	
"	"	L	44	<u>12</u>	23	45
Hairpins	#4	E	44	108	<u>23</u>	90
"	"	F	44	108	<u>23</u>	95
Cross Ties	#4	G	74	108	<u>33</u>	78
"	"	H	74	108	<u>33</u>	90
Spiral	#4	I	95	108	<u>58</u>	90
"	"	J	95	108	<u>58</u>	95

* Control Detail Failed

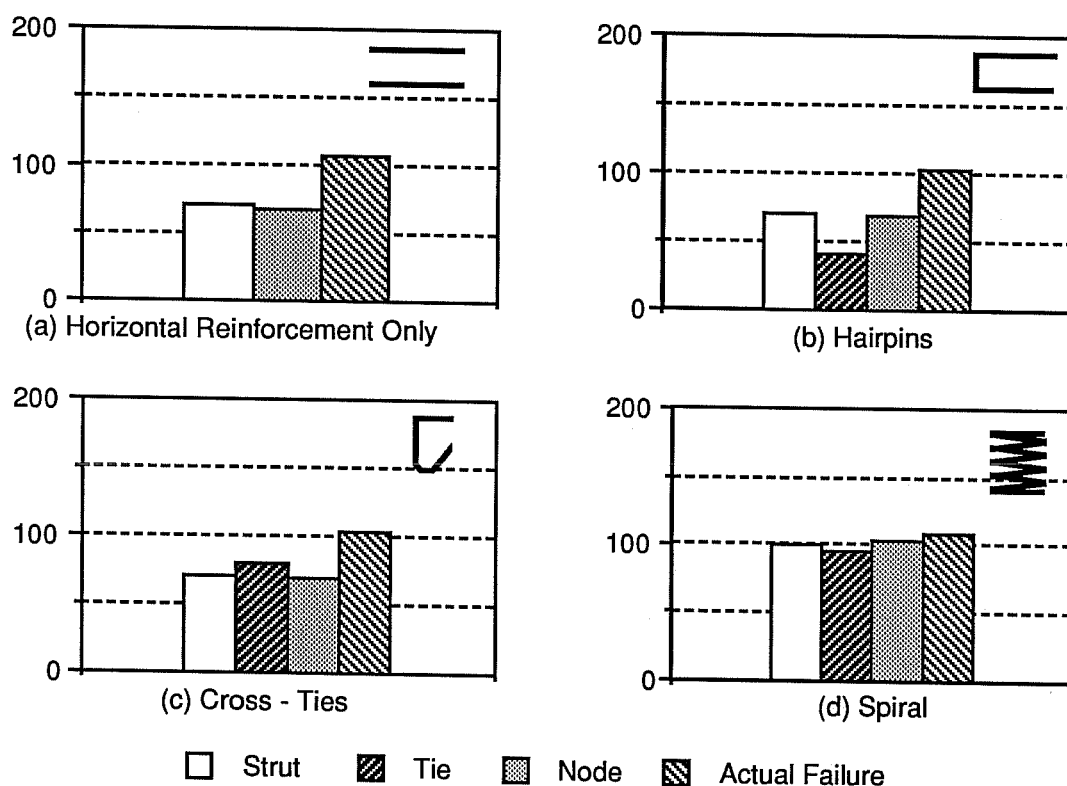


Figure 5.22 - Predicted Strut-and-Tie Component Failure Loads and Actual Failure Loads for Four-strand Anchors with Inclined Tendons

Table 5.7 - Strut and Tie Predicted Anchor Failure Loads for Anchors with Inclined Tendons

Reinforcement	Slab & Anchor		Strut-and-Tie Predicted			Actual Failure (Kips)
			Component Failures (Kips)			
			Strut	Tie	Node	
Horizontal Only	#5	G	70	0	<u>68</u>	105
"	"	H	70	0	<u>68</u>	110
Hairpins	#5	A	70	<u>40</u>	68	95
"	"	B	70	<u>40</u>	68	110
Cross Ties	#5	C	70	80	<u>68</u>	100
"	"	D	70	80	<u>68</u>	105
Spiral	#5	E	99	<u>96</u>	103	110
"	"	F	99	<u>96</u>	103	105 *

* Control Detail Failed

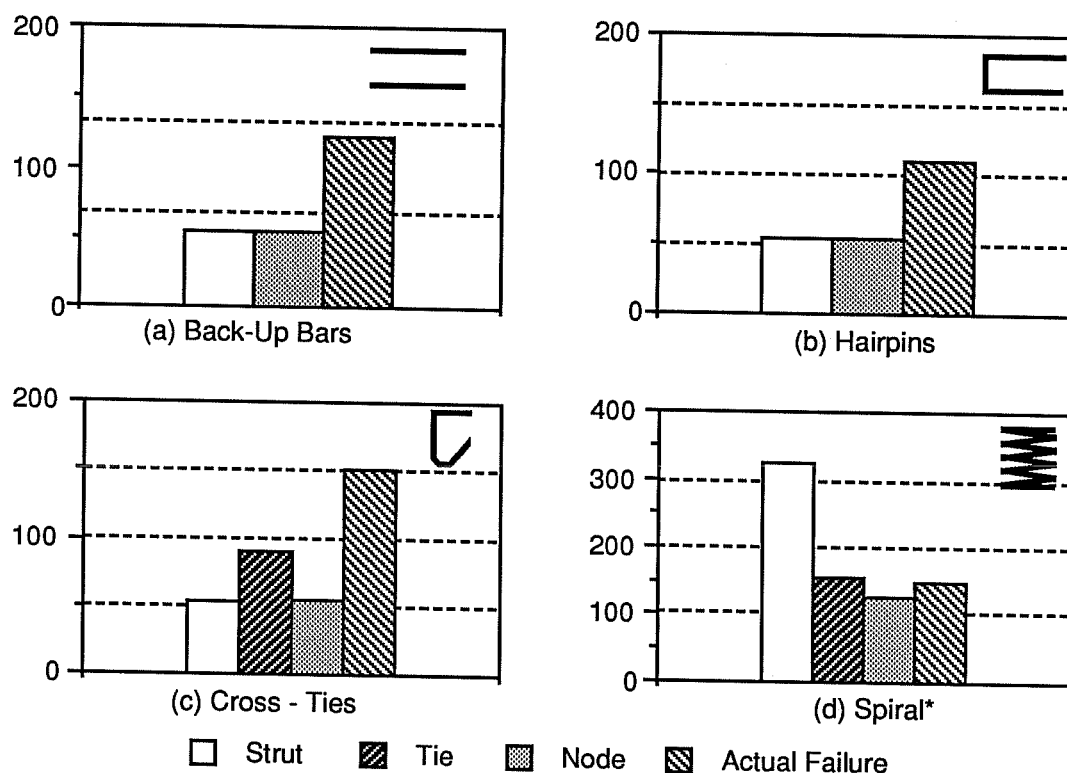


Figure 5.23 - Predicted Strut-and-Tie Component Failure Loads and Actual Failure Loads for Monostrand Anchors (* the spiral reinforced anchorage zones were not failed)

there were two layers ahead of the anchor. Node failure prediction was consistently accurate for all of the horizontally oriented four-strand anchors with and without inclined tendons (Figures 5.20 and 5.22), and the localized area of the failures indicates that the failures are occurring in the region of the node. The ratio of actual failure loads to node failure predictions for those anchors are 1.12 and 1.65 respectively. These values are conservative.

The values for vertically oriented anchors and horizontally oriented monostrand anchors were not as accurate (Figures 5.21 and 5.23). In fact, the values were extremely conservative. The equation used to predict node failure contains a term for the

Table 5.8 - Strut and Tie Predicted Anchor Failure Loads for Monostrand Anchors

Reinforcement	Slab & Anchor	Strut-and-Tie Predicted				Actual Failure (Kips)
		Component Failures		(Kips)		
		Strut	Tie	Node		
Back-Up	#6 G	54	0	<u>54</u>	95	
"	" H	54	0	<u>54</u>	125	
Hairpins	#6 A	54	7	<u>54</u>	100	
"	" B	54	7	<u>54</u>	145	
Cross Ties	#6 C	54	91	<u>54</u>	150	
"	" D	54	91	<u>54</u>	150	
Spiral	#6 E	325	156	<u>128</u>	>150**	
"	" F	325	156	<u>128</u>	>150**	

* Control Detail Failed

** Spiral Reinforced Anchor did not fail under maximum applicable load

maximum area of the portion of the concrete surface which is geometrically similar to and concentric with the anchorage. The condition of geometric similarity disallows most of the concrete surface around the vertically oriented and monostrand anchors in the experimental program.

Though the predicted node failures of the vertically oriented interior anchors were extremely conservative, the failure geometry (Figure 5.4a) involved node destruction which indicates that correct node failure predictions should be the most accurate for this series. The average ratio of actual failure loads to predicted node failure was 2.5 while the ratio for predicted tie failure is 0.79 which also indicates that the either the tie failure prediction was unconservative or that the anchorage zone failed at a strut or node.

Ideally, predicted strut and node failure loads should not be as conservative as they are in some cases. They should have values

around 1.0 when their failure controls, and they should have values of less than one when another component failure controls. However, if the values are going to be inaccurate, it is necessary that they are conservative.

5.4.3 Tie Failure Prediction

Two factors made the prediction of the anchorage zone failure load by calculation of the tie failure inaccurate. First complete omission of any contributions of the concrete tensile strength (Section 2.3.4) made the evaluation of tie strength unreliable. The concrete tensile strength is not considered in the predicted tie failure loads; therefore, tie strength values are very conservative estimates of the actual strength of uncracked anchorage zones. Also, the majority of failures produced crushing and spalling immediately ahead of the anchor which indicates node or strut failures rather than tie failures which should cause splitting of the slab.

The vertically oriented exterior anchor and the monostrand anchors did produce splitting of the slab. The failure of the vertically oriented exterior anchor (Figure 5.4b) vertical plane splitting, but the anchorage of some of the horizontal steel was insufficient to reach the yield strength of the bar and calculation of that strength was inaccurate. The back-up bars ahead of the exterior anchor are believed to have had sufficient anchorage. If only the back-up bars are considered, the predicted failure load is 12 kips. If the first row of horizontal reinforcing, which was insufficiently anchored, is also considered, the predicted failure load is 60 kips. The actual failure load was 45 kips.

The average ratios of actual failure load to tie predicted anchorage failure load for the four-strand anchors with inclined tendons (Figure 5.22) was 1.24 and was the most accurate prediction, but the failures did not cause splitting ahead of the anchor which

would indicate tie failure. The failure loads of the anchorages without vertical reinforcement were also as large as the failure loads of vertically reinforced anchorages; therefore, the accuracy of these loads is suspicious.

The monostrand anchors (Figure 5.14) failed by splitting apart vertical planes ahead of the anchor, which indicates that the failure was due to vertical plane bursting stress. The average ratio of failure load to predicted tie failure load was 1.65, but the effects of concrete tensile strength on the tie strength makes the predicted tie failure loads inaccurate even though they should control.

5.4.4 Strut-and-tie Model Predicted Failure

For every anchor tested in this investigation, the actual failure level was higher than the predicted failure level. The strut-and-tie model proved to be a consistently conservative procedure for predicting anchorage zone failure load levels in bridge decks.

5.5 Analysis Recommendations

Bridge deck post-tensioning anchors usually fail in their local zone. This makes analysis of the local zone the primary concern. Node failure, strut failure, vertical plane tie failure ahead of all anchors and horizontal plane tie failures ahead of exterior anchors should be analyzed with the strut-and-tie model.

5.6 Design Recommendations

5.6.1 General

In a 10 inch bridge deck, post-tensioning edge anchors which are similar to those examined and fail at service loads have been poorly constructed or loaded eccentrically. For the cases examined, unreinforced anchorage zones in 10 inch bridge decks should not fail

due to tendon jacking forces ($0.8f_{pu}$), but reinforcing should be added to the anchorage zone to provide general structural integrity.

5.6.2 Anchorage Reinforcing Details

Always provide vertical reinforcement. Spirals, hoops, and hairpin hoops performed best as anchorage zone reinforcement for bridge deck post-tensioned edge anchorages. These reinforcements provide confinement of the concrete ahead of the anchor. The hairpin hoop is the easiest to construct because it can be placed after installing post tensioning tendons or ducts. Both hoops and hairpin hoops should be placed in pairs, at least, ahead of an anchor. Cross ties and hairpins can also be used as vertical reinforcement. Edge anchor reinforcement can be designed with the strut-and-tie model as confining reinforcement, but it should also satisfy the requirements of a tie to carry reasonable anchor loads without any advantageous effects of concrete tensile strength.

For situations requiring extremely high loads a hairpin hoop or hoop can be used with a spiral, as shown in Figure 3.7, to provide a heavily reinforced anchorage zone.

5.6.3 Edge Distance

Exterior anchors with small edge distances have weaker anchorage zones and increase the importance of the horizontal plane stresses. A horizontal plane strut-and-tie model should be used ahead of exterior anchors to place sufficient bursting stress reinforcement.

5.6.4 Anchor Spacing and Stressing Sequence

Anchor spacing is of secondary importance and stressing sequence is of little importance for post-tensioned bridge deck edge

anchors. Whether an anchor's anchorage zone is isolated or shared with other anchors depends on anchor spacing and edge distance of the exterior anchors, but this only creates horizontal plane stresses ahead of interior anchors which can easily be carried by the minimum horizontal reinforcement required for bridge deck construction. Furthermore, strut failure is unaffected by adjacent loads, and node failure, which is assumed to be effected by anchor spacing (through effective bearing area), should not occur at service ($0.7f_{pu}$) or transfer loads ($0.8f_{pu}$); therefore, anchor spacing is of little consequence.

For exterior anchors with small edge distances, horizontal plane tie forces can be critical, and loading the adjacent interior anchor first can slightly reduce the horizontal plane stresses ahead of the exterior anchor. However, the exterior anchorage zone reinforcement should be designed to withstand the maximum applicable load for only that edge anchor; therefore, stressing sequence should not be considered to have harmful or beneficial effects on edge anchorage zones in bridge decks.

5.6.5 Anchor Orientation

Vertically oriented exterior anchors are the most likely anchors to fail due to horizontal plane bursting stresses because they can have small edge distances. Exterior anchor reinforcement should be designed with a strut-and-tie model. If vertical plane tie forces are found to be negligible, as in the vertical oriented anchors of this experimental program, reinforcement placed ahead of interior anchors should be designed solely as confinement reinforcement.

5.6.6 Anchor Types

The anchor type should not control the strength of an anchorage zone, but the size of the anchor in relationship to the

bridge deck thickness indicates whether horizontal plane or vertical plane stresses will be more prevalent in the slab.

5.7 Recommendations for AASHTO Bridge Design Specifications⁴

9.21.3.9 Multiple Slab Anchorages

9.21.3.9.1 Multiple slab anchorages are adjacent anchorages which are located on a slab or bridge deck edge.

9.21.3.9.2 Bursting forces which are in the plane of the slab can be reduced by loading closely-spaced anchors, but anchorage zones shall not depend on adjacent anchor loading for sufficient bursting strength. Bursting forces which are transverse to the plane of the slab need only be considered to be distributed directly ahead of the loaded anchor or vertical row of loaded anchors.

9.21.3.9.3 Vertical reinforcement shall be placed ahead of anchors to withstand bursting forces in accordance with sections 9.21.3.5 or 9.21.4.4. Concrete tensile strength shall be considered negligible in the design of the anchorage zone in accordance with section 9.21.3.5.3.

9.21.3.9.4 The multiple slab anchorage zones shall be designed in accordance with the requirements of sections 9.21.3.4, 9.21.3.5, and 9.21.5. Furthermore, any deck reinforcement may be considered anchorage zone reinforcement if the reinforcement is placed in the anchorage zone and the reinforcement possesses sufficient anchorage and development length.

C.9.21.3.9 Commentary on Multiple Slab Anchorages

C.9.21.3.9.2 Anchor spacing and stressing sequence only effect horizontal plane stresses. Critical bursting stresses are generally most severe ahead of the exterior anchor, and can be reduced by loading a close adjacent anchor; however, the confining forces provided by a close adjacent anchor should not be relied upon for anchorage zone strength. Furthermore, vertical stresses are concentrated directly ahead of the loaded anchor. Closely spaced anchors may distribute vertical bursting forces into adjacent anchorage zones, but the forces will redistribute if each anchorage zone is designed to independently carry its vertical bursting force.

C.9.21.9.4 Slabs and bridge decks typically have reinforcement for flexural strength and serviceability. Reinforcement provided for non-anchorage zone concerns can be considered anchorage zone reinforcement, but such reinforcement is still subject to the placement and capacity requirements of anchorage zone reinforcement.

Chapter 6 Summary and Conclusions

6.1 Summary of the Investigation

The purpose of the investigation was to evaluate the effects of anchor type, anchor orientation, spacing, edge distance and tendon inclination on post-tensioning anchorage zone capacity in bridge decks. Both analytical procedures and physical experiments were performed in the investigation.

Finite element and strut-and-tie modeling were used to predict bridge deck anchorage zone behavior. A variety of loading conditions were applied to analytical models. Those loading conditions included loading of an interior anchor only, an exterior anchor only, closely-spaced anchors, and distant anchors. Finally, the analytical predictions were compared to the experimental results and evaluated.

The physical experimental program incorporated the testing of 56 post-tensioning anchor pairs within 6 slabs. Characteristics such as anchor type, anchor orientation, tendon inclination, and anchorage zone reinforcement were varied. The most common anchorages were horizontally oriented four-strand anchors in a 10 inch bridge deck built at half-scale. Monostrand anchors, vertical oriented four-strand anchors, and horizontal oriented four-strand anchors with inclined tendons were also examined. Concrete and reinforcement strains were recorded during loading. Failure loads of individual anchors were determined except for a few cases where premature failure occurred at the opposite edge. The effects of variables on anchorage zone strength were evaluated.

6.2 Conclusions

For the cases examined, the strength of each anchorage zone was always sufficient to carry the expected transfer load levels ($0.8f_{pu}$) and service load levels ($0.7f_{pu}$) applied to the four-strand

and monostrand anchors in a 10 inch thick bridge deck. Bridge deck anchorage zones often combine the general zone and the local zone into virtually the same region of the slab. In most cases, the failure appeared to involve concrete crushing directly ahead of the anchor plate and separation of the confining concrete in the local anchorage zone. These failures indicate that the failure was propagated from the local zone. In contrast, all of the monostrand anchors and the vertically oriented exterior anchor with a small edge distance exhibited concrete splitting ahead of the anchor plate and along the tendon. The splitting extended into what is accepted as the general zone.

Bridge deck anchorage failures were generally localized failures. The interacting horizontal plane stresses never reached critical levels. Therefore, the effects of stressing sequence on the anchorage zones in bridge decks were negligible.

The strut-and-tie model produced consistently conservative predictions of anchorage zone capacity.

6.3 Recommendations

All post-tensioning anchorages should have confinement steel placed ahead of them to provide general structural integrity (i.e. hoops, hairpin hoops, or spirals). The following recommendations are made for the analysis and design of bridge deck anchorage zones similar to the ones in this investigation.

The strut-and-tie model should be used for the design of the post-tensioning anchorage zone. Vertical plane stresses, which are transverse to the plane of the bridge deck, need only be considered directly ahead of the loaded anchor. The analysis of those vertical plane stresses can be analyzed with a vertical plane model which neglects adjacent anchors in the horizontal plane. Slab horizontal temperature reinforcement should be sufficient to withstand horizontal stresses generated ahead of interior edge

anchors, but exterior edge anchors may require additional horizontal reinforcement. Stressing sequence and anchor spacing can be neglected if the previous conditions are met.

Appendix

Table A.1 - Calculated Concrete Stresses from Strain Gage Readings of Slab I During Alternate Anchoring Stressing Sequence

Calculated Stresses in Concrete from Horizontal Gages (psi)															
Gage # Position & Depth	1* A 1/4"	2* E-F 1/4"	3* H 1/4"	4 A 6"	5 A 24"	6 B 2"	7 B 6"	8 B 12"	9 C 2"	10 C 6"	11 C 9"	12 C 12"	13 C 48"	14* C 2"	15* C 8"
Load C	9	36	-3	-3	6	-75	-127	-15	-48	99	78	85	45	-66	123
Load G	15	72	0	0	6	-48	-118	-27	15	115	91	81	42	-45	145
Load E	6	24	-3	-3	6	6	-100	-33	99	111	78	81	63	-27	145
Load A	42	51	3	202	51	1313**	667**	12	115	199	157	139	27	39	241
Load B	51	69	0	163	87	983**	749**	130	115	184	127	117	45	84	235
Load D	63	Broken	3	175	90	1043**	748**	123	150	133	172	99	93	91	175
Load F	60	Broken	3	175	87	1070**	760**	126	166	145	81	99	96	115	193
Load H	57	Broken	3	181	85	1095**	800**	109	184	166	103	111	75	129	214

Calculated Stresses in Concrete from Horizontal Gages (psi)													
Gage # Position & Depth	16* C 9"	17* C 12"	18 H 16"	19 H 12"	20 H 48"	21 A 3"	22 A 8"	23* D 3"	24* D 8"	25 D 3"	26 D 8"	27 H 3"	28 H 8"
Load C	93	87	9	3	-3	0	3	Lost	21	12	24	-3	31
Load G	106	93	-48	-12	24	0	0	Lost	-15	6	24	6	21
Load E	97	81	-42	-15	27	0	-3	Lost	0	15	30	3	18
Load A	181	145	-36	-12	27	591**	51	Lost	-9	-18	18	3	15
Load B	157	136	-36	-12	21	582**	66	Lost	-6	-30	15	3	15
Load D	99	105	-21	-9	28	579**	66	Lost	Broken	Broken	111	4	18
Load F	108	105	-24	-18	40	579**	63	Lost	Broken	Broken	103	4	18
Load H	127	121	241	105	69	579**	60	Lost	Broken	Broken	97	1241**	187

* Gage Not Represented in Graphic
Broken = Gage Destroyed During Loading

** Stresses Exceed Tensile Strength of Concrete (361 psi)
Lost = Gage Previously Destroyed

Table A.2 - Calculated Concrete Stresses from Strain Gage Readings of Slab 1 During Adjacent Anchor Stressing Sequence

Position & Depth	Calculated Stresses in Concrete from Horizontal Gage (psi)										Horizontal Gages				
	1* A 1/4"	2* E-F 1/4"	3* H 1/4"	4 A 6"	5 A 24"	6 B 2"	7 B 6"	8 B 12"	9 C 2"	10 C 6"	11 C 9"	12 C 12"	13 C 48"	14* C 2"	15* C 6"
Load A	87	Lost	-23	211	57	1717**	1184**	154	78	75	78	60	-36	36	51
Load B	111	Lost	605***	117	81	1083**	1051**	377	61	33	33	27	-12	78	27
Load C	115	Lost	3262***	115	91	999**	818**	341	54	151	123	121	36	3	151
Load D	117	Lost	1557***	115	91	1047**	818**	332	85	109	81	105	81	21	115
Load E	117	Lost	1556***	117	91	1080**	839**	329	99	109	75	97	103	36	115
Load F	117	Lost	2032***	117	85	1113**	867**	332	121	121	78	97	109	54	130
Load G	117	Lost	13762***	117	87	1140**	897**	335	133	135	91	103	103	72	148
Load H	117	Lost	-4033	117	85	1156**	918**	344	148	151	103	111	87	87	166

Gage # Position & Depth	Calculated Stresses in Concrete from Horizontal Gages				Calculated Stresses in Concrete from Vertical Gages (psi)								
	16* C 9"	17* C 12"	18 H 16"	19 H 12"	20 H 48"	21 A 3"	22 A 8"	23* D 3"	24* D 8"	25 D 3"	26 D 8"	27 H 3"	28 H 8"
Load A	54	51	3	0	0	522	45	Lost	Lost	Lost	-3	0	0
Load B	24	45	6	3	-3	502	57	Lost	Lost	Lost	-6	0	0
Load C	121	139	15	3	9	498	60	Lost	Lost	Lost	12	0	0
Load D	75	103	24	6	12	498	57	Lost	Lost	Lost	111	3	0
Load E	69	91	30	6	30	498	57	Lost	Lost	Lost	111	0	0
Load F	75	91	27	-9	57	498	54	Lost	Lost	Lost	105	6	18
Load G	87	99	-36	-24	84	498	57	Lost	Lost	Lost	103	1138	166
Load H	103	112	169	97		498	57	Lost	Lost	Lost	103		

* Gage Not Represented in Graphic Broken = Gage Destroyed During Loading
 ** Stresses Exceed Tensile Strength of Concrete (psi) Lost = Gage Destroyed Previously

Table A.3 - Calculated Concrete Stresses from Strain Gage Readings of Slab 1 During Anchor A Failure Loading (ksi)

Calculated Stresses in Concrete from Horizontal Gages															
Gage # Position & Depth	1* A 1/4"	2* E-F 1/4"	3* H 1/4"	4 A 6"	5 A 24"	6 B 2"	7 B 6"	8 B 12"	9 C 2"	10 C 6"	11 C 9"	12 C 12"	13* C 48"	14* C 2"	15* C 6"
All to 35k	117	Lost	117	85	1156**	918**	344	148	151	103	111	87	87	166	
A to 40k	111	Lost	202	115	1261**	1036**	314	181	217	187	154	33	-18	196	
A to 56k	344	Lost	1677**	112	1506**	1202**	320	193	229	202	181	12	6	214	
A Failed	Broken	Lost	Broken	Broken	Broken	Broken	Broken	64	128	105	105	88	-37	108	

Calculated Stresses in Concrete from Vertical Gages (psi)														
Gage # Position & Depth	16* C 9"	17* C 12"	18* H 16"	19* H 12"	20* H 48"	Gage # Position & Depth	21 A 3"	22 A 8"	23* D 3"	24* D 8"	25* D 3"	26* D 8"	27* H 3"	28* H 8"
All to 35k	103	112	169	97	84	All to 35k	498**	57	Lost	Lost	Lost	103	1138**	166
A to 40k	148	154	166	103	81	A to 40k	778**	75	Lost	Lost	Lost	63	1193**	181
A to 56k	163	160	166	103	81	A to 56k	2513**	365**	Lost	Lost	Lost	63	1193**	181
A Failed	70	97	32	13	Broken	A Failed	Broken	Broken	Lost	Lost	Lost	84	467**	92

* Gage Not Represented in Graph
Broken = Gage Destroyed During Loading

** Stresses Exceed Tensile Strength of Concrete (361 psi)
Lost = Gage Destroyed During Previous Loading

Table A.4 - Calculated Concrete Stresses from Strain Gage Readings of Slab 1 During Anchor D Failure Loading (ksi)

Gage # Position & Depth	Calculated Stresses in Concrete from Horizontal Gages (psi)														
	1* A 1/4"	2* E-F 1/4"	3* H 1/4"	4* A 6"	5* A 2 1/4"	6* B 2"	7* B 6"	8* B 12"	9 C 2"	10 C 6"	11 C 9"	12 C 12"	13* C 48"	14* C 2"	15* C 6"
All to 35k	117	Lost	Lost	117	85	1156**	918**	344	148	151	103	111	87	87	166
D to 35k	121	Lost	Lost	118	88	1162**	918**	374**	136	145	97	111	91	75	151
D to 40k	117	Lost	Lost	121	85	1165**	921**	372**	130	135	91	109	97	63	136
D Failed	117	Lost	Lost	118	91	1144**	897**	350	112	129	93	121	106	30	99

Gage # Position & Depth	Calculated Stresses in Concrete from Horizontal Gages (psi)						Calculated Stresses in Concrete from Vertical Gages (psi)								
	16* C 9"	17* C 12"	18* H 6"	19* H 12"	20* H 48"		Gage # Position & Depth	21* A 3"	22* A 8"	23* D 3"	24* D 8"	25* D 3"	26 D 8"	27* H 3"	28* H 8"
All to 35k	103	112	169	97	84		All to 35k	498**	57	Lost	Lost	Lost	103	1138**	166
D to 35k	97	115	172	100	87		D to 35k	498**	54	Lost	Lost	Lost	81	1162**	175
D to 40k	91	108	175	100	87		D to 40k	498**	54	Lost	Lost	Lost	103	1162**	175
D Failed	86	109	187	106	93		D Failed	498**	54	Lost	Lost	Lost	223	1168**	169

* Gage Not Represented in Graph ** Stresses Exceed Tensile strength of Concrete (361 psi)
 Lost = Gage Destroyed Previously

Table A.5 -- Calculated Concrete Stresses from Strain Gage Readings of Slab 1 During Anchor H Failure Loading (ksi)

Calculated Stresses in Concrete from Horizontal Gages															
Gage # Position & Depth	1* A 1/4"	2* E-F 1/4"	3* H 1/4"	4* A 6"	5* A 24"	6* B 2"	7* B 6"	8* B 12"	9* C 2"	10* C 6"	11* C 9"	12* C 12"	13* C 48"	14* C 2"	15* C 6"
All to 35k	117	Lost	Lost	117	85	1156**	918**	344	148	151	103	111	87	87	166
H to 35k	Lost	Lost	Lost	Lost	Lost	Lost	Lost	Lost	64	134	111	111	82	-31	114
H to 45k	Lost	Lost	Lost	Lost	Lost	Lost	Lost	Lost	67	131	111	111	82	-31	114
H to 47k	Lost	Lost	Lost	Lost	Lost	Lost	Lost	Lost	64	131	111	111	82	-31	114
H to 52k	Lost	Lost	Lost	Lost	Lost	Lost	Lost	Lost	67	134	111	108	76	-31	111
H to 35k	Lost	Lost	Lost	Lost	Lost	Lost	Lost	Lost	65	136	111	111	77	-79	117
H to 42k	Lost	Lost	Lost	Lost	Lost	Lost	Lost	Lost	61	136	111	111	77	47	114

Calculated Stresses in Concrete from Vertical Gages (psi)													
Gage # Position & Depth	16* C 9"	17* C 12"	18* H 6"	19* H 12"	20* H 48"	21* A 3"	22* A 8"	23* D 3"	24* D 8"	25* D 3"	26* D 8"	27* H 3"	28* H 8"
All to 35k	103	112	169	97	84	All to 35k 498**	57	Lost	Lost	Lost	103	1138**	166
H to 35k	76	100	107	61	Lost	H to 35k	Lost	Lost	Lost	Lost	78	866**	143
H to 45k	76	97	110	61	Lost	H to 45k	Lost	Lost	Lost	Lost	78	875**	147
H to 47k	76	100	113	58	Lost	H to 47k	Lost	Lost	Lost	Lost	78	881**	147
H to 52k	73	100	110	20	Lost	H to 52k	Lost	Lost	Lost	Lost	78	881**	147
H to 35k	79	104	29	68	Lost	H to 35k	Lost	Lost	Lost	Lost	66	652**	186
H to 42k	77	101	57	89	Lost	H to 42k	Lost	Lost	Lost	Lost	69	745**	210

* Gage Not Represented in Graph ** Stresses Exceed Tensile Strength of Concrete (361 psi)
 Lost = Gage Destroyed Previously

Table A.6 - Calculated Reinforcement Stresses from Strain Gage Readings of Slab 2 on Lightly Reinforced Side During Alternate and Adjacent Anchor Loading Sequences (ksi)

Stresses in Horizontal #2 Reinforcing Bars									
Gage # Position & Depth	1* A 6"	2* A 20"	3 B 6"	4 B 20"	5* C 6"	6* C 20"	7* C 34"	8* H 6"	9* H 20"
Load C	0	.0	-.3	-.2	1.4	1.8	1.2	-.1	-.1
Load G	.1	.1	-.2	-.3	2.0	1.8	1.2	-.5	-.4
Load E	.2	.1	-.2	-.2	1.9	1.5	1.2	-.5	-.3
Load A	19.6	4.8	-.2	-.6	11.1	1.6	-.6	-.4	-.4
Load B	18.1	5.3	1.5	1.1	9.7	1.3	-.9	-.4	-.4
Load D	17.8	5.1	1.3	.8	5.9	1.2	1.2	-.4	-.3
Load F	17.9	5.0	1.3	.7	6.3	.9	1.1	-.5	-.2
Load H	17.9	5.0	1.3	.7	6.7	.9	.8	-.4	1.1

Stresses in Vertical #2 Reinforcing Bars								
Gage # Position & Depth	10 A 2"	11 A 2"	12 A 4"	13 A 4"	14 D 2"	15 D 4"	16 H 2"	17 H 4"
Load C	.1	.0	.1	.1	.1	.1	.0	.0
Load G	.2	.1	.2	.2	.2	.1	.1	.1
Load E	.2	.1	.2	.2	.1	.2	.1	.1
Load A	2.2	5.3	1.8	2.3	.2	.1	.1	.2
Load B	2.2	5.0	1.8	2.3	.2	1.0	.1	.2
Load D	2.0	4.8	1.6	2.1	3.9	1.8	.1	.2
Load F	2.0	4.7	1.5	2.1	3.9	1.8	.0	.1
Load H	2.0	4.7	1.5	2.0	3.9	1.7	6.9	3.5

Bars Stressed to Transfer Loads and Locked at 30 Kips for Readings
* Gages Passing Through Pre-formed Cracks

Stresses in Horizontal #2 Reinforcing Bars									
Gage Position & Depth	1* A 6"	2* A 20"	3 B 6"	4 B 20"	5* C 6"	6* C 20"	7* C 34"	8* H 6"	9* H 20"
Load A	12.3	2.4	.2	-.2	5.1	-.2	-.5	.0	.0
Load B	10.6	2.5	1.2	-.5	4.2	-.1	-.2	.0	.0
Load C	10.5	2.4	1.0	.8	5.2	1.7	.9	.2	.1
Load D	10.4	2.3	1.0	.7	2.5	1.7	1.4	.3	.1
Load E	10.5	2.3	1.1	.7	2.7	1.5	1.4	.3	.0
Load F	10.7	2.4	1.1	.8	3.1	1.4	1.4	.3	.0
Load G	10.9	2.5	1.2	.9	3.7	1.4	1.4	-.2	.3
Load H	10.6	2.2	.6	.7	Broken	1.3	1.3	.8	1.2

Stresses in Horizontal #2 Reinforcing Bars								
Gage Position & Depth	10 A 2"	11 A 2"	12 A 4"	13 A 4"	14 D 2"	15 D 4"	16 H 2"	17 H 4"
Load A	.8	3.3	1.0	1.4	.0	.0	.0	.0
Load B	.9	3.2	1.1	1.4	.0	.0	.1	.1
Load C	1.1	3.3	1.2	1.5	.1	.0	.1	.1
Load D	1.0	3.3	1.1	1.4	.7	1.7	.2	.2
Load E	1.1	3.3	1.1	1.5	3.5	1.8	.5	.5
Load F	1.2	3.4	1.2	1.6	3.5	1.8	.5	.5
Load G	1.3	3.5	1.4	1.7	3.6	1.8	.5	.5
Load H	.9	3.3	1.1	1.4	3.4	1.8	3.9	2.2

Bars Stressed to Transfer Loads and Locked at 30 Kips for Readings
*Gages Passed Through Pre-formed Cracks
Broken = Gage Destroyed During Loading

Table A.7 - Calculated Reinforcement Stresses from Strain Gage Readings of Slab 2 on Heavily Reinforced Side During Alternate and Adjacent Anchor Loading Sequences (ksi)

Stresses in Horizontal #3 Reinforcing Bars									
Gage # Position & Depth	21* A 5"	22* A 15"	23 B 5"	24 B 15"	25* C 5"	26* C 15"	27* C 25"	28* H 5"	29* H 15"
Load C	.1	-.1	-.3	-.1	.5	.9	.7	-.1	-.1
Load G	.2	-.0	-.2	-.1	.8	1.1	.7	-.1	-.4
Load E	.2	-.1	-.2	-.1	.9	1.7	.6	-.8	-.4
Load A	3.0	1.2	1.5	1.1	4.8	1.3	1.1	-.6	-.3
Load B	2.3	1.2	1.6	.8	4.4	1.3	.3	-.5	-.3
Load D	2.4	1.2	1.6	.7	3.1	.7	.5	-.5	-.3
Load F	2.4	1.2	1.6	.7	3.4	.7	.5	-.7	-.6
Load H	2.4	1.2	1.7	.7	3.8	.8	.4	3.0	2.5

Stresses in Vertical #2 Reinforcing Bars			
Gage # Position & Depth	30 A 2"	31 D 2"	32 H 2"
Load C	.0	.1	.0
Load G	.1	.2	.1
Load E	.1	.1	.1
Load A	3.7	.3	.1
Load B	3.7	.3	.1
Load D	3.6	1.4	.1
Load F	3.6	1.4	.0
Load H	3.6	1.4	3.3

Bars Stressed to Transfer Loads and Locked at 30 Kips for Readings
* Gages Passing Through Pre-formed Cracks

Stresses in Horizontal #3 Reinforcing Bars									
Gage Position & Depth	21* A 5"	22* A 15"	23 B 5"	24 B 15"	25* C 5"	26* C 15"	27* C 25"	28* H 5"	29* H 15"
Load A	1.7	1.1	.4	.0	2.9	.5	-.2	-.1	-.1
Load B	1.2	1.1	1.3	.6	2.5	.6	.0	-.2	-.2
Load C	1.3	1.1	1.1	.7	2.8	1.7	.6	.4	-.1
Load D	1.3	1.1	1.1	.7	1.3	.9	.9	.6	-.1
Load E	1.4	1.1	1.2	.7	1.5	.8	.9	.6	-.2
Load F	1.4	1.2	1.3	.8	1.9	.8	.9	.6	-.0
Load G	1.5	1.2	1.3	.8	2.2	.9	.8	-.4	-.3
Load H	1.4	1.1	1.3	.8	2.6	.9	.3	2.8	1.7

Stresses in Vertical #2 Reinforcing Bars			
Gage Position & Depth	30 A 2"	31 D 2"	32 H 2"
Load A	2.1	.1	.0
Load B	2.0	.1	.1
Load C	2.1	.2	.1
Load D	2.1	1.3	.1
Load E	2.2	1.2	.2
Load F	2.3	1.3	.2
Load G	2.3	1.3	.2
Load H	2.3	1.3	3.4

Bars Stressed to Transfer Loads and
Locked at 30 Kips for Reading
*Gages Passed Through Pre-formed Cracks

Table A.8 - Calculated Reinforcement Stresses from Strain Gage Readings of Slab 2 During Loading Anchor A to Failure

Stresses in Horizontal #2 Reinforcing Bars (ksi)										Stresses in Vertical #2 Reinforcing Bars (ksi)									
Gage # Position & Depth	1* A 6"	2* A 20"	3 B 6"	4 B 20"	5* C 6"	6* C 20"	7* C 34"	8* H 6"	9* H 20"	Gage # Position & Depth	10 A 2"	11 A 2"	12 A 4"	13 A 4"	14 D 2"	15 D 4"	16 H 2"	17 H 4"	
All 30k	10.8	2.6	.7	1.2	5.0	8.2	4.8	1.2	4.2	All 30k	1.4	.2	1.5	1.7	Lost	22.2	4.1	2.4	
A to 35k	13.6	2.9	.3	1.2	9.4	7.7	3.6	1.1	4.2	A to 35k	1.6	1.0	1.7	2.0	Lost	22.2	4.1	2.4	
A to 45k	18.5	4.0	.4	1.3	11.3	8.2	3.4	1.1	4.2	A to 45k	2.4	2.8	2.3	3.2	Lost	12.0	4.1	2.4	
A to 55k	24.6	5.3	.6	1.4	13.6	9.2	3.3	1.1	4.3	A to 55k	4.2	5.4	3.7	5.3	Lost	11.8	4.1	2.4	
A to 60k	29.4	6.5	.6	1.4	14.9	10.0	3.3	1.1	4.3	A to 60k	5.8	7.4	4.9	6.0	Lost	11.5	4.1	2.4	
A to 65k	33.1	7.1	.6	1.3	15.9	10.4	3.2	1.1	4.3	A to 65k	6.5	8.8	5.3	6.1	Lost	11.5	4.1	2.4	
A Failed	37.2	31.1	.3	1.4	12.4	11.9	4.4	1.1	4.3	A Failed	Broken	Broken	9.3	15.2	Lost	11.4	4.1	2.4	
A to 54k	240.6	32.5	.3	1.4	12.9	12.0	4.4	1.0	4.2	A to 54k	Broken	Broken	10.3	16.0	Lost	11.3	4.1	2.4	

Stresses in Horizontal #3 Reinforcing Bars (ksi)										Stresses in Vertical #2 Reinforcing Bars (ksi)									
Gage # Position & Depth	21* A 5"	22* A 15"	23 B 5"	24 B 15"	25* C 5"	26* C 15"	27* C 25"	28* H 5"	29* H 15"	Gage # Position & Depth	30 A 2"	31 D 2"	32 H 2"						
All 30k	1.6	1.3	1.4	.9	1.8	7	.5	3.0	2.0	All 30k	3.5	5.5	3.6						
A to 35k	1.9	1.5	1.6	1.0	4.7	2.0	.2	2.9	2.2	A to 35k	3.2	2.7	3.7						
A to 45k	2.7	1.9	1.8	1.0	9.1	2.4	.1	2.9	2.2	A to 45k	4.6	2.7	3.7						
A to 55k	3.7	3.3	1.9	1.0	7.8	3.1	.0	2.9	2.2	A to 55k	6.8	2.7	3.7						
A to 60k	5.6	4.5	2.0	1.0	8.7	3.7	.0	2.9	2.2	A to 60k	8.8	2.7	3.7						
A to 65k	7.4	6.1	2.1	1.0	9.7	4.1	.2	2.9	2.2	A to 65k	10.4	2.7	3.7						
A Failed	10.0	6.1	1.8	.9	8.1	4.5	.1	2.8	2.1	A Failed	15.1	2.7	3.7						
A to 54k	240.6	6.1	1.8	.9	8.3	4.4	.1	2.8	2.1	A to 54k	14.9	2.7	3.7						

Broken = Gage Destroyed During Loading Lost = Gage Destroyed Previously
 *Gages that pass through pre-formed cracks

Table A.9 - Calculated Reinforcement Stresses from Strain Gage Readings of Slab 2 During Loading Anchor D to Failure

Stresses in Horizontal #2 Reinforcing Bars (ksi)					Stresses in Vertical #2 Reinforcing Bars (ksi)													
Gage # Position & Depth	1* A 6"	2* A 20"	3 B 6"	4 B 20"	5* C 6"	6* C 20"	7* C 34"	8* H 6"	9* H 20"	Gage # Position & Depth	10 A 2"	11 A 2"	12 A 4"	13 A 4"	14 D 2"	15 D 4"	16 H 2"	17 H 4"
All 30k	10.6	.6	.7	1.0	1.7	1.3	1.3	.8	1.2	All 30k	.9	-.3	1.1	1.4	3.6	1.8	3.9	2.2
D to 50k	10.8	.6	.9	1.0	.6	1.5	1.9	1.2	4.0	D to 50k	1.2	-.0	1.3	1.6	7.9	3.8	3.9	2.2
D to 65k	10.7	.5	1.0	1.1	.3	2.0	2.6	1.3	3.9	D to 65k	1.1	-.1	1.2	1.4	13.8	7.3	3.9	2.2
D to 80k	10.8	.6	1.1	1.1	.3	2.6	3.0	1.3	4.0	D to 80k	1.3	.2	1.4	1.6	23.4	13.3	4.0	2.3
D to 90k	10.9	.7	1.1	1.1	.3	4.1	3.0	1.4	4.1	D to 90k	1.4	.2	1.5	1.7	56.9	25.9	4.1	2.4
D to 102k	10.9	.7	1.2	1.2	5.0	8.2	4.8	1.2	4.2	D to 102k	1.4	.2	1.5	1.7	Broken	22.2	4.1	2.4
D Failed	10.8	.8	.7	1.2	5.0	8.2	4.8	1.2	4.2	D Failed	1.4	.2	1.5	1.7	Broken	22.2	4.1	2.4

Stresses in Horizontal #3 Reinforcing Bars (ksi)					Stresses in Vertical #2 Reinforcing Bars (ksi)								
Gage # Position & Depth	21* A 5"	22* A 15"	23 B 5"	24 B 15"	25* C 5"	26* C 15"	27* C 25"	28* H 5"	29* H 15"	Gage # Position & Depth	30 A 2"	31 D 2"	32 H 2"
All 30k	1.4	1.1	1.3	.8	2.6	.9	.3	2.8	1.7	All 30k	2.3	1.3	3.4
D to 50k	1.6	1.2	1.5	.8	2.9	.5	.2	3.1	1.8	D to 50k	2.5	2.5	3.5
D to 65k	1.9	1.3	1.5	.8	1.4	.5	.6	3.1	1.9	D to 65k	2.7	4.7	3.6
D to 80k	1.7	1.3	1.3	.9	.9	.3	.6	3.2	2.0	D to 80k	2.7	6.7	3.6
D to 90k	1.7	1.2	1.3	.8	.5	.2	1.0	3.3	2.0	D to 90k	2.3	8.2	3.6
D to 102k	1.7	1.2	1.5	.8	.1	.1	1.1	3.3	2.0	D to 102k	2.3	8.8	3.6
D Failed	1.6	1.3	1.4	.9	1.8	.7	.5	3.0	2.0	D Failed	2.5	5.5	3.6

Broken = gage destroyed during loading
 *gages that pass through pre-formed cracks

Table A.10 - Calculated Reinforcement Stresses from Strain Gage Readings of Slab 2 During Loading Anchor H to Failure

Stresses in Horizontal #2 Reinforcing Bars (ksi)				Stresses in Vertical #2 Reinforcing Bars (ksi)													
Gage # Position & Depth	1* A 6"	2* A 20"	3 B 6"	4 B 20"	5* C 6"	6* C 20"	7* C 34"	8* H 6"	9* H 20"	10 A 2"	11 A 2"	12 A 4"	13 A 4"	14 D 2"	15 D 4"	16 H 2"	17 H 4"
All 30k	372.2	31.1	4	1.4	12.6	11.9	4.4	1.1	4.3	Lost	Lost	9.3	Lost	Lost	11.4	4.1	2.4
H to 45k	205.4	29.0	.5	.9	5.8	9.0	5.0	1.9	5.0	Lost	Lost	5.8	Lost	Lost	11.6	6.8	4.0
H to 55k	205.2	29.0	.5	1.0	6.1	9.1	5.0	2.7	5.5	Lost	Lost	5.9	Lost	Lost	11.6	8.2	5.5
H to 65k	204.9	29.0	.6	1.1	6.5	9.3	5.0	7.9	8.0	Lost	Lost	6.0	Lost	Lost	10.6	10.6	8.0
H to 75k	204.7	29.0	.7	1.1	6.9	9.5	5.0	12.4	10.7	Lost	Lost	6.0	Lost	Lost	10.6	14.4	10.0
H to 85k	204.5	28.8	.6	1.1	7.2	9.6	5.0	18.9	14.3	Lost	Lost	5.9	Lost	Lost	11.6	19.5	12.3
H to 90k	204.3	28.8	.5	1.0	5.5	8.9	5.2	20.7	21.4	Lost	Lost	5.9	Lost	Lost	11.6	28.5	11.3
H Failed	204.3	28.8	.5	1.0	5.5	8.9	5.2	20.9	15.9	Lost	Lost	5.9	Lost	Lost	11.7	19.2	6.7

Stresses in Horizontal #3 Reinforcing Bars (ksi)				Stresses in Vertical #2 Reinforcing Bars (ksi)									
Gage # Position & Depth	21* A 5"	22* A 15"	23 B 5"	24 B 15"	25* C 5"	26* C 15"	27* C 25"	28* H 5"	29* H 15"	Gage # Position & Depth	30 A 2"	31 D 2"	32 H 2"
All 30k	10.0	6.0	1.8	1.0	8.1	4.5	.2	2.9	2.1	All 30k	15.1	2.7	3.7
H to 45k	5.3	3.1	1.2	1.0	3.3	3.2	.6	4.8	3.8	H to 45k	3.7	2.7	9.0
H to 55k	5.4	3.1	1.2	1.0	3.5	3.5	.6	8.8	5.6	H to 55k	3.7	2.8	7.5
H to 65k	5.4	3.2	1.2	1.1	3.6	3.7	.7	6.6	7.6	H to 65k	3.8	2.8	10.4
H to 75k	5.4	3.2	1.2	1.1	3.8	3.9	.7	4.4	9.0	H to 75k	3.8	2.9	14.4
H to 85k	5.4	3.2	1.2	1.1	4.0	3.9	.7	13.5	12.2	H to 85k	3.7	2.9	23.7
H to 90k	5.4	3.2	1.2	1.1	4.0	3.9	.8	21.7	17.4	H to 90k	3.7	2.9	Broken
H Failed	5.4	3.1	1.2	1.1	3.3	3.4	.8	39.4	11.2	H Failed	3.7	2.9	Broken

Broken = Gage Destroyed During Loading Lost = Gage Destroyed Previously
 *Gages that pass through pre-formed cracks

Table A.11 – Calculated Concrete Stresses from Strain Gage Readings of Slab 3 in Unreinforced Anchorage Zones (psi)

Gage # Position & Depth	Horizontal				Vertical			
	1	2	3	4	5	6	7	8
	A 6"	C 6"	C 12"	A 3"	A 8"	B 3"	C 3"	C 8"
Load C	0	Lost	46	0	3	3	396	32
Load G	3	Lost	43	-3	3	0	396	32
Load K	3	Lost	46	-3	3	0	396	32
Load I	3	Lost	46	-3	3	-3	396	32
Load E	7	Lost	39	-3	3	-11	392	32
Load A	174	Lost	64	399	21	-46	364	18
Load B	139	Lost	46	402	36	770	360	43
Load D	146	Lost	53	402	32	713	364	39
Load F	146	Lost	50	399	32	709	357	36
Load H	146	Lost	50	395	36	706	357	39
Load J	146	Lost	50	395	32	713	357	36
Load L	146	Lost	53	395	32	709	353	36

Bars Stressed to Transfer Loads and Locked at 30 kips for Readings

Stresses in Concrete from Embedded Strain Gages								
Gage # Position & Depth	Horizontal			Vertical				
	1	2	3	4	5	6	7	8
	A 6"	C 6"	C 12"	A 3"	A 8"	B 3"	C 3"	C 8"
A to 50k	91	Lost	82	965	64	659	328	18
A to 60k	113	Lost	96	1421	93	652	317	14
A to 70k	254	Lost	118	2494	285	642	310	4
A to 75k	433	Lost	128	3588	936	642	306	0
A Failed	Broken	Lost	57	Broken	Broken	734	384	39
C to 50k	Lost	Lost	128	Lost	Lost	759	1218	106
C to 60k	Lost	Lost	146	Lost	Lost	762	1855	106
C to 70k	Lost	Lost	175	Lost	Lost	766	3142	280
C to 80k	Lost	Lost	188	Lost	Lost	686	Broken	Broken
C Failed	Lost	Lost	Broken	Lost	Lost	707	Broken	Broken

Broken = Gage Destroyed During Loading
Lost = Gage Destroyed Previously

Table A.12 - Calculated Reinforcement Stresses from Strain Gage Readings of Slab 3 During Alternate Anchor Stressing Sequence (Horizontal Oriented Four-strand Anchors, ksi)

Stresses in Reinforcement (ksi)														
Gage # Position Detail	9 F B-Bar	10 F HP	20 E B-Bar	21 E HP	11 H back	12 H ct	13 H ct	14 H ct	15 H ct	22 G back	23 G ct	24 G ct	25 G ct	26 G ct
Load C	0	0	0	0	0	0	0	0	0	0	0	0	0	0
Load G	0	0	0	0	0	0	0	0	0	-1	2	2	1	0
Load K	0	0	0	0	0	0	0	0	0	0	2	2	0	0
Load L	0	0	0	0	0	0	0	0	0	0	2	2	0	0
Load I	0	0	0	2	0	0	0	0	0	0	2	2	0	0
Load A	0	0	1	1	0	0	0	0	0	0	2	2	0	0
Load B	1	0	1	1	1	0	0	0	0	0	2	2	0	0
Load D	1	0	1	1	1	0	0	0	0	0	2	2	0	0
Load F	1	4	1	1	0	5	2	2	0	0	2	2	0	0
Load H	1	4	1	1	1	4	2	2	0	0	2	2	0	0
Load J	1	4	1	1	1	4	2	2	0	0	2	2	0	0
Load L	1	4	1	1	1	4	2	2	0	1	2	2	0	0

Stresses in Reinforcement (ksi)									
Gage # Position Detail	16 J back	17 J spir	27 I back	28 I spir	18 L back	29 K back			
Load C	0	0	0	0	0	0			
Load G	0	0	0	0	0	0			
Load K	0	0	0	0	0	0			
Load I	0	0	-1	0	0	0			
Load E	0	0	-1	0	0	0			
Load A	0	0	-1	0	0	0			
Load B	0	0	-1	0	0	0			
Load D	0	0	-1	0	0	0			
Load F	0	0	0	0	0	0			
Load H	0	0	0	0	0	0			
Load J	0	0	0	0	0	0			
Load L	3	0	1	0	2	2			

Bars Stressed to Transfer Loads and Locked at 30 kips for Readings

Table A.13 - Calculated Reinforcement Stresses from Strain Gage Readings of Slab 3 During Loading Anchors to Failure (Horizontal Oriented Four-strand Anchors, ksi)

Stresses in Reinforcement (ksi)					Stresses in Reinforcement (ksi)					Stresses in Reinforcement (ksi)					
Gage # Position Detail	9 F B-Bar	10 F HP	20 E B-Bar	21 E HP	Gage # Position Detail	11 H back	12 H ct	13 H ct	14 H ct	15 H ct	22 G back	23 G ct	24 G ct	25 G ct	26 G ct
E to 50k	0	3	0	4	H to 50k	-2	10	4	6	-1	-1	2	2	0	0
E to 60k	0	3	0	6	H to 60k	-2	11	4	8	-1	-1	2	1	0	0
E to 70k	0	3	-1	10	H to 70k	-3	15	6	12	-1	-1	2	1	0	0
E to 80k	0	3	-2	23	H to 90k	-2	Broken	16	Broken	-1	-1	2	1	0	0
E to 85k	0	3	-3	38	H to 100k	Broken	Broken	Broken	Broken	-1	-1	2	2	0	0
E Failed	0	3	-1	Broken	H Failed	Broken	Broken	Broken	Broken	14	0	2	2	0	0
F to 50k	-3	3	3	Lost	G to 50k	Lost	Lost	Lost	Lost	13	0	5	5	0	0
F to 60k	-4	4	3	Lost	G to 60k	Lost	Lost	Lost	Lost	13	-2	5	3	0	0
F to 70k	-5	6	3	Lost	G to 70k	Lost	Lost	Lost	Lost	13	-1	8	3	0	0
F to 80k	-6	12	2	Lost	G to 80k	Lost	Lost	Lost	Lost	13	2	12	7	0	0
F to 90k	-6	0	2	Lost	G to 85k	Lost	Lost	Lost	Lost	13	2	21	11	0	0
F Failed	9	0	1	Lost	G Failed	Lost	Lost	Lost	Lost	13	2	30	13	7	-1
														17	3

Stresses in Reinforcement (ksi)				Stresses in Reinforcement (ksi)			
Gage # Position Detail	16 J back	17 J spir	27 I back	Gage # Position Detail	18 L back	29 K back	
I to 50k	Lost	Lost	-5	K to 50k	3	-2	
I to 60k	Lost	Lost	-5	K to 60k	3	-3	
I to 70k	Lost	Lost	-1	K to 70k	3	-3	
I to 80k	Lost	Lost	-8	K to 80k	3	5	
I to 90k	Lost	Lost	-12	K Failed	3		
I to 94k	Lost	Lost	Broken				
I Failed	Lost	Broken	Broken	L to 50k	3	0	
J to 50k	0	1	0	L Failed	4	0	
J to 70k	-1	3	0				
J to 80k	-1	3	0				
J to 90k	-1	5	0				
J to 100k	-3	6	0				
J to 105k	-4	Broken	0				
J Failed	Broken	Broken	0				

Broken = Gage Destroyed Current Loading
 Lost = Gage Previously Destroyed

Table A.14 - Calculated Reinforcement Stresses from Strain Gage Readings of Slab 4 Ahead of Horizontal Oriented Four-strand Anchors (ksi)

Stresses in Reinforcement (ksi)																			
Gage Position & Detail	1		2		3		21		22		23		24		25		26		
	A	Back	A	Hoop	A	Hoop	B	Back	B	Hoop	B	Hoop	C	Back	C	Dbhlp	D	Dbhlp	
Load C	0	0	0	0	0	0	0	0	0	0	0	0	1	1	1	0	0	0	0
Load B	0	0	0	0	0	0	0	0	0	0	0	0	1	1	1	0	0	0	0
Load A	2	2	2	2	2	2	2	2	2	2	2	2	0	0	0	0	0	0	0
Load D	2	2	2	2	2	2	2	2	2	2	2	2	0	0	0	0	0	0	0
Load E	2	2	2	2	2	2	2	2	2	2	2	2	0	0	0	0	0	0	0
Load F	2	2	2	2	2	2	2	2	2	2	2	2	0	0	0	0	0	0	0
Load G	2	2	2	2	2	2	2	2	2	2	2	2	0	0	0	0	0	0	0
Load H	2	2	2	2	2	2	2	2	2	2	2	2	0	0	0	0	0	0	0
Load I	2	2	2	2	2	2	2	2	2	2	2	2	0	0	0	0	0	0	0
Load J	2	2	2	2	2	2	2	2	2	2	2	2	0	0	0	0	0	0	0
Load K	2	2	2	2	2	2	2	2	2	2	2	2	0	0	0	0	0	0	0
Load L	2	2	2	2	2	2	2	2	2	2	2	2	0	0	0	0	0	0	0

Bars Stressed to Transfer Loads and Locked at 30 kips for Readings

Stresses in Reinforcement (ksi)																			
Gage Position & Detail	1		2		3		21		22		23		24		25		26		
	A	Back	A	Hoop	A	Hoop	B	Back	B	Hoop	B	Hoop	C	Back	C	Dbhlp	D	Dbhlp	
A to 30k	6	2	7	2	3	2	3	3	1	1	1	1	1	1	1	1	1	1	5
A to 50k	7	3	8	7	3	3	3	3	1	1	1	1	1	1	1	1	1	1	4
A to 70k	9	7	12	8	3	3	3	3	1	1	1	1	1	1	1	1	1	1	4
A to 80k	16	19	21	12	3	3	3	3	1	1	1	1	1	1	1	1	1	1	4
A to 90k	26	48	48	21	3	3	3	3	1	1	1	1	1	1	1	1	1	1	4
A Failed	25	44	41	41	13	13	13	13	1	1	1	1	1	1	1	1	1	1	4
B to 30k	15	24	18	18	11	11	11	11	2	2	2	2	17	14	14	0	0	0	5
B to 50k	15	24	18	18	11	11	11	11	4	4	4	4	17	14	14	0	0	0	8
B to 70k	15	24	18	18	11	11	11	11	6	6	6	6	17	14	14	0	0	0	11
B to 80k	15	24	18	18	12	12	12	12	8	8	8	8	17	14	14	0	0	0	14
B to 90k	15	24	18	18	13	13	13	13	11	11	11	11	17	14	14	0	0	0	20
B to 100k	15	24	18	18	14	14	14	14	15	15	15	15	17	14	14	0	0	0	36
B Failed	15	24	18	18	Broken	Broken	Broken	Broken	29	29	29	29	17	14	14	0	0	0	Broken

Broken = Gage Destroyed During Loading
Lost = Gage Previously Destroyed

Table A.15 - Calculated Reinforcement Stresses from Strain Gage Readings of Slab 4 Ahead of Vertical Oriented Four-strand Anchors During Adjacent Anchor Stressing Sequence (ksi)

Stresses in Reinforcement (ksi)					
Gage Position & Detail	15 K Back	7 E Back	8 E Hp	27 F Back	28 F Hp
Load C	0	0	0	0	0
Load B	0	1	0	1	0
Load A	0	1	0	1	0
Load D	0	1	0	1	0
Load E	0	0	2	1	0
Load F	0	0	2	3	0
Load G	0	0	2	3	0
Load H	0	0	2	3	0
Load I	1	1	2	4	0
Load J	1	1	2	4	0
Load K	1	1	2	5	0
Load L	14	2	1	5	3

Stresses in Reinforcement (ksi)												
Gage Position & Detail	9 G Back	10 G Ct	11 G Ct	12 G Ct	29 H Back	30 H Ct	31 H Ct	32 H Ct	13 I Back	14 I Spir	33 J Back	34 J Spir
Load C	0	0	0	0	0	0	0	0	0	0	0	0
Load B	0	0	0	0	0	0	0	0	0	0	0	0
Load A	1	0	0	0	0	0	0	0	0	0	0	0
Load D	1	0	0	0	1	0	0	0	0	0	0	0
Load E	1	0	0	0	1	0	0	0	0	0	0	0
Load F	1	0	0	0	1	0	0	0	0	0	0	0
Load G	7	2	2	0	0	0	0	0	1	0	1	0
Load H	7	2	2	0	-1	2	0	0	1	0	1	0
Load I	7	2	2	0	-1	2	0	0	-1	1	1	0
Load J	8	2	2	0	-1	2	0	0	-1	1	0	2
Load K	8	2	2	0	0	2	1	0	0	1	0	2
Load L	9	2	2	0	1	1	1	0	1	1	2	2

Bars Stressed to Transfer Loads and Locked at 30 kips for Readings

Table A.16 - Calculated Reinforcement Stresses from Strain Gage Readings of Slab 4 Ahead of Vertical Oriented Four-strand Anchors During Loading Anchors to Failure (ksi)

Stresses in Reinforcement (ksi)			Stresses in Reinforcement (ksi)			Stresses in Reinforcement (ksi)				
Gage Position & Detail	15 K Back	14	Gage Position & Detail	7 E Back	8 Hp	Gage Position & Detail	13 I Back	14 Sp	33 J Back	34 J Spir
K to 30k	14		E to 30k	1	2	E to 30k	1	2	2	2
K to 50k	25		E to 50k	-1	4	E to 50k	-1	4	1	2
K to 60k	35		E to 60k	-1	5	E to 60k	-1	4	1	2
K to 65k	55		E to 70k	-2	7	E to 70k	-2	4	1	2
K Failed Broken			E to 80k	-3	8	E to 80k	-3	4	1	2
			E to 90k	-10	8	E to 90k	-10	3	1	2
			E Failed Broken		17	E Failed Broken		4	1	2
									0	2
L to 30k	Lost		F to 30k	Lost	17	F to 30k	Lost	3	0	2
L Failed	Lost		F to 50k	Lost	Lost	F to 50k	Lost	4	0	2
			F to 60k	Lost	Lost	F to 60k	Lost	6	0	2
			F to 70k	Lost	Lost	F to 70k	Lost	9	0	2
			F to 80k	Lost	Lost	F to 80k	Lost	13	0	2
			F to 90k	Lost	Lost	F to 90k	Lost	20	0	2
			F Failed	Lost	Lost	F Failed	Lost	24	0	2

Stresses in Steel Reinforcement			Stresses in Steel Reinforcement			Stresses in Steel Reinforcement				
Gage Position & Detail	10 G Ct	11 G Ct	Gage Position & Detail	31 H Ct	32 H Ct	Gage Position & Detail	13 I Back	14 Sp	33 J Back	34 J Spir
G to 30	3	3	G to 30	1	1	I to 30k	1	2	2	2
G to 50	4	4	G to 50	1	1	I to 50k	-1	2	1	2
G to 60	5	5	G to 60	1	1	I to 60k	-1	3	1	2
G to 70	5	5	G to 70	1	1	I to 70k	-2	5	1	2
G Failed Broken	14	9	G Failed Broken	1	1	I to 90k	-3	13	1	2
						I Failed	-13	0	0	2
H to 30	0	5	H to 30	2	2	J to 30k	15	-1	0	3
H to 50	0	5	H to 50	2	5	J to 50k	14	-1	-1	3
H to 60	0	5	H to 60	2	5	J to 60k	14	-1	-1	4
H to 70	0	5	H to 70	2	6	J to 70k	14	-1	-1	4
H to 75	0	5	H to 75	2	7	J to 80k	15	-1	1	5
H to 80	0	5	H to 80	2	7	J to 90k	15	-1	3	5
H to 85	0	5	H to 85	2	8	J to 05k	15	-1	5	8
H Failed	0	5	H Failed	2	8	J Failed	15	-1	5	8

Broken = Gage Destroyed During Loading
 Lost = Gage Destroyed Previously

Table A.17 - Calculated Reinforcement Stresses from Strain Gage Readings of Slab 5 During Adjacent Anchor Stressing Sequence (Horizontal Oriented Four-strand Anchors with Inclined Tendons, ksi)

Stresses in Reinforcement (ksi)													
Gage # Position & Detail	1 A Hor	2 A Hor	3 A Hp	11 B Hor	13 B Hp	4 C Hor	5 C Ct	6 C Ct	7 C Ct	14 D Hor	15 D Ct	16 D Ct	17 D Ct
Load C	0	0	0	-1	0	-1	1	1	0	0	0	0	0
Load B	0	0	0	-2	1	-1	1	1	0	0	0	0	0
Load A	0	0	2	-1	1	-1	1	0	0	0	0	0	0
Load D	0	0	1	-1	1	-1	1	0	1	0	0	0	0
Load E	0	0	1	-1	1	0	1	0	1	-1	0	0	1
Load F	0	0	1	-1	1	0	1	0	1	-1	0	0	1
Load G	0	0	2	-1	1	0	1	0	1	-1	0	0	1
Load H	0	0	2	-1	1	0	1	0	1	-1	8	3	1

Stresses in Reinforcement (ksi)							
Gage # Position & Detail	8 E Hor	9 E Spir	18 F Hor	19 F Spir	10 H Hor	20 H Hor	21 H Hor
Load C	0	0	0	0	0	0	0
Load B	0	0	0	0	0	0	0
Load A	0	0	0	0	0	0	0
Load D	-1	0	0	0	0	0	0
Load E	-1	2	0	0	0	0	0
Load F	0	2	1	2	0	0	0
Load G	0	2	1	2	-2	0	0
Load H	0	2	1	2	-1	0	0

Bars Stressed to Transfer Load Levels and Locked at 30 Kips for Gage Reading

Table A.18 - Calculated Reinforcement Stresses from Strain Gage Readings of Slab 5 During Loading Anchors to Failure (Horizontal Four-strand Anchors with Inclined Tendons, ksi)

Stresses in Reinforcement (ksi)						Stresses in Reinforcement (ksi)								
Gage # Position & Detail	1 A Hor	2 A Hor	3 A Hp	11 B Hor	13 B Hp	Gage # Position & Detail	4 C Hor	5 C Ct	6 C Ct	7 C Ct	14 D Hor	15 D Ct	16 D Ct	17 D Ct
A to 30k	0	0	2	-1	1	C to 30k	-1	1	1	1	-1	8	3	1
A to 50k	0	0	5	-1	1	C to 50k	-1	4	2	2	-1	8	3	1
A to 60k	0	1	6	-1	1	C to 60k	-1	6	2	1	-1	8	3	1
A to 70k	1	1	7	-1	1	C to 70k	-1	8	3	2	-1	8	3	1
A to 80k	2	1	10	-1	1	C to 80k	0	11	4	2	-1	8	3	1
A to 90k	3	1	13	-1	0	C to 90k	1	17	5	2	-1	8	3	1
A to 95k	4	1	17	-1	0	C to 100k	5	Broken	6	5	-1	8	3	1
A Failed	46	19	Broken	-1	1	C Failed	7	Broken	6	4	-1	8	3	1
B to 30k	38	16	Lost	-1	1	D to 30k	10	Lost	4	2	-2	8	3	1
B to 50k	38	16	Lost	-2	3	D to 50k	10	Lost	4	2	-2	5	3	1
B to 60k	38	16	Lost	-2	5	D to 60k	10	Lost	4	2	-2	5	3	1
B to 70k	38	16	Lost	-2	5	D to 70k	10	Lost	4	2	-2	6	3	2
B to 80k	38	16	Lost	-2	7	D to 80k	11	Lost	4	2	-2	8	3	2
B to 90k	38	16	Lost	-2	9	D to 90k	11	Lost	4	2	-2	8	3	2
B to 100k	38	16	Lost	-2	13	D to 100k	11	Lost	4	2	-2	11	3	2
B to 110k	38	16	Lost	-2	24	D to 105k	11	Lost	4	2	-2	Broken	11	2
B Failed	36	16	Lost	15	36	D Failed	11	Lost	4	2	-3	Broken	10	3

Stresses in Reinforcement (ksi)					Stresses in Reinforcement (ksi)			
Gage # Position & Detail	8 E Hor	9 E Spir	18 F Hor	19 F Spir	Gage # Position & Detail	10 G Hor	20 H Hor	21 H Hor
E to 30k	0	2	1	2	G to 30k	-2	0	0
E to 50k	-1	4	1	2	G to 50k	-3	0	0
E to 80k	-2	5	1	2	G to 60k	-3	0	0
E to 110k	-4	7	1	2	G to 70k	-2	0	0
F to 30k	-1	3	1	2	G to 80k	-2	0	0
F to 50k	0	3	1	4	G to 90k	-1	0	0
F to 80k	1	3	1	6	G to 100k	1	0	0
F to 110k	1	3	0	11	G to 105k	4	0	0
Reload	0	0	0	0	G Failed	16	0	0
E to 30k	-1	3	0	5	H to 30k	15	0	0
E to 80k	-3	5	1	5	H to 50k	15	0	0
E to 110k	-4	7	1	5	H to 60k	16	0	1
E at 110k	-4	7	1	5	H to 70k	16	0	1
F to 30k	0	2	0	5	H to 80k	16	0	1
F to 80k	1	2	-1	9	H to 90k	17	0	1
F to 110k	2	2	-1	12	H to 100k	17	0	1
F at 110k	2	2	-2	13	H to 110k	18	1	1
					H Failed	15	12	22

Bars Stressed to Transfer Load Level and Locked at 30 Kips for Gage Reading
 Broken = Gage Destroyed During Loading, Its Respective Anchor
 Lost = Gage Destroyed in During Loading of Another Anchor

Table A.19 – Calculated Reinforcement Stresses from Strain Gage Readings of Slab 6 During Adjacent Anchor Stressing Sequence (Monostrand Anchors, ksi)

Gage # Position & Detail	Stresses in Reinforcement (ksi)									
	10 G Back	11 G Hor	20 H Back	21 H Hor	22 H Hor	1 A Hor	2 A Hor	3 A Hp	12 B Hor	13 B Hp
Load C	0	Lost	0	0	0	0	0	0	0	0
Load B	0	Lost	0	0	0	0	0	0	1	-1
Load A	0	Lost	0	0	0	1	0	-1	1	-1
Load D	0	Lost	0	0	0	1	0	-1	1	-1
Load E	0	Lost	0	0	0	1	0	-1	1	-1
Load F	0	Lost	0	0	0	1	0	-1	1	-1
Load G	0	Lost	0	0	0	1	0	-1	1	-1
Load H	0	Lost	0	1	0	1	0	-1	1	-1

Gage # Position & Detail	Stresses in Reinforcement (ksi)								
	4 C Hor	5 C Ct	6 C Ct	7 C Ct	14 D Hor	15 D Ct	16 D Ct	17 D Ct	
Load C	1	1	1	0	0	0	0	0	
Load B	1	2	1	1	0	0	0	0	
Load A	1	2	1	1	1	0	0	0	
Load D	1	1	1	1	1	1	1	1	
Load E	1	1	1	1	1	2	1	1	
Load F	1	1	1	1	1	2	1	1	
Load G	1	1	1	1	1	2	1	1	
Load H	1	1	1	1	1	2	1	1	

Gage # Position & Detail	Stresses in Reinforcement (ksi)			
	8 E Hor	9 E Spir	18 F Hor	19 F Spir
Load C	0	0	0	0
Load B	0	0	0	0
Load A	0	0	0	0
Load D	0	0	0	0
Load E	0	0	0	0
Load F	0	1	0	1
Load G	0	1	0	1
Load H	0	1	1	1

Bars Stressed to Transfer Loads and Locked at 30 Kips for Readings

Table A.20 - Calculated Reinforcement Stresses from Strain Gage Readings of Slab 6 During Loading Anchors to Failure (Monostrand Anchors, ksi)

Stresses in Reinforcement (ksi)						Stresses in Reinforcement (ksi)					
Gage # Position & Detail	10 G Back	11 G Hor	20 H Back	21 H Hor	22 H Hor	Gage # Position & Detail	1 A Hor	2 A Hor	3 A Hp	12 B Hor	13 B Hp
G at 30k	0	Lost	0	1	0	A at 30k	1	0	-1	1	-1
G to 80k	1	Lost	0	0	1	A to 50k	1	0	0	2	-1
G to 110k	1	Lost	0	0	1	A to 60k	1	1	0	2	-1
H at 30k	2	Lost	0	1	0	A to 70k	1	1	1	2	-1
H to 50k	2	Lost	0	1	1	A to 80k	1	1	1	2	-2
H to 60k	2	Lost	0	2	1	A to 90k	1	1	2	2	-2
H to 70k	2	Lost	1	2	1	A to 100k	2	1	2	2	-1
H to 80k	2	Lost	1	3	1	A failed	18	7	Broken	2	-1
H to 90k	4	Lost	1	2	1	B at 30k	15	8	Lost	1	-1
H to 95k	4	Lost	1	2	1	B to 80k	14	8	Lost	3	2
H Failed	3	Lost	1	2	1	B to 110k	14	8	Lost	3	2
G at 30k	1	Lost	0	0	0	B at 30k	1	1	Lost	0	2
G to 100k	1	Lost	0	0	1	B to 100k	1	1	Lost	3	2
G to 120k	1	Lost	0	0	1	B to 120k	1	1	Lost	4	5
G Failed	6	Lost Broken	0	0	1	B to 140k	1	1	Lost	14	23
						B to 145k	1	1	Lost	18	33
						B Failed	3	2	Lost	72	Broken

Stresses in Reinforcement (ksi)						Stresses in Reinforcement (ksi)							
Gage # Position & Detail	4 C Hor	5 C Ct	6 C Ct	7 C Ct	14 D Hor	15 D Ct	16 D Ct	17 D Ct	Gage # Position & Detail	8 E Hor	9 E Spir	18 F Hor	19 F Spir
C at 30k	1	1	1	1	1	3	1	1	E at 30k	0	0	1	1
C to 80k	2	2	2	2	0	3	1	1	E to 80k	0	2	0	1
C to 110k	2	2	2	2	0	3	2	1	E to 110k	0	2	0	1
D at 30k	1	2	2	1	1	3	1	1	F at 30k	0	1	0	1
D to 80k	1	2	2	1	1	10	5	1	F to 80k	0	2	1	1
D to 110k	1	2	2	1	2	17	8	1	F to 110k	0	2	2	3
C at 30k	3	3	4	1	0	8	4	1	E at 30k	2	1	4	2
C to 100k	5	6	6	1	0	8	4	1	E to 100k	2	3	3	2
C to 120k	6	7	7	2	0	9	4	1	E to 120k	2	3	3	1
C to 140k	10	15	15	7	-1	13	12	2	E to 140k	0	1	1	1
C to 150k	20	20	20	10	-1	16	15	6	E to 145k	-1	1	1	0
C at 150k	51	10	25	10	0	17	17	9					
C Failed	281	Broken	25	8	0	16	15	9					
D at 30k	0	Lost	0	0	0	-2	0	0	F at 30k	0	0	0	0
D to 100k	-1	Lost	0	1	1	14	8	1	F to 100k	1	1	1	1
D to 120k	-1	Lost	0	1	1	19	11	1	F to 120k	2	1	1	1
D to 140k	-2	Lost	0	1	1	24	16	1	F to 140k	2	1	1	1
D to 150k	-2	Lost	0	4	2	28	19	1	F to 145k	3	1	2	1
D at 150k	-4	Lost	0	6	6	29	20	1					
D Failed	6	Lost	1	6	6	20	15	1					

Broken = Gage Destroyed During Loading
 Lost = Gage Previously Destroyed

Bibliography

- 1 American Association of State Highway and Transportation Officials (AASHTO); Standard Specifications for Highway Bridges; AASHTO; 1983
- 2 ACI Committee 209; "Prediction of Creep, Shrinkage, and Temperature Effects in Concrete Structures"; ACI Manual of Concrete Practice, Part 1, Materials and General Properties of Concrete; Report ACI 209R-82; American Concrete Institute; 1987.
- 3 Bergmeister, K.; Breen, J. E.; Jirsa, J. O.; Kreger, M. E.; "Detailing for Structural Concrete"; Research Report 1127-3F; Center for Transportation Research Bureau of Engineering Research, The University of Texas at Austin; May, 1990.
- 4 Breen, J.; Burdet, O.; Sanders, D.; Wolmann, G.; Roberts, C.; Falconer, B.; "Proposed Post-Tensioned Anchorage Zone Provisions for Inclusion in the AASHTO Bridge Specifications"; Unpublished Draft; The University of Texas at Austin; 1990.
- 5 Burdet, O. L.; "Analysis and Design of Anchorage Zones in Post-Tensioned Concrete Bridges"; Ph.D. Dissertation, The University of Texas at Austin; May 1990.
- 6 Burdet, O. L.; "Computation and Display of Principal Stresses Using PRIN6"; Unpublished User's Manual, The University of Texas at Austin; 1990.
- 7 Burgess, J. A., Breen, J. E., and Poston, R. W.; "Anchorage Cracking of Post-Tensioned Bridge Decks with Closely-Spaced Anchors"; Unpublished Masters Report, The University of Texas at Austin; 1986.
- 8 Hibbit, Karlsson, and Sorenson Providence, RI; "ABAQUS Users' Guide".
- 9 Libby, James R.; "Critique of a post-tensioned roof slab failure", Concrete International Concrete International, ACI, Volume 7, No. 10; Oct. 1985, pp 28-32.

Bibliography (cont.)

- 10 Post-Tensioning Institute; Post-Tensioning Manual; Chapter 6, Section 6.2; 4th Ed., 1985.
- 11 Roberts, C.; "Behavior and Design of the Local Anchorage Zone in Post-Tensioned Concrete"; Unpublished Masters Thesis, The University of Texas at Austin; May 1990.
- 12 Sanders, D. H.; "Design and Behavior of Post-Tensioned Concrete Anchorage Zones"; Ph. D. Dissertation, The University of Texas at Austin; August 1990.
- 13 Sanders, D. H.; Breen, J. E.; and Duncan, R. R.; "Strength and Behavior of Closely Spaced Post-Tensioned Monostrand Anchorages"; Ferguson Structural Engineering Laboratory, Bureau of Engineering Research, The University of Texas at Austin; Oct. 1987.
- 14 Schlaich, J.; Schafer, K.; and Jennewein, M.; "Toward a Consistent Design of Structural Concrete"; PCI Journal; Prestressed Concrete Institute; Vol. 32, No. 3; May/June 1987; pp. 74-150.

Vita

Brian Albert Falconer was born in Evanston, Illinois on June 20, 1965 as the son of Robert Allen Falconer and Marian Jeanette Falconer. In 1983, he graduated from the University City Senior High School in University City, Missouri, and enrolled in The University of Kansas at Lawrence. He was awarded a Bachelor of Science Degree in Architectural Engineering from the University of Kansas in May of 1988. In August of that same year, he enrolled in the Graduate School of The University of Texas at Austin.

Permanent Address: 5 Provence Drive
 Lake Saint Louis, Missouri

This thesis was typed by Brian A. Falconer.